Targeting Ataxia telangiectasia mutated (ATM) and DNA dependent protein kinase catalytic subunit (DNA-PKcs) for synthetic lethality application in breast cancer

Nada Mohammed Albarakati

BSc, MSc

Academic Unit of Clinical Oncology,
Division of Cancer and Stem Cells,
University of Nottingham,
Nottingham, UK

Thesis submitted to the University of Nottingham
for the degree of Doctor of Philosophy

July 2015

Abstract

BRCA1 germ-line mutations predispose to hereditary breast and ovarian cancers. Cells lacking functional BRCA1 protein are deficient in the homologous recombination (HR) DNA repair pathway. Base excision repair (BER) is essential for processing base damage induced by endogenous and exogenous sources. Recently, BRCA1 was shown to transcriptionally regulate expression of genes involved in BER such as *OGG1*, *NTH1*, *APE1* and *XRCC1*. The primary aim of the work described in this thesis was to investigate whether targeting the double-strand break (DSB) pathway in BRCA1-BER deficient cells using ATM or DNA-PKcs inhibitors would be synthetically lethal.

Firstly, DNA repair gene and protein expression in BRCA1 deficient and BRCA1 proficient cells were investigated. Initially the RT² Profiler™ DNA Repair PCR Array was used to investigate the expression of 84 DNA repair genes. Data demonstrated down-regulation of several DNA repair mRNAs in BRCA1 mutant/knockdown cell lines as compared to BRCA1 proficient cell lines. Quantitative real time PCR (RT-qPCR) was performed for selected DNA repair genes (*APE1*, *XRCC1*, *SMUG1*, *Pol ß*, *Lig3*, *ATM* and *DNA-PKcs*) and confirmed statistically significant down-regulation of these genes in BRCA1 mutant/knockdown cell lines as compared to BRCA1 wild type/control cell lines. Protein expression of APE1, XRCC1, SMUG1, Pol ß, Lig3, ATM and DNA-PKcs was assessed by western blot analysis and showed down-regulation consistent with the results of mRNA expression. These results suggest that BRCA1 deficiency may be associated with a global defect in the BER pathway.

Secondly, as BRCA1 deficient cells demonstrated evidence of BER deficiency, these cells may be amenable to a synthetic lethality approach by targeting additional DSB repair targets. To examine this, BRCA1 deficient cells were targeted by ATM inhibitors (KU55933 and KU60019). Data demonstrated that BRCA1 mutant/knockdown cell lines were significantly more sensitive to ATM inhibition than BRCA1 proficient cell lines. Functional studies were conducted to understand the mechanism behind this selective cytotoxicity of ATM inhibitors in BRCA1 deficient cells. BRCA1 deficient cells treated with ATM inhibitors showed significant increase in DSB formation compared to untreated BRCA1 deficient cells. Cell cycle progression was arrested significantly at G2/M phase in treated BRCA1 HeLa cells as compared to untreated BRCA1 HeLa cells. On the other hand, MDA-MB-436 cells showed a modest increase in G2/M arrest after 48 hours treatment which suggests disturbed cell cycle progression. BRCA1 deficient cell lines also demonstrated increased levels for apoptosis in response to ATM inhibition. This *in vitro* study suggests that a potential synthetic lethality relationship exists between BRCA1 deficiency and ATM inhibition.

In light of the observed BRCA1/ATM synthetic lethality relationship, BRCA1 deficient cells were targeted with DNA-PKcs inhibitors (NU7441 and NU7026) to investigate whether these drugs would also induce synthetic lethality. Data demonstrated that BRCA1 mutant/knockdown cell lines were significantly more sensitive to DNA-PKcs inhibition than BRCA1 proficient cell lines. Functional studies showed that BRCA1

deficient cells treated with DNA-PKcs inhibitors have a significant increase in DSB formation as compared to untreated BRCA1 deficient cells. The formation of DSBs was followed by a modest arrest at G1 phase and induction of apoptosis. This *in vitro* study suggests that a potential synthetic lethality relationship exists between BRCA1 deficiency and DNA-PKcs inhibition.

Finally, BRCA1 deficient cells were targeted by ATM or DNA-PKcs inhibitor in combination with cisplatin to investigate whether it would enhance the observed synthetic lethality. The results of both combination treatments induced hypersensitivity in BRCA1 deficient cells compared to BRCA1 deficient cells treated with cisplatin alone. Significant increase in DSB formation was observed in BRCA1 mutant/knockdown cells treated with the combination of ATM inhibitor/cisplatin or DNA-PKcs inhibitor/cisplatin compared to each inhibitor alone. Cell cycle analysis showed significant G2/M arrest and induction of apoptosis in BRCA1 deficient cells treated with the combination treatments compared to each inhibitor alone. These results support the hypothesis that cisplatin increases the efficacy of ATM and DNA-PKcs inhibition in BRCA1 deficient cells. Taken together, this study provides the pre-clinical evidence that ATM and DNA-PKcs could be alternative synthetic lethality targets in BRCA1 deficient breast cancer.

Publication arising from this thesis

Albarakati N, Abdel-Fatah TM, Doherty R, Russell R, Agarwal D, Moseley P, Perry C, Arora A, Alsubhi N, Seedhouse C, Rakha EA, Green A, Ball G, Chan S, Caldas C, Ellis IO, Madhusudan S. Targeting BRCA1-BER deficient breast cancer by ATM or DNA-PKcs blockade either alone or in combination with cisplatin for personalized therapy. Mol Oncol. 2015 Jan;9(1):204-17. doi: 10.1016/j.molonc.2014.08.001. Epub 2014 Aug 27.

Poster presentations

Nada Albarakati, Tarek Abdel Fatah, Paul Moseley, Stephen Chan, Claire Seedhouse, Ian Ellis, Srinivasan Madhusudan. A novel synthetic lethality application targeting ATM and DNA-PKcs in BRCA1 deficient cancer cells. National Cancer Research Institute (NCRI), Cancer Conference. Liverpool, UK (Nov, 2013).

Nada Albarakati, Rebeka Sultana, Srinivasan Madhusudan. Synthetic lethal targeting of BRCA1 deficient cells by ATM and DNA-PKcs inhibitors for personalized cancer therapy. The 6th Saudi Scientific International Conference. The Brunel University, UK (Oct, 2012).

Other related publications

Sultana R, Abdel-Fatah T, Abbotts R, Hawkes C, **Albarakati N**, Seedhouse C, Ball G, Chan S, Rakha EA, Ellis IO, Madhusudan S. Targeting XRCC1 deficiency in breast cancer for personalized therapy. Cancer Res. 2013 Mar 1;73(5):1621-34.

Abdel-Fatah TM, **Albarakati N**, Bowell L, Agarwal D, Moseley P, Hawkes C, Ball G, Chan S, Ellis IO, Madhusudan S. Single-strand selective monofunctional uracil-DNA glycosylase (SMUG1) deficiency is linked to aggressive breast cancer and predicts response to adjuvant therapy. Breast Cancer Res Treat. 2013 Dec;142(3):515-27.

Abdel-Fatah TM, Russell R, Agarwal D, Moseley P, Abayomi MA, Perry C, **Albarakati N**, Ball G, Chan S, Caldas C, Ellis IO, Madhusudan S. DNA polymerase β deficiency is linked to aggressive breast cancer: a comprehensive analysis of gene copy number, mRNA and protein expression in multiple cohorts. Mol Oncol. 2014 May;8(3):520-32.

Abdel-Fatah TM, Russell R, **Albarakati N**, Maloney DJ, Dorjsuren D, Rueda OM, Moseley P, Mohan V, Sun H, Abbotts R, Mukherjee A, Agarwal D, Illuzzi JL, Jadhav A, Simeonov A, Ball G, Chan S, Caldas C, Ellis IO, Wilson DM 3rd, Madhusudan S. Genomic and protein expression analysis reveals flap endonuclease 1 (FEN1) as a key biomarker in breast and ovarian cancer. Mol Oncol. 2014 May 13.

Sultana R, Abdel-Fatah T, Perry C, Moseley P, **Albarakti N**, Mohan V, Seedhouse C, Chan S, Madhusudan S. Ataxia telangiectasia mutated and Rad3 related (ATR) protein kinase inhibition is synthetically lethal in XRCC1 deficient ovarian cancer cells. PLoS One. 2013; 8(2):e57098.

Acknowledgements

I would like to express my sincere gratitude to my supervisor Dr. Srinivasan Madhusudan for all his support and guidance in order to complete this project.

My sincerest appreciation to the Ministry of Higher Education, Saudi Arabia for the financial support while doing my PhD at the University of Nottingham.

I would like to thank past and current members of the DNA Repair Group at the University of Nottingham (Dr. Mohammed Zubair, Dr. Rebeka Sultana, Dr. Rachel Abbotts, Dr. Christina Perry and Dr. Rachel Doherty) for their support, ideas and friendship.

I am deeply grateful to Dr. Claire Seedhouse, Academic unit of Haematology for her ideas and support with PCR work. I would also like to thank other members of the Academic unit of Oncology for their technical support, advice and friendship during my time spent in the department.

Finally, I would like to express my deepest and heartfelt appreciation to my parents and family who have given me continuous support throughout this study time.

Table of Contents

Abstract 2

Publication arising from this thesis 5

Acknowledgements 7

Table of Contents 8

List of Abbreviations 13

List of Figures 15

List of Tables 19

1. Introduction 21

1.1. DNA damage 24

1.1.1. Base damage 25

1.1.2. Backbone damage 26

1.2. DNA repair 27

1.2.1. DNA repair pathways 28

1.2.1.1. Direct repair 28

1.2.1.2. Base excision repair 28

1.2.1.3. Nucleotide excision repair 32

1.2.1.4. Mismatch repair 33

1.2.1.5. Double strand break repair 34

1.2.1.5.1. Homologous recombination 37

1.2.1.5.2. Non-homologous end joining 38

1.3. Ataxia telangiectasia mutated (ATM) 39

1.3.1. Role of ATM in the cellular response 40

1.4. DNA dependent protein kinase catalytic subunit (DNA-PKcs) 42

1.4.1. Role of DNA-PKcs in the cellular response 42

1.5. The development of ATM and DNA-PKcs inhibitors 44

1.6. Breast Cancer 45

1.7. The BRCA1 tumour suppressor gene 48

1.7.1. Role of BRCA1 in DNA damage response and repair 50

1.7.2. Role of BRCA1 in cell cycle regulation 51

1.7.3. Role of BRCA1 in transcriptional regulation 52

1.8. BRCA1 and cancer 52

1.9. Synthetic lethality 53

1.9.1. Synthetic lethality between BRCA and PARP 54

1.9.2. Alternative synthetic lethality targets 57
1.10. Hypothesis and Aims 58
2. Materials and Methods 61
2.1. Materials 61
2.2. Cell lines and culture media 61
2.2.1. HeLa SilenciX® cells 61
2.2.2. Breast cancer cells 62
2.3. Methods 62
2.3.1. Subculture of cell lines 63
2.3.2. Cryopreservation of cell lines 63
2.3.3. AQueous non-radioactive cell proliferation assay (MTS assay) 64
2.3.3.1. Background principles 64
2.3.3.2. Assay 64
2.3.3.3. Data analysis 65
2.3.4. Clonogenic survival assay 65
2.3.4.1. Background principles 65
2.3.4.2. Plating efficiency 65
2.3.4.3. Clonogenic assay 66
2.3.4.4. Data analysis 67
2.3.5. γH2AX immunofluorescence microscopy assay 67
2.3.5.1. Background principles 67
2.3.5.2. Assay 68
2.3.5.3. Data analysis 69
2.3.6. Flow cytometric analyses for cell cycle 69
2.3.6.1. Background principles 69
2.3.6.2. Assay 70
2.3.6.3. Data analysis 70
2.3.7. Annexin V flow cytometric analyses for Apoptosis 71
2.3.7.1. Background principles 71
2.3.7.2. Assay 73
2.3.7.3. Data analysis 73
2.3.8. DNA repair gene expression profiling 74
2.3.8.1. Background principles 74
2.3.8.2. RNA extraction 74
2.3.8.3. cDNA Synthesis 75
2.3.8.4. RT² Profiler™ DNA Repair PCR Array 76
2.3.8.5. Quantitative real time PCR (RT-qPCR) 77

2.3.8.6. Data analysis 78
2.3.9. Western Blot analysis 79
2.3.9.1. Background principles 79
2.3.9.2. Preparation of cell lysate 79
2.3.9.3. Protein quantification (Bradford assay) 80
2.3.9.4. Preparation of cell lysates for electrophoresis 80
2.3.9.5. Polyacrylamide gel electrophoresis and Protein transfer 80
2.3.9.6. Immunoblotting 81
2.3.9.7. Primary antibodies 82
2.3.9.8. Data analysis 82
3. DNA repair profiling in BRCA1 deficient and proficient cells 84
3.1. Introduction 84
3.1.1. BRCA1 mutation in breast cancer cell lines 85
3.1.2. Rationale for the study 86
3.1.2.1. Aims 87
3.2. Materials and Methods 88
3.3. Results 89
3.3.1. Determination of BRCA1 expression in cell lines 89
3.3.1.1. Western blot analysis demonstrates reduced BRCA1 protein expression 89
3.3.1.2. RT- qPCR demonstrate reduced BRCA1 mRNA expression 90
3.3.2. RT^2 Profiler DNA Repair PCR Array 92
3.3.3. Optimisation of the purified RNA for RT-PCR 95
3.3.4. BRCA1 deficiency is associated with multiple altered DNA repair gene expression profile 100
3.3.5. DNA repair protein expression is down-regulated in BRCA1 deficient cell lines compared to BRCA1 proficient cell lines. 106
3.3.6. Quantitative real time PCR (RT-qPCR) in BRCA1 deficient and BRCA1 proficient cells. 108
3.3.7. Quantification of DNA repair mRNA and protein expression in BRCA1 deficient and BRCA1 proficient cells. 110
3.3.8. Growth inhibition MTS assay in response to MMS 117
3.4. Discussion and conclusions 118
3.4.1. Loss of BRCA1 expression links to a global reduction in mRNA and proteins involved in Base excision repair pathway 118
3.4.1.1. BRCA1 deficient cell lines are hypersensitive to MMS 119
3.4.2. Loss of BRCA1 expression is associated with reduction in expression of Homologous recombination factors 120
3.4.3. Loss of BRCA1 expression is associated with reduction in expression of Non-homologous end joining factors 122

3.4.4. Loss of BRCA1 expression is associated with reduction in expression of other DNA repair factors 123

3.4.5. Conclusions 125

4. Targeting BRCA1 deficiency in breast cancer for personalized therapy using ATM inhibitors (KU55933 & KU60019) 127

4.1. Introduction 127

4.1.1. Rationale for study 129

4.2. Aims 129

4.3. Results 130

4.3.1. Clonogenic cell survival and Growth inhibition in response to ATM inhibitors (KU55933 & KU60019) 130

4.3.2. Growth inhibition and clonogenic cell survival in response to PARP inhibitors 135

4.3.3. γH2AX focus immunofluorescence microscopy assay 137

4.3.3.1. γH2AX formation in response to ATM inhibitors 138

4.3.4. Cell cycle analysis by propidium iodide flow cytometry after treatment with ATM inhibitors 141

4.3.5. Apoptosis detection by annexin V-FITC flow cytometry after treatment with ATM inhibitors 145

4.4. Discussion and conclusions 149

4.4.1. Conclusions 153

5. Targeting BRCA1 deficiency in breast cancer for personalized therapy using DNA-PKcs inhibitors (NU7441 & NU7026) 157

5.1. Introduction 157

5.1.1. Rationale for study 158

5.2. Aims 158

5.3. Results 159

5.3.1. Clonogenic cell survival and Growth inhibition in response to DNA-PKcs inhibitors (NU7441 & NU7026) 159

5.3.2. γH2AX focus immunofluorescence microscopy assay 164

5.3.2.1. γH2AX formation in response to DNA-PKcs inhibitors 164

5.3.3. Cell cycle analysis by propidium iodide flow cytometry after treatment with DNA-PKcs inhibitors 166

5.3.4. Apoptosis detection by annexin V-FITC flow cytometry after treatment with DNA-PKcs inhibitors 170

5.4. Discussion and conclusions 173

5.4.1. Conclusions 177

6. Cisplatin in combination with Ataxia telangiectasia mutated (ATM) or DNA dependent protein kinase catalytic subunit (DNA-PKcs) inhibitor in BRCA1 deficient cells 180

6.1. Introduction 180

6.1.1. Rationale for study 181

6.2. Aims 181
6.3. Results 182
6.3.1. Clonogenic cell survival assay in response to Cisplatin 182
6.3.2. Clonogenic cell survival assay in cells treated with KU55933 or NU7441 in combination with cisplatin 183
6.3.3. γH2AX immunofluorescence microscopy in response to KU55933 or NU7441 in combination with cisplatin 186
6.3.4. Flow cytometric cell cycle analysis in response to ATM inhibitor (KU55933) or DNA-PKcs inhibitor (NU7441) in combination with Cisplatin 190
6.3.5. Apoptosis detection by annexin V-FITC flow cytometry in response to KU55933 or NU7441 in combination with cisplatin 193
6.4. Discussion and conclusions 197
6.4.1. Conclusions 200
7. General Discussion and suggestions for future studies 203
7.1. Summary of key findings 211
References 212
APPENDIX A. ΔΔCt Method 248
APPENDIX B. DNA repair genes assayed in Qiagen RT^2 Profiler DNA Repair 249
APPENDIX C. Other related DNA repair genes under-expressed in BRCA1 deficient cell lines compared to BRCA1 proficient cell lines. 251
APPENDIX D. Evaluation of drug interaction 251

List of Abbreviations

µg	Microgram
µl	Microliter
µM	Micromolar
AP	Apurinic/Apyrimidinic
APE1	Human apurinic /apyrimidinic endonuclease 1
ATM	Ataxia telangiectasia mutated
ATR	Ataxia-telangiectasia and Rad3-related
BER	Base excision repair
bp	Base pair
BRCA1	Breast cancer susceptibility 1
BRCA2	Breast cancer susceptibility 2
Ct	Threshold cycle
DMSO	Dimethyl sulfoxide
DNA	Deoxyribonucleic acid
DNA-PK	DNA-protein kinase
DNA-PKcs	DNA dependent protein kinase catalytic subunit
DSB	Double strand break
FEN1	Flap structure specific endonuclease 1
H2AX	H2A histone family, member X
HR	Homologous recombination
IC_{50}	Inhibitory concentration of an inhibitor that results in death of 50% of cell population
kDa	kilodalton
L	Litre

M	Molar
MMR	Mismatch Repair
MMS	Methyl methane sulphonate
MRN	MRE11/RAD50/NBS1 complex
NER	Nucleotide excision repair
NHEJ	Non homologous end joining
PARP1	Poly (ADP-Ribose) Polymerase 1
PBS	Phosphate buffered saline
PI	Propidium iodide
PI3K	Phosphatidylinositide 3-kinase
Pol β	DNA polymerase beta
RNA	Ribonucleic acid
RNAse	Ribonuclease
rpm	rotation per minute
SD	Standard deviation
SEM	Standard error of the mean
SL	Synthetic lethality
SSB	Single strand DNA break
XRCC1	X-ray repair cross complementing gene 1
γH2AX	Phosphorylated H2AX

List of Figures

FIGURE 1.1. THERAPEUTIC TARGETING OF THE HALLMARKS OF CANCER. 22

FIGURE 1.2. SOURCES CAUSING DNA DAMAGE AND CORRESPONDING REPAIR PATHWAY. 25

FIGURE 1.3. BASE EXCISION REPAIR (BER) PATHWAY. 31

FIGURE 1.4. DOUBLE STRAND BREAK (DSB) REPAIR PATHWAY. 36

FIGURE 1.5. THE STRUCTURE DOMAIN OF BRCA1. 49

FIGURE 1.6. SYNTHETIC LETHALITY. 53

FIGURE 1.7. HYPOTHETICAL SYNTHETIC LETHALITY IN BRCA1/ BER DEFICIENT CELLS, BY ATM OR DNA-PKCS INHIBITORS. 59

FIGURE 2.1. ANNEXIN V FLOW CYTOMETRY MECHANISM (V-FITC). 72

FIGURE 2.2. ANNEXIN V AND PI STAINING. 72

FIGURE 3.1. BRCA1 PROTEIN EXPRESSION IN THE CELL LINES STUDIED BY WESTERN BLOT 89

FIGURE 3.2. QUANTIFICATION OF BRCA1 PROTEIN EXPRESSION 90

FIGURE 3.3. QUANTIFICATION OF BRCA1 MRNA EXPRESSION 91

FIGURE 3.4. ILLUSTRATION OF QRT-PCR AMPLIFICATION PLOT. 93

FIGURE 3.5. RT^2 PROFILER PCR ARRAY PLATE LAYOUT. 94

FIGURE 3.6. OPTIMISATION OF RNA CONCENTRATION FOR RT^2 PCR. 96

FIGURE 3.7. MELTING CURVE ANALYSIS FOR HELA CELLS WITH 1 µG TOTAL RNA PER ARRAY. 97

FIGURE 3.8. AMPLIFICATION PLOTS FOR RT^2 PROFILER DNA REPAIR ARRAY. 98

FIGURE 3.9. MELTING CURVES FOR RT^2 PROFILER PCR ARRAY. 99

FIGURE 3.10. SCATTER PLOT COMPARING DNA REPAIR GENE EXPRESSION IN BRCA1 HELA DEFICIENT CELLS AGAINST CONTROL HELA BRCA1 PROFICIENT CELLS. 101

FIGURE 3.11. SCATTER PLOT COMPARING DNA REPAIR GENE EXPRESSION IN BRCA1 DEFICIENT MDA-MB-436 CELLS AGAINST CONTROL BRCA1 PROFICIENT MCF7 CELLS. 102

FIGURE 3.12. REPRESENTATIVE WESTERN BLOT ANALYSIS OF BASE EXCISION REPAIR PROTEINS IN BRCA1 DEFICIENT AND PROFICIENT CELL LINES. 107

FIGURE 3.13. REPRESENTATIVE WESTERN BLOT ANALYSIS OF ATM AND DNA-PKCS EXPRESSION. 108

FIGURE 3.14. QUANTIFICATION OF BASE EXCISION REPAIR PROTEINS EXPRESSION (LEFT) AND QUANTITATIVE REAL TIME PCR (RT-QPCR) SHOWING MRNA EXPRESSION (RIGHT) IN BRCA1 DEFICIENT AND PROFICIENT HELA CELL LINES. 112

FIGURE 3.15. QUANTIFICATION OF BASE EXCISION REPAIR PROTEINS EXPRESSION (LEFT) AND QUANTITATIVE REAL TIME PCR (RT-QPCR) SHOWING MRNA EXPRESSION (RIGHT) IN BRCA1 DEFICIENT AND PROFICIENT BREAST CANCER CELL LINES. 114

FIGURE 3.16. QUANTIFICATION OF ATM AND DNA-PKCS PROTEIN (LEFT) AND QUANTITATIVE REAL TIME PCR (RT-QPCR) SHOWING MRNA EXPRESSION (RIGHT) IN BRCA1 DEFICIENT AND PROFICIENT HELA CELL LINES. 115
FIGURE 3.17. QUANTIFICATION OF ATM AND DNA-PKCS PROTEIN EXPRESSION (LEFT) AND QUANTITATIVE REAL TIME PCR (RT-QPCR) SHOWING MRNA EXPRESSION (RIGHT) IN BRCA1 DEFICIENT AND PROFICIENT BREAST CANCER CELL LINES. 116
FIGURE 3.18. MMS TREATMENT IN BRCA1 DEFICIENT AND PROFICIENT CELLS. 117
FIGURE 4.1. CLONOGENIC SURVIVAL ASSAY OF ATM INHIBITOR (KU55933). 131
FIGURE 4.2. CLONOGENIC SURVIVAL ASSAY OF INHIBITOR KU55933 (24 HOURS TREATMENT PROTOCOL). 132
FIGURE 4.3. MTS CELL GROWTH INHIBITION ASSAYS OF ATM INHIBITOR (KU55933). 133
FIGURE 4.4. CLONOGENIC SURVIVAL ASSAY OF ATM INHIBITOR (KU60019). 134
FIGURE 4.5. MTS CELL GROWTH INHIBITION ASSAYS OF PARP INHIBITOR (NU1025). 135
FIGURE 4.6. CLONOGENIC SURVIVAL ASSAY OF PARP INHIBITOR (3-AMINOBENZAMIDE). 136
FIGURE 4.7. REPRESENTATIVE PHOTOMICROGRAPHIC OF IMMUNOFLUORESCENCE MICROSCOPY ASSAY FOLLOWING KU55933 TREATMENT FOR 24 HOURS AND 48 HOURS. 137
FIGURE 4.8. REPRESENTATIVE PHOTOMICROGRAPHIC OF IMMUNOFLUORESCENCE MICROSCOPY ASSAY FOLLOWING KU55933 TREATMENT 5 μM AND 10 μM FOR 48 HOURS. 138
FIGURE 4.9. IMMUNOFLUORESCENCE MICROSCOPY STAINING FOR ΓH2AX FOCI FORMATION FOLLOWING KU55933 TREATMENT FOR 48 HOURS. 139
FIGURE 4.10. IMMUNOFLUORESCENCE MICROSCOPY STAINING FOR ΓH2AX FOCI FORMATION FOLLOWING KU60019 TREATMENT FOR 48 HOURS. 140
FIGURE 4.11. REPRESENTATIVE GRAPHS OF FLOW CYTOMETRIC CELL CYCLE ANALYSIS FOLLOWING KU55933 TREATMENT. 142
FIGURE 4.12. FLOW CYTOMETRIC CELL CYCLE ANALYSIS FOLLOWING KU55933 TREATMENT FOR 48 HOURS. 143
FIGURE 4.13. FLOW CYTOMETRIC CELL CYCLE ANALYSIS FOLLOWING KU60019 TREATMENT FOR 48 HOURS. 144
FIGURE 4.14. REPRESENTATIVE GRAPHS OF FLOW CYTOMETRY IMAGES FOR APOPTOSIS ASSAY FOLLOWING KU55933 TREATMENT. 146
FIGURE 4.15. APOPTOSIS DETECTION BY ANNEXIN V-FITC FLOW CYTOMETRY IN KU55933 TREATED CELLS. 147
FIGURE 4.16. APOPTOSIS DETECTION BY ANNEXIN V-FITC FLOW CYTOMETRY IN KU60019 TREATED CELLS. 148
FIGURE 4.17. PROPOSED MODEL OF SYNTHETIC LETHALITY BETWEEN ATM INHIBITORS AND BRCA1-BER DEFICIENT SYSTEM. 155

FIGURE 5.1. CLONOGENIC SURVIVAL ASSAY OF DNA-PKCS INHIBITOR (NU7441). 160
FIGURE 5.2. CLONOGENIC SURVIVAL ASSAY OF INHIBITOR NU7441 (24 HOUR TREATMENT PROTOCOL). 161
FIGURE 5.3. MTS CELL GROWTH INHIBITION ASSAYS OF DNA-PKCS INHIBITOR (NU7441). 162
FIGURE 5.4. CLONOGENIC SURVIVAL ASSAY OF DNA-PKCS INHIBITOR (NU7026). 163
FIGURE 5.5. IMMUNOFLUORESCENCE MICROSCOPY STAINING FOR ΓH2AX FOCI FORMATION FOLLOWING NU7441 TREATMENT FOR 48 HOURS. 165
FIGURE 5.6. IMMUNOFLUORESCENCE MICROSCOPY STAINING FOR ΓH2AX FOCI FORMATION FOLLOWING NU7026 TREATMENT FOR 48 HOURS. 166
FIGURE 5.7. REPRESENTATIVE GRAPHS OF FLOW CYTOMETRIC CELL CYCLE ANALYSIS FOLLOWING NU7441 TREATMENT. 167
FIGURE 5.8. FLOW CYTOMETRIC CELL CYCLE ANALYSIS FOLLOWING NU7441 TREATMENT FOR 48 HOURS. 168
FIGURE 5.9. FLOW CYTOMETRIC CELL CYCLE ANALYSIS FOLLOWING NU7026 TREATMENT FOR 48 HOURS. 169
FIGURE 5.10. APOPTOSIS DETECTION BY ANNEXIN V-FITC FLOW CYTOMETRY IN NU7441 TREATED CELLS. 171
FIGURE 5.11. APOPTOSIS DETECTION BY ANNEXIN V-FITC FLOW CYTOMETRY IN NU7026 TREATED CELLS. 172
FIGURE 5.12. PROPOSED MODEL OF SYNTHETIC LETHALITY BETWEEN DNA-PKCS INHIBITORS AND BRCA1-BER DEFICIENT SYSTEM. 178
FIGURE 6.1. CLONOGENIC SURVIVAL ASSAY OF CISPLATIN. 182
FIGURE 6.2. CLONOGENIC SURVIVAL ASSAY OF ATM INHIBITOR (KU55933) IN COMBINATION WITH CISPLATIN. 184
FIGURE 6.3. CLONOGENIC SURVIVAL ASSAY OF DNA-PKCS INHIBITOR (NU7441) IN COMBINATION WITH CISPLATIN. 185
FIGURE 6.4. IMMUNOFLUORESCENCE MICROSCOPY STAINING FOR ΓH2AX FOCI FORMATION FOLLOWING ATM INHIBITOR (KU55933) IN COMBINATION WITH CISPLATIN FOR 48 HOURS EXPOSURE. 187
FIGURE 6.5. IMMUNOFLUORESCENCE MICROSCOPY STAINING FOR ΓH2AX FOCI FORMATION FOLLOWING DNA-PKCS INHIBITOR (NU7441) IN COMBINATION WITH CISPLATIN FOR 48 HOURS EXPOSURE. 189
FIGURE 6.6. FLOW CYTOMETRIC CELL CYCLE ANALYSIS FOLLOWING ATM INHIBITOR (KU55933) IN COMBINATION WITH CISPLATIN 191
FIGURE 6.7. FLOW CYTOMETRIC CELL CYCLE ANALYSIS FOLLOWING DNA-PKCS INHIBITOR (NU7441) IN COMBINATION WITH CISPLATIN 192

FIGURE 6.8. APOPTOSIS DETECTION BY ANNEXIN V-FITC FLOW CYTOMETRY IN RESPONSE TO ATM INHIBITOR (KU55933) IN COMBINATION WITH CISPLATIN 195
FIGURE 6.9. APOPTOSIS DETECTION BY ANNEXIN V-FITC FLOW CYTOMETRY IN RESPONSE TO DNA-PKCS INHIBITOR (NU7441) IN COMBINATION WITH CISPLATIN 196
FIGURE 6.10. WORKING MODEL FOR CISPLATIN AND ATM OR DNA-PKCS INHIBITOR AS A SYNTHETIC LETHALITY STRATEGY IN BRCA1-BER DEFICIENT CELLS. 201

List of Tables

TABLE 2.1. REACTION MIX FOR RT² PROFILER™ DNA REPAIR PCR ARRAY.....76
TABLE 2.2. REACTION MIX FOR QUANTITATIVE REAL TIME PCR (RT-QPCR).....77
TABLE 2.3. QUANTITECT® PRIMERS USED IN RT-QPCR ANALYSIS. 78
TABLE 2.4. PRIMARY ANTIBODIES USED IN WESTERN BLOT. 82
TABLE 3.1. BRCA1 MUTATIONS IN BREAST CANCER CELL LINES. 85
TABLE 3.2. BREAST CANCER CELL LINES USED IN THIS PROJECT.....88
TABLE 3.3. BASE EXCISION REPAIR GENES UNDER-EXPRESSED IN BRCA1 DEFICIENT CELL LINES COMPARED TO BRCA1 PROFICIENT CELL LINES. 103
TABLE 3.4. HOMOLOGOUS RECOMBINATION GENES UNDER-EXPRESSED IN BRCA1 DEFICIENT CELL LINES COMPARED TO BRCA1 PROFICIENT CELL LINES.....104
TABLE 3.5. NON-HOMOLOGOUS END JOINING GENES UNDER-EXPRESSED IN BRCA1 DEFICIENT CELL LINES COMPARED TO BRCA1 PROFICIENT CELL LINES.....104
TABLE 3.6. NUCLEOTIDE EXCISION REPAIR GENES UNDER-EXPRESSED IN BRCA1 DEFICIENT CELL LINES COMPARED TO BRCA1 PROFICIENT CELL LINES.....105
TABLE 3.7. MISMATCH REPAIR GENES UNDER-EXPRESSED IN BRCA1 DEFICIENT CELL LINES COMPARED TO BRCA1 PROFICIENT CELL LINES. 106
TABLE 3.8. QUANTITATIVE REAL TIME PCR (RT-QPCR) FOR MULTIPLE DNA REPAIR GENES IN BRCA1 DEFICIENT CELLS.....109
TABLE 3.9. QUANTITATIVE REAL TIME PCR (RT-QPCR) FOR MULTIPLE DNA REPAIR GENES IN BRCA1 DEFICIENT CELLS.....109

Chapter 1

Background

1. Introduction

Cancer is a class of complex diseases caused by genetic, epigenetic or translational changes that force the transformation of normal cells into malignant cells (Baylin and Jones, 2011). The major limitations of existing anticancer agents are that their efficacy is restricted by specificity, toxicity and the development of drug resistance. The search for new targeted, less toxic treatments and methods to improve the specificity and effectiveness of existing therapies is a major focus of cancer research.

In the early 1900s, Paul Ehrlich (German chemist) defined “Chemotherapy” as the use of chemicals to treat disease; he was also the first to use animal models successfully in screening a series of chemicals for their potential activity against diseases. Ehrlich's accomplishment remains the cornerstone in cancer drug development (DeVita and Chu, 2008). Since then cancer research has produced a complex and rich foundation of information which has revealed that cancer is a disease involving dynamic changes in the genome. To provide an overview of the complex biological data about cancer, researchers identify six essential features to transform normal cells into cancer cells. These features were referred to as “Hallmarks of cancer” by Hanahan and Weinberg (shown in Figure 1.1), and include; sustaining growth signals, insensitivity to antigrowth signals, resisting cell death, limitless replicative potential, inducing angiogenesis, activating invasion and metastasis (Hanahan and Weinberg, 2000).

Almost ten years after that and with an increasing body of research, Hanahan and Weinberg suggested two additional hallmarks and two enabling characteristics. The new emerging hallmarks are; deregulating cellular energetics and avoiding immune destruction, while tumor-promoting inflammation and genome instability and mutation are enabling characteristics (Hanahan and Weinberg, 2011).

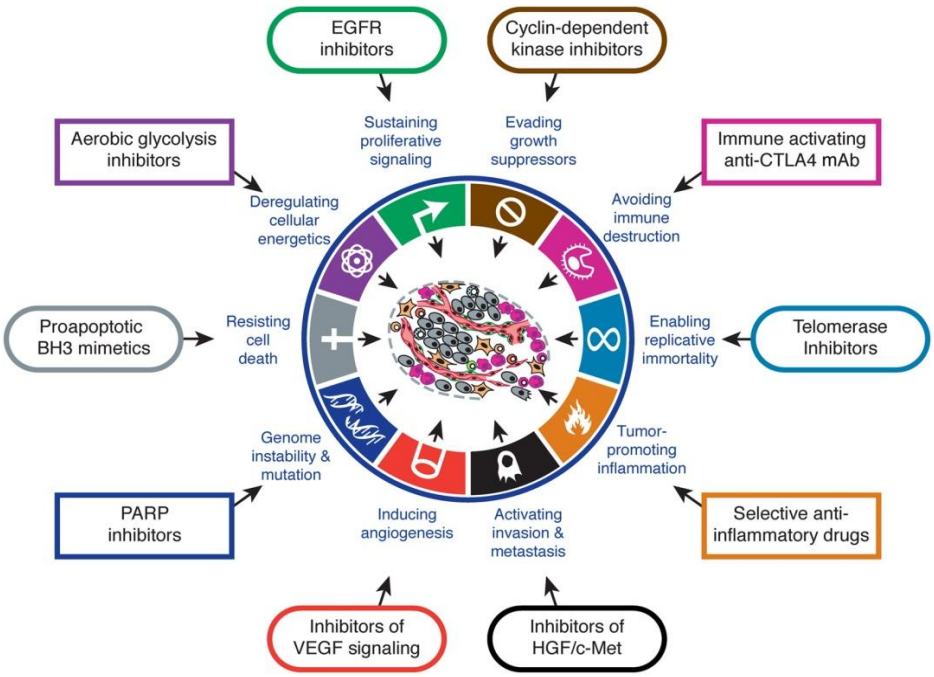

Figure 1.1. Therapeutic Targeting of the Hallmarks of Cancer.

Each 'characteristic' can be targeted with a class of drug which is either in clinical trials or in some cases approved for clinical use in treating certain forms of human cancer. Adapted from (Hanahan and Weinberg, 2011). Copyright© 2011 by Elsevier with permission conveyed through Copyright Clearance Center Inc.

Genomic instability and mutation are described as "Enabling Characteristics" as cells develop new ways to use different DNA repair pathways and damage signalling to avoid cell death. One novel approach in the treatment of cancer is

to potentiate the effect of the chemotherapy drug in damaging the DNA by targeting DNA repair mechanisms responsible for repairing this damage. In other words, this field is interested in combining a DNA repair inhibitor with the right DNA damaging agent.

One such novel target is Poly (ADP-ribose) polymerase 1 (PARP1). PARP1 is an enzyme that plays an essential role in single strand break repair (SSBR), a pathway that is related to the base excision repair (BER) pathway. Inhibition of SSBR pathway is associated with accumulation of SSBs; without repair the SSB would be converted to a double strand break (DSB) lesion during DNA replication (Dantzer et al., 2000, Hoeijmakers, 2001, Schreiber et al., 2006).

In 2005, two Nature papers reported that cells deficient in the Breast Cancer Susceptibility genes *BRCA1* and *BRCA2* were 100 to 1000 fold more sensitive to PARP inhibition than BRCA heterozygote or wild type control cell lines (Bryant et al., 2005, Farmer et al., 2005). Both of these studies were reported independently by two groups using deficient models of BRCA1 and BRCA2 with different PARP inhibitors, which provide evidence that this sensitivity in BRCA mutant cells was due to PARP inhibition. The hypothesis was that with the mutation in *BRCA* genes cells are defective in the Homologous Recombination (HR) pathway and targeting PARP will inactivate the SSBR pathway inducing 'Synthetic Lethality'.

'Synthetic Lethality' is the process by which cancer cells are selectively targeted by the inactivation of two or more genes or pathways that causes cell death, whereas inactivation in only one of them is not lethal (Kaelin, 2005, Ashworth, 2008). Since then several studies have been conducted to investigate this hypothesis. Now there is evidence that cells with defects in the

HR pathway, or where the *BRCA* gene is silenced by epigenetic changes, are sensitive to PARP inhibitors (Ashworth, 2008), widening the therapeutic potential for these agents.

Chapter one of this thesis sets out to provide the background information on DNA damage and repair pathways in mammalian cells, where mechanism of both base excision repair (BER) and double strand break (DSB) repair will be studied in some detail. Following that the progress to date in the development of inhibitors for DSB repair, and the biological role of ATM and DNA-PKcs will be presented. Understanding the concept of "synthetic lethality" between BRCA and PARP in the treatment of cancers defective in HR DNA repair will follow. Finally, alternative synthetic lethality targets will be investigated.

1.1.DNA damage

DNA is under constant attack from various destructive agents including endogenous, as well as exogenous sources summarised in Figure 1.2. Endogenous damage may result from spontaneous base loss or various types of base modification (for instance; cytosine deamination, converting it to uracil) caused by exposure to metabolic products such as reactive oxygen species, or mispairing errors introduced during replication (Lindahl, 1993, Gates, 2009). Exogenous damage has many sources including; UV light, X-rays or gamma radiation, thermal disruption or chemical exposure. DNA damage types can be broadly subdivided into base damage and backbone damage (Hoeijmakers, 2001).

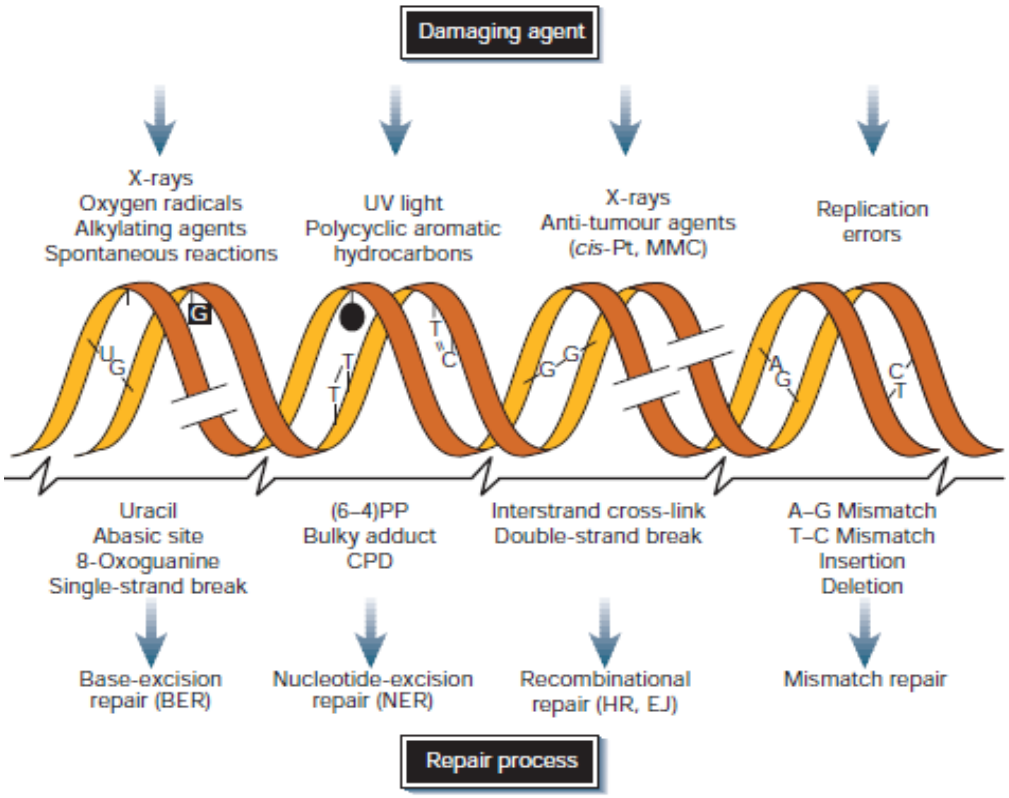

Figure 1.2. Sources causing DNA damage and corresponding repair pathway.

Specific DNA damage is categorized by possible endogenous or exogenous sources and the corresponding DNA repair pathway for each type of damage. Adapted from (Hoeijmakers, 2001). Copyright© 2001 by Nature Publishing Group with permission conveyed through Copyright Clearance Center Inc.

1.1.1. Base damage

Deamination

Cytosine residues in DNA can undergo hydrolytic deamination converting them to uracil residues. Up to 500 deamination of cytosine events take place in human cells per day. Other deamination reactions include conversion of adenine to hypoxanthine, 5-methylcytosine to thymine and guanine to xanthine

(Lindahl, 1993). Hydrolysis of the glycosidic bonds holding a base to the DNA backbone is also common (Gates, 2009).

Oxidation

One of the causes of DNA base damage is exposure to reactive oxygen species generated during either normal cellular oxygen metabolism, from exposure to UV light or a wide range of other exogenous sources. A frequent oxidative lesion is 8-hydroxyguanine (8-oxoG); this mutagenic lesion shows preference to pair with adenine rather than cytosine during replication. This lesion is estimated to occur at a rate of up to 500 events per day, the same rate as cytosine deamination (Tudek et al., 2003, Gates, 2009).

Alkylation

Another source of DNA base damage is where an alkyl group attaches to the DNA base giving alkylation products such as O^2-alkylthymine, O^4-alkylthymine, O^6-methylguanine and O^6- ethylguanine. This binding may prevent DNA replication causing mutation or cell death. Alkylation can be generated by both endogenous sources (for instance; oxidative by-product or cellular methyl donors such as *S*-adenosylmethionine) and exogenous sources (fuel combustion, tobacco exposure or anticancer therapies e.g. cisplatin) (Engelbergs et al., 2000, Fu et al., 2012).

1.1.2. Backbone damage

The DNA backbone is under constant exposure to environmental and endogenous agents that create thousands of lesions per cell each day (Lindahl,

1993). While some of these lesions like abasic sites or SSB are considered to be toxic, DSB are considered to be the most harmful. There are three major classes of DSB structures that can be toxic if not repaired.

(1) Two-ended DNA double-strand break, created by direct fracture of a DNA duplex. (2) One-ended DNA double-strand break, created when a replication fork encounters a DNA single-strand break. (3) Daughter strand gap, created when lagging or leading strand progression is inhibited by a DNA lesion (Helleday et al., 2007).

1.2.DNA repair

The accurate and efficient repair of DNA damage is essential for normal cellular function and maintenance of genomic stability (Figure 1.2) (Hoeijmakers, 2001). Genomic instability in cancer cells is often related to deficiency in one or more of the DNA repair pathways, which can account for the development of a more malignant phenotype (Hoeijmakers, 2009).

Cells have two strategies to use for damage recognition and to initiate DNA damage responses. Direct recognition is the simplest form of repair (one step) where particular DNA damage can be repaired by cognate proteins (usually an enzyme). The second DNA damage response is multi-step recognition, where several proteins are involved and each one has a particular job to do, starting from recognition of the damage and ending with sealing the new DNA strand. DNA repair pathways can be divided into five categories; direct repair, base excision repair (BER), nucleotide excision repair (NER), mismatch repair (MMR) and double strand break repair (DSB) which includes, homologous

recombination (HR) and non homologous end joining (NHEJ) pathways (Sancar et al., 2004).

1.2.1. DNA repair pathways

1.2.1.1. Direct repair

Several mechanisms exist to directly reverse certain DNA damaging lesions, for instance direct reversal of the O^6-methyl group from O^6-methylguanine (O^6-MeGua) by Methylguanine DNA Methyltransferase (MGMT). MGMT is a small enzyme of 20 kDa which forms a low stable complex with the DNA backbone at the damage site. It was believed that the enzyme flips-out the O^6-MeGua base and the methyl group is transferred to an active site cysteine. However, O^6-MeGua if not repaired can cause errors by mispairing with thymine during replication, causing G:C to A:T transitions or a strand break (Lindahl et al., 1988, Sancar et al., 2004, Luo et al., 2010).

1.2.1.2. Base excision repair

BER is a complex pathway responsible for accurate removal of DNA bases that have been damaged by alkylation or oxidation, along with a variety of other lesions including base deamination and single strand breaks that could otherwise cause mutations during replication. BER in mammalian cells consists of two major sub-pathways that differ from each other in the length of the region they repair and in the subsets of enzymes involved (Figure 1.3). The short patch repair (SP-BER) pathway replaces single nucleotides, whereas the

long patch repair (LP-BER) pathway replaces 2-10 nucleotides. Initiation of BER is thought to be by the DNA glycosylase family proteins, which remove the damaged base creating an abasic site (apurinic/apyrimidinic, AP site). Apurinic/apyrimidinic endonuclease 1 (APE1) then cleaves the phosphodiester bond 5' to the AP site leaving a nick with 5'deoxyribose-5-phosphate (5'dRP) and 3'-hydroxyl group (3'OH). The second step of BER is adding the first nucleotide to the 3'-end of the AP site and removing the 5' terminal sugar residue (by the process of β-elimination) by DNA polymerase β (Pol β). Normally, this reaction continues through the SP-BER sub-pathway where DNA Ligase 3 and X-ray repair cross complementing gene 1 (XRCC1) complex then complete the repair.

On the other hand, when the 5'-end is resistant to β-elimination the repair process proceeds through the LP-BER sub-pathway. In this sub-pathway, replication factor C (RF-C) recruits proliferating cell nuclear antigen (PCNA) onto the AP site. PCNA acts as a DNA sliding clamp for the DNA polymerase δ and ε (Poly δ/ε) which performs DNA synthesis to remove the 5' terminal sugar residue as part of a flap. As an alternative, Pol β and Rad9-Rad1-Hus1 complex (9-1-1) was found to have a similar structure as PCNA. The flap is then removed by flap endonuclease (FEN1) and DNA Ligase 1 completes LP-BER sub-pathway by ligating the DNA ends (Fortini and Dogliotti, 2007, Hegde et al., 2008, Abbotts and Madhusudan, 2010, Balakrishnan et al., 2009).

Poly(ADP-ribose) polymerases (PARPs) have been suggested to be involved in the regulation of the BER process, by binding to the AP site until the appropriate enzyme becomes available to process the repair (Khodyreva et

al., 2010, Yelamos et al., 2011). Once PARP1 is activated it catalyses the successive transfer of ADP-ribose units from the substrate nicotinamide adenine dinucleotide (NAD+) to a variety of acceptor nuclear proteins. This automodification attracts other DNA damage repair enzymes to the site such as, Pol ß, Ligase 3 and XRCC1 (Schreiber et al., 2006, Megnin-Chanet et al., 2010). However, PARP1 does not play a major role in catalysis of DNA damage processing via either base excision repair pathway (Allinson et al., 2003, Strom et al., 2011).

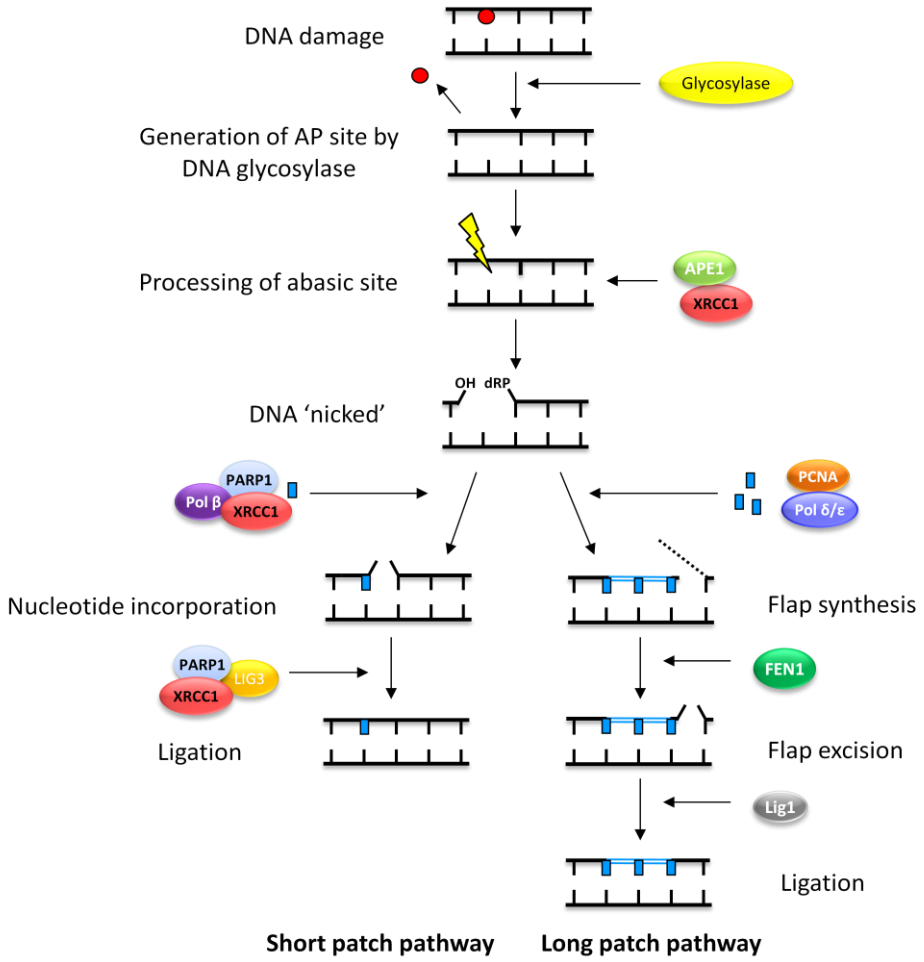

Figure 1.3. Base Excision Repair (BER) pathway.

A damaged base is removed by a DNA glycosylase to generate an AP site. The repair patch may be a single nucleotide repair short patch (SP-BER) or a 2–10 nucleotide long patch (LP-BER). When the base damage is removed by one of the glycosylase family, APE1 (apurinic/apyrimidinic endonuclease 1) cleaves the 5' bond to the site and recruits DNA polymerase (Pol β-δ-ε) to fill in the gap that is ligated by Ligase 3 (Lig3) /XRCC1 (X-ray cross-complementing protein 1) complex. When the AP site is generated by hydrolytic glycosylases, or by spontaneous hydrolysis, repair usually proceeds through the LP-BER sub-pathway. APE1 cleaves the 5' phosphodiester bond, and the RF-C/PCNA-Poly complex carries out repair synthesis and nick translation, displacing several nucleotides. The flap structure is cleaved off by FEN1 (flap endonuclease) and the LP-BER is ligated by Ligase 1. PARP1/ poly(ADP-ribose) polymerase 1; PCNA/ proliferating cell nuclear antigen; OH/ hydroxyl group; dRP/ deoxyribose phosphate. Adapted from (Abbotts and Madhusudan, 2010).

1.2.1.3. Nucleotide excision repair

Nucleotide excision repair (NER) recognises and repairs base lesions associated with DNA helical distortion, including these produced by UV light or platinum chemotherapy. More than 25 proteins/complexes have been identified in eukaryotic cells which are required to complete NER. This pathway can be divided into two main sub pathways; global genome repair (GGR) and transcription-coupled repair (TCR), depending on the complexes that initiate repair. TCR removes lesions from the transcribed DNA strand of transcriptionally active genes when encountered by RNA polymerase II, restoring transcriptional activity and preventing apoptosis. GGR performs this process with poor efficiency, instead removing lesions on non-transcribed strands and transcriptionally inert genes to avoid replication fork stalling and chromosomal breakages. The key event in this pathway is incision of the damaged strand from each side of a lesion, releasing up to 32 nucleotides of the damaged DNA strand (Wood, 1997, Sugasawa, 2010).

The clinical consequences of defective NER are demonstrated by three syndromes associated with defects of NER proteins; xeroderma pigmentosum (XP), cockayne syndrome (CS) and the photosensitive form of trichothiodystrophy (TTD). Individuals with inherited XP syndrome exhibit severe sun-sensitivity, freckling and a 1000-fold increase in skin cancer including squamous and basal cell cancers as well as melanomas. Mutations in XP genes (*XPA*, *XPB*, *XPC*, *XPD*, *XPE*, *XPF* or *XPG*) can be identified in these patients. 20% of all XP patients, those with more than one mutation in XP genes, exhibit neurological abnormalities in addition to their XP symptoms. These symptoms include deafness, speach and walking disability

because of primary neuronal degradation. CS patients with mutation in *CSA* and *CSB* genes may exhibit sun-sensitivity and skin cancer though less than XP patients. CS symptoms include growth retardation, cachexia, neurological and mental developmental delays, cataracts, retinopathy, deafness, dental caries, and characteristic facies with a thin face, flat cheeks, and prominent tapering nose. TTD patients with mutations in *TTD-A*, *XPB* and *XPD* genes also show sun-sensitivity though no increased skin cancer risk. TTD symptoms are erythema, ichthyosis-like skin changes, nail and other neuroectodermal dysplasias, and short, brittle sulphur-deficient hair (Robbins et al., 1991, Thoms et al., 2007, Kraemer et al., 2007).

1.2.1.4. Mismatch repair

Mismatch repair (MMR) is the main pathway that recognises and repairs lesions/errors introduced during DNA replication. This pathway is initiated when a complex of MSH2 and MSH6 recognizes the mismatch. A range of combinations of MSH2 and either MSH6 or MSH3 are formed, which specify the type of mismatch recognized. After that, MSH proteins recruit MLH1 and its binding partners, post–meiotic-segregation increased 1 (PMS1) protein and post–meiotic-segregation increased 2 (PMS2) protein. An exonuclease removes the DNA lesion, a DNA polymerase synthesizes a new strand, and finally, a DNA Ligase completes the repair. A defect in MMR brings on a mutator phenotype, which causes a predisposition to cancer. MMR status also affects meiotic and mitotic recombination, DNA damage signalling and apoptosis (Jiricny, 2006, Li, 2008, Modrich and Lahue, 1996).

MMR deficiency is associated with three diseases, Hereditary Nonpolyposis Colorectal Cancer (HNPCC) syndrome, Muir – Torre syndrome, and Turcot syndrome. HNPCC patients often develop colon cancer and other visceral tumours such as endometrial, ovarian, stomach, kidney, and small intestinal cancers. In 80% of all HNPCC patients mutations in the *hMLH1*, *hMSH2*, *hMSH6*, and *hPMS2* MMR genes can be identified. Muir – Torre syndrome patients present with sebaceous carcinomas, colon cancer, and other visceral tumours such as endometrial, ovarian, stomach, kidney, and small intestinal cancers. Mutations in *hMSH1* and *hMSH2* genes can be identified in these patients. Turcot syndrome is caused by mutations in *hMSH1* and *hPMS2* genes. Turcot syndrome is associated with gliomas, lymphomas, colon cancer and other visceral tumours such as endometrial, ovarian, stomach, kidney, and small intestinal cancers (Peltomaki, 2003, Chung and Rustgi, 2003, Thoms et al., 2007).

1.2.1.5. Double strand break repair

DNA double strand breaks (DSBs) are the most lethal class of damage in DNA. DSBs, if left unrepaired or inappropriately repaired, can lead to cell death or to a variety of genetic mutations, translocations and chromosome loss (Hoeijmakers, 2001). This kind of lesion could be generated directly, following exposure to ionizing radiation, or indirectly during the processing of other DNA adducts or at stalled replication forks. DSB damage is repaired by one of the DSB repair sub-pathways illustrated in Figure 1.4, homologous recombination (HR) which is error-free or Non-homologous end joining (NHEJ) which is error-prone. The balance between these two sub pathways

differs between cell types of a single species and also differs between different cell cycle phases within a single cell type (O'Driscoll and Jeggo, 2006, Brandsma and Gent, 2012). In addition to classical HR and NHEJ there is an alternative DSB repair pathway:

Single Strand Annealing (SSA) pathway is activated when HR or NHEJ pathways cannot complete the repair. After resection of the break complementary stretches in the single strand DNA anneal, followed by the deletion of the intervening sequence and one of the repeat sequences. Some researchers categorize this pathway as an alternative for HR and others for NHEJ (Ivanov et al., 1996, Gottlich et al., 1998, Stark et al., 2004, Brandsma and Gent, 2012).

Microhomology-mediated end joining (MMEJ) is a subset of Alternative Non-homologous end joining (A-NHEJ). Repair by this pathway starts by resection of the 5' – 3' by MRN complex and then RPA binds to the DNA strand ends for protection. Where microhomologous regions are uncovered the DNA overhangs anneal, followed by DNA polymerase filling the gap and DNA Ligase sealing the strand. MMEJ is always associated with DNA deletions (McVey and Lee, 2008).

Alternative Non-homologous end joining (A-NHEJ) is an error prone pathway considered as a major source of genetic instability. Like SSA, A-NHEJ is thought to be activated when HR or NHEJ pathways cannot complete the repair. This pathway is not fully understood yet, however several proteins have been found to play a role in A-NHEJ including; PARP1, MRN complex, Ligase 3, Ligase 1 and XRCC1 (Brandsma and Gent, 2012, Dueva and Iliakis, 2013).

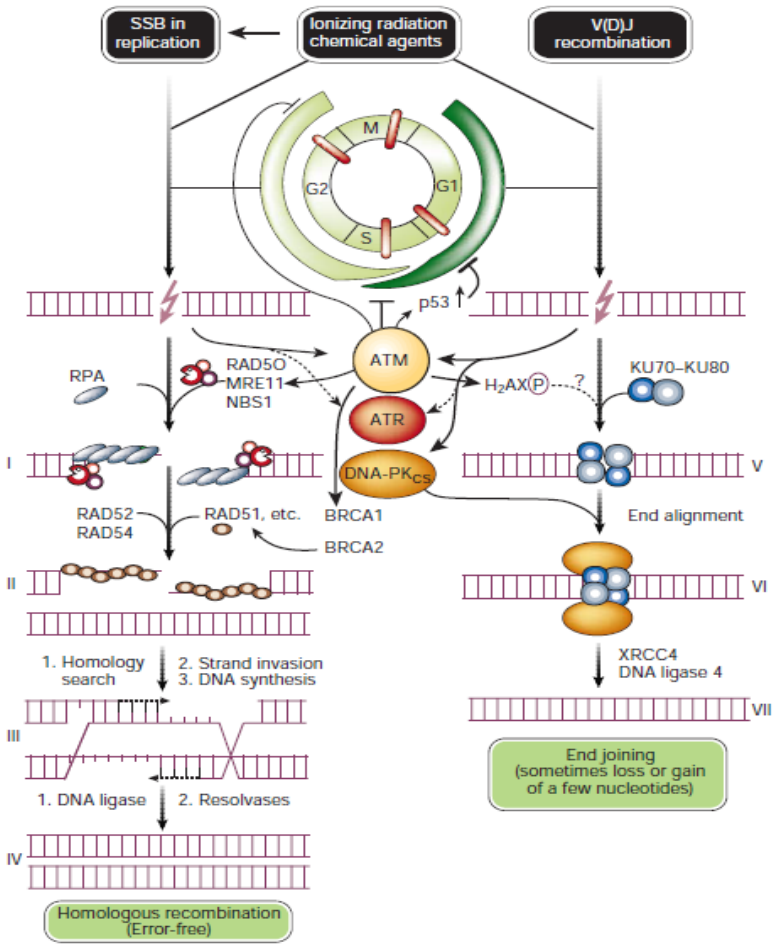

Figure 1.4. Double Strand Break (DSB) repair pathway.

Homologous recombination (HR): (I) Following DSB, MRN complex and Rad51 localises to DSB via BRCA2. (II) Rad51 and related proteins assemble the pre-synaptic filament. (III) Rad51 and Rad54 identify homologous sequence of DNA and facilitate invasion into break site and new sequence of DNA is synthesised. (IV) Exchanged ends, (Holliday junctions), are rejoined by resolvases. **Non-Homologous end joining (NHEJ)**: (V) Heterodimer of Ku70/Ku80 binds to exposed DNA initiating NHEJ. (VI) The active protein kinase DNA-PK complex (Ku70/Ku80 + DNA-PKcs) brings the ends of DSB for processing prior to religation. (VII) MRN complex, FEN1 and Artemis remove excess DNA ends. New DNA is synthesised by a DNA polymerase and ligation occurs via XRCC4 and DNA Ligase 4. DSB = double strand break, MRN = Mre11-Rad50-NBS1, XRCC2/3/4 = X-ray cross complementation group 2/3/4, V(D)J = Variable, diversity and joining, BRCA1/2 = breast cancer susceptibility 1/2. Adapted from (Hoeijmakers, 2001), Copyright© 2001 by Nature Publishing Group with permission conveyed through Copyright Clearance Center Inc.

1.2.1.5.1. Homologous recombination

Homologous recombination (HR) pathway provides an error free repair of DSB. HR pathway takes place during late S phase and G2/M phase when homologous chromatids are available. HR involves multiple steps as presented in Figure 1.4, recognition of the DSB damage by the ataxia telangiectasia mutated (ATM) is the first sensor of DSB. ATM in turn activates multiple genes involved in HR repair, cell cycle arrest and apoptosis. Substrates for ATM phosphorylation include; BRCA1, p53, CHK2, histone H2AX and MRN complex (MRE11/RAD50/NBS1). The MRN complex then resects the DNA strand 5' to 3' generating 3'ends of single stranded DNA (ssDNA) on either side of the DSB (Bakkenist and Kastan, 2004). The resulting SSB ends are then coated by Replication Protein A (RPA) protein which in turn recruits other proteins (including; Rad17/Rfc2-5, Rad9/Hus1/Rad1 and ATR/ATRIP) which form foci at the damaged site. RAD52 proteins then replace RPA proteins forming a ring to protect the SSB from exonucleolytic digestion.

At this stage RAD52 competes with the KU complex of the NHEJ pathway and may determine sub-pathway selection between HR and NHEJ. RPA displacement is accomplished through the action of two proteins, BRCA1 and BRCA2. RAD51 and its related proteins (RAD51B, RAD51C, RAD51D, RAD54, XRCC2 and XRCC3) along with RPA, stimulate the activity of DNA strand exchange, with the complementary strand forming a heteroduplex while unpaired recipient DNA forms a D-loop. Conversely BRCA2 binds to RAD51, this complex binds to the exposed SSB and enables the loading of RAD51 to the SSB. Then DNA polymerases synthesize a new strand. The final step of the

HR repair is the sealing of the strands by DNA Ligase (Takata et al., 1998, Christmann et al., 2003, Li and Heyer, 2008).

1.2.1.5.2. Non-homologous end joining

The Non-homologous end joining (NHEJ) pathway is more commonly used for DSB repair by mammalian cells (Figure 1.4). NHEJ functions in all phases of cell cycle, especially in the G1 phase. It is an error-prone pathway as it does not rely on sister chromatids (homologous template) for repair. This results in short deletions or insertion of incorrect base pairs. After DSB induction, the first step towards repair through NHEJ is the binding of a heterodimeric complex consisting of the proteins KU70 and KU80 to the DNA damaged ends forming a ring shaped structure to protect the DNA from exonuclease digestion. Following DNA binding, the KU heterodimer recruits the catalytic subunit of the DNA dependent protein kinase (DNA-PKcs) thereby forming the active DNA-PK complex. DNA-PKcs is activated by interaction with a ssDNA at the site of DSB. In the following step, DNA-PKcs recruits XRCC4 which forms a stable complex with Ligase 4. The XRCC4/Ligase 4 complex binds to the ends of DNA molecules and brings both ends together with complementary but non- ligatable ends. This complex cannot directly re-ligate most of the DSBs before both ends are processed. Processing of DSBs is performed by the MRN complex, which has the role of removing the excess of DSB strands at the 3' flaps. While flap endonuclease 1 (FEN1) is responsible for removal of the 5' overhangs. Another protein involved in processing overhangs is the protein Artemis, which acts in a complex with DNA-PK.

Artemis acquires endonuclease activity, degrading single-strand overhangs and hairpins, which seems to be necessary for processing 5' and 3' overhangs during NHEJ. This pathway is sometimes associated with gain or loss of a few nucleotides if internal microhomologies are used for annealing before sealing. This implies the involvement of DNA polymerases or Artemis to create compatible ends. Finally, ligation is achieved by the actions of XRCC4/Ligase 4 complex (Takata et al., 1998, Christmann et al., 2003, Burma et al., 2006, Khanna and Jackson, 2001).

1.3. Ataxia telangiectasia mutated (ATM)

The *Ataxia Telangiectasia Mutated* (*ATM*) gene product was identified in 1995, based on its role in a rare, inherited disorder Ataxia Telangiectasia. The gene responsible for this disorder was mapped to chromosome 11q22-23. ATM protein is around 370 kDa and contains about 3056 amino acid residues. The 400 amino acids residues of its C-terminal region highly matched to the catalytic subunit of phosphatidylinositol-3 kinases (PI-3 kinases) (Savitsky et al., 1995, Rotman and Shiloh, 1998).

The catalytic site of ATM is within the C-terminal PI-3 domain, although it is believed that the rest of this large protein is responsible for receiving signals (working as a DNA damaging sensor) to regulate downstream targets. Several proteins interact with ATM including CHK2 and p53 (Rotman and Shiloh, 1998).

1.3.1. Role of ATM in the cellular response

ATM is a nuclear protein, the levels of which do not change when cells are exposed to ionizing radiation (IR). However, the protein kinase activity of ATM increases 2 to 3 fold following cellular exposure to IR, as determined by immunoprecipitation kinase assays (Canman et al., 1998, Banin et al., 1998, Chan et al., 1998). Bakkenist *et al* demonstrated that ATM containing a serine to alanine mutation at amino acid 1981 failed to support IR-induced phosphorylation of p53 or cell cycle arrest, suggesting that serine 1981 phosphorylation is critical for the function of ATM. Moreover, serine 1981-phosphorylated ATM localizes to nuclear foci in response to DNA damage (Bakkenist and Kastan, 2003).

The ATM signalling pathway is activated following DSBs. ATM is recruited to the damaged sites, however it is not clear if ATM interacts with damaged DNA directly or indirectly.

It was previously thought that ATM activation primarily requires direct binding to MRN complex. However recent studies has shown that PARP1 may control ATM phosphorylation and mediates the earliest recruitment of MRE11 and NBS1 to DNA damage (Rupnik et al., 2008, Haince et al., 2008, Haince et al., 2007).

Once ATM is activated, it may be released from the site of the DSB, enabling phosphorylation of several downstream substrates, such as chromatin bound histone H2AX and BRCA1 which lead to a variety of effects on DNA repair, cell cycle and apoptosis (Kurz and Lees-Miller, 2004). H2AX gets phosphorylated immediately after DNA damage by ATM on its C-terminal

serine residue 139 and is referred to as (γH2AX) forming foci, which can be observed by using immunofluorescence (Rogakou et al., 1999). In 2001 Burma *et al* showed that once ATM is activated at a DSB, it immediately activates γH2AX at the damaged site. This very early event could then initiate the recruitment of several DNA repair proteins (Burma et al., 2001). In terms of its role in cell cycle regulation, ATM interacts with a number of downstream substrates including proteins that activate the G1 (p53 and Nbs1), S (CHK2, BRCA1 and MRN) or G2/M (CHK1, CHK2 and Rad17) checkpoints. Activation of ATM-dependent cell cycle checkpoints would be expected to allow DNA repair, thereby enabling cells to survive. Studies proposed that considerable cross-talk exists between different ATM substrates and that several of them act in more than one cellular processes (Kurz and Lees-Miller, 2004).

Since ATM functions at the centre of a signalling network that controls different cellular responses, modulation of ATM function has become an area of interest for the treatment of cancer. Studies illustrated that ATM signalling pathways can be targeted in several ways to treat cancer. For instance, inhibition of ATM by the small molecule inhibitor (KU55933) increases the cytotoxicity of chemotherapeutic agents and IR in breast, colon and lung carcinoma cell lines (Crescenzi et al., 2008). Similarly, targeting p53 mutated cancer cells by inhibiting ATM increases cytotoxicity compared with proficient p53 cell lines (Smith et al., 2010).

1.4.DNA dependent protein kinase catalytic subunit (DNA-PKcs)

The DNA-dependent protein kinase (DNA-PK) holoenzyme consists of two subunits: the first component is the heterodimer complex KU, comprising of two enzymes KU70 (approximately 70 kDa) and KU80 (80 kDa). The second component of DNA-PK is a large polypeptide that corresponds to DNA-PK catalytic subunit (DNA-PKcs) (Hartley et al., 1995). The *DNA-PKcs* gene was mapped to chromosome 8q11 (Connelly et al., 1998). DNA-PKcs protein is around 460 kDa with approximately 3500 amino acid residues. The carboxy-terminal end of DNA-PKcs consists of 380 amino acid residues that fall into the phosphatidylinositol-3 kinase (PI-3 kinase) superfamily (Poltoratsky et al., 1995, Hartley et al., 1995, Kurimasa et al., 1999).

1.4.1. Role of DNA-PKcs in the cellular response

DNA-PKcs is a nuclear protein and recruitment to the DSB results in translocation of the heterodimer KU inward on the dsDNA allowing DNA-PKcs to directly interact with DSB ends (Yoo and Dynan, 1999, Calsou et al., 1999). DNA-PKcs was found to have unlimited kinase activity in the absence of KU heterodimer and DNA DSBs (Hammarsten and Chu, 1998, West et al., 1998). The kinase activity of DNA-PKcs is essential for NHEJ and the DNA damage response. DNA-PKcs can phosphorylate several nuclear proteins including KU heterodimer (Chan et al., 1999), XRCC4 (Leber et al., 1998), Ligase 4 (Wang et al., 2004), Artemis (Weterings and Chen, 2008), H2AX (Stiff et al., 2004) and p53 (Shieh et al., 1997). Recently it was found that

DNA-PKcs phosphorylates NHEJ Werner syndrome protein (WRN) that is required for efficient DSB repair (Kusumoto-Matsuo et al., 2014).

Following induction of a DSB, DNA-PKcs is phosphorylated at more than 40 sites. The best characterized DNA-PKcs phosphorylation cluster is the threonine 2609. Phosphorylation of threonine 2609 cluster is important for NHEJ. Recently Zhang *et al* demonstrated that knock-in mutant mice with human *DNA-PKcs* lacking a functional threonine 2609 are highly sensitive to replication stress agents which confer early lethality. In addition, the threonine 2609 phosphorylation cluster has been found to associate with other DNA repair proteins. For example, DNA-PKcs phosphorylation at the threonine 2609 is important for the coordination between ATM and Artemis in DNA DSB repair (Zhang et al., 2011, Davis et al., 2014a).

Regarding DNA-PKcs phosphorylations role in DNA repair, it is proposed that DNA-PK holoenzyme functions as a scaffolding protein to bring the broken DNA ends together and assists in the localisation of repair factors (Davis et al., 2014a). Moreover, DNA-PKcs phosphorylation has a role in regulation of cell cycle arrest in response to DSB. Chen *et al.*'s illustrated that DNA-PKcs functions primarily in the G1 phase (Chen et al., 2005). Conversely, DNA-PKcs plays a direct role in the suppression of apoptosis. Le Romancer *et al* demonstrated that cleavage and inactivation of DNA-PK during apoptosis is expected to switch off the function of kinase in DNA repair. In mammalian cells, loss of DNA-PK due to mutations increases sensitivity to treatments that induce DSBs (Le Romancer et al., 1996).

1.5. The development of ATM and DNA-PKcs inhibitors

To date, several DSB repair inhibitors have been described. **Wortmannin** is a non-specific inhibitor of PI-3 kinase. It is known to block ATM as well as DNA-PKcs (Rosenzweig et al., 1997). In 2004, the first small molecule to target ATM kinase **KU55933** (2-morpholin-4-yl-6- thianthren-1-yl-pyran-4-one) was developed. KU55933 potentiates the cytotoxicity of IR and chemotherapeutic agents in cell lines (Hickson et al., 2004). In 2008 **CP466722**, a specific inhibitor of ATM [2-(6, 7-dimethoxyquinazolin-4-yl)-5-(pyridin- 2-yl)-2H-1, 2, 4-triazol-3-amine], was identified. CP466722 inhibited ATM dependent phosphorylation events and resulted in G2/M cell cycle arrest. CP466722 shows similarity to KU55933 inhibitor in rapidly and potently inhibiting ATM over a period of several hours and demonstrates reasonable stability in tissue culture (Rainey et al., 2008). In 2009, **KU60019** (2-[(2R, 6S)-2, 6-dimethylmorpholin- 4-yl]-N-[5-(6-morpholin-4-yl-4-oxo-4H-pyran-2-yl)-9H-thioxanthen-2-yl]-acetamide), another specific inhibitor of ATM kinase was developed. KU60019 is an improved analogue of KU55933, and has been shown to be around 10 times more potent than KU55933 at radiosensitizing human glioma cells (Golding et al., 2009).

After initial use of Wortmannin for DNA-PKcs inhibition, **LY294002** (2-(4-morpholinyl)-8-phenylchromone) was developed. LY294002 is non-specific DNA-PKcs inhibitor and more toxic than Wortmannin (Vlahos et al., 1994, Davidson et al., 2013). A number of inhibitors have been generated using LY294002 as a template. **NU7026** (2- (morpholin-4-yl)-benzo [h]chomen-4-one), is over 50 fold more selective for DNA-PKcs than to other PI-3Ks

including ATM and ATR. NU7026 alone had no effect on cell cycle distribution although it increases DSB levels (Willmore et al., 2004). **NU7441** inhibitor (2-N-morpholino-8-dibenzothiophenyl-chromen-4-one) is more potent and specific to DNA-PKcs, (IC_{50} of only 14 nmol/L) and has at least 100 fold selectivity for DNA-PKcs compared with other PI-3K family kinases. NU7441 inhibitor has proved to be not only a potent chemo- and radio-sensitiser but also a powerful tool to study the biology of DNA-PKcs (Leahy et al., 2004, Zhao et al., 2006, Tavecchio et al., 2012, Davidson et al., 2013).

1.6. Breast Cancer

Every day, thousands of women around the world are diagnosed with breast cancer. In 2008 almost 1.4 million women were diagnosed with breast cancer worldwide and around 459,000 deaths were recorded. Incidence rates were much higher in more developed countries with 71.7 per 100,000 compared to 29.3 per 100,000 in less developed countries, whereas the corresponding mortality rates were 17.1 per 100,000 and 11.8 per 100,000 respectively. The highest incidence rates were recorded in Western Europe, Australia/New Zealand and Northern Europe, whilst rates were lowest in Eastern Africa and Middle Africa (Youlden et al., 2012). There is a 0.5% overall increase in incidence annually. However, observed improvements in breast cancer survival especially in developed countries over recent decades have been attributed to the introduction of population-based screening using mammography, improved education and the systemic use of adjuvant therapies (Rosso et al., 2010, Gunsoy et al., 2014).

There are a number of factors that contribute to an increase risk of breast cancer, such as:

(1) Age, about 2 out of 3 invasive breast cancers are found in women over the age of 50. (2) Diet, there is an increase in breast cancer risk by 13% with the higher level of fat intake. (3) Tobacco exposure in all its forms (smoking, and including second-hand smoke). (4) Alcohol consumption, alcohol has been described as being one of the most constant enhancers of breast cancer risk. (5) Body size, obesity if associated with an increased risk of breast cancer (Youlden et al., 2012, McCormack and Boffetta, 2011, Gunsoy et al., 2014). (6) Family history, having a first degree relative with breast cancer can increase a woman's risk by two fold. This risk is greater if the relative has been diagnosed before the age of 50 (Pharoah et al., 1997). Family history accounts for 5-10% of the total number of cases of breast cancer and often involves germline mutations in breast cancer susceptibility genes such as *BRCA1* and *BRCA2*, or others like *p53, PTEN, ATM, CHK2* and *RAD51* (Lose et al., 2006, Flanagan et al., 2010).

A wide variety of clinical and pathological factors are regularly used to categorize breast cancer patients in order to assess prognosis and determine the appropriate therapy. These factors include;

(1) Age at diagnosis, women under the age of 40 often have a more aggressive cancer with higher mortality and recurrence rates in comparison with older women. Younger patients are more likely to have poor clinical characteristics, e.g. larger tumour size and higher histological grade, lymphatic vessel invasion and the involvement of lymph nodes. This is why this group is classified as

high risk and approximately 80% of these patients are offered adjuvant cytotoxic treatment (Kroman et al., 2000, van der Sangen et al., 2008, Schnitt, 2010). (2) Tumour size, it has been established that the rate of distant recurrence increases in patients with large tumours as opposed to smaller tumours (Koscielny et al., 2009). However, tumour size alone is an unreliable prognostic factor in breast cancer (Foulkes et al., 2009). (3) Lymph node status, it is thought to be the second most prominent factor in gauging the probability of survival, after tumour size (Vorgias et al., 2001). (4) Hormone receptor expression, estrogen receptors (ER) and progesterone receptors (PR) located within the cell nucleus have prognostic value in breast cancer patients (Fisher et al., 1986, Garicochea et al., 2009). The prognostic and predictive importance of assessment of ER expression in breast cancer is well established; e.g. patients with ER-positive tumours have more favourable prognostic characteristics than patients with ER-negative tumours which relapse earlier. Patients with ER positive breast cancer will usually receive hormonal therapy; however the added value of PR assessment is controversial. PR status in ER- positive breast cancer might be used to help guide clinical management, as high levels of PR expression may identify a subset of ER-positive patients most likely to benefit from hormonal therapy (Hefti et al., 2013). (5) Histological type, the histological type of invasive breast cancer presents valuable prognostic information. A few histologic types of invasive carcinoma have better prognostic value than others. Ductal carcinoma of no special type, accounting for up to 70% of all breast cancers, has the worst prognosis, whereas tubular breast cancer demonstrates the best prognosis (Martinez and Azzopardi, 1979, Fisher et al., 1975, Ellis et al., 1992, Rakha et

al., 2010). (6) Molecular classification, gene expression profiling has been used to define breast cancer subtypes based on the molecular characteristics and its association with clinical outcome. This classification groups tumours into five molecular subtypes; (a) Luminal A (breast cancer with the highest expression of ER receptor and expression of keratin 18 and 19 in luminal mammary cells, this class is the most common subtype, representing 50–60% of the total). (b) Luminal B (similar to luminal A but has moderate expression of ER receptor, luminal B molecular profile makes up between 10- 20% of all breast cancers). (c) Basal like (ER- negative and high expression of cytokeratin 5, cytokeratin 17, the basal-like subtype represents 10–20% of all breast carcinomas). (d) Normal breast-like (expression of genes known to be expressed in normal mammary tissue, account for about 5–10% of all breast carcinomas). (e) HER2 positive (high expression of the HER2 gene and other genes associated with the HER2 pathway and/or HER2 amplicon located in the 17q12 chromosome, 15-20% of all breast cancers correspond to this molecular subtype) (West et al., 2001, Eroles et al., 2012).

1.7.The BRCA1 tumour suppressor gene

The *Breast Cancer susceptibility 1* (*BRCA1*) gene was identified by Mary King's group in 1990; this gene was mapped to chromosome 17q21 then cloned by Mark Skolnick's group in 1994. BRCA1 gene contains 24 exons, 22 coding exons and 2 non-coding exons. The identification of *BRCA1* gene was a significant breakthrough in the management of breast and ovarian cancers (Hall et al., 1990, Miki et al., 1994).

BRCA1 protein is around 220 kDa and is a highly phosphorylated nuclear protein. BRCA1 contains nuclear import and export signals, allowing movement between the nucleus and cytoplasm to enable BRCA1 to perform its functions. BRCA1 contains about 1863 amino acid residues (Figure 1.5) including an N-terminal RING domain, two nuclear localization signals (NLSs), and two C-terminal BRCA1 Carboxyl Terminal (BRCT) domains of around 110 amino acid residues (Miki et al., 1994, Venkitaraman, 2002, Silver and Livingston, 2012). These domains interact with several proteins and contribute to multiple functions of BRCA1, including in DNA damage response and repair, cell cycle regulation, and transcriptional regulation.

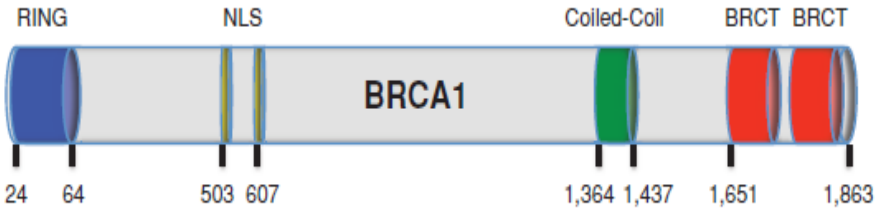

Figure 1.5. The Structure Domain of BRCA1.

Two domains of BRCA1 that are frequently mutated in families with hereditary breast and ovarian cancer are the N-terminal RING domain and the C-terminal BRCT repeats. Both could contribute to tumour suppressing functions of BRCA1. NLS = nuclear localisation signal, BRCT = BRCA1 carboxyl terminal. Adapted from (Silver and Livingston, 2012). Copyright© 2012 by American Association for Cancer Research with permission conveyed through Copyright Clearance Center Inc.

1.7.1. Role of BRCA1 in DNA damage response and repair

One of the first links between BRCA1 and DNA repair was the functional interaction between BRCA1 and RAD51 suggesting a role for BRCA1 in genomic instability (Scully et al., 1997). Since then many studies have shown that BRCA1 plays a vital role in the HR pathway (Moynahan et al., 1999). In addition BRCA1 is also involved in the initial detection of DNA damage. Moreover, BRCA1 has roles in other DNA repair pathways such as:

(1) **NER:** BRCA1 has shown direct control of global genomic repair (GGR) a sub-pathway of NER pathway through *XPC*, *DDB2* and *GADD45* genes, suggesting that deficiency in BRCA1 is followed by deficiency in GGR/NER (Hartman and Ford, 2002).

(2) **NHEJ:** the role of BRCA1 in the NHEJ pathway is uncertain, although several studies suggest a major role of BRCA1 in NHEJ and the maintenance of genomic integrity (Zhong et al., 2002, Bau et al., 2004), while others did not (Moynahan et al., 1999, Merel et al., 2002).

(3) BRCA1 has been suggested to stimulate the activity of three **BER** enzymes; OGG1 (8-oxoguanine DNA glycosylase), NTH1 (homolog of endonuclease III), and APE1. These enzymes mediate repair of three signature oxidative lesions, 8-oxoguanine, thymine glycol and abasic sites, respectively. BRCA1 regulation of BER enzymes was found to be through a transcriptional mechanism involving the transcription factor OCT1 (Octamer-binding transcription factor 1). The exact mechanism by which the BRCA1/OCT1 complex regulates the BER pathway, and whether or not there is a physiologically important defect in BER that can be therapeutically targeted in

BRCA1 deficient cells, remains to be answered (Saha et al., 2010). A previous study has shown that BRCA1 in collaboration with APE1 down regulates levels of reactive oxygen species, oxidized DNA and nitrated proteins (Saha et al., 2009).

1.7.2. Role of BRCA1 in cell cycle regulation

BRCA1 is involved in cell cycle regulation, a function that may allow adequate time for DNA repair to occur in cells. The phosphorylation of BRCA1 is required to activate cell cycle arrest after DNA damage. For instance, in response to ionizing irradiation, ATM phosphorylates BRCA1 on serine 1387 which is required to activate S phase arrest. On the other hand, BRCA1 phosphorylation on serine 1423 has a direct role in G2/M cell cycle arrest (Xu et al., 2002). Cell cycle regulation is controlled by a family of cyclin dependent kinases and their endogenous inhibitors acting at a variety of cell cycle checkpoints. For example, BRCA1 phosphorylation has been shown, through p53 dependent and independent pathways, to stimulate the transcription of the $p21^{CIP1/WAF1}$ leading to G1/S cycle arrest (Chai et al., 1999, Mullan et al., 2006). BRCA1 participates in the G1/S checkpoint response indirectly through CHK2 and p53 phosphorylation (Foray et al., 2003). Recently, DNA-PKcs was shown to activate the CHK2–BRCA1 pathway during mitosis to ensure chromosomal stability (Shang et al., 2014).

1.7.3. Role of BRCA1 in transcriptional regulation

BRCA1 may regulate transcription by interacting with a core component of transcription RNA called polymerase II, BRCA1 is also a co-activator or co-repressor of a number of known transcription factors (Irminger-Finger et al., 1999). For example, BRCA1 has been reported to regulate the oestrogen receptor alpha (ERα). The ability of BRCA1 to induce expression of ERα is dependent on the transcription factor OCT1, which is required to recruit BRCA1 to the ERα promoter (Gorski et al., 2009). In addition, BRCA1 has been shown to interact with the C-terminus of p53 and alter the transcriptional activity of p53 by re-directing it from activation of pro-apoptotic target genes to other genes involved in cell cycle arrest and DNA repair (Chai et al., 1999). Interestingly, mutations in p53 are common in BRCA mutated cancers and that this loss of p53 function may be important in tumourgenesis (Mullan et al., 2006).

1.8. BRCA1 and cancer

Germ-line mutations in *BRCA1* predispose to breast and ovarian cancer development. *BRCA1* mutation carriers have an 80% lifetime risk of developing breast cancer and 40-50% risk of developing ovarian cancer (Risch et al., 2001). In addition, *BRCA1* mutations increase the risk of other types of cancer, such as pancreatic and prostate cancers. Children (both male and female) of a carrier have a 50% chance of inheriting the mutation in their germline, where one defective allele is sufficient to predispose to cancer (Thompson and Easton, 2002). If there is somatic loss of function of the

second allele then a tumour is likely to develop. This is known as the Knudson two hit hypothesis for tumour suppressor genes (Knudson, 1971).

1.9. Synthetic lethality

Synthetic lethality is defined as a genetic combination of mutations in two or more genes/pathways that leads to cell death, whereas a mutation in only one of them does not (Figure 1.6). Synthetic is used here for its ancient Greek meaning: the combination of two entities to form something new. This phenomenon was first discovered from the investigation of fruit flies in 1922 by Calvin Bridge. Sturtevant replicated these results in *Drosophila pseudoobscura* in 1956 (Rehman et al., 2010, Kaelin, 2005, Nijman, 2011). Synthetic lethality represents a new approach of targeting DNA repair pathways with cancer therapies based on the genetic background of the tumour.

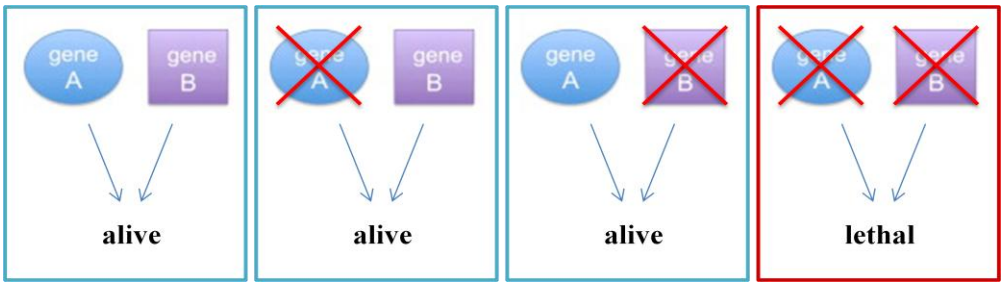

Figure 1.6. Synthetic Lethality.

Deletion of either gene A or gene B does not affect cell viability whereas inactivation of both at the same time is synthetically lethal. Adapted from (Nijman, 2011).

1.9.1. Synthetic lethality between BRCA and PARP

The well known synthetic lethality relationship to date is targeting *BRCA* mutation with PARP1 inhibitors (Farmer et al., 2005, Bryant et al., 2005). PARP1 plays a role in single strand break repair (SSBR), a pathway related to BER. Inhibition of SSBR is associated with accumulation of DSBs, which can be exploited in a subset of cancers possessing defects in DSB repair. *BRCA* gene products have a role in the HR pathway (Venkitaraman, 2002). BRCA deficient cells have impaired HR repair (Moynahan et al., 1999). The PARP1/BRCA synthetic lethality model proposes that targeting BRCA deficient tumours, which are HR deficient, with PARP inhibitor leads to accumulation of SSBs. This is followed by the formation of DSBs during DNA replication, leading to cell death (Farmer et al., 2005, Bryant et al., 2005). A study by Farmer *et al* demonstrated reduced survival of BRCA1 and BRCA2 deficient cell lines after treatment with PARP1 inhibitors (KU0058684 and KU0058948). Both treated BRCA deficient cell lines showed G2/M cell cycle arrest and apoptosis. In addition, Bryant *et al*, demonstrated that PARP1 inhibitors (NU1025 and AG14361) were more effective in BRCA2 deficient cell lines as compared to BRCA2 proficient cell lines. Treatment of BRCA2 deficient cell lines resulted in induction of γH2AX foci formation (representing DNA DSBs). Both of these studies were reported independently and concluded that BRCA deficient cells were selectively sensitive to PARP1 inhibition.

The PARP1/BRCA synthetic lethality model was then translated into clinical trials. A Phase I clinical trial of PARP inhibitor was conducted with Olaparib (known previously as AZD2281 and then KU0059436) in a cohort of patients

with BRCA deficient tumours. The study demonstrated that Olaparib has antitumor activity in *BRCA* mutation carriers. In addition, a Phase II clinical trial of Olaparib in BRCA deficient tumours showed positive proof of the PARP1/BRCA synthetic lethality concept (Fong et al., 2010, Balmana et al., 2011, Audeh et al., 2010, Tutt et al., 2010). The outcomes of both Phase I and II clinical trials provided evidence that PARP inhibitors could be used as a new treatment in BRCA deficient tumours (Chan and Mok, 2010, Balmana et al., 2011).

Recent studies have, however, illustrated some problems with PARP inhibition, including a lack of specificity. The PARP family of enzymes consists of at least 17 members and each one of them has a different structure and function (Rouleau et al., 2010, Mangerich and Burkle, 2011, Underhill et al., 2011). PARP1 for instance is involved in: telomere length, organizing the spindle apparatus, localization and activation of p53 and also the SSBR pathway (Mangerich and Burkle, 2011). Recent studies have evaluated a series of 185 inhibitors of PARP, including the best-known inhibitors being tested clinically such as Olaparib, ABT-888 and Rucaparib, for the specificity to bind to the catalytic domains of 13 of the 17 human PARP family members. In this study they determined that majority of the inhibitors bind to multiple targets and are therefore not specific (Wahlberg et al., 2012). Resistance to PARP inhibition is also an emerging problem. Potential resistance mechanisms include: altered NHEJ capacity and restoration of, or increase in, HR capacity (Montoni et al., 2013). Moreover, although BRCA1 deficient tumours are sensitive to PARP1, *BRCA1* hypomorphic mutant tumours can restore BRCA1

expression and are therefore insensitive to PARP inhibition (Drost et al., 2011). Another potential resistance mechanism involves Tumor Suppressor p53 Binding Protein 1 (53BP1), which binds to the central DNA-binding domain of p53. Bunting *et al*, demonstrated that loss of 53BP1 can restore the HR pathway in BRCA1 deficient cells. The mechanism for this is the promotion of ATM function and therefore this may be overcome by the use of ATM inhibitors (Bunting et al., 2010). On the other hand, because most agents that would be combined with a PARP inhibitor are already administered at or near a maximum dose, the addition of another potentiating agent is likely to increase toxicity as well as efficacy. For instance, a phase II trial was conducted involving 40 patients with metastatic malignant melanoma treated with PARP inhibitor (AG014699) in combination with temozolomide. Results showed that 18% of the study subjects demonstrated partial responses, with notable side effects such as, temozolomide-related myelosuppression and one toxic death (Plummer et al., 2006, Pacher and Szabo, 2007). More recently a phase I trial was terminated; this study was designed to determine the maximum tolerated dose and safety profile of Olaparib in combination with topotecan in solid tumours. The most common side effects reported were fatigue and gastrointestinal adverse events similar to the ones previously reported in Olaparib monotherapy studies. However, unexpected high haematological toxicities were observed even with substantially lower doses of both agents (Samol et al., 2012).

1.9.2. Alternative synthetic lethality targets

The discovery of the synthetic lethality (SL) relationship between BRCA and PARP has become the paradigm for a new class of rational cancer therapies. Several novel SL candidates have also been recently investigated. For instance, RAD51D deficiency showed sensitivity to PARP inhibitor suggesting a possible SL target (Loveday et al., 2011). Similarly, Mantle Cell Lymphoma (MCL) deficient in both ATM and p53 are more sensitive to the PARP inhibitor (Olaparib) than cells lacking ATM function alone. Suggesting that inhibition of both ATM and PARP may have efficacy in targeting p53 deficient malignancies (Williamson et al., 2012). Similar sensitivity is observed in MRE11 deficient cells with PARP1 inhibitor (ABT-888) treatment (Vilar et al., 2011).

The emerging problems with PARP inhibition led our group to investigate alternative SL targets. For example, we have shown that targeting Apurinic/apyrimidinic endonuclease (APE1), a central component of the BER pathway, with a small molecule inhibitor induces SL in HR deficient cell lines (Mohammed et al., 2011, Sultana et al., 2012). Similarly, targeting APE1 in Phosphatase and tensin homolog (PTEN) deficient melanoma cell lines induces SL (Abbotts et al., 2014a). In addition, targeting X-ray repair cross complementing gene 1 (XRCC1) deficient cell lines with DSB repair inhibitors (ATM or DNA-PKcs) or SSB break repair inhibitor (ATR) results in SL (Sultana et al., 2013a, Sultana et al., 2013b).

1.10. Hypothesis and Aims

The base excision repair (BER) pathway is critical for processing DNA damage caused by alkylation, oxidation, single strand breaks and base deamination (Dianov and Hubscher, 2013). The well known synthetic lethality relationship to date is targeting *BRCA* mutated tumours (HR deficient) with PARP1 inhibitors. However with the emerging problems using PARP inhibition, several novel synthetic lethality candidates have been recently investigated within the BER pathway. On the other hand, studies suggest a cross talk between BRCA1 and BER (Alli et al., 2009). In a more recent study, a functional interaction between Pol ß and BRCA1 was demonstrated (Masaoka et al., 2013), implying a potential role for Pol ß in BRCA1 mediated DSB repair. In addition, BRCA1 has also been shown to be involved in the transcriptional regulation of BER factor such as OGG1, NTH1 and APE1 (Saha et al., 2010). As a result, the hypothesis of this study is that with the essential role of BRCA1 in regulating several BER factors, such as APE1, Pol ß, OGG1 and NTH1, then BRCA1 deficient cell lines may have impaired BER factors which leads to accumulation of SSBs followed by the formation of DSBs during the DNA replication process. Therefore, it is suggested that BRCA1 deficient cells are reliant on the DSB pathway for cellular survival. Accordingly targeting the DSB pathway by ATM or DNA-PKcs inhibition in BRCA1-BER deficient cell lines may induce synthetic lethality (Figure 1.7).

The aims of this research project are as follows:

1. To investigate DNA repair mRNA and protein expression in BRCA1 deficient and proficient cell lines.

2. To investigate if targeting BRCA1 deficiency by ATM inhibitors (KU55933 & KU60019) is synthetically lethal.
3. To investigate if targeting BRCA1 deficiency by DNA-PKcs inhibitors (NU7441 & NU7026) is synthetically lethal.
4. To investigate if targeting BRCA1 deficiency by ATM or DNA-PKcs inhibitor in combination with cisplatin is synthetically lethal.

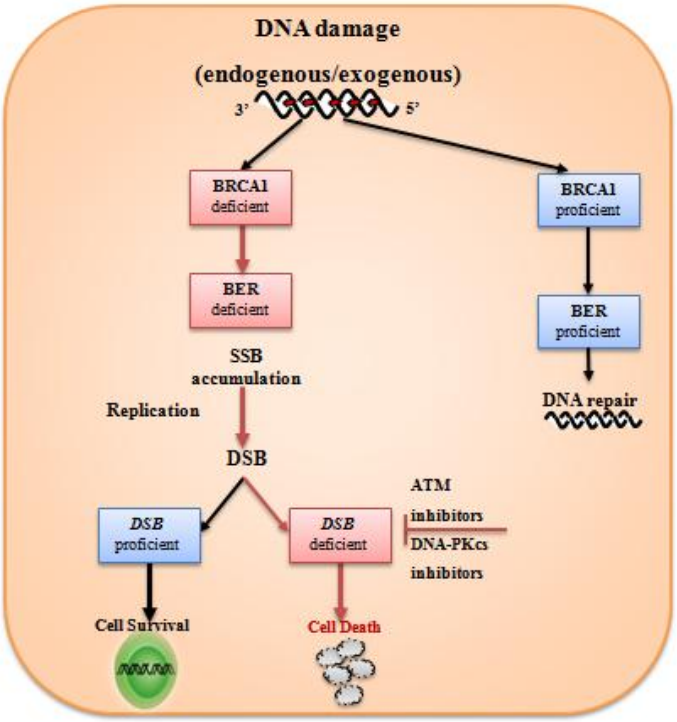

Figure 1.7. Hypothetical synthetic lethality in BRCA1/ BER deficient cells, by ATM or DNA-PKcs inhibitors.

Impaired BER factors in BRCA1 deficient cell lines leads to accumulation of SSBs followed by the formation of DSBs during the DNA replication process. Therefore, it is suggested that cells are reliant on the DSB pathway for cellular survival. Targeting the DSB pathway by ATM or DNA-PKcs inhibition may induce synthetic lethality leading to cell death.

Chapter 2

Materials and Methods

2. Materials and Methods

2.1. Materials

KU55933 [2-(4-Morpholinyl)-6-(1-thianthrenyl)-4*H*-pyran-4-one], KU60019 [(2*R*,6*S*-rel)-2,6-Dimethyl-*N*-[5-[6-(4-morpholinyl)-4-oxo-4*H*-pyran-2-yl]-9*H*-thioxanthen-2-yl-4-morpholineacetamide], NU7441 [8-(4-Dibenzothienyl)-2-(4-morpholinyl)-4*H*-1-benzopyran-4-one], NU7026 [2-(4-Morpholinyl)-4*H*-naphthol[1,2-*b*]pyran-4-one], and NU1025 [8-Hydroxy-2-methyl-4(3*H*)-quinazolinone] were purchased from Tocris Bioscience (UK), while (3-AB) 3-aminobenzamide was purchased from Sigma (UK). All compounds were dissolved in 100 % v/v dimethyl sulphoxide (DMSO) to give 5 or 10 mM stock solutions, and stored at -20°C. Cisplatin solution was obtained from Pharmacy, Nottingham City Hospital, UK and stored at room temperature.

2.2. Cell lines and culture media

2.2.1. HeLa SilenciX® cells

Human cervical adenocarcinoma adherent cell lines, BRCA1 HeLa SilenciX (Adherent HeLa cells silenced for BRCA1 (Accession Number: NM_007295)) and Control HeLa SilenciX (Adherent HeLa cells transfect with control shRNA), were purchased from Tebu-Bio (www.tebu-bio.com) and were grown in DMEM medium (with L-Glutamine 580mg/L, 4500 mg/L D-Glucose, with 110mg/L Sodium Pyruvate) (Invitrogen,UK) supplemented with 10% FBS, 1% penicillin/streptomycin and 125 μg/ml Hygromycin B (Invitrogen,UK). BRCA1 HeLa SilenciX cells were used between passage 20

and 34; Control HeLa SilenciX cells were used between passage 48 and 60. All materials were obtained from (Sigma/PAA, UK) unless otherwise stated. To make it easier for discussion of the results, BRCA1 deficient HeLa SilenciX cells are referred to as **BRCA1 HeLa** and Control BRCA1 proficient HeLa SilenciX cells are referred to as **Control HeLa**.

2.2.2. Breast cancer cells

Human breast adenocarcinoma adherent cell lines, **MCF7** (hemizygous for BRCA1 wild type used between passage 25 and 38), and **MDA-MB-436** (*BRCA1* mutated used between passage 17 and 29), were used in this study. MDA-MB-436 cells are homozygous for a 5396 + 1G>A mutation in the splice donor site of exon 20 resulting in loss of the wild-type *BRCA1* allele. Analysis has identified two *BRCA1* transcript lengths; one transcript had skipped exon 20 (predicting an in-frame deletion of 28 amino acids in the encoded BRCA1 proteins) and the second transcript had spliced at a cryptic splice site in intron 20 (5396 + 88/89) (predicting an insertion of 7 amino acids encoded by intron sequences followed by a termination codon) (Merajver et al., 1995, Elstrodt et al., 2006).

MCF7 cells were obtained from ATCC® and were maintained with RPMI-1640 supplemented with 10% FBS and 1% penicillin/streptomycin. MDA-MB-436 cells were obtained from CLS and were grown in DMEM: Ham's F12 supplemented with 2 mM L-glutamine, 10% FBS and 1% penicillin/streptomycin. All materials were obtained from Sigma/PAA (UK).

2.3.Methods

2.3.1. Subculture of cell lines

All cell lines were cultured at 37ºC in a humidified incubator with 5% CO_2 and 95% air. To subculture, all cells were handled separately with their own reagents and under sterile conditions. Medium was removed and cells washed twice with phosphate buffered saline (PBS) (without Ca_{2+} and Mg_{2+}). Cells were detached from the flask by adding 5 ml or less of 0.5mg/ml trypsin-EDTA (Sigma/PAA, UK) and incubated for 5 minutes at 37ºC. Medium was used to deactivate the trypsin and the suspension was centrifuged at 1000 rpm for 5 minutes to remove residual trypsin. The pellet was resuspended in medium, mixed well and split into a new tissue culture flask. All cell lines were routinely confirmed to be mycoplasma negative.

2.3.2. Cryopreservation of cell lines

Cells were cryopreserved at a low passage number for future use. Prior to freezing cells were trypsinised and counted using a haemocytometer. 1 x 10^6 cells were resuspended in 1 ml of freezing medium, stored in a cryovial at -80ºC overnight, and then transferred to liquid nitrogen for long term storage. Freezing medium consisted of complete medium for the cell line + 10% DMSO, with the exception of HeLa cells where the freezing medium was 50% FBS + 40% PBS +10% DMSO. Cells were recovered from liquid nitrogen by thawing rapidly in a water bath at 37°C. The cells were then resuspended in 9 ml fully supplemented culture medium and centrifuged at 1000 rpm for 5 minutes in order to remove traces of DMSO. The medium was then removed

and the pellets were resuspended in medium and transferred to tissue culture flasks.

2.3.3. AQueous non-radioactive cell proliferation assay (MTS assay)

2.3.3.1. Background principles

MTS assay (Promega, UK) is frequently used for screening different compounds to determine if they have effects on cell proliferation or show direct cytotoxic effects that eventually lead to cell death.

MTS solution is composed of a tetrazolium compound [3-(4, 5-dimethylthiazol-2-yl)-5-(3-carboxymethoxyphenyl)-2-(4-sulfophenyl)-2H-tetrazolium, inner salt; MTS] and an electron coupling reagent phenazine methosulfate (PMS). Cells reduce MTS into a formazan product that is soluble in tissue culture medium; formazan is produced by dehydrogenase enzymes that are only found in metabolically active cells (Riss et al., 2011, Cory et al., 1991).

2.3.3.2. Assay

To evaluate the cytotoxicity of varying doses of inhibitors (KU55933, NU7441 or NU1025), MTS assays were performed according to the manufacturer's recommendation. 500 - 2000 cells, in 200 µl of medium, were seeded into each well of a 96-well plate. Cells were allowed to adhere for 24 hours, followed by incubation with varying concentrations of inhibitors. The MTS assay was performed on day 6.

2.3.3.3. Data analysis

On day 6, 20 µl of MTS reagent was added to each well, and the plate was incubated for 3-4 hours at 37ºC in the dark. Formazan absorbance was measured at 490 nm using a plate reader (FLUOstar OPTIMA, UK/ Infinite® F50, UK). Percentage of the absorbance was determined by comparison to a control population of untreated cells.

This assay was performed three times, each time in triplicate. Graphs were produced and statistical analysis performed using the Microsoft Excel 2010 and GraphPad prism software version 6.02.

2.3.4. Clonogenic survival assay

2.3.4.1. Background principles

The clonogenic survival assay allows a determination of cell survival after exposure to potentially cytotoxic agents. The assay measures viable cells that have undergone at least 5-6 rounds of replication to produce a colony and have therefore survived the drug exposure (Munshi et al., 2005).

2.3.4.2. Plating efficiency

Cell lines were plated into 6-well plates at varying densities. Plates were incubated for 12-14 days under normal incubator conditions, then media was removed and wells were fixed (with methanol and acetic acid mixture) for 10 minutes. Plates were stained with crystal violet and colonies counted manually.

2.3.4.3. Clonogenic assay

HeLa SilenciX cells (200-500 cells/well) and Breast cancer cells (300-900 cells/well) where seeded in a 6-well plate. Cells were allowed to adhere for 24 hours. Compounds (KU55933, KU60019, NU7441, NU7026 or 3-Aminobenzamide) were added at the indicated concentrations, with a control for each cell line that did not receive drug. The plates were left in the incubator for 14 days. After incubation, the media was discarded, cells were fixed (with methanol and acetic acid mixture) and colonies stained with crystal violet and counted manually.

To evaluate cisplatin chemopotentiation cells were seeded as above and after 24 hours cells were exposed to cisplatin for 16 hours. Plates were then washed twice with PBS, fresh media added and plates placed in an incubator with or without inhibitors 14 days then they were fixed and stained as above. All assays were performed in duplicate and repeated three times.

A second clonogenic survival assay method was also employed to determine validity of the previously described protocol. In this method, cells lines were plated as previously described, cells were allowed to adhere for 24 hours, after which inhibitory compound was added at varying concentrations. Cells were incubated for 24 hours, after which the plates were gently washed with PBS and the medium replaced without inhibitor. Plates were again incubated for 14 days prior to staining as previously described.

2.3.4.4. Data analysis

Blue stained visible colonies with ≥ 50 cells were counted manually and surviving fraction was calculated as follows:

Surviving Fraction (SF) = [No. of colonies formed / (No. of cells seeded x Plating efficiency)].

Plating efficiency was calculated by:

Plating Efficiency (PE) = (No. of colonies formed / No. of cells seeded) x 100.

When comparing between the two clonogenic protocols, and in the clonogenic combination study, the inhibitory concentration of an inhibitor that result in the death of 50% of the cell population (IC_{50}) was calculated using curve fitting with nonlinear regression analysis. This assay was performed three times. Graphs were produced and statistical analysis performed using the Microsoft Excel 2010 and GraphPad prism software version 6.02.

2.3.5. γH2AX immunofluorescence microscopy assay

2.3.5.1. Background principles

The histone protein H2AX is one of three types of histone H2A found in eukaryotic cells and has been shown to be involved in DNA repair and is a central component of signalling pathways activated in response to DNA double strand breaks. Within minutes of a DNA double strand break, H2AX becomes rapidly phosphorylated by ATM, ATR or DNA-PK, on a serine 139 residue forming γH2AX foci, each foci is thought to correspond to one double strand break within the nucleus (Rogakou et al., 1998, Rogakou et al., 1999, Paull et

al., 2000). This focus can be detected using antibody staining and fluorescence microscopy.

2.3.5.2. Assay

100,000 cells per well were seeded onto sterile coverslips in 6-well plates. Cells were allowed to adhere for 24 hours, and then cells were incubated in medium containing ATM inhibitors (KU55933/KU60019) or DNA-PKcs inhibitors (NU7441/NU7026). After 24 and 48 hours treatment, cells were washed with PBS and fixed with ice-cold 100% methanol for 10 minutes. After rehydrating in PBS, cells were permeabilized in blocking buffer [KCM buffer (120mM potassium chloride, 20mM sodium chloride, 10mM Tris-HCl, 1mM EDTA, 0.1% Triton X-100) with 2% bovine serum albumin, 10% milk powder, and 10% normal goat serum] for one hour. Cells were incubated with primary anti phospho-histone H2AX (Ser139) antibody (mouse monoclonal antibody, Millipore Corp., dilution 1:200) in blocking buffer at room temperature for 1 hour. After incubation, the cells were washed in KCM buffer and incubated with secondary anti-mouse antibody (polyclonal goat anti-mouse immunoglobulins, DAKO, dilution 1:200) at room temperature for 1 hour in the dark, followed by 2-3 washes in KCM buffer. Coverslips were air dried at room temperature, stained with DAPI (Vectashield Hard Set, Vector Laboratories Inc., Burlingame, USA) and stored overnight at 4°C before analyses.

To evaluate cisplatin chemopotentiation, cells were seeded as above and after 24 hours cells were exposed to cisplatin for 16 hours. Plates were then washed twice with PBS, fresh media added and plates placed in an incubator

with or without inhibitors for 24 and 48 hours then washed and fixed as above. Immunofluorescence microscopy was then performed as described below.

2.3.5.3. Data analysis

Images were obtained using Olympus BX40 microscope and the images captured by cellSens (Vers 1.4) Imaging Software and camera (Olympus). Cells containing γH2AX foci were determined in 100 cells per slide in three separate experiments. Nuclei containing more than six γH2AX foci were considered positive. This method (> 6 γH2AX foci) of quantification has been shown to be reliable. Moreover, the basal level of γH2AX foci for the cell lines used in the present study (Breast cancer and HeLa cell lines) has previously been shown to be a maximum of 6 (Farmer et al., 2005, Bryant et al., 2005, Sultana et al., 2012). The student t-test was used to calculate if there is a significant difference in sensitivity between mutant/knockdown cells before and after treatment with inhibitors. A p-value ≤ 0.05 was defined as a significant relationship. Graphs were produced and statistical analysis performed using the Microsoft Excel 2010 and GraphPad prism software version 6.02.

2.3.6. Flow cytometric analyses for cell cycle

2.3.6.1. Background principles

Distribution of cell cycle by flow cytometry is a widely used procedure. This assay is based on analysis of the cellular DNA content after staining cells with the fluorescent DNA binding dye, propidium iodide (PI). This method

reveals distribution of cells in three major phases of the cycle (G1, S and G2/M) (Ormerod and Kubbies, 1992, Pozarowski and Darzynkiewicz, 2004).

2.3.6.2. Assay

100,000 cells were plated in to T25 flasks, and were allowed to adhere for 24 hours. Inhibitory compound was added and after 48 hours treatment, cells were collected by trypsinization and centrifugation (1000 rpm for 5 minutes). The cell pellets were fixed in 70% ethanol in PBS, incubated at 4^{o}C overnight to allow fixation and then stored under these conditions until FACS analyses. Prior to FACS analysis, fixed cells were centrifuged and the pellet was resuspended in 500 µl PBS containing propidium iodide (PI) (2 µg/ml) and DNAse-free RNase A (10 µg/ml). After incubation at 37^{o}C for 1 hour, samples then were analysed.

To evaluate cisplatin chemopotentiation cells were seeded as above and after 24 hours cells were exposed to cisplatin for 16 hours. Plates were then washed twice with PBS, fresh media added and placed in an incubator with or without inhibitors 48 hours. Cell cycle analysis was then performed.

2.3.6.3. Data analysis

Samples were analysed on a Cytomics F500 flow cytometer (Beckman Coulter, USA) using a 488nm laser for excitation and a 620nm bandpass filter for collection of data. Data was analysed using FlowJo 7.6.1 (Tree Star, Ashland, USA). At least 50,000 cells from each cell suspension were analysed. This assay was performed three times; the student t-test was used to calculate if there is a significant difference in sensitivity between mutant/knockdown

cells before and after treatment with inhibitors. A p-value ≤0.05 was defined as a significant relationship. Graphs were produced and statistical analysis performed using the Microsoft Excel 2010 and GraphPad prism software version 6.02.

2.3.7. Annexin V flow cytometric analyses for Apoptosis

2.3.7.1. Background principles

Programmed cell death (Apoptosis), is a common form of cell death in eukaryotes and during embryonic development. It is characterized by chromatin condensation, altering in cell volume and translocation of membrane phosphatidylserine (PS) from the inner side of the plasma membrane to the surface (Figure 2.1). Annexin V is a Ca^{2+}-dependent phospholipid-binding protein with a high affinity for PS. Staining with Annexin V is used in conjunction with a second dye such as propidium iodide (PI) for identification of early and late apoptotic cells (Figure 2.2). Viable cells with intact membranes are negative (reject) to PI, whereas dead cells with damaged membranes are positive (permeable) to PI. Therefore, viable cells are both Annexin V and PI negative, early apoptotic cells are Annexin V positive and PI negative, late apoptotic cells are Annexin V and PI positive, finally necrotic cells are Annexin V negative and PI positive (Koopman et al., 1994, Riccardi and Nicoletti, 2006).

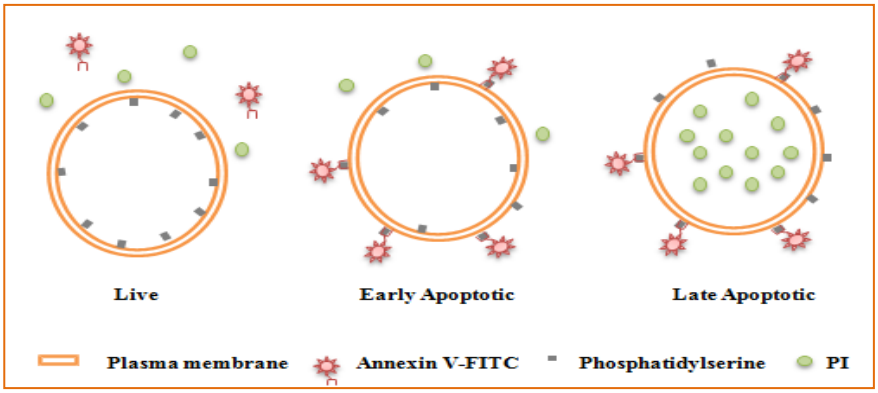

Figure 2.1. Annexin V flow cytometry mechanism (V-FITC).

In early apoptosis, phosphatidylserine, which is located inside the plasma membrane, transposes to the cell outer surface. Annexin V is a human vascular anticoagulant, with high affinity for PS. Annexin V-FITC/PI staining method is widely used in the detection of early apoptosis. Adapted from (www.flow-cytometry.us).

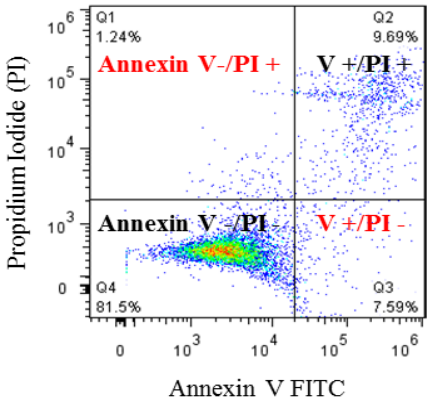

Figure 2.2. Annexin V and PI Staining.

Viable cells are both Annexin V and PI negative, early apoptosis cells are Annexin V positive and PI negative, late apoptosis cells are Annexin V and PI positive, finally necrotic are Annexin V negative and PI positive.

2.3.7.2. Assay

Cells were grown to sub-confluence (70-80 %) and harvested. 100,000 cells were plated in to T25 flasks and were allowed to adhere for 24 hours. Inhibitory compound was added and cells were collected after 24 and 48 hours exposure. Cells were trypsinized and centrifuged at 1000 rpm for 5 minutes. The cell pellets were washed twice with ice-cold PBS and then resuspend in Binding buffer (BioLegend, UK) at a concentration of $1x10^6$ cell/ml. 5 µl of FITC Annexin V (ImmunoTools, Germany) and 5 µl PI were added to 100 µl of the cell solution and incubated for 15 minutes at room temperature in the dark. 400 µl of the Binding buffer was then added and the sample analysed by FACS.

To evaluate cisplatin chemopotentiation cells were seeded as above and after 24 hours cells were exposed to cisplatin for 16 hours. Plates were then washed twice with PBS, fresh media added and placed in an incubator with or without inhibitors for 24 and 48 hours. Cell cycle analysis was then performed.

2.3.7.3. Data analysis

Samples were analysed on a Cytomics F500 flow cytometer (Beckman Coulter, USA) using a 488nm laser for excitation and a 575nm bandpass filter for collection of data. Data was analysed using FlowJo 7.6.1 (Tree Star, Ashland, USA). At least 20,000 cells from each cell suspension were analysed. This assay was performed three times; the student t-test was used to calculate if there is a significant difference in sensitivity between mutant/knockdown cells before and after treatment with inhibitors. Percentage of the absorbance was determined by comparison to a control population of untreated cells. A p-

value ≤0.05 was defined as a significant relationship. Graphs were produced and statistical analysis performed using Microsoft Excel 2010 and GraphPad prism software version 6.02.

2.3.8. DNA repair gene expression profiling

2.3.8.1. Background principles

To determine the human DNA repair gene profile in BRCA1 deficient cell lines, RT-qPCR array was performed using the DNA repair RT² Profiler™ PCR Array (Qiagen, UK). This array represents 84 key genes involved in the Base excision, Nucleotide excision, Mismatch, Double-strand break, and other DNA repair pathways. Additionally, quantitative real time PCR (RT-qPCR) using QuantiTect® Primers (Qiagen, UK) was performed to confirm up/down gene expression.

2.3.8.2. RNA extraction

Total cellular RNA was isolated using the RNeasy mini kit (Cat No; 74104, Qiagen) according to the manufacturer's instructions. Briefly, 350 µl of Buffer RLT was added to the 2 x 10^6 pelleted cells, and then vortexed. 350 µl of 70% ethanol was mixed with the lysate and then 700 µl of the lysate was transferred to an RNeasy spin column. The sample was then centrifuged for 15 seconds at 10,000 rpm. The flow through was discarded and 350 µl of Buffer RW1 was added to the RNeasy spin column to wash the membrane. The sample was centrifuged for 15 seconds at 10,000 rpm, and the flow through was discarded.

DNA digestion was performed to eliminate genomic DNA contamination using the DNase digestion kit (Cat No; 79254, Qiagen). 70 µl of Buffer RDD and 10 µl of DNase I stock solution was added into a 0.5 ml eppendorf. This DNase I incubation mix was centrifuged for 15 seconds at 10,000 rpm. 80 µl of the DNase I mix was then added directly to the RNeasy spin column membrane, and incubated at room temperature for 15 minutes. 350 µl of Buffer RW1 was added to the RNeasy spin column, and the sample was centrifuged for 15 seconds at 10,000 rpm. The flow through was discarded and 500 µl of Buffer RPE was added to the RNeasy spin column to wash the membrane. The sample was centrifuged for 15 seconds at 10,000 rpm. 500 µl of Buffer RPE was added to the RNeasy spin column to wash the membrane, and the sample was centrifuged for 2 minutes at 10,000 rpm. Following centrifugation, the RNeasy spin column was carefully placed in a new 1.5 ml eppendorf, and 40 µl of RNase-free water was added directly to the spin column membrane. The sample was centrifuged for 1 minute at 10,000 rpm to elute the RNA.

The concentration (µg/µl) of the eluted RNA was performed by measuring absorbance ratio at 260:280 nm using a spectrophotometer system (Nanodrop 2000c, Thermo Scientific, USA) and RNA aliquots were then stored at -80ºC.

2.3.8.3. cDNA Synthesis

Equal amounts of RNA (0.5 µg) were reverse transcribed to form cDNA using RT² First Strand Kit (Cat No; 79254330401, Qiagen). For each RNA sample 2 µl GE (DNA elimination buffer) and nuclease-free water was added to bring the total volume of genomic DNA elimination mixture to 10 µl. The genomic DNA elimination mixture was centrifuged for 10 seconds at 10,000

rpm. The mixture was incubated at 42°C for 5 minutes. Following incubation, the genomic DNA elimination mixture was chilled on ice for at least one minute. For preparation of the room temperature cocktail, 4 µl of 5X RT Buffer 3 (BC3), 1 µl of Primer & External Control Mix (P2), 2 µl of RE3 (RT Enzyme Mix 3), and 3 µl of nuclease free water were added to a sterile 1.5 mL eppendorf. The 10 µl of RT cocktail was added to the genomic DNA elimination mixture. The reaction was incubated at 42°C for 15 minutes and the reaction was stopped by heating at 95°C for 5 minutes. Following heating, 91 µl of nuclease free water was added to the cDNA and held on ice until the array was prepared or the cDNA was stored at -80ºC.

2.3.8.4. RT² Profiler™ DNA Repair PCR Array

To evaluate the expression of 84 DNA repair genes, cDNA samples were mixed with RT^2 SYBR Green Mastermix (Qiagen) according to the supplier's instructions. Briefly, the PCR component mix was prepared as follow;

Table 2.1. Reaction mix for RT² Profiler™ DNA Repair PCR Array

Reagent	Volume
RT^2 SYBR Green Mastermix	1350 µl
cDNA synthesis reaction	102 µl
RNase-free water	1248 µl
Total	**2700 µl**

25 µl of the mix was added to each well of the PCR array plate (Cat No: PAHS-042ZC). The plate was sealed using optical adhesive film and centrifuged for 1 minute to remove bubbles. RT PCR was performed on an Applied Biosystems 7500 FAST cycler, the cycler conditions were; initial 1:10

minutes at 95ºC; followed by 2-41:15 seconds at 95ºC, then 1 minute at 60ºC. Quality controls included within the array plates confirmed the lack of DNA contamination and successfully tested for RNA quality and PCR performance.

2.3.8.5. Quantitative real time PCR (RT-qPCR)

To confirm up/down regulation of gene expression as shown by RT² Profiler™ DNA Repair PCR Array, quantitative real time PCR (RT-qPCR) using QuantiTect® Primers (Qiagen, UK) was performed according to the supplier's instructions. Briefly, the PCR component mix was prepared as follow;

Table 2.2. Reaction mix for Quantitative real time PCR (RT-qPCR).

Reagent	Volume
cDNA from RT^2 First Strand synthesis	2 µl
10x QuantiTect primer	1 µl
SYBR Green Mastermix	5 µl
RNase-free water	2 µl
Total	**10 µl**

PCR mix was added to each well of the PCR plate (Applied Biosystems®, UK). The plate was sealed using optical adhesive film and centrifuged for 1 minute to remove bubbles. RT qPCR was performed on an ABI prism 7700 (Applied Biosystems) using SYBR green detection (Applied Biosystems®, UK). Thermal cycler conditions included incubation at 95ºC for 10 minutes followed by 40 cycles of 95ºC for 15 seconds and 60ºC for 1 minute. Following the 40 cycles, the products were heated from 60ºC to 95ºC over 20 minutes to allow melting curve analysis to be done. This allowed the

specificity of the products to be determined (single melting peak) and confirmed the absence of primer-dimers. The housekeeping gene *GAPDH* was used to standardise the samples and the relative expression of *BRCA1*, *XRCC1*, *APE1*, *SMUG1*, *Pol ß*, *Lig3*, *ATM* and *DNA-PKcs* were therefore calculated as the ratio between the expression of test gene and the expression of housekeeping gene. Positive and negative controls (no template) were included in each experiment and all reactions were performed three times.

Table 2.3. QuantiTect® Primers used in RT-qPCR analysis.

Gene Symbol	Source	Catalog no.
APE1	Qiagen	QT00012474
XRCC1	Qiagen	QT00016688
SMUG1	Qiagen	QT00002317
Pol ß	Qiagen	QT00088655
Lig3	Qiagen	QT00017115
ATM	Qiagen	QT00061593
DNA-PKcs	Qiagen	QT00086828
BRCA1	Qiagen	QT00039305
GAPDH	Qiagen	QT00079247
ß2M	Applied Biosystems	Forward /GAGTATGCCTGCCGTGTG Reverse /AATCCAAATGCGGCATCT

2.3.8.6. Data analysis

Raw data from both real-time PCR methods were uploaded using a PCR array data analysis template available at http://pcrdataanalysis.sabiosciences.com/pcr/arrayanalysis.php. The integrated Web-based software package for the PCR array system automatically performed all comparative threshold cycle ($\Delta\Delta C_t$)–based fold-change calculations from the uploaded data. For these calculations, GAPDH was used for normalization of the data. After normalization, the relative expression of each gene was averaged for the two samples in each cell line. Fold changes in average gene expression were expressed as the difference in expression of

BRCA1 deficient cells compared with BRCA1 proficient cells (control). Statistical significance determined for the RT² Profiler™ Array using the Bonferroni correction for multiple testing, with p values less than 0.05 (threshold $p < 0.000595 = 0.05/84$). RT-qPCR statistical significance determined using t test, with p values less than 0.05. Analysis performed using GraphPad prism software version 6.02.

2.3.9. Western Blot analysis

2.3.9.1. Background principles

Western blot is a method developed more than 30 years ago (Burnette, 1981). This process involves separation of specific proteins in given cells or tissue extract on a sodium dodecyl sulphate (SDS)-polyacrylamide gel, followed by electrophoresis transfer to a nitrocellulose membrane and detected using specific antibodies (primary antibodies) that bind to the target protein. Horseradish peroxidise (HRP) enzyme conjugated secondary antibodies were used to bind with their specific primary antibodies which can be detected using ECL™ chemiluminescent system. Visualisation of the immune complex was performed using X-ray film.

2.3.9.2. Preparation of cell lysate

70-80% confluent cells were washed with PBS, trypsinised and counted using a haemocytometer. The cell pellet was resuspended in media, 1×10^6 or 2×10^6 cells were lysed using 100 µl of RIPA buffer (20 mM Tris, 150 mM NaCl, 1% Nonidet p-40, 0.5% sodium deoxycholate, 1 mM EDTA, 0.1% SDS; Sigma) containing 10% of protease inhibitor (Sigma) and 1% of phosphatase

inhibitor cocktails 2 and 3 (Sigma). The lysate was incubated on ice for 1 hour, then repeatedly aspirated with a fine-gauge needle and incubated overnight at -20°C. Next day lysates were centrifuged at 13000 rpm for 20 minutes at 4°C and the supernatant was stored at -20°C.

2.3.9.3. Protein quantification (Bradford assay)

Bradford assay (Bio-Rad, UK) is a method based on binding Coomassie dye to protein (Bradford, 1976). Differential colour change occurs in response to the protein concentration. Briefly, 10 µl of protein were mixed with 250 µl assay solution in 96-well plate. The absorbance value was measured at 595 nm by plate reader (FLUOstar OPTIMA, UK/ Infinite® F50, UK) with in 1 hour. A protein standard curve was generated using bovine serum albumin (BSA) against corresponding protein concentrations. The determination of the protein concentration, in respective cell lysates, was carried out to ensure equal loading of protein in the wells of western blot gel.

2.3.9.4. Preparation of cell lysates for electrophoresis

Equal volumes (20 – 50 µg) of protein were mixed with 5 µl lithium dodecyl sulphate (LDS) sample buffer (Expedeon, UK), 1 µl Dithiothreitol (DTT) (Invitrogen, UK) and dH_2O. The mix was incubated at 70ºC for 10 minutes, and then placed on ice.

2.3.9.5. Polyacrylamide gel electrophoresis and Protein transfer

Samples were loaded onto precast SDS 4-12% gels (Expedeon, UK) and were run in 3-(N-morpholino) propanesulphonic acid-sodium dodecyl sulphate

(MOPS-SDS) running buffer (Expedeon), at a constant voltage of 125-200 V for 60-120 minutes.

Using the Xcell II Blot Module (Invitrogen), proteins were transferred to a nitrocellulose membrane (Whatman, GE Healthcare) in transfer buffer [20% (v/v) methanol, 50 mM Tris-HCl, and 380 mM glycine] by application of a 25V current for 60-120 minutes.

2.3.9.6. Immunoblotting

Membranes were blocked by incubation with PBS-T (PBS, 0.05% Tween 20) containing 5% non-fat milk for 60 minutes at room temperature. Membranes were incubated with primary antibody diluted in blocking buffer for 60 minutes at 37ºC or overnight at 4^{o}C. The membranes were washed 3 times (5 minutes each) with PBS-T. Protein expression was examined by application of HRP-labelled secondary antibody (Dako, Denmark) at 1:1000 dilution in blocking buffer for 60 minutes at room temperature. The membranes were washed 3 times (5 minutes each) with PBS-T and detected on photographic film using ECL reagent (GE Healthcare).

2.3.9.7. Primary antibodies

Table 2.4. Primary antibodies used in Western blot.

Antigen	Antibody	MW	Source	Catalog no.	Dilution
APE1	Rabbit	37 kDa	Novus	NB 100-101	1:1000
XRCC1	Mouse	85 kDa	Neomarkers	MS-434-PO	1:150
SMUG1	Goat	37 kDa	Acris	APO884PU-N	1:1000
Pol ß	Rabbit	38 kDa	Abcam	Ab26343	1:1000
Lig3	Rabbit	113 kDa	Abcam	Ab96576	1:1000
BRCA1	Rabbit	220 kDa	Santa Cruz	Sc-642	1:150
ATM	Goat	350 kDa	Abcam	ab2631	1:1000
DNA-PKcs	Rabbit	460 kDa	Abcam	ab32566	1:1000
ß -actin	Mouse	42 kDa	Sigma	A2228	1:10000

2.3.9.8. Data analysis

Photographic films were scanned and analysed using Image Studio Lite (Ver 3.1) (Li-Cor, USA). β-actin was used for normalization of the data. This assay was performed in two or three independent experiments; the student t-test was used to calculate the significant difference between control cells and mutant/knockdown cells. A p-value ≤ 0.05 was defined as significant. Graphs were produced and statistical analysis performed using the GraphPad prism software version 6.02.

Chapter 3

DNA repair profiling in BRCA1 deficient and proficient cells

3. DNA repair profiling in BRCA1 deficient and proficient cells

3.1. Introduction

Germ-line mutations in the *BRCA1* gene are one of the most common causes of hereditary forms of breast and ovarian cancers. *BRCA1* mutation carriers have 80% lifetime risk of developing breast cancer, and 40-50% risk of developing ovarian cancer (Risch et al., 2001). In addition, *BRCA1* mutations increase the risk of other types of cancer, such as pancreatic and prostate cancers (Thompson and Easton, 2002). Moreover, in sporadic breast cancer, epigenetic mechanisms of gene inactivation are now well recognized as a potential alternative to genetic mutation in the silencing of the *BRCA1* promoter in up to 11-14% of tumours (Turner et al., 2004). Dysfunctional BRCA pathway may also contribute to a 'BRCAness' phenotype in about 25% of cancers (Turner et al., 2004), where breast cancers do not harbour germline *BRCA* mutations but display similar phenotypes including HR deficiency. The term 'BRCAness' is a phenotype which refers to molecular and histopathological characteristics observed in a subset of breast cancers that exhibit similarity to BRCA deficient tumours, including 'basal phenotype' and 'triple negative' (oestrogen receptor, progesterone receptor and HER2 negative) cancers (Turner et al., 2004, Matros et al., 2005). This chapter investigated, whether BRCA1 deficient cells compared to BRCA1 proficient cells exhibit altered profile of DNA repair expression.

3.1.1. BRCA1 mutation in breast cancer cell lines

Four established breast cancer cell lines with *BRCA1* mutation have been reported, HCC1937 was the first BRCA1 deficient cell line reported in 1998. HCC1937 was derived from a germline *BRCA1* mutation carrier (Tomlinson et al., 1998). In 2006 Elstrodt and colleagues screened 41 human breast cancer cell lines and found three to be *BRCA1* mutant (summarised in Table 3.1), the same results were confirmed by analysis of 51 human breast cancer cell lines in 2013 (Elstrodt et al., 2006, Riaz et al., 2013).

Cell line	*BRCA1 Mutation status*	*BRCA1 transcript expression*	*Exon*	*ER*	*PGR*	*P53*	*EGFR*
MDA-MB-436	5396 + 1G>A	++*	20	-	-	-	+
SUM1315M02	185delAG	+	2	-	-	-	+
SUM149PT	2288delT	+	11	-	-	-	+
HCC1937	5382insC	++	20	-	-	-	+

Table 3.1. BRCA1 mutations in breast cancer cell lines.

ER, estrogen receptor; EGFR, epidermal growth factor receptor; PGR, progesterone receptor. For transcript expression: (+, low transcript levels); (++, normal transcript levels); (++*, Two transcript lengths that both differ from the wild type sequence). For protein expression: (+, expression) and (-, no expression) (Tomlinson et al., 1998, Elstrodt et al., 2006, Riaz et al., 2013).

3.1.2. Rationale for the study

As discussed previously (section 1.7.1) BRCA1 plays a role in many DNA repair pathways including, BER, NER, MMR, HR and NHEJ. Therefore in this chapter, a comprehensive analysis of the DNA repair pathway genes in BRCA1 deficient cells compared to proficient cells will be described using the RT² Profiler™ DNA Repair PCR Array (as described in section 2.3.8.4.). The RT² Profiler PCR Array has the advantage of combining RT-PCR performance with the ability of microarrays to detect the expression of 84 DNA repair genes simultaneously.

BRCA1 has been suggested to stimulate the activity of three BER enzymes (see section 1.7.1); OGG1, NTH1 and APE1. These enzymes mediate repair of three signature oxidative lesions; 8-oxoguanine, thymine glycol and abasic sites, respectively (Saha et al., 2010). A more recent study supports these findings and has confirmed down-regulation of the same enzymes in BRCA1 deficient cells, it also suggested XRCC1 to be regulated by BRCA1 (De Summa et al., 2014). XRCC1 protein associates with Pol ß, and Lig3, to form a complex that repairs the single strand DNA breaks generated during the BER process. In addition, recent studies suggest a cross talk between BRCA1 and other BER genes. For instance, a functional interaction between Pol ß and BRCA1 (Masaoka et al., 2013) has been described, and an association between low SMUG1 protein expression and loss of BRCA1 expression (Abdel-Fatah et al., 2013). For this reason in the current study BER genes (APE1, XRCC1, SMUG1, Pol ß and Lig3) will be investigated for a potential link with BRCA1 deficiency. In addition, as the main aim of this study is to investigate synthetic lethality in a BRCA1 deficient system by targeting the DSB pathway, ATM (a

key enzyme in HR) and DNA-PKcs (a key enzyme in NHEJ) genes will be investigated as well. Therefore, the selected genes (*BRCA1*, *APE1*, *XRCC1*, *SMUG1*, *Pol ß*, *Lig3*, *ATM* and *DNA-PKcs*) will be investigated using the RT² Profiler™ Array and then further assessment of the results will be carried out by quantitative real time PCR (RT-qPCR) using QuantiTect® Primers (as described in section 2.3.8.5.). Finally, the mRNA expression of the selected genes will be compared with protein expression using western blot analysis.

3.1.2.1. Aims

The aims of this chapter were as follows:

1. To explore DNA repair expression in BRCA1 proficient and deficient cell lines using RT² Profiler™ DNA Repair PCR Array.
2. To confirm up or down regulation of selected DNA repair genes in a panel of BRCA1 proficient and deficient cell lines using Quantitative real time PCR (RT-qPCR).
3. To investigate alteration in protein expression of selected DNA repair factors in BRCA1 proficient and deficient cell lines using western blot analysis.

3.2. Materials and Methods

Materials and methods for the assays listed are described in full in Chapter 2.

BRCA1 deficient **MDA-MB-436** breast cancer cells and BRCA1 proficient **MCF7** breast cancer cells were used in this study (Table 3.2). A second set of BRCA1 proficient and deficient cell line model was also used; **BRCA1 deficient HeLa SilenciX cells** and **Control BRCA1 proficient HeLa SilenciX cells.**

To make it easier for discussion of the results, BRCA1 deficient HeLa SilenciX cells are referred to as **BRCA1 HeLa** and Control BRCA1 proficient HeLa SilenciX cells are referred to as **Control HeLa**.

Cell line	*BRCA1 Mutation status*	*BRCA1 transcript expression*	*ER*	*PGR*	*P53*	*EGFR*
MDA-MB-436	5396 + 1G>A	+*	-	-	-	+
MCF7	Wild type	+	+	+	+	-

Table 3.2. Breast cancer cell lines used in this project.

ER, estrogen receptor; EGFR, epidermal growth factor receptor; PGR, progesterone receptor. For transcript expression: (+, normal transcript levels); (+*, Two transcript lengths that both differ from the wild type sequence). For protein expression: (+, expression) and (-, no expression) (Elstrodt et al., 2006, Riaz et al., 2013).

3.3. Results

3.3.1. Determination of BRCA1 expression in cell lines

3.3.1.1. Western blot analysis demonstrates reduced BRCA1 protein expression

The protein expression of BRCA1 was determined in all cell lines by western blotting. Briefly, cell lysates were prepared from 70-80% confluent cells and loaded onto polyacrylamide gels as described in section 2.3.9. BRCA1 was resolved on precast SDS 4-12% gels. Following electrophoresis, proteins were electrotransferred onto nitrocellulose and probed for target protein using specific antibody (Table 2.4). Recombinant BRCA1 protein (Sigma/UK, 0.02µl) was also run as control on the gel, moreover as a loading control; β-actin antibody was used.

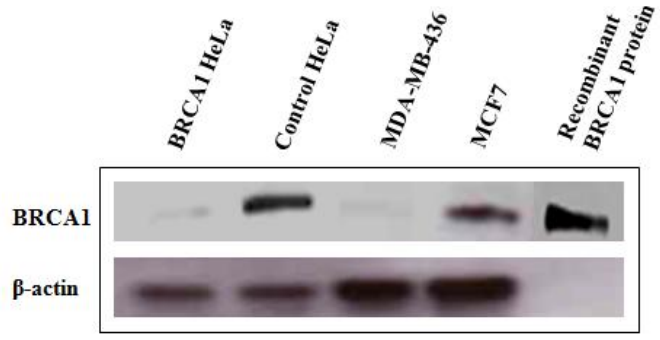

Figure 3.1. BRCA1 protein expression in the cell lines studied by western blot

Whole cell protein lysates were collected for each cell line and 50 µg samples were separated by electrophoresis on denaturing polyacrylamide gels as described in section 2.3.9. Recombinant BRCA1 protein was also run as control on the gel. Blot was probed using specific BRCA1 antibody with predicted molecular weight 220 kDa. As a loading control, β-actin antibody (42 kDa) was used.

As expected, MDA-MB-436 and BRCA1 HeLa cell lines are BRCA1 deficient (Figure 3.1), when compared to MCF7 and Control HeLa cell lines. Quantification of protein expression is shown in Figure 3.2. Significant under-expression of BRCA1 protein was confirmed in BRCA1 HeLa (fold change mean = 0.09, $p < 0.0001$) and MDA-MB-436 cells (fold change mean = 0.07, $p = 0.0001$) compared to Control HeLa and MCF7 cells respectively.

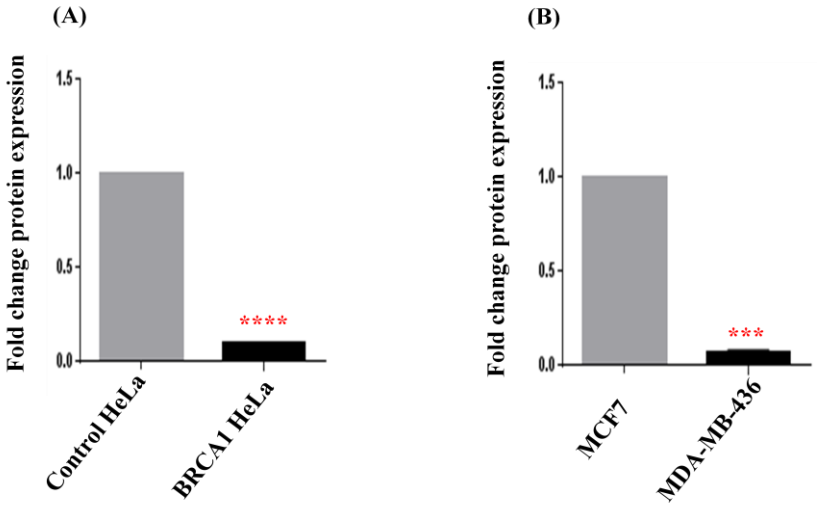

Figure 3.2. Quantification of BRCA1 protein expression

(A) Relative BRCA1 expression in BRCA1 HeLa cells was calculated in comparison to Control HeLa cells. **(B)** Relative BRCA1 expression in MDA-MB-436 cells was calculated in comparison to MCF7 cells. Values plotted are means ± SD of the fold-change (ratio of protein/ß-actin normalized to control) *** $p<0.001$ and **** $p<0.0001$.

3.3.1.2. RT- qPCR demonstrate reduced BRCA1 mRNA expression

After confirming low expression of BRCA1 protein in BRCA1 HeLa and MDA-MB-436 cells, mRNA expression was determined by RT-qPCR as described in section 2.3.8.5. Relative expression were calculated for each cell line and compared to their respective control cell lines. The mRNA expression

of housekeeping genes *ß2-microglobulin* (*ß2M*) and *GAPDH* (primer details in Table 2.3) were used to standardise the samples. The relative expression of BRCA1 mRNA was calculated as the ratio between the expression of *BRCA1* gene and the expression of the housekeeping gene. Negative control was included in each experiment. As both housekeeping genes showed similar results, GAPDH was used for all subsequent experiments. Data as expected (Figure 3.3) demonstrated low mRNA expression of BRCA1 in BRCA1 HeLa cells compared to Control HeLa (mean fold change = 0.16; p = 0.0015). Low BRCA1 mRNA expression was also seen in MDA-MB-436 cells compared to MCF7 cells (mean fold change = 0.09; p = 0.0026).

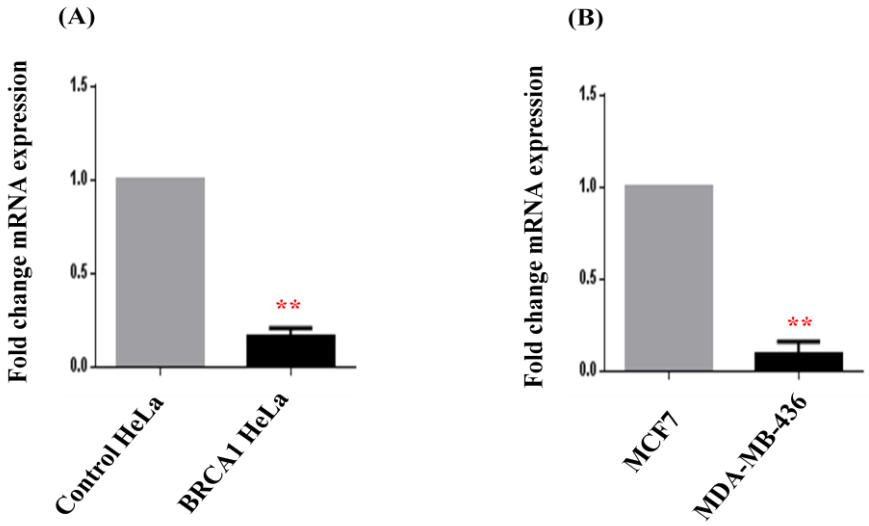

Figure 3.3. Quantification of BRCA1 mRNA expression

(A) Relative BRCA1 expression in BRCA1 HeLa cells was calculated in comparison to Control HeLa cells. **(B)** Relative BRCA1 expression in MDA-MB-436 cells was calculated in comparison to MCF7 cells. The housekeeping gene *GAPDH* was used to standardise the samples and the relative expression level of BRCA1 was therefore calculated as the ratio between the level of gene of interest and the level of housekeeping gene. Negative control (no template) was included in each experiment and all reactions were run in triplicate ** $p<0.01$.

3.3.2. RT^2 Profiler DNA Repair PCR Array

Real-time (RT-PCR) is a highly sensitive and reliable method for gene expression analysis. RT^2 Profiler PCR Arrays has the advantage of combining RT-PCR performance and the ability of microarrays to detect the expression of many genes simultaneously. RT^2 Profiler PCR array from Qiagen is a high throughput assay which allows analysis of the gene expression profiles in chosen cell populations. It consists of two step reverse transcription RT-PCR reaction: firstly isolated RNA and then converted to cDNA. Secondly the cDNA in combination with gene specific primers and a PCR master mix which contains a SYBR Green (which fluoresces when bound to double-stranded DNA (dsDNA)), subjected to thermal cycling.

Baseline fluorescence represents the background 'noise' fluorescence, which refers to the signal level during the initial cycles and it is automatically determined by the PCR cycler software. RT-PCR phases can be broken up into three sections; Exponential phase; each PCR cycle results in a doubling of dsDNA product which increases fluorescent signal until a pre-specified threshold is reached. This threshold cycle (C_t) is the cycle number at which fluorescent signal of the reaction crosses the baseline threshold, and is dependent upon the initial concentration of the primer target within the sample. Linear phase; the reaction components are being consumed, gradually reducing reaction efficiency and products are starting to degrade. Plateau phase; the reaction has stopped, no more products are being made and if left long enough, the PCR products will begin to degrade. Graphical representation of C_t can be observed using amplification plots (Figure 3.4). By normalising the C_t of the gene of interest against the C_t of a housekeeping gene using $\Delta\Delta C_t$ method

($\Delta\Delta C_t$ calculation method listed in APPENDIX A), gene expression can be compared in different samples (lifetechnologies, 2012, Qiagen, 2011).

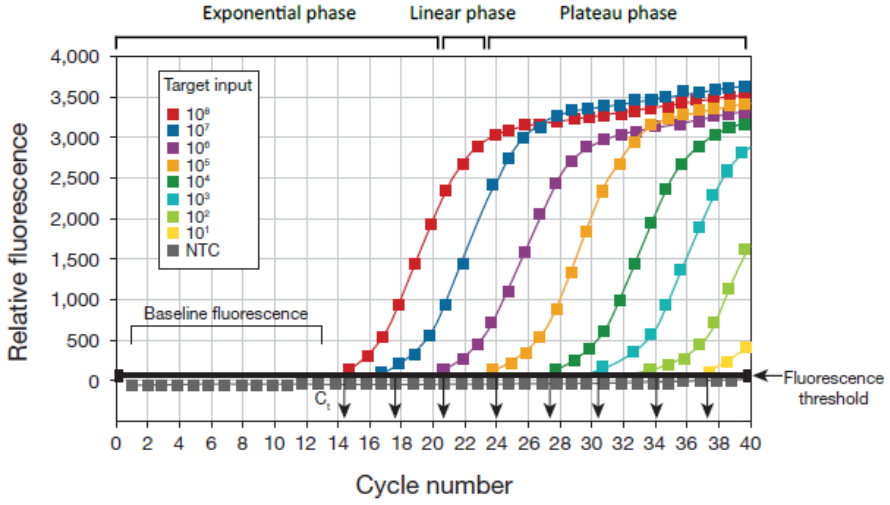

Figure 3.4. Illustration of qRT-PCR amplification plot.

Plot represents the accumulation of product over the duration of the qRT-PCR. The samples used to create the plots are a dilution series of the target DNA sequence. Adapted from (lifetechnologies, 2012).

The Qiagen RT^2 Profiler PCR array is performed in a 96-well format (Figure 3.5), allowing analysis of 84 genes simultaneously. In addition to 5 housekeeping genes, the genomic DNA control (GDC) that specifically detects non-transcribed genomic DNA contamination with a high level of sensitivity. The reverse-transcription control (RTC) that tests the efficiency of the reverse-transcription reaction performed with the RT^2 First Strand Kit by detecting a template synthesized from the kit's built-in external RNA control. The positive PCR control (PPC) consists of a pre-dispensed artificial DNA sequence and the assay that detects it. This control tests the efficiency of the polymerase chain reaction itself. Genes assessed in the RT^2 Profiler DNA PCR Array are listed in APPENDIX B.

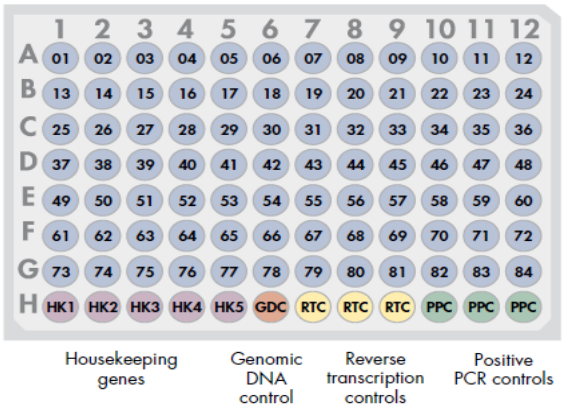

Figure 3.5. RT^2 Profiler PCR Array plate layout.

Wells A1 to G12 each contain a real-time PCR assay for a DNA repair pathways related gene. Wells H1 to H5 contain a housekeeping genes panel to normalize array data (HK1-5). Well H6 contains a genomic DNA control (GDC). Wells H7 to H9 contain replicate reverse-transcription controls (RTC). Wells H10 to H12 contain replicate positive PCR controls (PPC). Adapted from (Qiagen, 2011).

Fluorescent reference dye (Rn), in this case SYBR Green, is normalised against ROX which is a passive reference dye contained within the PCR master mix. In amplification plots ΔRn scale, which is plotted against cycle number on a Log10, is a subtraction of baseline fluorescence from Rn. To demonstrate if the amplification was successful, post-amplification melting curve analysis can be performed. After thermo-cycling is completed, fluorescence of the PCR product is recorded while temperature is increased. When the melting point (T_m) is reached it is followed by a sudden decrease in fluorescent signal. T_m may be affected by multiple factors like (DNA length, and the presence of base mismatches); therefore different PCR products display different melting characteristics. By plotting change in Fluorescence

against change in Temperature (–ΔF/ΔT) to give a melting profile, it is possible to detect the presence of nonspecific product or 'primer-dimers' (binding of homologous primers to self rather than template) as additional peaks on the melting curve. To avoid presence of non-specific product, optimise the concentration of RNA was needed to find the concentration that gives successful amplification with less background noise (lifetechnologies, 2012, Qiagen, 2011).

3.3.3. Optimisation of the purified RNA for RT-PCR

High-quality RNA is essential for obtaining good, RT-PCR results. The most important prerequisite for any gene expression analysis experiment is consistently high-quality RNA from every experimental sample. So the concentration (µg/µl) of the purified RNA was performed by measuring absorbance ratio at 260 : 280 nm using a spectrophotometer system (Nanodrop 2000c, Thermo Scientific, USA) before every assay.

Optimisation of purified RNA for RT-PCR was carried out at different concentrations; starting with 1 µg total RNA per array. Amplification plot for the RT^2 Profiler array demonstrated successful amplification (Figure 3.6), however some background noise were detected. Melting curve analysis for both HeLa cell lines is summarised in Figure 3.7. Three nonspecific products (melting peaks) detected in Control HeLa cells, and one nonspecific product was detected with BRCA1 HeLa cells.

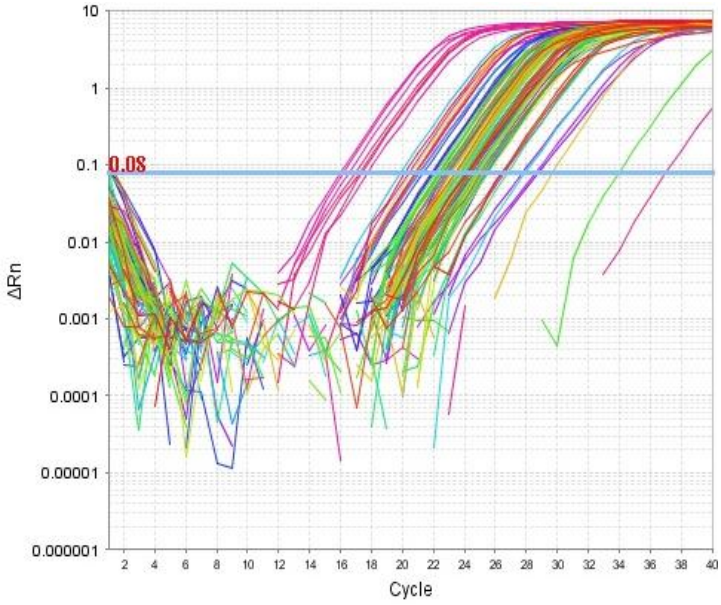

Figure 3.6. Optimisation of RNA concentration for RT^2 PCR.

Amplification plot for RT^2 Profiler DNA Repair Array, using 1 µg total RNA per array. Product is indicated by exponential fluorescence accumulation with increasing cycle number. Plot demonstrates successful amplification, though some background noise is detected.

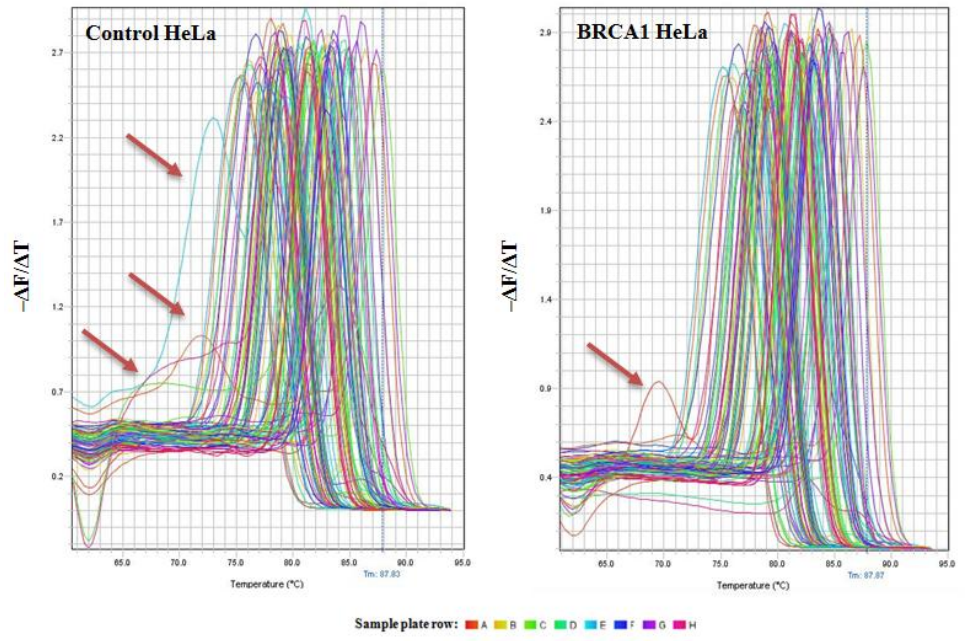

Figure 3.7. Melting curve analysis for HeLa cells with 1 µg total RNA per array.

The presence of nonspecific product is observed as additional peaks to the left of the melting curve. Three nonspecific products (melting peaks) are seen in Control HeLa cells, and one nonspecific product was seen with BRCA1 HeLa.

As mentioned above, using 1 µg total RNA per array showed successful amplification, however some background noise in amplification plot along with nonspecific product detected in melting curves. Therefore the total RNA was reduced using 0.5 µg which shows successful amplification of all 84 primers for each of the cell lines (see Figure 3.8). Successful melting curve analysis for all the cell lines is summarised in Figure 3.9 with every specific product for all the 84 target genes.

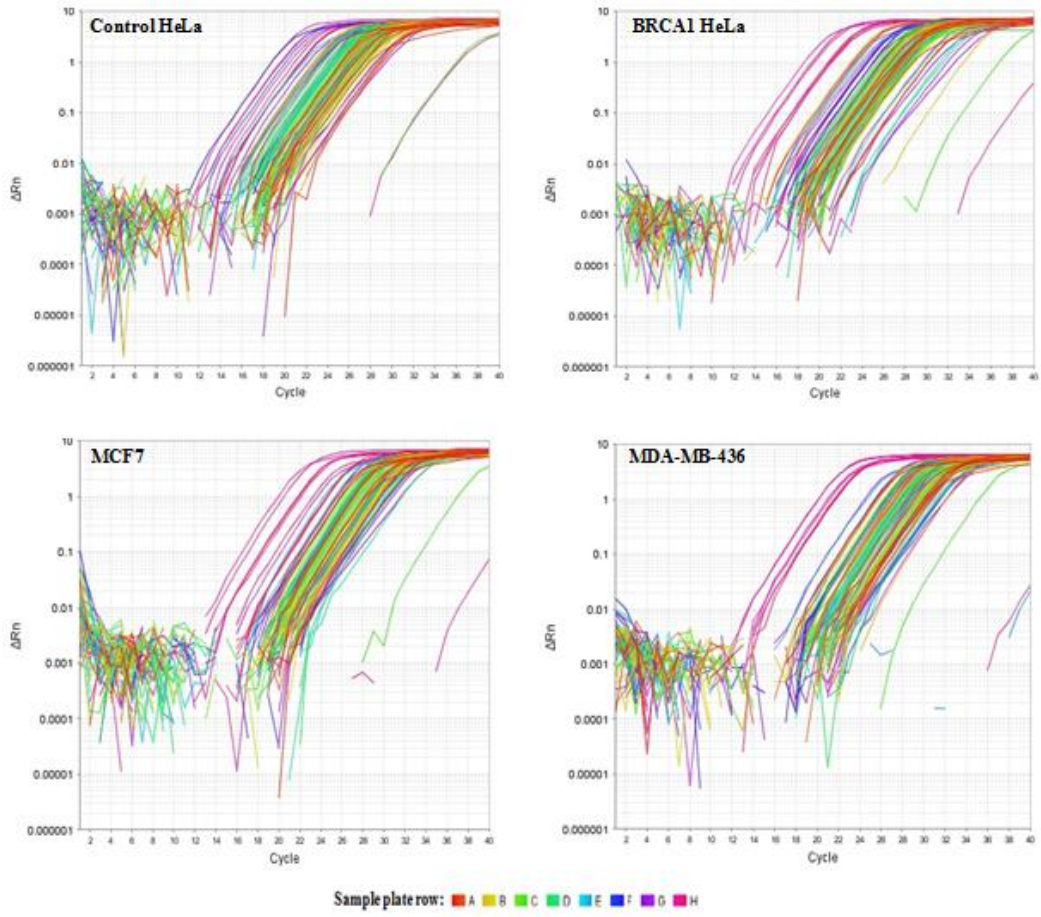

Figure 3.8. Amplification plots for RT^2 Profiler DNA Repair Array.

Amplification of PCR product is indicated by exponential fluorescence accumulation with increasing cycle number.

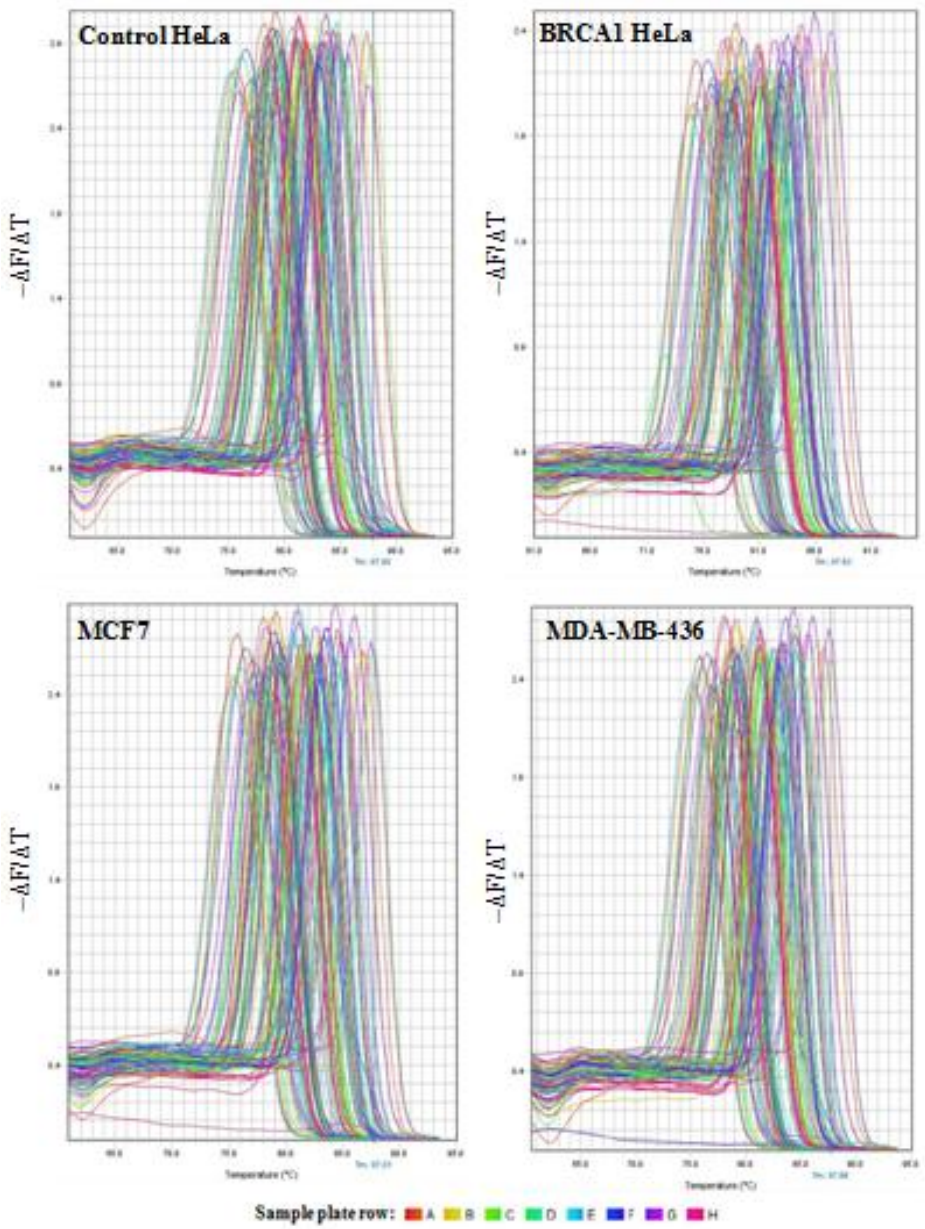

Figure 3.9. Melting curves for RT^2 Profiler PCR Array.

Single melting peaks are observed for all the 84 primers assayed with all the cell lines, indicating high specificity.

3.3.4. BRCA1 deficiency is associated with multiple altered DNA repair gene expression profile

To investigate whether BRCA1 deficiency is associated with an altered DNA repair gene expression, both breast cancer (MDA-MB-436 and MCF7) and HeLa cell lines (BRCA1 HeLa deficient cells and Control HeLa proficient cells) were used to investigate mRNA expression by using RT^2 PCR DNA repair profile assay as described in section 2.3.8.4. Data analysis as described in section 2.3.8.6 was performed by importing the raw RT^2 PCR DNA repair profile assay data into a Qiagen analysis template that can compare multiple experimental replicates for one cell line against multiple experimental replicates of the control cells. The integrated Web-based software package for the PCR array system automatically performed all comparative threshold cycle ($\Delta\Delta C_t$)–based fold-change calculations from the uploaded data. For these calculations, GAPDH was used for normalization of the data. Scatter plots were charted to compare gene expression in BRCA1 wild type MCF7 cells to MDA-MB-436 and Control HeLa cells to BRCA1 HeLa cells as illustrated in Figure 3.10 and Figure 3.11.

A number of genes were initially observed to be under-expressed in BRCA1 deficient cell lines compared to BRCA1 proficient cells (though not statistically significant), including: BER factors (Table 3.3) such as (*APE1*, *Pol ß*, *SMUG1*, *NTHL1*, *UNG*, *FEN1*, *OGG1*, *NEIL1* and *XRCC1*); HR factors (Table 3.4) such as (*RAD21*, *RAD51*, *RAD54L* and *ATM*); NHEJ factors (Table 3.5) such as (*DNA-PKcs*, *LIG4*, *XRCC5* and *XRCC6*); NER factors (Table 3.6) such as (*ERCC1*, *ERCC2*, *ERCC3*, *ERCC4* and *ERCC5*) and MMR factors

(Table 3.7) such as (*MLH1*, *MSH2*, *MLH3*, *MSH3*, *MSH4* and *MSH5*). Other related DNA repair gene expressions results are shown in APPENDIX C.

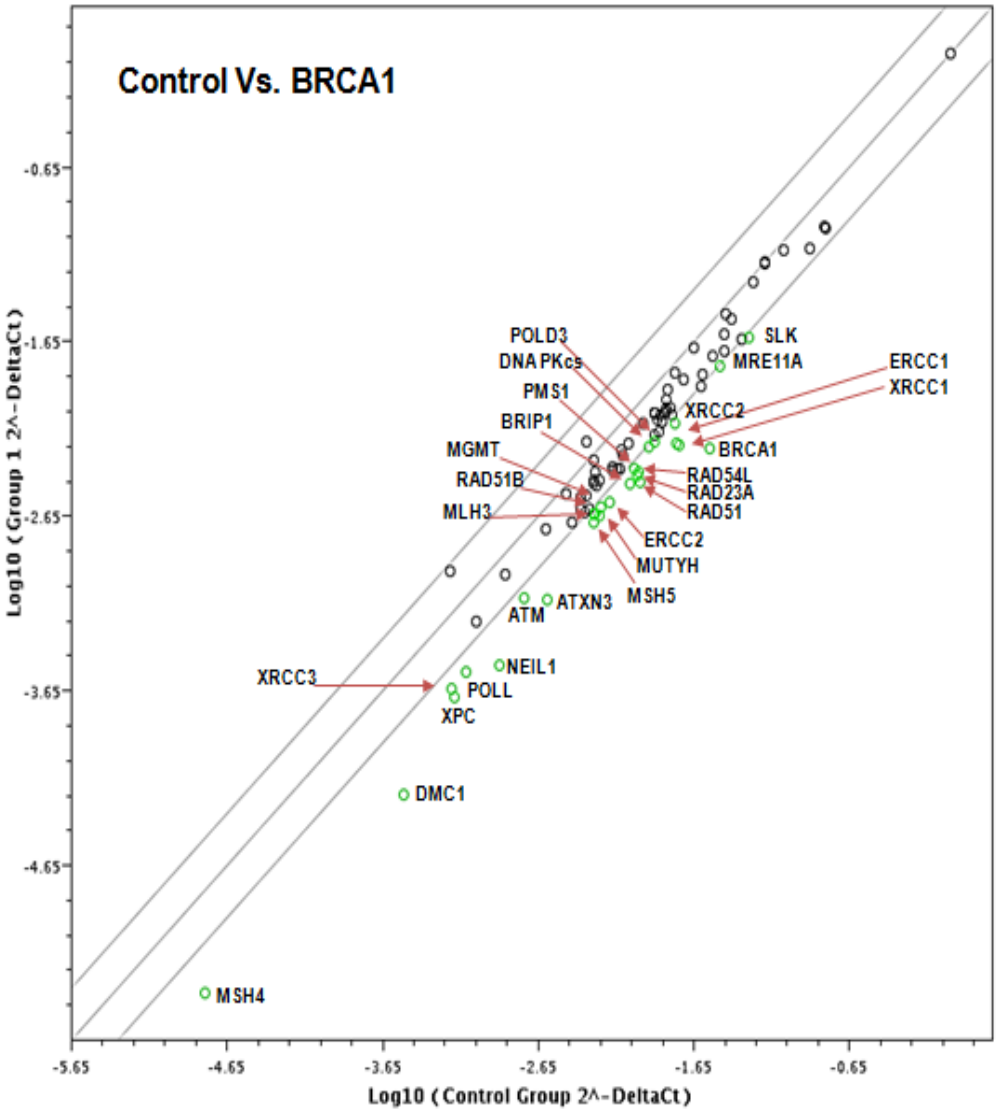

Figure 3.10. Scatter plot comparing DNA repair gene expression in BRCA1 HeLa deficient cells against Control HeLa BRCA1 proficient cells.

The area outside the grey lines indicates two-fold change in gene expression in BRCA1 HeLa deficient cells compared to Control HeLa proficient cells. Green circles indicate gene under-expression. Data are from 4 independent experiments.

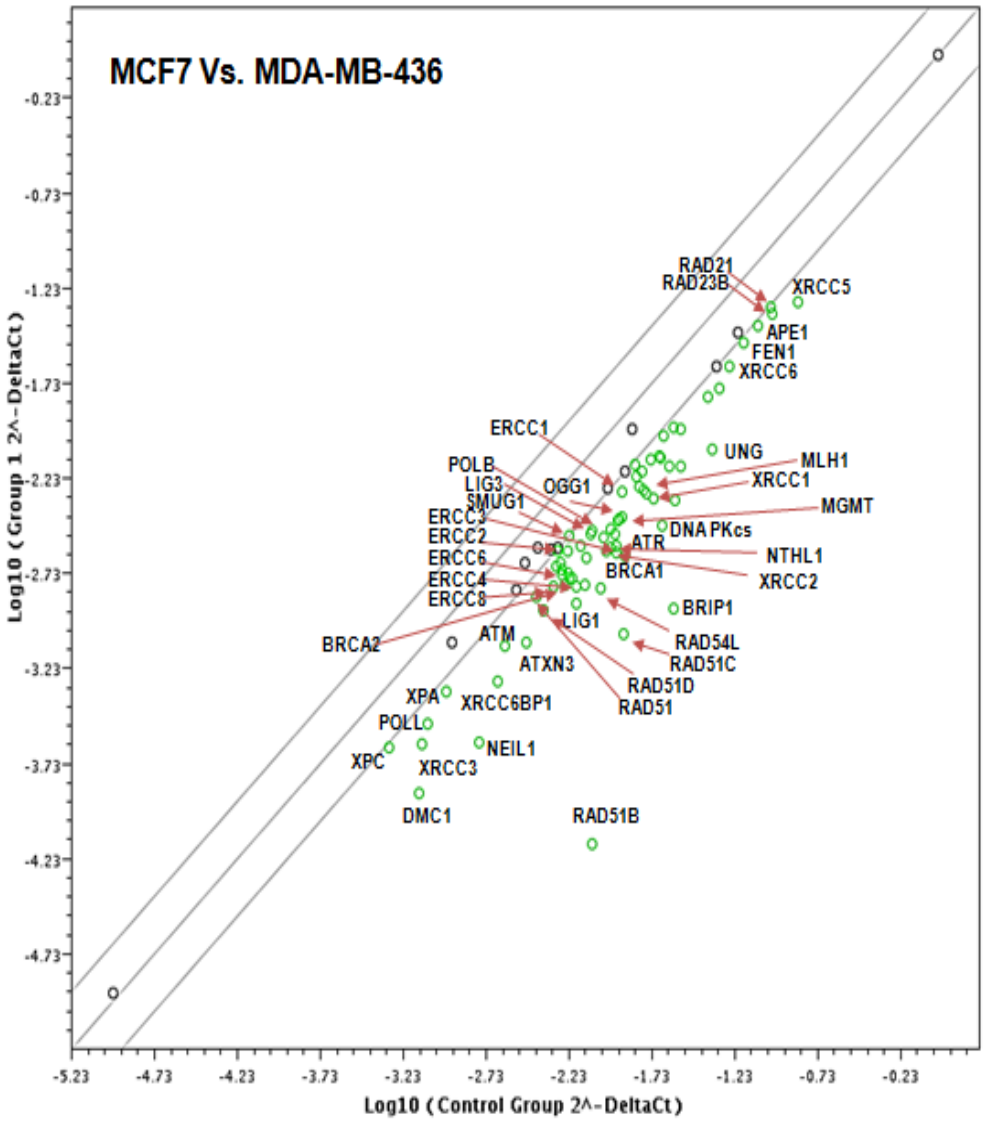

Figure 3.11. Scatter plot comparing DNA repair gene expression in BRCA1 deficient MDA-MB-436 cells against Control BRCA1 proficient MCF7 cells.

The area outside the grey lines indicates two-fold change in gene expression in BRCA1 deficient MDA-MB-436 cells compared to Control BRCA1 proficient MCF7 cells. Green circles indicate gene under-expression. Data are from 3 independent experiments.

	Fold Change	*P Value*	*Fold Change*	*P Value*
Base Excision Repair pathway				
	BRCA1 HeLa cells compared to Control HeLa cells.		***MDA-MB-436 cells compared to MCF7 cells***	
APE1	**0.9409**	0.884684	**0.3727**	0.129971
APE2	**1.3159**	0.513565	**0.4227**	0.186305
PARP1	**0.867**	0.734063	**0.3466**	0.104084
PARP2	**0.5142**	0.113767	**0.4542**	0.225598
PARP3	**0.6157**	0.24867	**0.74**	0.643637
Pol ß	**0.4801**	0.081162	**0.3508**	0.108061
SMUG1	**0.8477**	0.694167	**0.3244**	0.084292
NTHL1	**0.7368**	0.467355	**0.1743**	0.007565
UNG	**0.6014**	0.2264	**0.1367**	0.002386
FEN1	**0.9652**	0.932845	**0.3687**	0.125779
OGG1	**0.8994**	0.800667	**0.2696**	0.044589
NEIL1	**0.1794**	**4.97E-05**	**0.1284**	0.001735
NEIL2	**1.0452**	0.916272	**0.4597**	0.232758
NEIL3	**0.7661**	0.525954	**0.172**	0.007128
XRCC1	**0.46**	0.065009	**0.2161**	0.019016
CCNO	**0.6362**	0.281997	**0.5398**	0.343677
LIG3	**0.5202**	0.120232	**0.2258**	0.022699
MUTYH	**0.5441**	0.147802	**0.3013**	0.065909

Table 3.3. Base excision repair genes under-expressed in BRCA1 deficient cell lines compared to BRCA1 proficient cell lines.

Statistical significance determined using the Bonferroni correction for multiple testing, with p values less than 0.05 (threshold $p < 0.000595 = 0.05/84$).

	Fold Change	*P Value*	*Fold Change*	*P Value*
Homologous recombination pathway				
	BRCA1 HeLa cells compared to Control HeLa cells.		***MDA-MB-436 cells compared to MCF7 cells***	
BRCA1	**0.2858**	0.002997	**0.1102**	0.000774
BRCA2	**0.8036**	0.602818	**0.1888**	0.010779
RAD21	**0.7465**	0.486529	**0.3336**	0.092238
RAD50	**0.598**	0.221385	**0.4154**	0.177557
RAD51	**0.4348**	0.047867	**0.1967**	0.01287
RAD51B	**0.5634**	0.17243	**0.0035**	**1.35E-16**
RAD51C	**0.6507**	0.306534	**0.0366**	**6.01E-07**
RAD51D	**0.2415**	0.000771	**0.2555**	0.036586
RAD54L	**0.569**	0.179889	**0.1526**	0.004084
RAD52	**0.4867**	0.086983	**0.5749**	0.395073
XRCC2	**0.6684**	0.337792	**0.1455**	0.003244
XRCC3	**0.6135**	0.245154	**0.2486**	0.033003
ATM	**0.6491**	0.30388	**0.2646**	0.04166
DMC1	**0.1552**	**1.12E-05**	**0.1049**	**0.000592**

Table 3.4. Homologous recombination genes under-expressed in BRCA1 deficient cell lines compared to BRCA1 proficient cell lines.

Statistical significance determined using the Bonferroni correction for multiple testing, with p values less than 0.05 (threshold $p < 0.000595 = 0.05/84$).

	Fold Change	*P Value*	*Fold Change*	*P Value*
Non-homologous end joining pathway				
	BRCA1 HeLa cells compared to Control HeLa cells.		***MDA-MB-436 cells compared to MCF7 cells***	
DNA-PKcs	**0.3941**	0.027044	**0.1417**	0.00285167
XRCC4	**0.7831**	0.560666	**0.1958**	0.0126124
XRCC5	**0.9085**	0.819398	**0.2602**	0.0391621
XRCC6	**0.966**	0.934363	**0.3028**	0.0670124
XRCC6BP1	**1.2011**	0.662691	**0.1237**	0.00143637
LIG4	**0.8472**	0.692972	**0.225**	0.0223933

Table 3.5. Non-homologous end joining genes under-expressed in BRCA1 deficient cell lines compared to BRCA1 proficient cell lines.

Statistical significance determined using the Bonferroni correction for multiple testing, with p values less than 0.05 (threshold $p < 0.000595 = 0.05/84$).

	Fold Change	*P Value*	*Fold Change*	*P Value*
Nucleotide Excision repair pathway				
	BRCA1 HeLa cells compared to Control HeLa cells.		***MDA-MB-436 cells compared to MCF7 cells***	
BRIP1	**0.6094**	0.238695	**0.0207**	**6.21E-09**
LIG1	**0.8041**	0.603755	**0.138**	0.002504
ATXN3	**0.5322**	0.133711	**0.167**	0.006227
RAD23A	**0.3338**	0.009237	**0.3472**	0.104664
RAD23B	**1.1663**	0.71429	**0.3608**	0.117858
RPA1	**0.8723**	0.745059	**0.3048**	0.068525
CCNH	**0.8436**	0.685694	**0.3193**	0.079999
CDK7	**0.9395**	0.881941	**0.3411**	0.099029
DDB1	**0.9989**	0.997897	**0.4437**	0.212276
DDB2	**0.6038**	0.230168	**0.0931**	**0.000303**
PNKP	**0.513**	0.112515	**0.2365**	0.027241
POLL	**0.3423**	0.010967	**0.331**	0.089917
RPA3	**0.3167**	0.006392	**0.2927**	0.059662
SLK	**0.6866**	0.37098	**0.4019**	0.161845
ERCC1	**0.4388**	0.050344	**0.3989**	0.15841
ERCC2	**0.5797**	0.19469	**0.4072**	0.167956
ERCC3	**0.8955**	0.792752	**0.2168**	0.019293
ERCC4	**0.677**	0.353311	**0.1761**	0.00792
ERCC5	**0.7557**	0.505017	**0.7899**	0.717002
ERCC6	**0.7167**	0.428061	**0.314**	0.075715
ERCC8	**0.6865**	0.370706	**0.2744**	0.047489
XAB2	**0.7547**	0.503003	**0.4005**	0.160214
XPA	**0.8541**	0.707449	**0.2709**	0.045366
XPC	**0.6286**	0.269452	**0.348**	0.105382

Table 3.6. Nucleotide excision repair genes under-expressed in BRCA1 deficient cell lines compared to BRCA1 proficient cell lines.

Statistical significance determined using the Bonferroni correction for multiple testing, with p values less than 0.05 (threshold $p < 0.000595 = 0.05/84$).

	Fold Change	*P Value*	*Fold Change*	*P Value*
Mismatch repair pathway				
	BRCA1 HeLa cells compared to Control HeLa cells.		***MDA-MB-436 cells compared to MCF7 cells***	
POLD3	**0.6115**	0.24197	**0.2132**	0.018015
PMS1	**0.4435**	0.053395	**0.266**	0.04247
PMS2	**0.7229**	0.439965	**0.3196**	0.080299
MLH1	**0.7251**	0.444321	**0.2236**	0.021839
MSH2	**0.8477**	0.694213	**0.3276**	0.086968
MLH3	**0.6227**	0.259804	**0.2389**	0.028331
MSH3	**0.7749**	0.543888	**0.2801**	0.051116
MSH4	**0.3285**	0.00828	**0.6991**	0.582307
MSH5	**0.3414**	0.010783	**0.1551**	0.004409
MSH6	**0.6342**	0.27871	**0.3555**	0.112648
MPG	**0.7868**	0.568232	**0.2445**	0.031002
TREX1	**0.8607**	0.721094	**0.7439**	0.649341

Table 3.7. Mismatch repair genes under-expressed in BRCA1 deficient cell lines compared to BRCA1 proficient cell lines.

Statistical significance determined using the Bonferroni correction for multiple testing, with p values less than 0.05 (threshold $p < 0.000595 = 0.05/84$).

3.3.5. DNA repair protein expression is down-regulated in BRCA1 deficient cell lines compared to BRCA1 proficient cell lines.

The RT² Profiler™ Array suggested reduced expression of several mRNAs involved in BER, HR, NHEJ, NER and MMR in BRCA1 deficient cell lines as compared to BRCA1 proficient cell lines. As discussed previously (section 3.1.2.) selected DNA repair factors (APE1, XRCC1, SMUG1, Pol ß, Lig3, ATM and DNA-PKcs) will be investigated. To determine the protein expression of these factors, western blots were performed as described in section 2.3.9. Western blots results of BER, HR and NHEJ factors are shown in Figure 3.12 and Figure 3.13. Reduced expression of XRCC1, APE1, SMUG1, Pol ß and lig3, along with both ATM and DNA-PKcs proteins were

observed in BRCA1 deficient cell lines as compared to BRCA1 proficient cell lines.

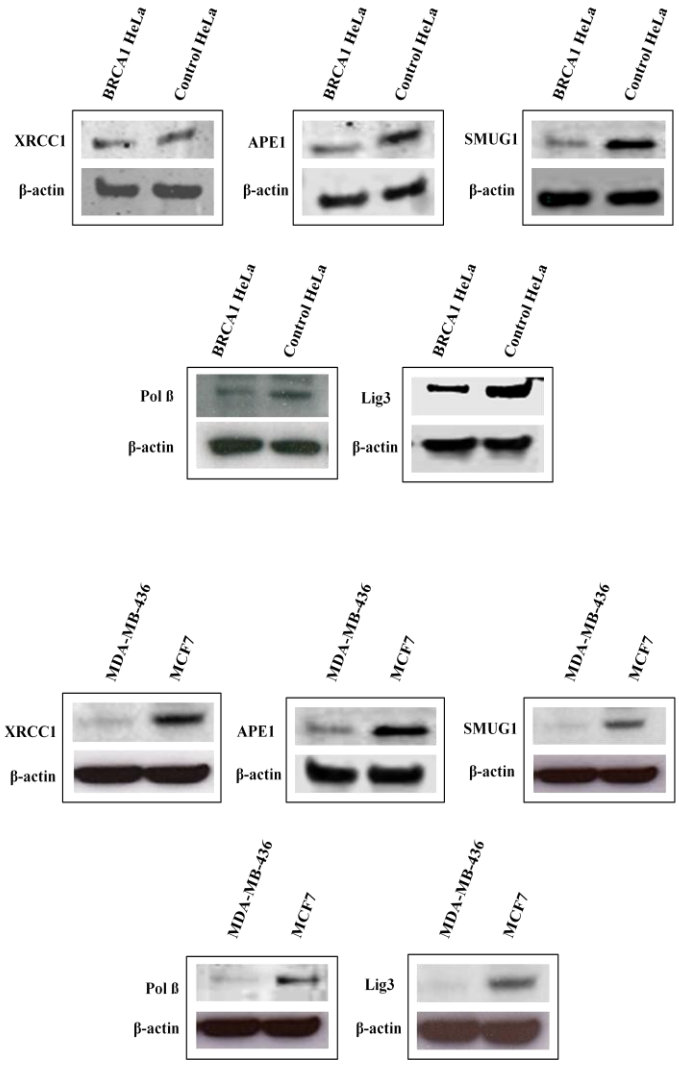

Figure 3.12. Representative western blot analysis of Base Excision Repair proteins in BRCA1 deficient and proficient cell lines.

BER Proteins (XRCC1, APE1, SMUG1, Pol ß and Lig3) expression shows down-regulation in BRCA1 deficient cell lines (BRCA1 HeLa and MDA-MB-436) compared to BRCA1 proficient cell lines (Control HeLa and MCF7). Whole cell protein lysates were collected for each cell line and 25 or 50 µg samples were separated by electrophoresis on denaturing polyacrylamide gels as described in section 2.3.9. Blot was probed using specific antibodies with predicted molecular weight (XRCC1, 80 kDa; APE1, 37 kDa; SMUG1, 37 kDa; Pol ß, 38 kDa and Lig3, 113 kDa). As a loading control, β-actin antibody (42 kDa) was used.

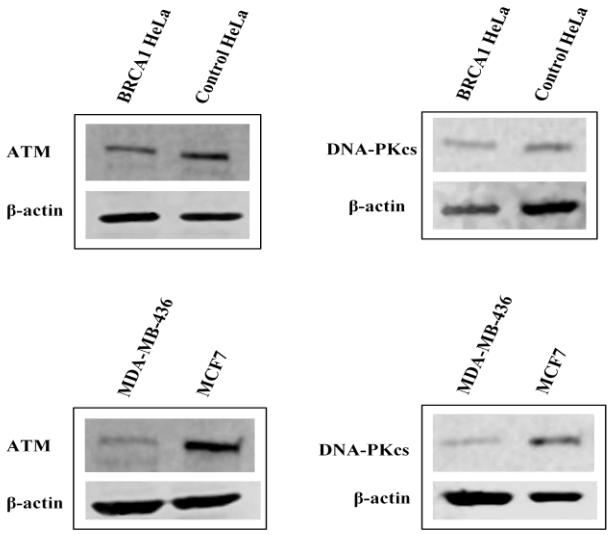

Figure 3.13. Representative western blot analysis of ATM and DNA-PKcs expression.

ATM and DNA-PKcs are down-regulated in BRCA1 deficient cell lines (BRCA1 HeLa and MDA-MB-436) compared to BRCA1 proficient cell lines (Control HeLa and MCF7). Whole cell protein lysates were collected for each cell line and 25 or 50 µg samples were separated by electrophoresis on denaturing polyacrylamide gels as described in section 2.3.9. Blot was probed using specific antibodies with predicted molecular weight (ATM, 350 kDa and DNA-PKcs, 460 kDa). As a loading control, β-actin antibody (42 kDa) was used.

3.3.6. Quantitative real time PCR (RT-qPCR) in BRCA1 deficient and BRCA1 proficient cells.

Quantitative real time PCR (RT-qPCR) using QuantiTect® Primers (Qiagen, UK) was performed as described in section 2.3.8.5 for the selected DNA repair factors; BRCA1, APE1, XRCC1, SMUG1, Pol ß, Lig3, ATM and DNA-PKcs (discussed previously section 3.1.2.). mRNA expression is shown in Table 3.8

for breast cancer cell lines and mRNA expression for HeLa cell lines is shown in Table 3.9.

	Fold Change	*P Value*
APE1	**0.0716**	0.0057
XRCC1	**0.0406**	0.0007
SMUG1	**0.0533**	0.0029
Pol ß	**0.2487**	0.0.033
Lig3	**0.2720**	0.0257
ATM	**0.0165**	0.0002
DNA-PKcs	**0.0584**	0.0019
BRCA1	**0.0938**	0.0026

Table 3.8. Quantitative real time PCR (RT-qPCR) for multiple DNA repair genes in BRCA1 deficient cells.

DNA repair mRNA expression in MDA-MB-436 compared to MCF7 cells. Statistical significance determined using t test, with p values less than 0.05.

	Fold Change	*P Value*
APE1	**0.3622**	0.0081
XRCC1	**0.3150**	0.0151
SMUG1	**0.5100**	0.0469
Pol ß	**0.3100**	0.0166
Lig3	**0.5678**	0.0004
ATM	**0.2750**	0.0285
DNA-PKcs	**0.2300**	0.0454
BRCA1	**0.1627**	0.0015

Table 3.9. Quantitative real time PCR (RT-qPCR) for multiple DNA repair genes in BRCA1 deficient cells.

DNA repair mRNA expression in BRCA1 HeLa cells compared to Control HeLa cells. Statistical significance determined using t test, with p values less than 0.05.

3.3.7. Quantification of DNA repair mRNA and protein expression in BRCA1 deficient and BRCA1 proficient cells.

Relative quantification of mRNA and protein expression for XRCC1, APE1, SMUG1, Pol ß, Lig3, ATM and DNA-PKcs was performed. BRCA1 HeLa cells, expressed relatively low DNA repair factors compared to Control HeLa cells, as demonstrated in Figure 3.14 and Figure 3.16. MDA-MB-436 cells expressed relatively low DNA repair factors compared to MCF7 cells, as demonstrated in Figure 3.15 and Figure 3.17.

Western blot results were analysed using Image Studio (Li-Cor, Lincoln, USA) as described in section 2.3.9.8. RT-qPCR results were analysed as described in section 2.3.8.6. These assays were performed in two or more independent experiments. The student t-test was used to investigate the difference in expression of DNA repair proteins between BRCA1 proficient and BRCA1 deficient cell lines.

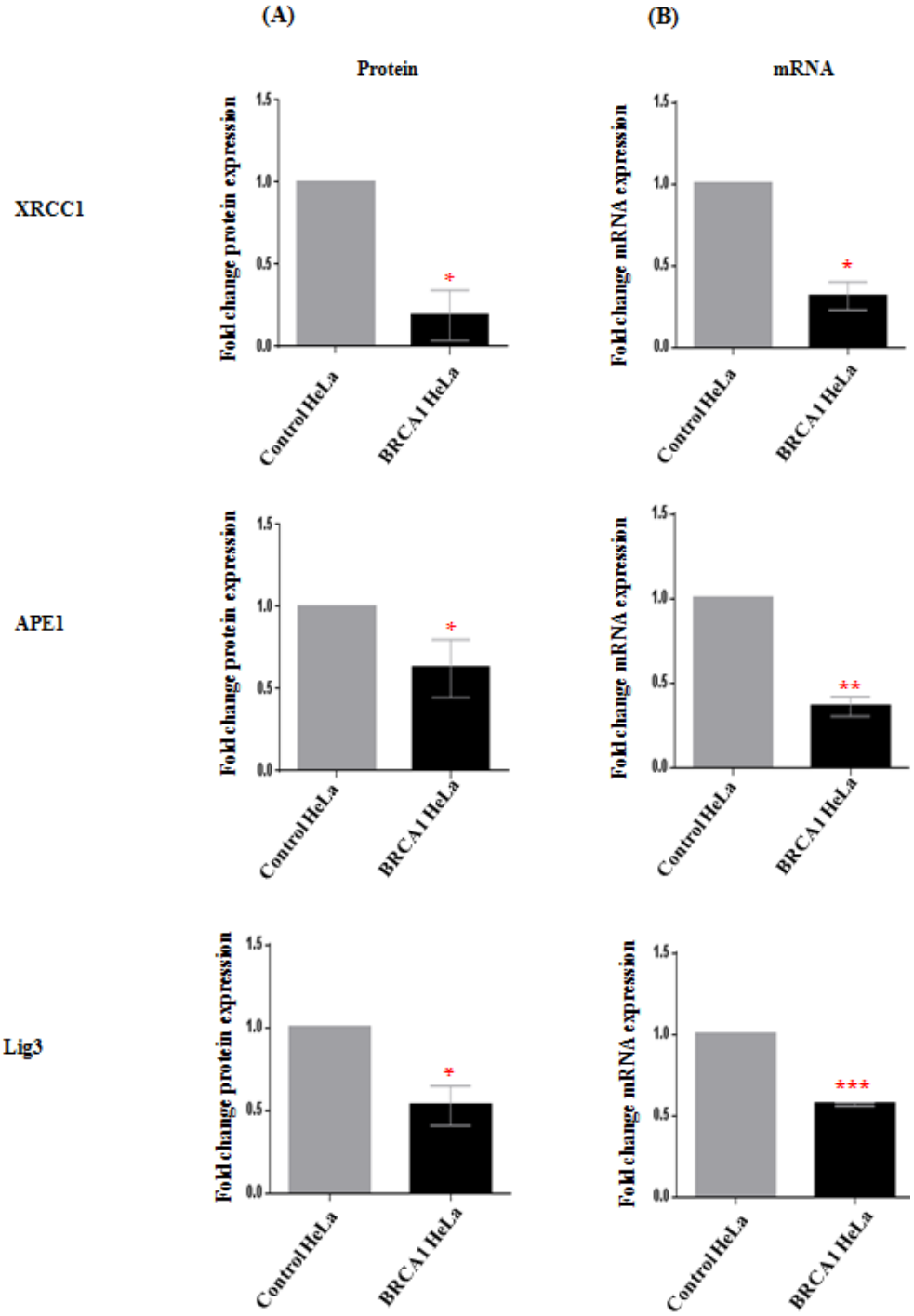
(A)
Protein
(B)
mRNA
XRCC1
APE1
Lig3
Fold change protein expression
Fold change mRNA expression
1.5
1.0
0.5
0.0
*
**
***
Control HeLa
BRCA1 HeLa

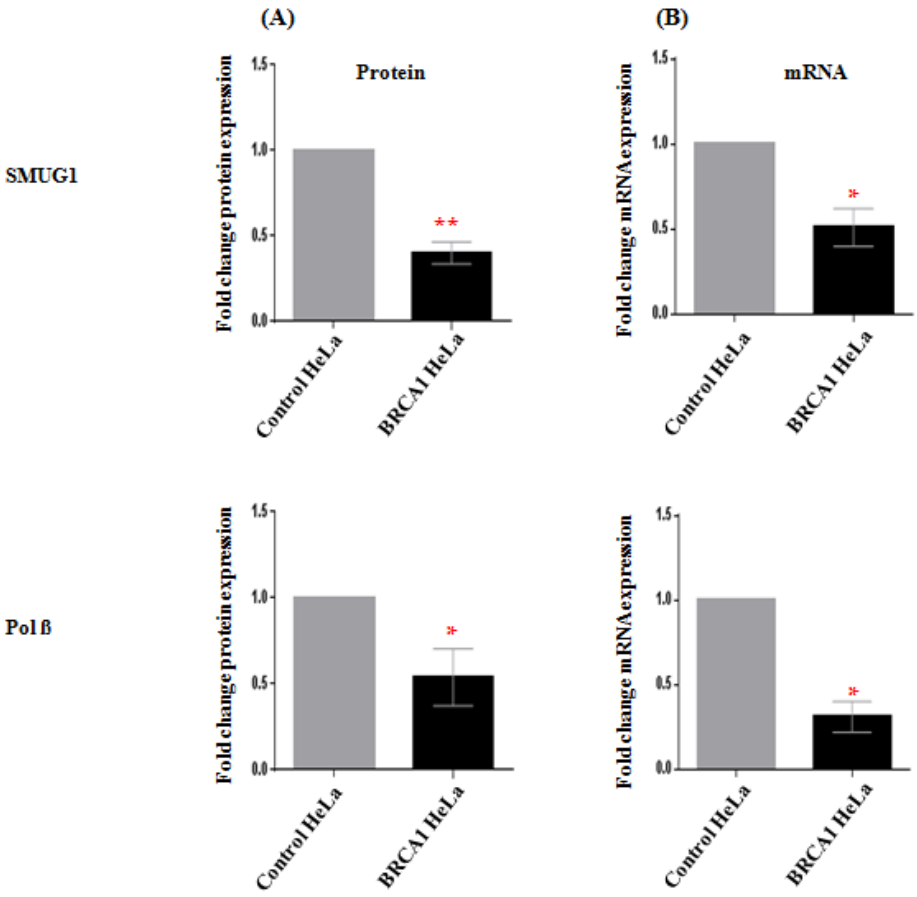

Figure 3.14. Quantification of Base Excision Repair proteins expression (left) and quantitative real time PCR (RT-qPCR) showing mRNA expression (right) in BRCA1 deficient and proficient HeLa cell lines.

(A) Showing protein expression, values plotted are means ± SD of the fold-change (ratio of protein/ß-actin normalized to control) and **(B)** mRNA expression, values plotted are means ± SD of the fold-change (ratio of mRNA/GAPDH normalized to control). * $p<0.05$, ** $p<0.01$ and *** $p<0.001$, p value was assessed by t-test compared to Control HeLa cell line. Graphs were produced and statistical analysis performed using GraphPad prism.

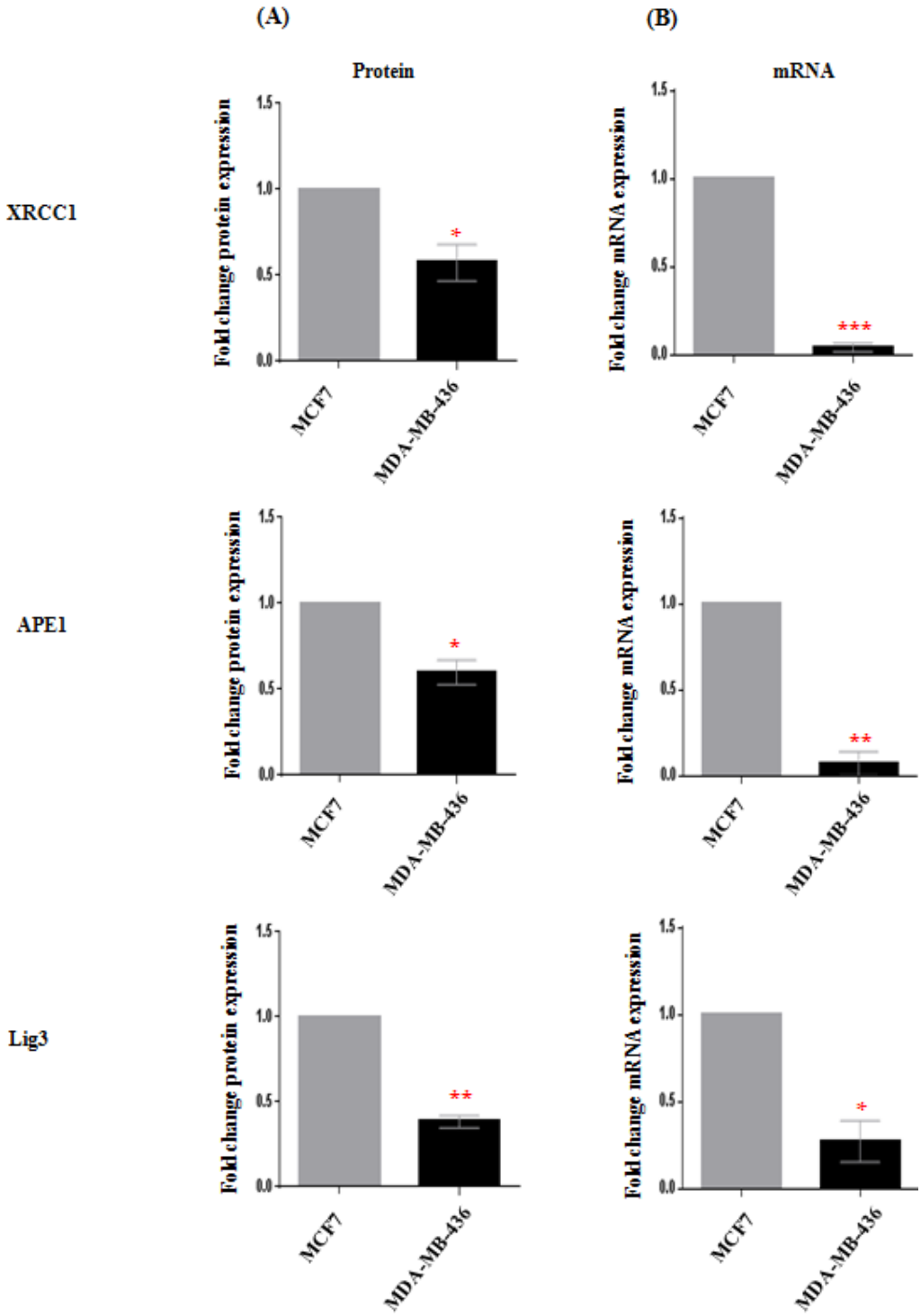
(A)
Protein
(B)
mRNA
XRCC1
APE1
Lig3
Fold change protein expression
Fold change mRNA expression
1.5
1.0
0.5
0.0
*
**
***
MCF7
MDA-MB-436

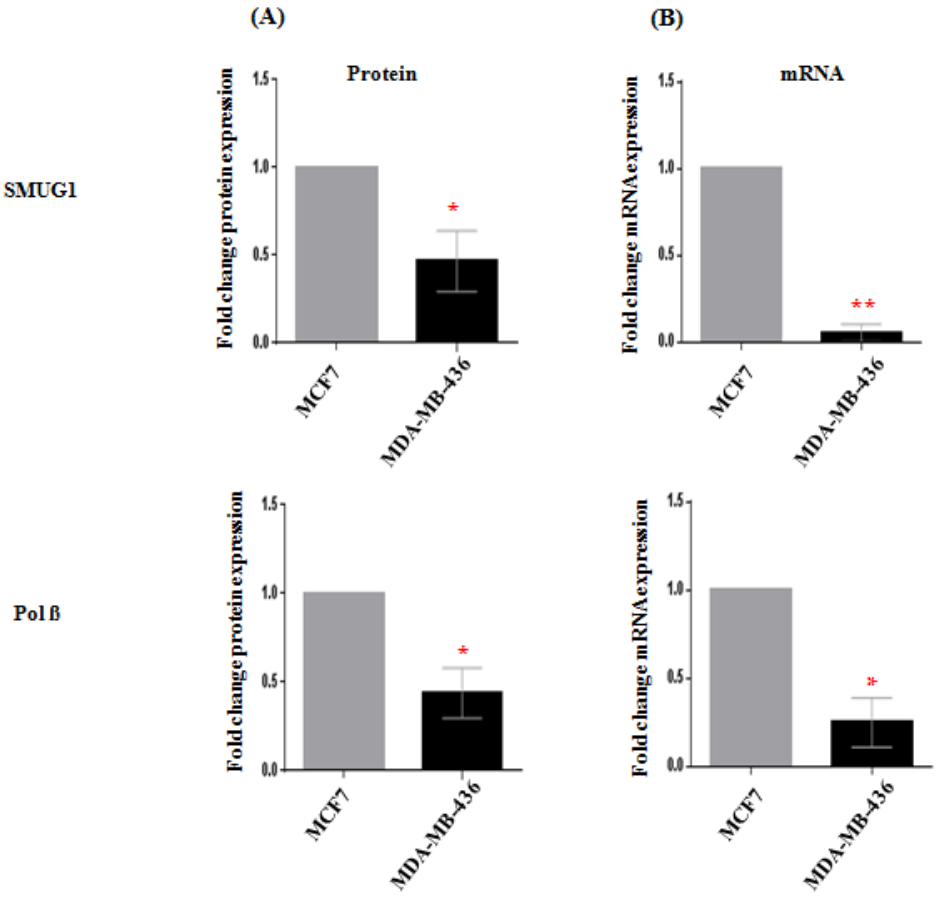

Figure 3.15. Quantification of Base Excision Repair proteins expression (left) and quantitative real time PCR (RT-qPCR) showing mRNA expression (right) in BRCA1 deficient and proficient breast cancer cell lines.

(A) Showing protein expression, values plotted are means ± SD of the fold-change (ratio of protein/ß-actin normalized to control) and **(B)** mRNA expression, values plotted are means ± SD of the fold-change (ratio of mRNA/GAPDH normalized to control). * $p<0.05$, ** $p<0.01$ and *** $p<0.001$, p value was assessed by t-test compared to MCF7 cell line. Graphs were produced and statistical analysis performed using GraphPad prism.

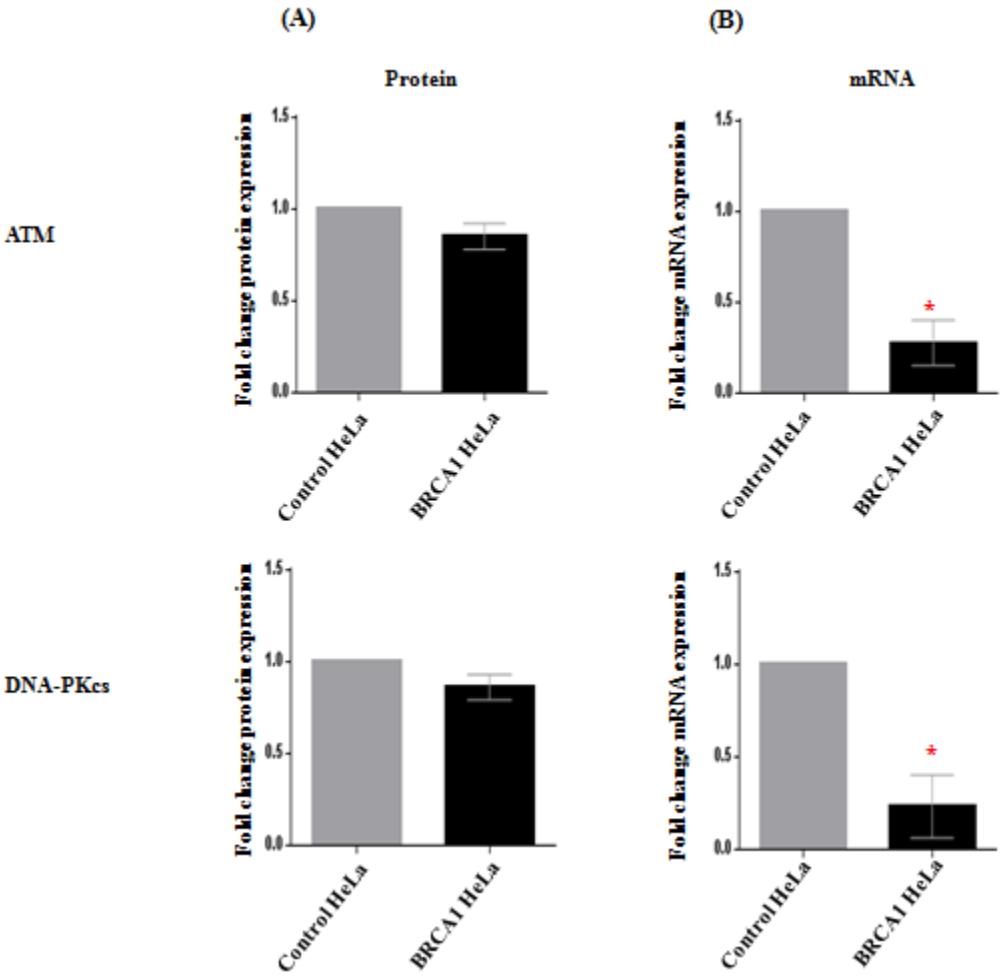

Figure 3.16. Quantification of ATM and DNA-PKcs protein (left) and quantitative real time PCR (RT-qPCR) showing mRNA expression (right) in BRCA1 deficient and proficient HeLa cell lines.

(A) Showing protein expression, values plotted are means ± SD of the fold-change (ratio of protein/ß-actin normalized to control) and **(B)** mRNA expression, values plotted are means ± SD of the fold-change (ratio of mRNA/GAPDH normalized to control). * $p<0.05$, p value was assessed by t-test compared to Control HeLa cell line. Graphs were produced and statistical analysis performed using GraphPad prism.

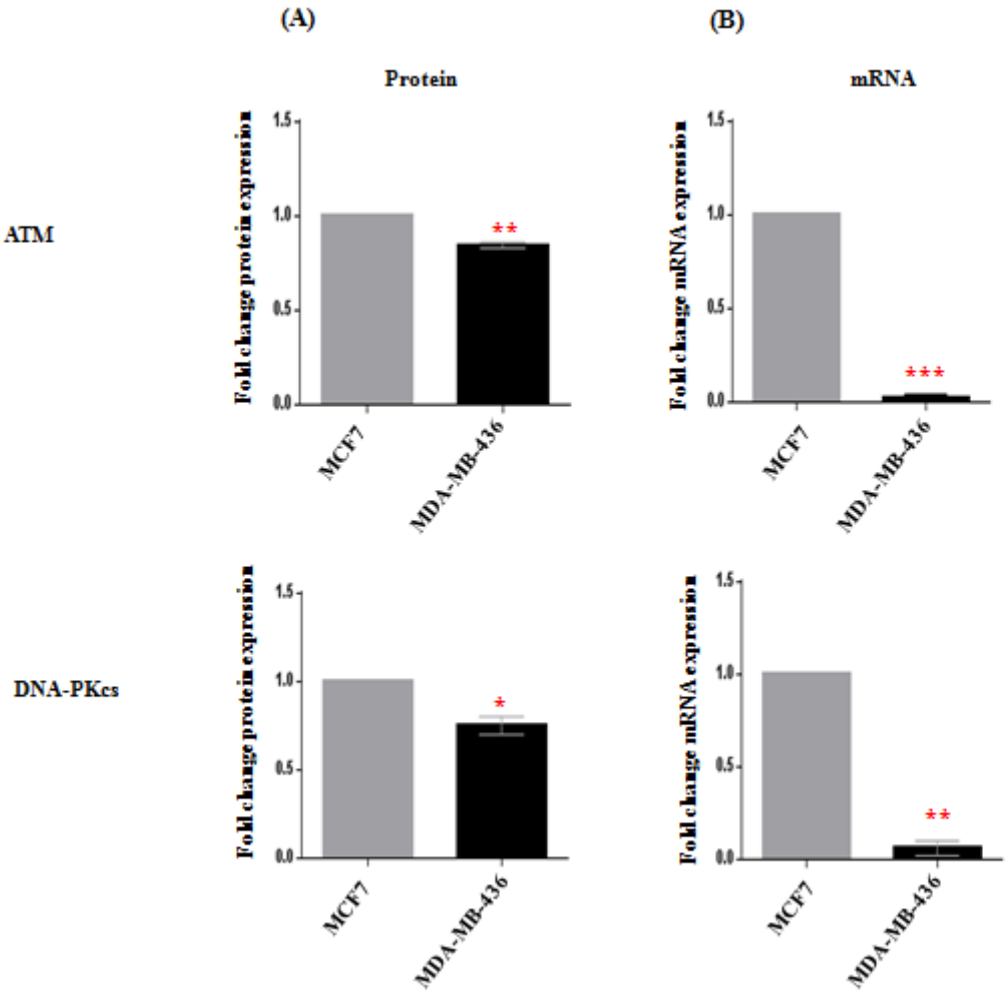

Figure 3.17. Quantification of ATM and DNA-PKcs protein expression (left) and quantitative real time PCR (RT-qPCR) showing mRNA expression (right) in BRCA1 deficient and proficient breast cancer cell lines.

(A) Showing protein expression, values plotted are means ± SD of the fold-change (ratio of protein/ß-actin normalized to control) and **(B)** mRNA expression, values plotted are means ± SD of the fold-change (ratio of mRNA/GAPDH normalized to control). * $p<0.05$, ** $p<0.01$ and *** $p<0.001$, p value was assessed by t-test compared to MCF7 cell line. Graphs were produced and statistical analysis performed using GraphPad prism.

3.3.8. Growth inhibition MTS assay in response to MMS

BRCA1 deficient cells demonstrate low BER factors as shown. To test whether low BER expression confers phenotypic consequence, MMS (alkylating agent) in BRCA1 proficient and deficient cells was investigated. MTS assay was used to determine cell growth inhibition in response to MMS treatment (0.00 µM to 800 µM) for 72 hours in BRCA1 mutated MDA-MB-436 cells and control MCF7 cells. As shown in Figure 3.18, BRCA1 mutated MDA-MB-436 cells were more sensitive to MMS than control MCF7 cells. The data concurs with a previous study by Masaoka *et al*, who demonstrated similar MMS sensitivity in BRCA1 deficient cells (Masaoka et al., 2013).

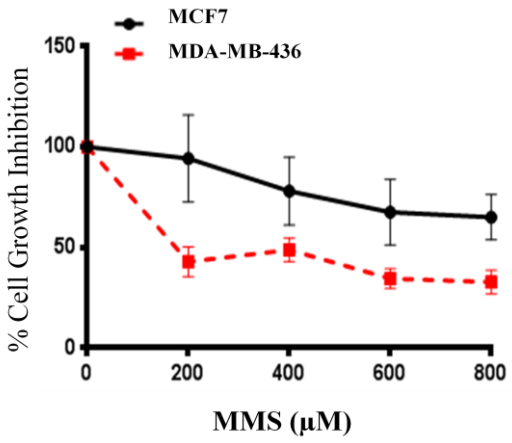

Figure 3.18. MMS treatment in BRCA1 deficient and proficient cells.

BRCA1 deficient cells exhibited decreased cell growth after exposure for 72 hours to MMS, compared to BRCA1 proficient cell line. Data are shown as the mean and SD values for each concentration from 2 independent experiments.

3.4. Discussion and conclusions

3.4.1. Loss of BRCA1 expression links to a global reduction in mRNA and proteins involved in Base excision repair pathway

In a recent publication, BRCA1 has been suggested to stimulate the activity of three BER enzymes; OGG1 (8-oxoguanine DNA glycosylase), NTH1 (homolog of endonuclease III), and APE1 (apex nuclease 1). These enzymes mediate repair of three signature oxidative lesions; 8-oxoguanine, thymine glycol and abasic sites, respectively (Saha et al., 2010). A more recent study supports these findings, and has confirmed down-regulation of APE1, NTH1, OGG1 as well as XRCC1 in BRCA1 mutated and sporadic breast cancers (De Summa et al., 2014). XRCC1 protein associates with Pol ß, and Lig3, to form a complex that repairs the single strand DNA breaks generated during the BER process (Saha et al., 2010). Other studies suggest a cross talk between BRCA1 and other BER genes e.g. Pol ß and SMUG1 (Masaoka et al., 2013, Abdel-Fatah et al., 2013), highlighting additional BER factors that may be associated with BRCA1 expression. For these reasons in the current study BER factors; APE1, XRCC1, SMUG1, Pol ß and Lig3 were investigated. To achieve this, the RT² Profiler™ Array was conducted first to investigate 84 DNA repair genes in BRCA1 deficient cell lines as compared to BRCA1 proficient cell lines. However, the establishment of a statistical significance threshold that adequately controls the proportion of false-positive findings is not a trivial issue. Therefore, due to the sample size and number of arrays statistical significance was determined using a Bonferroni correction to adjust for multiple testing, with corrected p values set at less than 0.05 (threshold $p <$

0.000595 = 0.05/84). Thus, the current RT² Profiler array results did not always reach statistical significance and further independent replicates are required. Further assessment of the results was carried out using quantitative real time PCR (RT-qPCR) for the selected DNA repair genes as discussed above. Finally, the mRNA expression of the selected genes was compared with protein expression using western blot.

In the current study, expression of several BER mRNAs were found to be down-regulated in both BRCA1 mutant/knockdown cell lines (see Table 3.3); low mRNA expression was demonstrated for *APE1*, *OGG1* and *NTHL1* genes which was consistent with the results published by Saha *et al*. mRNAs of the selected BER genes also showed down-regulation. Interestingly many other BER mRNAs showed down-regulation including; *PARP1*, *PARP2*, *PARP3*, *NEIL1*, *NEIL3*, *UNG*, *FEN1*, *MUTYH* and *CCNO*. Targeted assessment in individual primer assays may be useful to further assess these genes. Conversely, individual RT-qPCR analysis for *XRCC1*, *APE1*, *LIG3*, *SMUG1* and *Pol ß* mRNA expression demonstrated significant reduction in both mutant/knockdown BRCA1 cell lines as compared to proficient BRCA1 cell lines (see Table 3.8 and Table 3.9). This reduction was linked to reduction in protein expression (see Figure 3.14 and Figure 3.15). These results suggest that there may be impairment in key BER factors in BRCA1 deficient cells, which may cause different types of unrepaired single strand breaks.

3.4.1.1. BRCA1 deficient cell lines are hypersensitive to MMS

In this section of the study the efficacy of the alkylating agent in DNA damage formation in BRCA1 deficient and proficient cells was investigated.

Methyl methane sulphonate (MMS) is an alkylating agent, damage induced by MMS is repaired by BER pathway. MMS acts by methylating DNA on N7-deoxyguanosine and N3-deoxyadenosine, creating adducts that are substrates for BER. At high concentrations of MMS, the frequency of methylation events overwhelms BER capacity and induce replication fork stalling, resulting in cytotoxic levels of DSB formation (Stevnsner et al., 1993, Masaoka et al., 2013). A number of studies have shown that BRCA1/BER deficient cell lines were hypersensitive to MMS compared to their wild type matched controls (Bridge et al., 2005, Masaoka et al., 2013). In this study MMS was confirmed to be selectively toxic to BRCA1/BER mutated human cancer cell line (MDA-MB-436) compared to MCF7 proficient cell line by using MTS assay. This result suggests impairment in BER. However, measuring BER efficiency should be conducted in BRCA1 deficient cell lines in the future studies.

3.4.2. Loss of BRCA1 expression is associated with reduction in expression of Homologous recombination factors

The first report of a role for BRCA1 in genomic stability and double strand break repair, by Scully and colleagues, suggested a functional interaction between BRCA1 and RAD51 in both the meiotic and mitotic cell cycles. This in turn suggests an important role for BRCA1 in controlling genomic stability (Scully et al., 1997). This association was corroborated by a later report by Chen and colleagues, who observed the presence of both BRCA1 and RAD51 on the damaged DNA site in meiotic cells (Chen et al., 1998). This finding was followed by the first functional evidence for the role of BRCA1 in HR repair pathway through its direct interaction with RAD51 (Moynahan et al., 1999).

Subsequent observations that agents causing recombinogenic lesions like cisplatinum and ionizing radiation, do not induce formation of RAD51 foci in BRCA1 deficient cells, suggesting that disruption of BRCA1 was associated with markedly reduced expression of RAD51 (Bhattacharyya et al., 2000, Bindra et al., 2004). In the current study, reduced BRCA1 expression in mutant/knockdown cell lines was associated with a reduction in *RAD51* expression at mRNA (see Table 3.4) in both mutant/knockdown cell lines. Several other HR mRNA expressions were also observed to be down-regulated in both mutant/knockdown cell lines; low mRNA expression was demonstrated for RAD51 related family (*RAD51B*, *RAD51C* and *RAD51D*), *RAD50*, *RAD52*, *XRCC3*, *BRCA2* and *DMC1*. In addition, *RAD54L* and *XRCC2* were also down-regulated in both mutant/knockdown cell lines. Recently, RAD21 has been suggested as a potential *BRCA1* mutation status dependent predictive and prognostic marker in familial breast cancer (Yan et al., 2012). In the present study low mRNA expression of *RAD21* in both mutant/knockdown cell lines was demonstrated. ATM is believed to be the first sensor in DSB and a key player in HR pathway. ATM activates multiple genes involved in HR repair, cell cycle arrest and apoptosis. Substrates for ATM phosphorylation include; BRCA1, p53, CHK2, histone H2AX and MRN complex (Bakkenist and Kastan, 2004). In this study low mRNA expression of *ATM* in BRCA1 mutant/knockdown cell lines was demonstrated using RT^2-PCR array. Then *ATM* was assessed in individual RT-qPCR which showed significant mRNA reduction in both mutant/knockdown BRCA1 cell lines compared to proficient BRCA1 cell lines (see Table 3.8 and Table 3.9). Gene expression was associated with protein expression for ATM (see Figure 3.16 and Figure 3.17).

Taken together, these results suggest that BRCA1 deficiency may associate with a global defect in HR repair expression. However, individual primer assays may be useful to further assess these genes.

3.4.3. Loss of BRCA1 expression is associated with reduction in expression of Non-homologous end joining factors

BRCA1 interacts with the Rad50/Mre11/Nbs1 complex that occupies a central role in DNA double-strand break repair mediated by HR and NHEJ. Zhong and colleagues suggested a BRCA1 role in NHEJ. They investigated Brca1-deficient mouse embryonic fibroblasts cell extracts and found that it exhibit reduced end-joining activity independent of the endogenous protein amounts of DNA LIG4, KU80 (known as XRCC5), and KU70 (known as XRCC6) (Zhong et al., 2002). In the current study, reduced BRCA1 expression in mutant/knockdown cell lines was associated with a reduction in *LIG4*, *XRCC5* and *XRCC6* expression at mRNA confirming Zhong *et al* results (see Table 3.5). In addition, *XRCC4* show down-regulation at the mRNA expression in mutant/knockdown cell lines. DNA-PKcs is known to have a critical role in NHEJ pathway. Recently, Shang and colleagues reported that DNA-PKcs is the upstream regulator of the CHK2–BRCA1 pathway (Shang et al., 2014). In this study low mRNA expression of *DNA-PKcs* was demonstrated in mutant/knockdown cell lines by RT^2-PCR array (see Table 3.5). Then *DNA-PKcs* was assessed in individual RT-qPCR which showed significant mRNA reduction in both mutant/knockdown BRCA1 cell lines compared to proficient BRCA1 cell lines (see Table 3.8 and Table 3.9). Also,

gene expression was consistent with protein expression in DNA-PKcs (see Figure 3.16 and Figure 3.17). Taken together, these results suggest that BRCA1 deficiency is associated with impairment in NHEJ expression.

3.4.4. Loss of BRCA1 expression is associated with reduction in expression of other DNA repair factors

BRCA1 has been suggested to control Nucleotide excision repair (NER), through the p53 protein which regulates NER by transcriptional regulation of genes involved in the recognition of adducts in genomic DNA. Loss of p53 function results in deficient global genomic repair (GGR), a subset of NER that targets and removes lesions from the whole genome. BRCA1 specifically enhances the GGR pathway, independent of p53, and can induce p53-independent expression of the NER genes *XPC*, *DDB2*, and *GADD45* (Hartman and Ford, 2002). In the current study, reduced BRCA1 expression in mutant/knockdown cell lines was associated with a reduction in *XPC* and *DDB2* expression at mRNA consistent with the data published by Hartman and Ford (see Tabel 3.6). In addition, a panel of NER factors also shows down-regulation at the mRNA expression. For instance; *CCNH*, *RPA3*, *ERCC1*, *ERCC4*, *ERCC6*, *ERCC8*, *BRIP1*, *LIG1*, *ATXN3*, *RAD23A*, *RPA1*, *CDK7*, *DDB1*, *DDB2*, *PNKP*, *POLL*, *SLK*, *ERCC2*, *ERCC3*, *ERCC5*, *XAB2* and *XPA*.

The role of BRCA1 in MMR pathway is still not understood, however recently a report by Song and colleagues demonstrated that mutation in *BRCA1* was followed by mutation in *MSH6* and *MSH2* (Song et al., 2014). In the current

study, reduced BRCA1 expression in mutant/knockdown cell lines was associated with a reduction in *MSH6* and *MSH2* expression at mRNA supporting Song *et al* results (see Table 3.7). Moreover, a panel of MMR mRNA expressions were observed to be down-regulated in both mutant/knockdown cell lines including; *POLD3*, *PMS1*, *PMS2*, *MLH1*, *MLH3*, *MSH3*, *MSH4*, *MSH5*, *MPG* and *TREX1*. These results suggest that BRCA1 deficiency may associate with a global defect in NER and MMR expression. However, further investigation is needed to measure the efficiency of these pathways.

Taken together, the main aim of this chapter was to investigate a potential impairment in DNA repair pathways within BRCA1 deficient cells. To achieve this, RT² Profiler™ Array was conducted first to investigate 84 DNA repair genes in BRCA1 deficient cell lines compared to BRCA1 proficient cell lines. Data demonstrated down-regulation in several DNA repair mRNAs however; the results did not always give statistical significance. Further assessment of the results was carried out using quantitative real time PCR (RT-qPCR) for selected DNA repair genes (*APE1*, *XRCC1*, *SMUG1*, *Pol ß*, *Lig3*, *ATM* and *DNA-PKcs*) which had previously been shown to have a potential link with BRCA1 (Abdel-Fatah et al., 2013, Masaoka et al., 2013, De Summa et al., 2014). Data for individual primers demonstrated statistically significant down-regulation of the selected DNA repair genes. This highlights the difference between the two PCR methods, where both showed consistent down-regulation but data was not statistically significant with the RT² Profiler™ Array. This can have two explanations. Firstly the efficiency, specificity and sensitivity of

primers can differ. Secondly, and more importantly, the average threshold cycle (Ct) should be in the range of 15 to 35 which is considered as a strong positive reaction. Ct values greater than 35 are considered as a weak reaction. Ct value is negatively associated with the concentration of nucleic acids detected. Ct values are classified in subsequent categories of Ct < 25, Ct 25-35 and Ct 35-40. In the present study both Ct values for both PCR methods were in the range of 18 to 33. However the percentage distributions of Ct values were different. In the RT² Profiler™ Array 66% of Ct values were < 25 and 34% between 25 and 35, whereas by RT-qPCR around 90% of Ct values were 25-35 and 10% were < 25. This suggests that the reason for having consistent but not statistically significant results in RT² Profiler™ Array was because of the distribution of the Ct values. It is worth mentioning that a previous study demonstrated similar results when they compared a quantitative RT-PCR array (qPCR-array) with an oligonucleotide microchip (microarray) (Chen et al., 2009). For future work this problem can be avoided by further dilution of the cDNA.

3.4.5. Conclusions

These *in vitro* studies suggested that BRCA1 has been linked to a possible defect in BER, HR, NHEJ, NER and MMR, via mechanisms that are not fully understood. This chapter described the assessment of DNA repair factors expressions in BRCA1 mutant/knockdown cell lines. Selected DNA repair factors (APE1, XRCC1, SMUG1, Pol ß, Lig3, ATM and DNA-PKcs) were observed to be down-regulated at the mRNA and/or protein expression. Taken together, these results suggest that BRCA1 deficiency may be associated with a global defect in DNA repair.

Chapter 4

Targeting BRCA1 deficiency for personalized therapy using ATM inhibitors (KU55933 & KU60019)

4. Targeting BRCA1 deficiency in breast cancer for personalized therapy using ATM inhibitors (KU55933 & KU60019)

4.1. Introduction

BRCA1 facilitates the efficient resolution of DNA double-strand breaks (DSBs) through homologous recombination (HR) (Huen et al., 2010, Caestecker and Van de Walle, 2013). Cells lacking functional BRCA1 protein have impaired HR, and thus are suggested to depend on the more error-prone non-homologous end joining (NHEJ) pathway leading to chromosomal instability that drive breast cancer development (Huen et al., 2010). BER pathway is critical for processing DNA damage caused by alkylation, oxidation, ring saturation, single strand breaks and base deamination (Dianov and Hubscher, 2013).

PARP1 (poly [ADP-ribose] polymerase 1) plays a role in single strand break repair (SSBR), a BER related pathway (Langelier and Pascal, 2013). The DNA repair intermediates generated during SSBR/BER, if unrepaired, may get converted to toxic DSBs (Dianov and Hubscher, 2013). PARP1 inhibition is synthetically lethal in BRCA deficient cells (Farmer et al., 2005, Bryant et al., 2005). Although it should be noted that recent studies illustrated some problems with PARP inhibition (Edwards et al., 2008, Montoni et al., 2013, Fojo and Bates, 2013). For instance, PARP family of enzymes consist of at least 17 members, each one of them has a different structure and function (Rouleau et al., 2010, Mangerich and Burkle, 2011, Underhill et al., 2011). So there are issues with specificity of current inhibitions under development. Moreover, a recent study evaluated a series of 185 inhibitors of PARP,

including the best-known inhibitors being tested clinically such as Olaparib, ABT-888 and Rucaparib, for the specificity to bind to the catalytic domains of 13 of 17 human PARP family members. In this study they determined that the majority of the inhibitors bind to multiple targets (Wahlberg et al., 2012).

Emerging studies suggest a cross talk between BRCA1 and BER factors. BRCA1 mutated and basal-like breast cancer cells were found to be sensitive to oxidative DNA damage induced by hydrogen peroxide (H_2O_2) treatment. The increased sensitivity was associated with defective BER as assessed by cell based BER assay in BRCA1 deficient cells (Alli et al., 2009). In a more recent study, BRCA1 deficient cells were sensitive to alkylating agent Methyl methane sulphonate (MMS) and functional interaction between Pol ß and BRCA1 was demonstrated in that study (Masaoka et al., 2013) implying a potential role for Pol ß in BRCA1 mediated DSB repair. In addition, BRCA1 has also been shown to be involved in the transcriptional regulation of BER factor such as OGG1, NTH1, XRCC1 and APE1 (Saha et al., 2010, De Summa et al., 2014).

Ataxia telangiectasia mutated (ATM) is a key component of HR pathway. ATM is a serine/threonine kinase that activates over a hundred proteins involved in DNA damage response, DNA repair, cell cycle regulation, apoptosis and other pathways (Kurz and Lees-Miller, 2004, Chaudhary and Al-Baradie, 2014). The ATM signalling pathway is activated following DSBs. ATM is recruited to the damaged sites, however it is not clear if ATM interacts with damaged DNA directly or indirectly. It was previously thought that ATM activation primarily requires direct binding to MRN complex which is a sensor of DSBs (Chaudhary and Al-Baradie, 2014). However recent studies have

shown that PARP1 may control ATM phosphorylation and mediates the earliest recruitment of MRE11 and NBS1 to DNA damage (Rupnik et al., 2008, Haince et al., 2008, Haince et al., 2007).

4.1.1. Rationale for study

Data presented in Chapter 3 of this thesis suggested that BRCA1 deficiency is associated with reduced expression of several factors involved in BER. In this chapter it was investigated if such BRCA1-BER deficient cells could be targeted by blockade of ATM for personalized therapy.

4.2. Aims

The aims of this study were as follows:

1. To investigate the effect of ATM inhibitors (KU55933 and KU60019) on cell viability and growth using clonogenic cell survival and MTS assays.
2. To confirm the effect of PARP inhibitors (NU1025 and 3-Aminobenzamide) on cell viability and growth using clonogenic cell survival and MTS assays.
3. To test the hypothesis that DNA double strand breaks accumulate in cells after exposure to ATM inhibitors in BRCA1 deficient cells.
4. To determine the effect of ATM inhibitors on cell cycle in BRCA1 deficient cells.
5. To explore induction of apoptosis in BRCA1 deficient cells after treatment with ATM inhibitors.

4.3. Results

4.3.1. Clonogenic cell survival and Growth inhibition in response to ATM inhibitors (KU55933 & KU60019)

The plating efficiencies (which is a measure of a cells ability to form colonies) of the HeLa cell lines were around 60% to 98% in this study, this is consistent with the previous published literature which showed the high plating efficiency of HeLa cells (Puck and Fisher, 1956, Rafferty, 1985). On the other hand, previous studies showed plating efficiency of breast cancer cell lines around 29% to 55% (Mukherjee et al., 2005, Mukherjee and Martin, 2006, Ware et al., 2007, Zhang et al., 2014, Karasawa et al., 2014, Duangmano et al., 2012). In this present study plating efficiencies for MCF7 and MDA-MB-436 cells in clonogenic assay were around (45% to 58%) and (24% to 54%), respectively. It is possible that one of the reasons for this slight increase/decrease in plating efficiencies is due to the specific culture conditions (e.g. cell culture media and FBS concentrations) and cell seeding number in different studies.

Clonogenic survival assays were performed to test whether BRCA1 deficient cells are sensitive to ATM inhibition. BRCA1 mutated (MDA-MB-436) and knockdown cell lines (BRCA1 HeLa cells) along with BRCA1 proficient MCF7 cells and Control HeLa cell lines were treated with increasing concentrations of KU55933 ($C_{21}H_{17}NO_3S_2$) which is a potent, selective and competitive ATM kinase inhibitor. Results are shown in Figure 4.1.

IC_{50} values were calculated using nonlinear regression, with the proviso that in BRCA1 proficient cell lines (Control HeLa and MCF7) cytotoxicity did not

approach 50% in some cases, thus impairing extrapolation. Clonogenic assay demonstrated that BRCA1 HeLa cells, are more sensitive to KU55933 compared to Control HeLa cells (mean IC_{50}= 2.911 ± 0.21 vs. mean IC_{50}= 9.160 ± 1.6). Similarly, increased sensitivity was also demonstrated in BRCA1 mutated MDA-MB-436 cells compared to control MCF7 cells (mean IC_{50}= 6.39 ± 0.43 vs. mean IC_{50}= 9.23 ± 0.48).

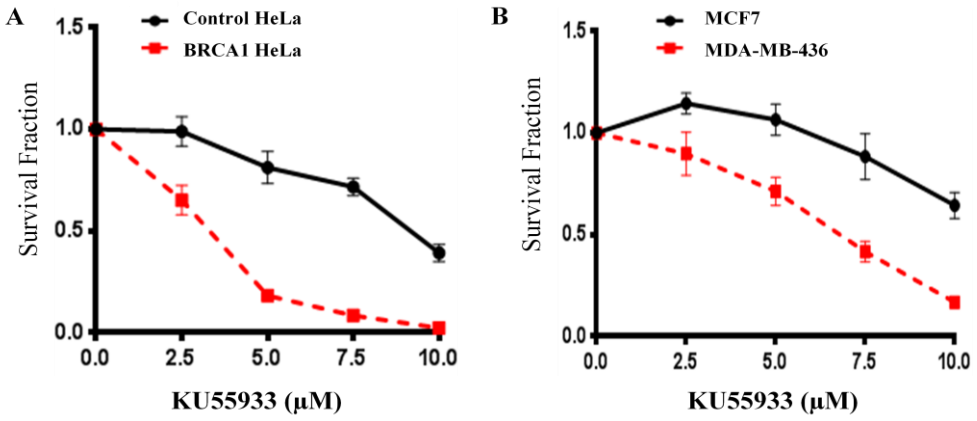

Figure 4.1. Clonogenic survival assay of ATM inhibitor (KU55933).

Cell lines with reduced BRCA1 expression exhibited decreased colony forming ability after treatment with KU55933 inhibitor for 14 days, compared to BRCA1 proficient cell lines. (A) BRCA1 HeLa cells compared to Control HeLa cells. (B) MDA-MB-436 cells compared to MCF7 cells. Plating efficiencies of cell lines with standard error were as follows: (A) Control HeLa- 85.83% ± 3.433%; BRCA1 HeLa- 74.10% ± 4.054% (B) MCF7- 45.71% ± 4.69%; MDA-MB-436- 36.73% ± 3.67%. Clonogenic data are shown as the mean and SD values for each concentration from ≥ 3 independent experiments.

In general, increasing concentrations of KU55933 inhibitor reduced the colony forming ability in BRCA1 deficient cells compared to the BRCA1 proficient cells. To validate further, an alternative clonogenic assay protocol was performed, where cells were treated with ATM inhibitor for 24 hours then

culture media was replaced with fresh media and the remaining assay was conducted as described in 2.3.4.3. Results are illustrated in Figure 4.2.

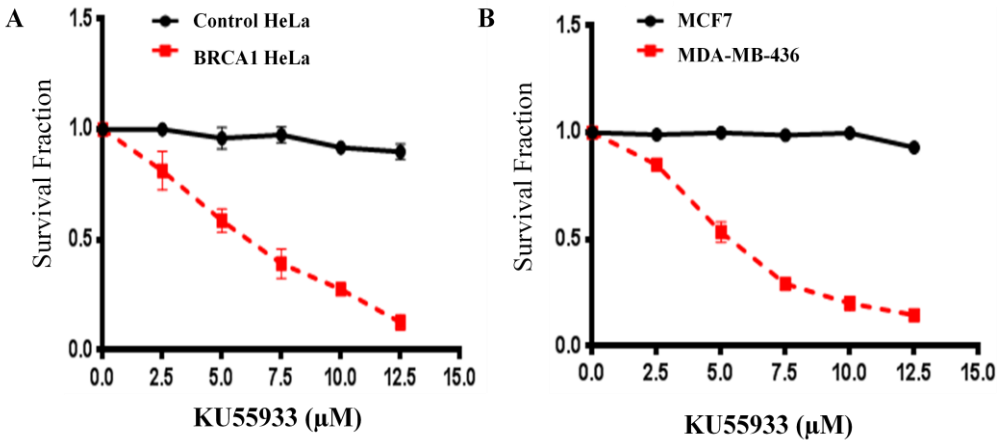

Figure 4.2. Clonogenic survival assay of inhibitor KU55933 (24 hours treatment protocol).

Cell lines with reduced BRCA1 expression exhibited decreased colony forming ability after treatment with KU55933 inhibitor for 24 hours. (A) BRCA1 HeLa cells compared to Control HeLa cells. (B) MDA-MB-436 cells compared to MCF7 cells. Plating efficiencies of cell lines with standard error were as follows: (A) Control HeLa- 83.30% ± 3.30%; BRCA1 HeLa- 86.80% ± 6.80% (B) MCF7- 48.78% ± 4.33%; MDA-MB-436- 53.62% ± 1.94%. Clonogenic data are shown as the mean and SD values for each concentration from 2 independent experiments.

The alternative clonogenic assay results demonstrated that BRCA1 HeLa cells are more sensitive to KU55933 than Control HeLa cells (mean IC_{50}= 5 ± 0.24 vs. IC_{50} above the maximum level tested). Similarly, sensitivity was demonstrated in BRCA1 mutated MDA-MB-436 cells compared to control MCF7 cells (mean IC_{50}= 4.45 ± 0.23 vs. IC_{50} above the maximum level tested). Both the 24 hour KU55933 treatment protocol and the 14 day treatment protocol, provide evidence that increasing concentration of KU55933

inhibitor reduces the colony forming ability of BRCA1 deficient cell lines compared to the BRCA1 proficient cell lines. The 14 day treatment protocol was used for all further clonogenic assays described in the rest of the thesis.

For additional validation, the proliferation assay (MTS assay) was used to determine cell growth in response to KU55933. As shown in Figure 4.3, BRCA1 deficient HeLa cells were more sensitive to KU55933 than the Control HeLa cells. Similar sensitivity was demonstrated in BRCA1 mutated MDA-MB-436 cells compared to control MCF7 cells.

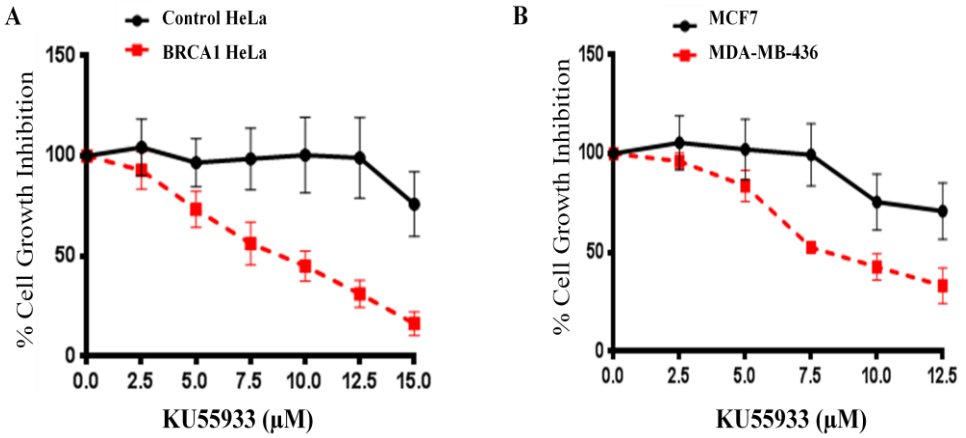

Figure 4.3. MTS cell growth inhibition assays of ATM inhibitor (KU55933).

Cell lines with reduced BRCA1 expression exhibited decreased cell growth after treatment with KU55933 inhibitor for 6 days, compared to BRCA1 proficient cell lines. (A) BRCA1 HeLa cells compared to Control HeLa cells. (B) MDA-MB-436 cells compared to MCF7 cells. Data are shown as the mean and SD values for each concentration from ≥ 2 independent experiments.

For further validation, KU60019 ($C_{30}H_{33}N_3O_5S$), another ATM potent kinase inhibitor, was investigated (Golding et al., 2009). As shown in Figure 4.4 clonogenic cell survival assays, BRCA1 HeLa cells are more sensitive to KU60019 than Control HeLa cells. Similar sensitivity was also demonstrated in BRCA1 mutated MDA-MB-436 cells compared to control MCF7 cells. Taken together, these data provide strong evidence that BRCA1 deficient cells are sensitive to ATM inhibition.

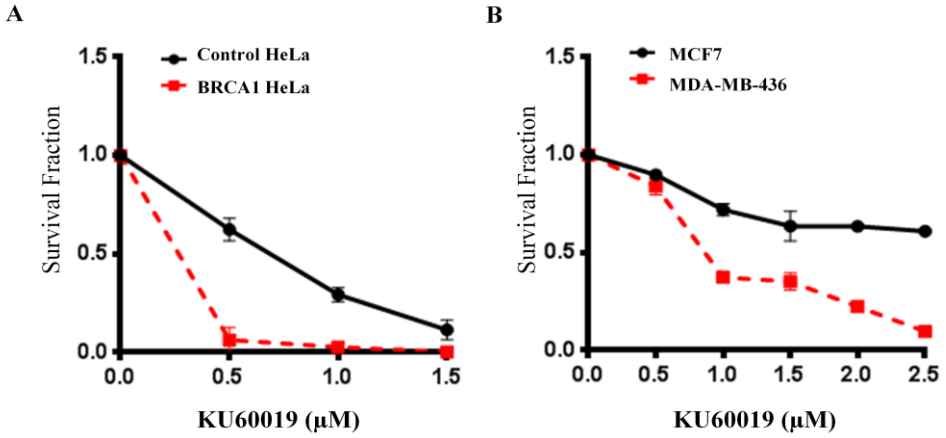

Figure 4.4. Clonogenic survival assay of ATM inhibitor (KU60019).

Cell lines with reduced BRCA1 expression exhibited decreased colony forming ability after treatment with KU60019 inhibitor for 14 days, compared to BRCA1 proficient cell lines. (A) BRCA1 HeLa cells compared to Control HeLa cells. (B) MDA-MB-436 cells compared to MCF7 cells. Plating efficiencies of cell lines with standard error were as follows: (A) Control HeLa- 87.75% ± 5.75%; BRCA1 HeLa- 67.00% ± 17.00% (B) MCF7- 61.36% ± 4.21%; MDA-MB-436- 46.00% ± 4.25%. Clonogenic data are shown as the mean and SD values for each concentration from ≥ 2 independent experiments.

4.3.2. Growth inhibition and clonogenic cell survival in response to PARP inhibitors

MTS cell growth assays were performed using NU1025 ($C_9H_8N_2O_2$) a well characterised inhibitor of PARP (Bowman et al., 1998, Griffin et al., 1998, Sultana et al., 2012), as a positive control drug to induce lethality in this model system. Figure 4.5 demonstrates that BRCA1 HeLa cells were more sensitive to NU1025 than the Control HeLa cells. Similar sensitivity was also demonstrated in BRCA1 mutated MDA-MB-436 cells compared to control MCF7 cells. This result is consistent with previous studies that demonstrated similar sensitivity in BRCA1 deficient cells to NU1025 (Bryant et al., 2005, Sultana et al., 2012).

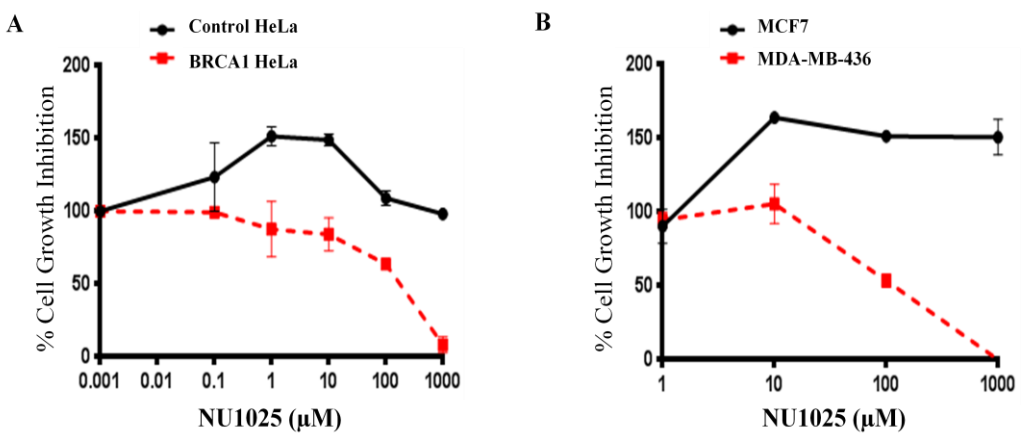

Figure 4.5. MTS cell growth inhibition assays of PARP inhibitor (NU1025).

Cell lines with reduced BRCA1 expression exhibited decreased cell growth after treatment with NU1025 inhibitor for 6 days, compared to BRCA1 proficient cell lines. (A) BRCA1 HeLa cells compared to Control HeLa cells. (B) MDA-MB-436 cells compared to MCF7 cells. Data are shown as the mean and SD values for each concentration from ≥ 2 experiments.

For additional validation, 3-Aminobenzamide ($C_7H_8N_2O$) another PARP inhibitor, was investigated (Purnell and Whish, 1980). As shown in Figure 4.6, BRCA1 HeLa cells are more sensitive to 3-Aminobenzamide compared to Control HeLa cells. Similar sensitivity was also demonstrated in BRCA1 mutated MDA-MB-436 cells compared to control MCF7 cells. This result is consistent with a previous study that showed sensitivity in BRCA1 deficient cells to 3- Aminobenzamide (Bryant et al., 2005). Functional analyses in cells were then carried out to investigate ATM inhibition in BRCA1 deficient cells.

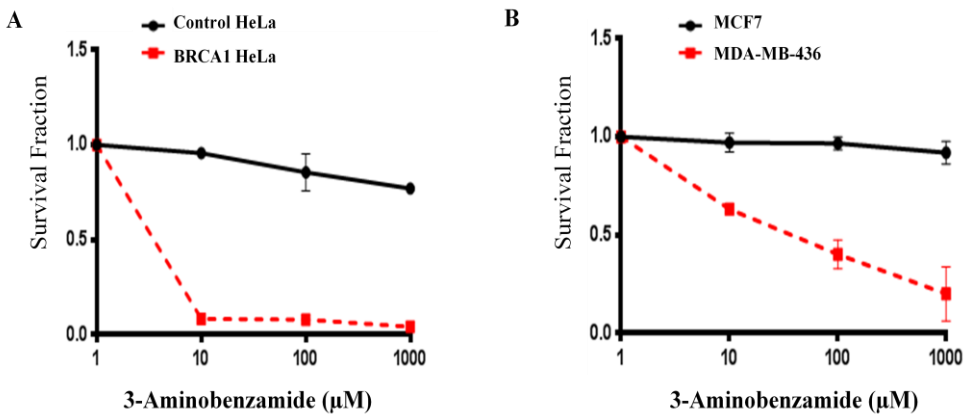

Figure 4.6. Clonogenic survival assay of PARP inhibitor (3-Aminobenzamide).

Cell lines with reduced BRCA1 expression exhibited significantly decreased colony forming ability after treatment with 3-Aminobenzamide inhibitor for 14 days, compared to BRCA1 proficient cell lines. (A) BRCA1 HeLa cell line compared to Control HeLa. (B) MDA-MB-436 compared to MCF7. Plating efficiencies of cell lines with standard error were as follows: (A) Control HeLa- 98.17% ± 1.83%; BRCA1 HeLa- 98.33% ± 0.33% (B) MCF7- 64.06% ± 0.94%; MDA-MB-436- 64.61% ± 0.72%. Clonogenic data are shown as the mean and SD values for each concentration from ≥ 2 independent experiments.

4.3.3. γH2AX focus immunofluorescence microscopy assay

To determine whether DSBs accumulate after treatment with KU55933, DSBs were measured using the γH2AX immunofluorescence microscopy assay. As described in Chapter 2 section 2.3.5, cells were treated with 10 µM of KU55933 for 24 hours and 48 hours. As shown in Figure 4.7, after 48 hours of treatment, a significant increase in foci formation was observed in BRCA1 deficient cells. Cells were then treated with 5 µM of KU55933 for 48 hours as shown in Figure 4.8, but no significant accumulation of γH2AX foci in BRCA1 deficient cells was observed. The data support a dose response effect of ATM inhibition in BRCA1 deficient cells.

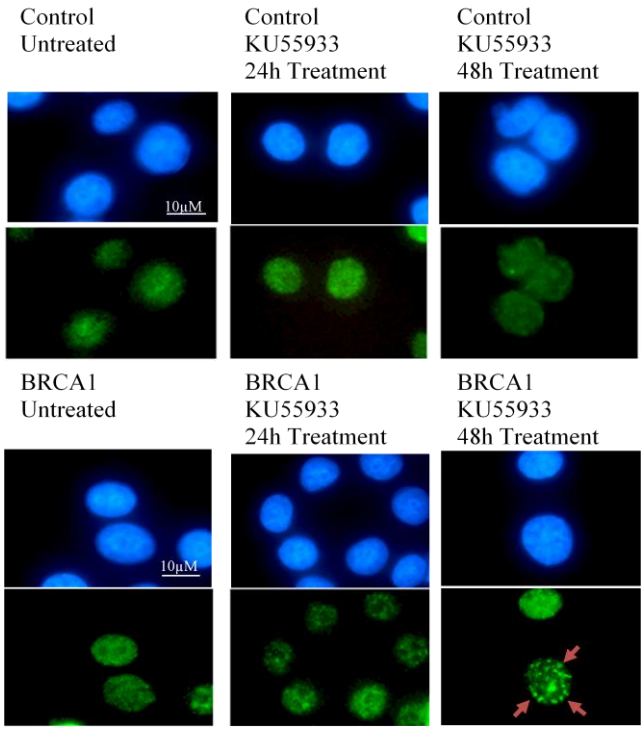

Figure 4.7. Representative photomicrographic of Immunofluorescence microscopy assay following KU55933 treatment for 24 hours and 48 hours.

BRCA1 HeLa cells and Control HeLa cells, were treated with 10 µM for 24 and 48 hours, then fixed and stained with γH2AX primary and FITC-conjugated secondary antibodies. DAPI was used as a nuclear stained showing in blue and γH2AX foci detected fluoresce in green.

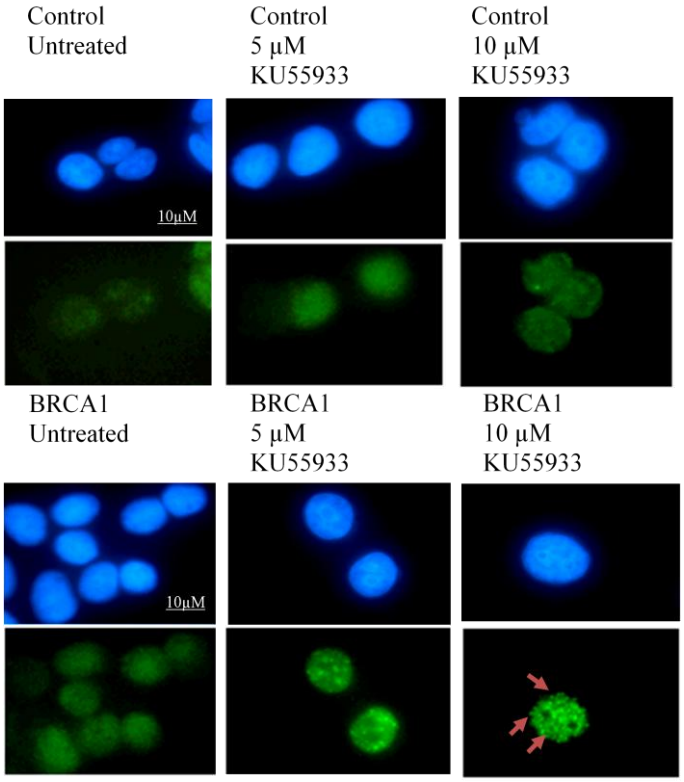

Figure 4.8. Representative photomicrographic of Immunofluorescence microscopy assay following KU55933 treatment 5 µM and 10 µM for 48 hours.

BRCA1 HeLa cells and Control HeLa cells, were treated with 5 µM and 10 µM for 48 hours, then fixed and stained with γH2AX primary and FITC-conjugated secondary antibodies. DAPI was used as a nuclear stained showing in blue and γH2AX foci detected fluoresce in green.

4.3.3.1. γH2AX formation in response to ATM inhibitors

BRCA1 proficient and BRCA1 deficient cell lines following treatment with 10 µM of KU55933 for 48 hours are shown in Figure 4.9. The data demonstrates a statistically significant increase in the accumulation of γH2AX foci in treated BRCA1 HeLa cells compared to untreated BRCA1 HeLa cells (mean 66.50% ± 6.5 vs. mean 20.50% ± 3.5; p = 0.02) and compared to corresponding treated Control HeLa cells (mean 8.00% ± 3.00; p = 0.014).

Similar results were also observed in treated MDA-MB-436 cells in which accumulation of γH2AX foci were significantly higher compared to untreated MDA-MB-436 cells (mean 88.00% ± 4.0 vs. 5.50% ± 0.50; p = 0.002) and compared to corresponding treated MCF7 cells (mean 4.50% ± 1.50; p = 0.0026).

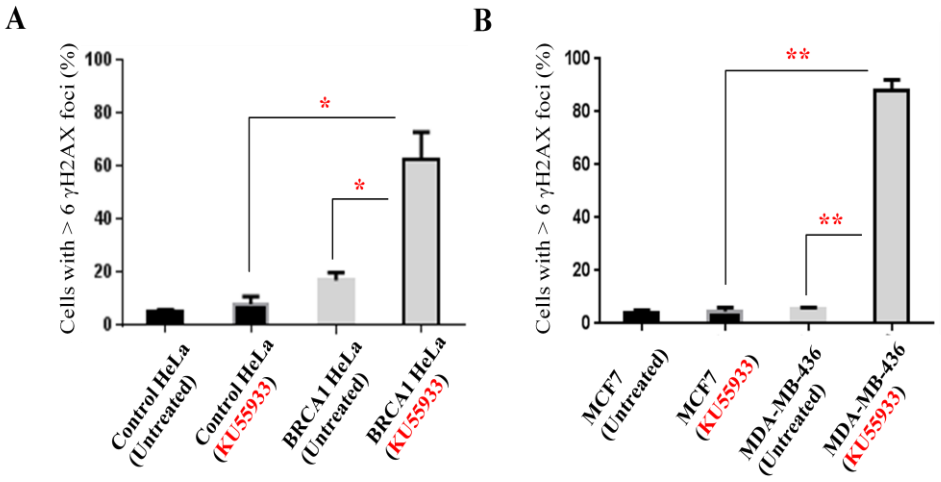

Figure 4.9. Immunofluorescence microscopy staining for γH2AX foci formation following KU55933 treatment for 48 hours.

(A) BRCA1 HeLa cells compared to Control HeLa cells. (B) MDA-MB-436 cells compared to MCF7 cells. Data are shown as the mean and SD values for each concentration from ≥ 3 independent experiments. * $p<0.05$ and ** $p<0.01$, p value was assessed by a t-test comparing BRCA1 deficient cell lines to BRCA1 proficient cell lines. Graphs were produced and statistical analysis performed using GraphPad prism.

For further validation KU60019, another ATM inhibitor, was investigated. Treatment with 1μM of KU60019 produced similar results as with KU55933. As shown in Figure 4.10, a statistically significant increase in the accumulation of γH2AX foci in treated BRCA1 HeLa cells compared to untreated BRCA1 HeLa cells (mean 41.50% ± 4.5 vs. 10% ± 1.0; p = 0.02), and compared to corresponding treated Control HeLa cells (mean 5.00% ± 1.00; p = 0.015)

were observed. Similar results were also observed in treated MDA-MB-436 cells in which accumulation of γH2AX foci was significantly higher compared to untreated MDA-MB-436 cells (mean 71.50% ± 2.5 vs. 17.50% ± 1.5; p = 0.002), and compared to the corresponding treated MCF7 cells (mean 37.50% ± 1.5; p = 0.007). Although MDA-MB-436 cells were more sensitive to KU60019 inhibitor, MCF7 cells showed a similar change (from 10% to 37.50%). This result infers that KU60019 inhibitor maybe toxic to MCF7.

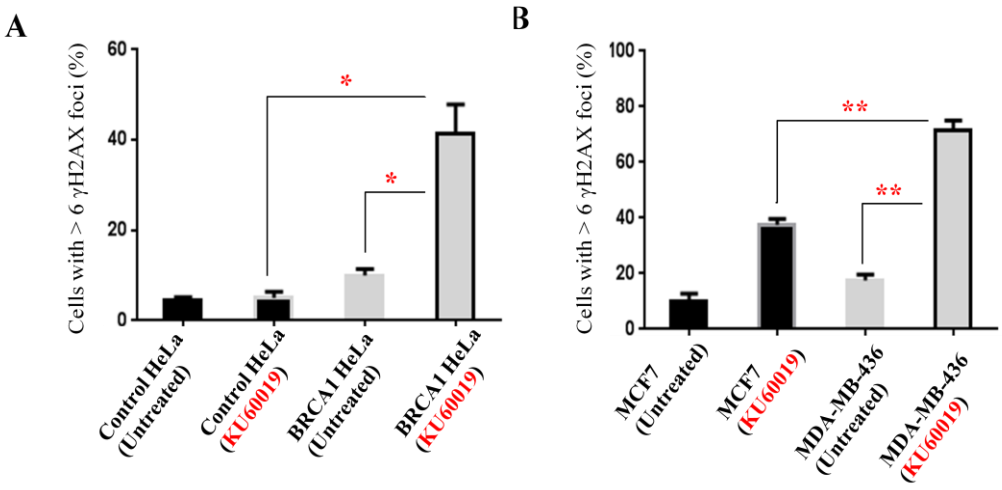

Figure 4.10. Immunofluorescence microscopy staining for γH2AX foci formation following KU60019 treatment for 48 hours.

(A) BRCA1 HeLa cells compared to Control HeLa cells. (B) MDA-MB-436 cells compared to MCF7 cells. Data are shown as the mean and SD values for each concentration from ≥ 2 independent experiments. * $p<0.05$ and ** $p<0.01$, p value was assessed by a t-test comparing BRCA1 deficient cell lines to BRCA1 proficient cell lines. Graphs were produced and statistical analysis performed using GraphPad prism.

4.3.4. Cell cycle analysis by propidium iodide flow cytometry after treatment with ATM inhibitors

DSB formation induces cell cycle checkpoint activation to trigger cell cycle arrest to allow DNA repair, if the damage is extensive then this process can initiate apoptosis (Kurz and Lees-Miller, 2004). To evaluate cell cycle progression, Propidium iodide (PI) flow cytometry was used as described in Chapter 2, section 2.3.6.

Cells were treated for 24 hours and 48 hours with 10 µM or 20 µM of KU55933 (Figure 4.11). Although no significant difference was observed after 24 hours, at 48 hours in BRCA1 deficient cells treated with 10 µM KU55933 exhibited a significant increase in G2/M phase arrest compared to control cells was observed. On the other hand, at 20 µM concentration conducts apoptosis was evident, illustrated by the loss of cells count.

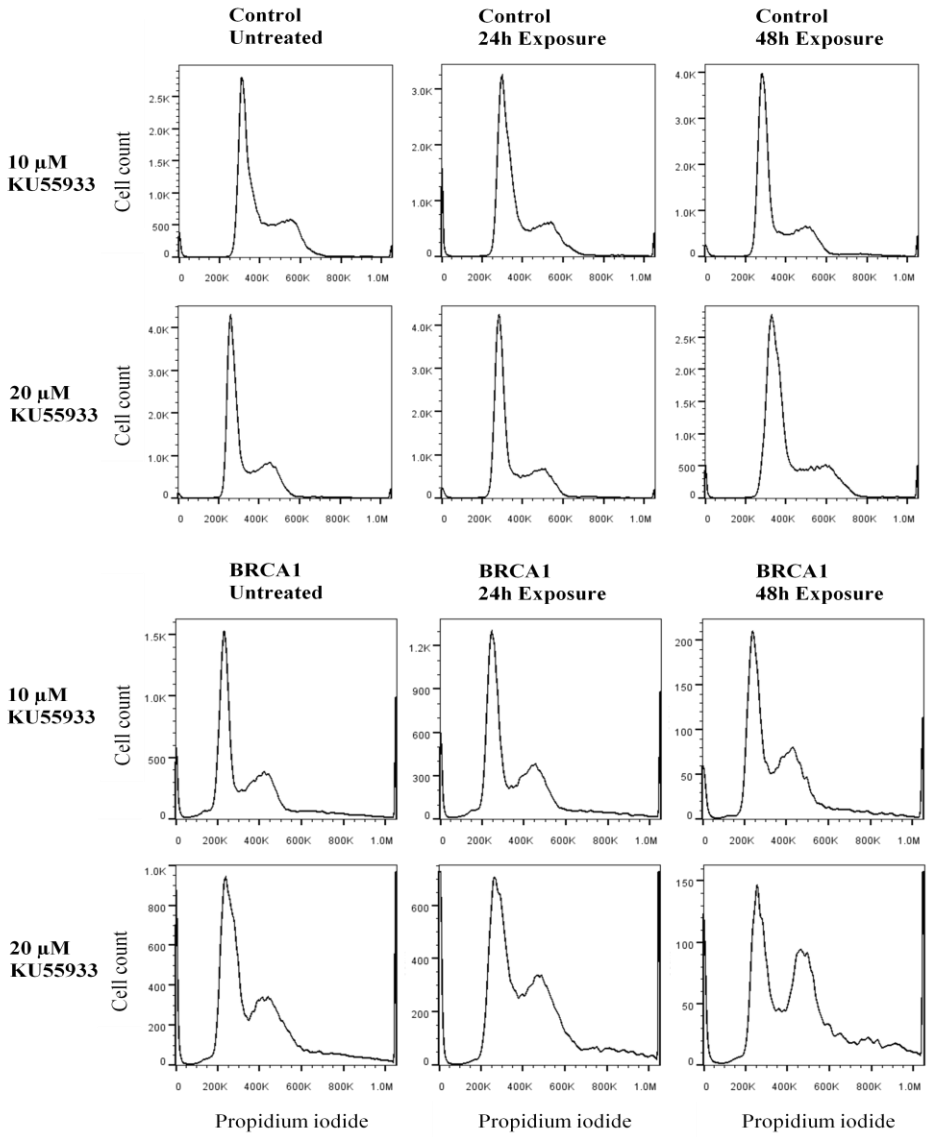

Figure 4.11. Representative graphs of flow cytometric cell cycle analysis following KU55933 treatment.

BRCA1 HeLa cells and Control HeLa cells were treated with 10 µM and 20 µM for 24 hours and 48 hours. Y axis represents cell count and propidium iodides detected fluorescence is shown on the X axis.

Results for BRCA1 proficient and BRCA1 deficient cells following treatment with 10 µM (KU55933) for 48 hours are shown in Figure 4.12. The data demonstrate a statistically significant G2/M arrest in treated BRCA1 HeLa cells compared with untreated BRCA1 HeLa cells (mean 26.60% ± 0.40 vs. 20.50% ± 1.50; p = 0.05), and compared to corresponding treated Control

HeLa cells (mean 21.50% ± 0.50; p = 0.0154). Results of treated MDA-MB-436 cells demonstrate an increase in G2/M arrest compared to MDA-MB-436 untreated cells, though this is not significant (mean 32.45% ± 2.75 vs. mean 27.60% ± 2.9; p = 0.3). The observed G2/M arrest was significantly higher in treated MDA-MB-436 cells compared to treated MCF7 cells (mean 20.30% ± 0.50; p = 0.0491). Conversely, Control HeLa and MCF7 cells did not show the same increase (i.e. ~5%) as with BRCA1 deficient cells. (Control HeLa and MCF7 cells, G2/M arrest mean 21.50% to 22.55% and 19% to 20.30%, respectively).

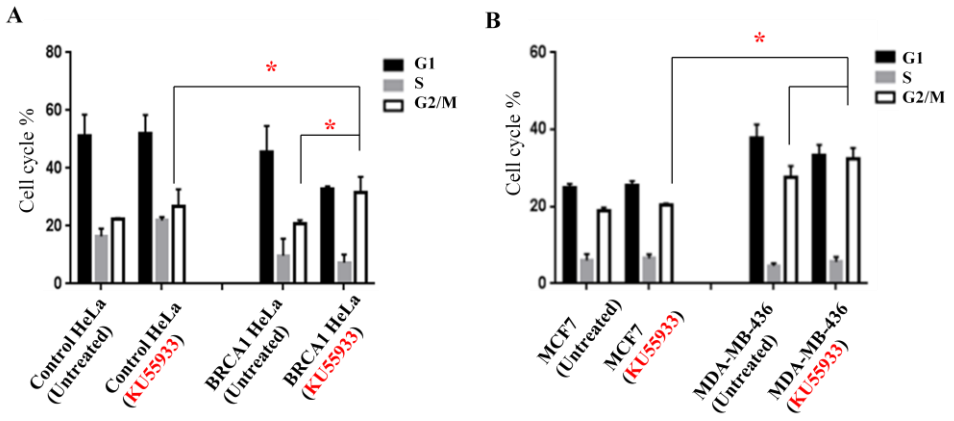

Figure 4.12. Flow cytometric cell cycle analysis following KU55933 treatment for 48 hours.

(A) BRCA1 HeLa cells compared to Control HeLa cells. (B) MDA-MB-436 cells compared to MCF7 cells. Data are shown as the mean and SD values for each concentration from ≥ 3 independent experiments. * p≤ 0.05, p value was assessed by a t-test comparing BRCA1 deficient cell lines to BRCA1 proficient cell lines. Graphs were produced and statistical analysis performed using GraphPad prism.

For further validation KU60019, another ATM inhibitor, was investigated. Treatment with 1μM of KU60019 produced similar results as with KU55933.

As shown in Figure 4.13, a statistically significant G2/M arrest in treated BRCA1 HeLa cells was demonstrated as compared to untreated BRCA1 HeLa cells (mean 31.55% ± 0.55 vs. 26.9% ± 0.2; p = 0.015), and as compared to the corresponding treated Control HeLa cells (mean 23.80% ± 0.10; p = 0.005). A similar, although not statistically significant, G2/M arrest was also observed in treated MDA-MB-436 cells compared to untreated MDA-MB-436 cells (mean 34.60% ± 0.40 vs. 28.30% ± 1.7; p = 0.06). A statistically significant G2/M was observed in treated MDA-MB-436 cells as compared to treated MCF7 cells (mean 25.15% ± 1.15; p = 0.0162). In contrast, Control HeLa cells and MCF7 did not show the same increase (G2/M arrest mean 19.5% to 23.8% and 25.70% to 25.15%, respectively).

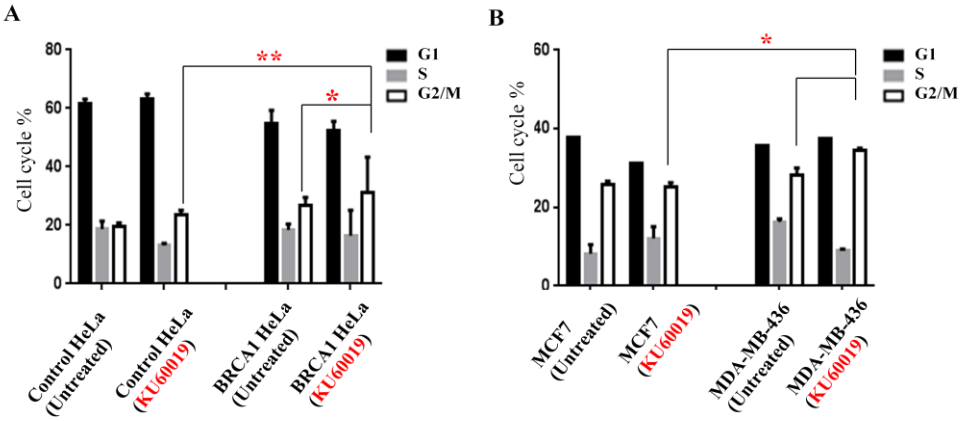

Figure 4.13. Flow cytometric cell cycle analysis following KU60019 treatment for 48 hours.

(A) BRCA1 HeLa cells compared to Control HeLa cells. (B) MDA-MB-436 cells compared to MCF7 cells. Data are shown as the mean and SD values for each concentration from ≥ 2 independent experiments. * $p<0.05$ and ** $p<0.01$, p value was assessed by a t-test comparing BRCA1 deficient cell lines to BRCA1 proficient cell lines. Graphs were produced and statistical analysis performed using GraphPad prism.

4.3.5. Apoptosis detection by annexin V-FITC flow cytometry after treatment with ATM inhibitors

Annexin V was used in conjunction with a propidium iodide (PI) for identification of late apoptotic cells as described in Chapter 2, section 2.3.7. Viable cells with intact membranes are negative (reject) to PI, whereas dead cells with damaged membranes are positive (permeable) to PI. Therefore, viable cells are both Annexin V and PI negative, early apoptosis cells are Annexin V positive and PI negative, late apoptosis cells are Annexin V and PI positive, necrotic cells are Annexin V negative and PI positive (Koopman et al., 1994, Riccardi and Nicoletti, 2006).

Cells were treated for 24 hours and 48 hours with 10 μM of KU55933. As shown in Figure 4.14, although no significant increase in apoptosis after 24 hours was evident, at 48 hours in BRCA1 deficient cells treated with 10 μM of KU55933 showed significant increase in apoptosis compared to control cells was observed.

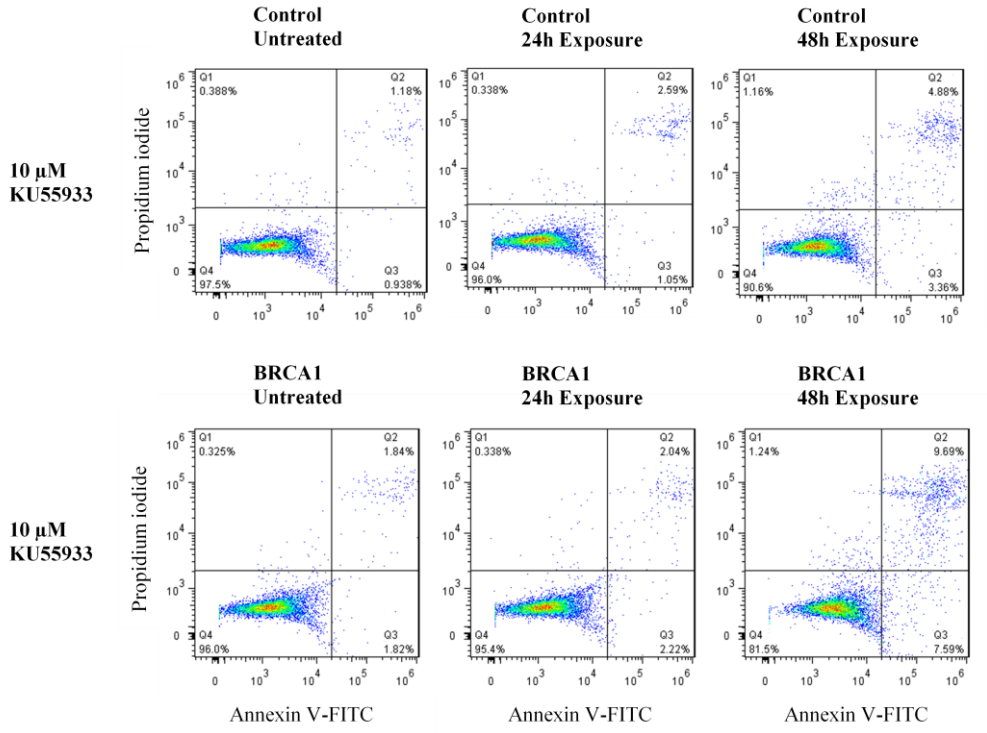

Figure 4.14. Representative graphs of flow cytometry images for apoptosis assay following KU55933 treatment.

Cells were treated with 10 µM of KU55933 for 24 hours or 48 hours, then stained with annexin V-FITC and propidium iodide (PI), and analysed by two-colour flow cytometry. Viable cells are both Annexin V and PI negative [bottom left quadrant], early apoptosis cells are Annexin V positive and PI negative [bottom right quadrant], late apoptosis cells are Annexin V and PI positive [top right quadrant], necrotic cells are Annexin V negative and PI positive [top left quadrant].

Results for BRCA1 proficient and BRCA1 deficient cells following treatment with 10 µM (KU55933) for 48 hours are shown in Figure 4.15, data were normalised against baseline apoptotic fraction (untreated cells) to determine the percentage increase in apoptosis. The data demonstrate a statistically significant increase in apoptosis with treated BRCA1 HeLa cells compared to untreated BRCA1 HeLa cells (mean 11.12% vs. 3.6%; p =

0.0014). Similar results were also observed in treated MDA-MB-436 cells, in which a significant increase in apoptosis as compared to untreated MDA-MB-436 cells was observed (mean 13.1% vs. 4.8%; $p < 0.0001$). On the other hand, Control HeLa and MCF7 cells did not show the same rate of increase (mean 3.9% to 5.7% and 3.17% to 7.5%, respectively).

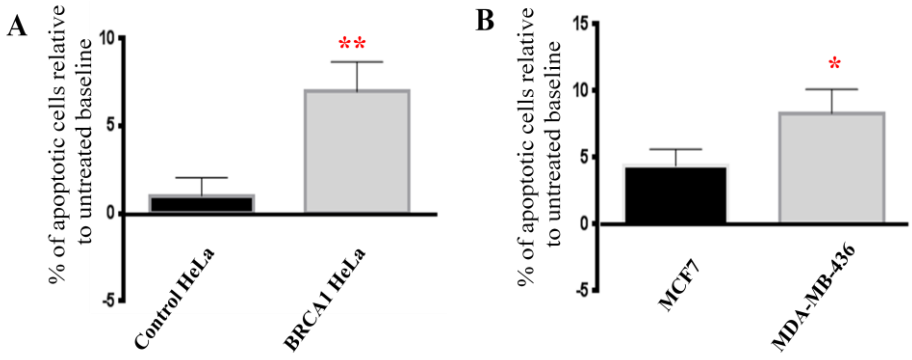

Figure 4.15. Apoptosis detection by annexin V-FITC flow cytometry in KU55933 treated cells.

Treatment with KU55933 inhibitor was associated with a significant increase in apoptotic cells. Data were normalised against baseline apoptotic fraction to determine the percentage increase in apoptosis. (A) BRCA1 HeLa cells compared to Control HeLa cells. (B) MDA-MB-436 cells compared to MCF7 cells. Data are shown as the mean and SD values for each concentration from ≥ 3 experiments. * $p<0.05$ and ** $p<0.01$, p value was assessed by a t-test comparing BRCA1 deficient cell lines to BRCA1 proficient cell lines. Graphs were produced and statistical analysis performed using GraphPad prism.

For further validation KU60019, another ATM inhibitor, was investigated. Treatment with 1μM of KU60019 produced similar results as with KU55933. As shown in Figure 4.16, the data demonstrates a statistically significant increase in apoptosis in treated BRCA1 HeLa cells compared to the

corresponding untreated BRCA1 HeLa cells (mean 9.56% vs. 5.53%; p = 0.037). A similar increase was also observed in treated MDA-MB-436 cells as compared to untreated MDA-MB-436 cells (mean 8.99% vs. 4.68%; though was not significant). Conversely, Control HeLa and MCF7 cells did not show the same rate of increase (mean 4% to 3.8% and 3.97% to 5.9%, respectively).

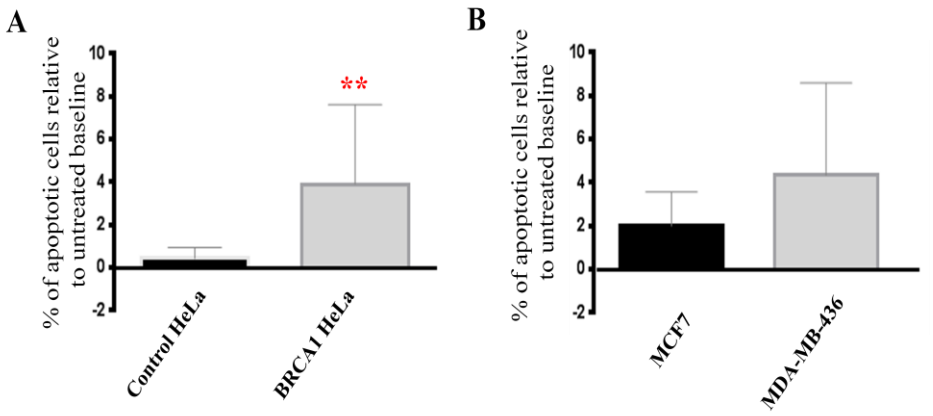

Figure 4.16. Apoptosis detection by annexin V-FITC flow cytometry in KU60019 treated cells.

Treatment with KU60019 inhibitor was associated with an increase in apoptotic cells. Data were normalised against baseline apoptotic fraction to determine the percentage increase in apoptosis. (A) BRCA1 HeLa cells compared to Control HeLa cells. (A) BRCA1 HeLa cells compared to Control HeLa cells. (B) MDA-MB-436 cells compared to MCF7 cells. Data are shown as the mean and SD values for each concentration from ≥ 3 experiments. ** $p<0.01$, p value was assessed by a t-test comparing BRCA1 deficient cell lines to BRCA1 proficient cell lines. Graphs were produced and statistical analysis performed using GraphPad prism.

4.4. Discussion and conclusions

BER is a highly conserved pathway, responsible for repairing the vast majority of endogenous DNA damage including alkylation, oxidation, ring saturation, single strand breaks and base deamination. Defects in BER have been genetically linked to cancer risk. For instance, Pol ß was found to play an important role in suppressing carcinogenesis since 30% of human tumors investigated to date carry *Pol ß* mutations (Sobol et al., 2002, Starcevic et al., 2004, Wallace, 2014). More recently in our group, a study was undertaken in breast cancer and found that low Pol ß is associated with poor survival (Abdel-Fatah et al., 2014). In addition, XRCC1 another key factor in BER, recently shown that loss of XRCC1 was associated with poor survival in breast cancer. Moreover, XRCC1 deficiency was highly associated with loss of other DNA repair factors, such as BRCA1 and p53 (Sultana et al., 2013a). Recent data indicate a cross talk between BRCA1 and BER factors. Saha *et al* study for instance showed that BRCA1 is involved in the transcriptional regulation of *OGG1*, *NTH1*, *XRCC1* and *APE1* (Saha et al., 2010). In agreement with this data, Chapter 3 of this thesis has shown that reduced BRCA1 expression in mutant/knockdown cell lines was associated with a significant reduction in several BER genes at the mRNA and protein expression. As BRCA1 deficient cells were shown to be BER deficient, cells may be more reliant on backup DSB repair pathways to maintain cellular survival. Blocking DSB repair should cause selective toxicity in BRCA1-BER deficient cells. The aim of this chapter was to investigate if targeting BRCA1 deficiency by ATM inhibitors (KU55933 or KU60019) is synthetically lethal.

Clonogenic survival assays (inhibitor exposure for total assay period) were conducted first to evaluate the cytotoxicity of ATM inhibitors against BRCA1 knockdown HeLa cells and BRCA1 mutated MDA-MB-436 cells, using Control HeLa and MCF7 cells as BRCA1 proficient controls, respectively. Then an alternative clonogenic assay protocol was performed (inhibitor exposure for 24 hours of assay period). For additional validation, the proliferation assay (MTS assay) was used to determine cell growth in response to ATM inhibitor. Results of all assays showed both KU55933 and KU60019 inhibitors induced significant cytotoxicity in BRCA1 deficient cells compared to BRCA1 proficient cells. These data suggest that BRCA1 deficient cells are reliant on ATM to maintain cellular survival.

To validate the cell line system used in the current study, clonogenic survival assay and MTS assay using PARP inhibitors (NU1025 and 3-Aminobenzamide) against BRCA1 deficient and proficient cell lines were performed. As predicted, both inhibitors induced significant cytotoxicity in BRCA1 deficient cells. These results support previously published data showing selective sensitivity to PARP inhibitors (in particular; NU1025 and 3-Aminobenzamide) in BRCA1 deficient models (Bryant et al., 2005, Sultana et al., 2012). Several functional studies were conducted to understand the mechanism behind this selective cytotoxicity of ATM inhibitors to BRCA1 deficient system. BRCA1 deficient cell lines were previously demonstrated to express reduced expression of several DSB repair factors (Chapter 3). The baseline level of DSBs damage present in these cells was assessed using γH2AX immunofluorescence microscopy assay, which is a well validated marker of DSBs. BRCA1 deficient cell lines treated with ATM inhibitors

(KU55933 or KU60019) for 48 hours were associated with a statistically significant increase in the accumulation of γH2AX foci compared to untreated BRCA1 deficient cells. Interestingly MCF7 cells showed a slight increase after KU60019 inhibitor treatment but not with KU55933, this result infers that KU60019 may be toxic to MCF7 (Figure 4.10B); this could be linked to the slight increase in apoptosis as well (Figure 4.16B).

These results support the hypothesis that ATM inhibition in BRCA1-BER deficient cells causes DSB accumulation which cannot be repaired due to an actual defect in DSB pathway. Moreover accumulation of γH2AX foci in cells treated with ATM inhibitors has been reported in previous publications (Shaheen et al., 2011, Sultana et al., 2013a). Although phosphorylation of H2AX is ATM dependent, accumulation of γH2AX foci in BRCA1 deficient cells was observed. One possible explanation for this finding is that other factors such as ATR or DNA-PKcs may be involved. Further mechanistic studies are required to clarify additional pathways.

DSB formation induces cell cycle checkpoint activation to trigger cell cycle arrest to allow DNA repair, or if the DNA damage is extensive can initiate apoptosis (Kurz and Lees-Miller, 2004). Cell cycle progression was arrested significantly at G2/M phase in treated BRCA1 HeLa cells compared to untreated BRCA1 HeLa cells (after treatment with ATM inhibitors for 48 hours). BRCA1 mutated MDA-MB-436 cells showed a modest increase in G2/M arrest, though it was not significant (Figure 4.12 and 4.13). It should be noted that the flow cytometry assay was conducted after 24 and 48 hours, and to confirm G2/M arrest in MDA-MB-436 cells different time points should be tested in the future.

These increases in G2/M arrest support previously published data showing G2/M arrest after ATM inhibition (Sultana et al., 2013a, Lee et al., 2013, Nadkarni et al., 2012, Jazayeri et al., 2006). ATM phosphorylates Ser1423 of BRCA1 which is required for G2/M checkpoint activation (Cortez et al., 1999, Xu et al., 2001, Wu et al., 2010); in agreement with previous studies the current study shows that in the absence of BRCA1 and ATM, cells arrest in G2/M phase giving the cell time to repair. This could explain the survival data since the arrest in G2 would allow more NHEJ repair in BRCA1 deficient after blocking HR. Though it is interesting that ATM inhibition leads to G2/M arrest, one possible explanation is the overlapping function between ATM/CHK2 and ATR/CHK1 pathways which share many substrates (Smith et al., 2010). This overlapping function was seen in p53 deficient cells which rely on ATM and ATR to control the checkpoint signalling to survive after DNA damage (Reinhardt et al., 2007). G2/M arrest could then be followed by apoptosis. A flow cytometry-based apoptosis detection assay was performed. Results demonstrated that BRCA1 deficient cell lines treated with ATM inhibitors for 48 hours exhibited an increase in apoptosis rate compared to untreated BRCA1 deficient cell lines. These results support those previously published showing ATM inhibitor KU55933 treatment triggers apoptosis in different cancer cell lines (Sultana et al., 2013a, Li and Yang, 2010, Korwek et al., 2012) which again highlighted the importance of ATM in DNA repair and cell survival.

The data presented here support that ATM maybe a promising alternative synthetic lethality target. This study suggests that ATM inhibition is responsible for the synthetic lethality in BRCA1 deficient cells, and also

suggests that ATM inhibitors must be evaluated further as an alternative synthetic lethality strategy in *in vivo* models. A model for synthetic lethality is shown in Figure 4.17. In brief, impaired expression of BER factors in BRCA1 deficient cell lines leads to an increase accumulation of unrepaired SSBs which is followed by the formation of DSBs during DNA replication process. Therefore, it is suggested that cells are reliant on DSB pathway for cellular survival. Targeting the DSB pathway by ATM inhibition would lead to the observed synthetic lethality. In contrast, in cells that are proficient in DSB repair the DSBs would be repaired and cells would survive.

A limitation of this chapter is that this synthetic lethality study was restricted to two ATM inhibitors. KU60019 is known as an improved analogue of KU55933 (Golding et al., 2009) although the current results did not show this. For example accumulation of γH2AX foci was significantly higher in MDA-MB-436 compared to untreated cells, though KU60019 was slightly toxic to MCF7 also. As a result more tests with KU60019 are needed using different cell lines. Another limitation was with cell cycle analysis which showed G2/M arrest increase with ATM treatment in BRCA1 HeLa cells, though MDA-MB-436 cells increase was not significant. This could be because samples were analysed after 24 and 48 hours. However, more time points should be tested in the future to monitor cells response after different treatment.

4.4.1. Conclusions

These *in vitro* studies demonstrate that a potential synthetic lethality relationship exists between BRCA1 deficiency and targeting the DSB pathway using ATM inhibitors (KU55933 or KU60019). The data suggests that ATM

inhibitors are selectively toxic to BRCA1 deficient cells. Also DNA DSBs accumulate following treatment with these inhibitors. In addition these data have shown a significant G2/M phase arrest in treated BRCA1 HeLa cells compared to untreated BRCA1 HeLa cells. As MDA-MB-436 cells showed a modest increase in G2/M arrest after 48 hours, this suggests that different time points should be tested in the future. Moreover, ATM inhibitor treatment triggers apoptosis in BRCA1 deficient cell lines.

These findings represent an alternative synthetic lethality strategy in targeting BRCA1 deficiency, which can potentially overcome PARP inhibition challenges. On the other hand, the global defect in DNA repair proved in BRCA1 deficient cells in particular the impaired BER factors expression, gives a wider role for using ATM inhibitors in cancers defective in BER in the absence of germline BRCA1 mutations. However, investigations with more BER deficient cell lines are required.

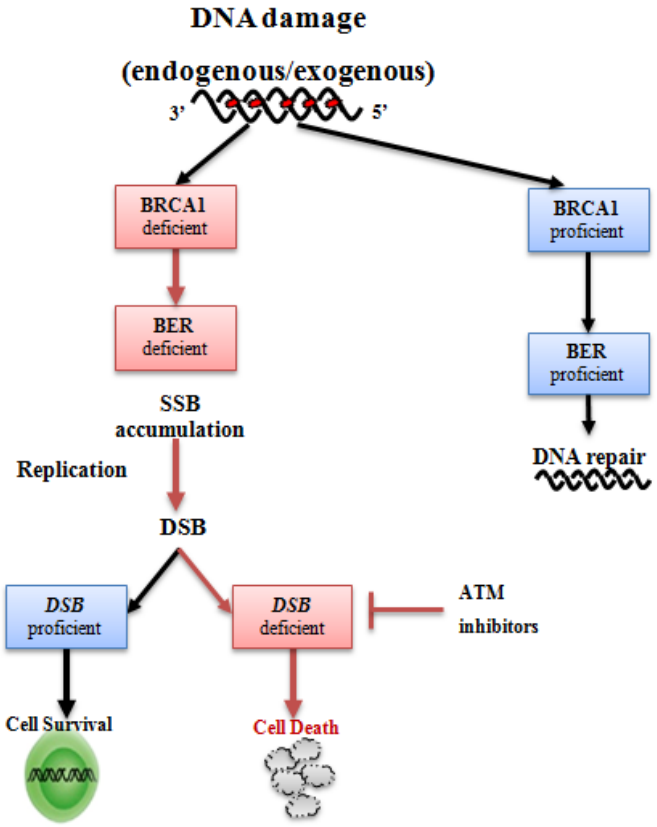

Figure 4.17. Proposed model of synthetic lethality between ATM inhibitors and BRCA1-BER deficient system.

Chapter 5

Targeting BRCA1 deficiency for personalized therapy using DNA-PKcs inhibitors (NU7441 & NU7026)

5. Targeting BRCA1 deficiency in breast cancer for personalized therapy using DNA-PKcs inhibitors (NU7441 & NU7026)

5.1. Introduction

BRCA1 facilitates the efficient resolution of DNA double-strand breaks (DSBs) through homologous recombination (HR) (Huen et al., 2010, Caestecker and Van de Walle, 2013). Cells lacking functional BRCA1 protein have impaired HR, and thus are suggested to depend on the more error-prone non-homologous end joining (NHEJ) pathway which is able to function at all stages of the cell cycle and does not require the presence of a homologous template. The NHEJ pathway is suggested to lead to chromosomal instability that leads to breast cancer development (Huen et al., 2010). It has been assumed that targeting the molecular machinery driving the DNA damage response, particularly the NHEJ pathway, with small molecule inhibitors will effectively enhance the efficacy of current cancer treatments that generate DNA damage (Kashishian et al., 2003, Davidson et al., 2013).

DNA-dependent protein kinase catalytic subunit (DNA-PKcs) is a key component of NHEJ pathway. DNA-PKcs has been shown to phosphorylate a large number of proteins, including NHEJ factors such as KU70/KU80, XRCC4, Lig3, XLF, WRN and Artemis along with other DNA damage response proteins including H2AX and p53. Recruitment of DNA-PKcs to the DNA-PK complex results in translocation of a heterodimer KU70/KU80 inward on the DNA, this is more likely to allow DNA-PKcs to bind directly to the damage resulting in the activation of the catalytic activity of the enzyme (Davis and Chen, 2013). Studies show that even with the absence of

heterodimer KU70/KU80, DNA-PKcs has unlimited kinase activity (West et al., 1998, Hammarsten and Chu, 1998). In addition synthetic lethality has been observed with PARP deficient cells targeted with DNA-PKcs inhibitor NU7026 (Veuger et al., 2003).

5.1.1. Rationale for study

Chapter 3 of this thesis suggested that BRCA1 deficiency is associated with reduced mRNA and/or protein expression of several factors involved in BER, HR and NHEJ. Data presented in Chapter 4 suggested a potential synthetic lethality relationship between BRCA1 deficiency and ATM inhibitors. In this chapter the aim was to investigate if BRCA1-BER deficient cells could be targeted by blockade of DNA-PKcs for personalized therapy.

5.2. Aims

The aims of this study were as follows:

1. To investigate the effect of DNA-PKcs inhibitors (NU7441 and NU7026) on cell viability and growth using clonogenic cell survival and MTS assays.
2. To test the hypothesis that DNA double strand breaks accumulate in cells after treatment with DNA-PKcs inhibitors in BRCA1 deficient cells.
3. To determine the effect of DNA-PKcs inhibitors on cell cycle in BRCA1 deficient cells.
4. To explore induction of apoptosis in BRCA1 deficient cells after treatment with DNA-PKcs inhibitors.

5.3. Results

5.3.1. Clonogenic cell survival and Growth inhibition in response to DNA-PKcs inhibitors (NU7441 & NU7026)

Clonogenic survival assays were performed to test whether BRCA1 deficient cells are sensitive to DNA-PKcs inhibition. BRCA1 mutated (MDA-MB-436) and knockdown (BRCA1 HeLa cells) cell lines along with MCF7 cells and Control HeLa cell lines were treated with increasing concentrations of NU7441 ($C_{25}H_{19}NO_3S$) which is a potent, selective and competitive DNA-PKcs kinase inhibitor. Results are shown in Figure 5.1.

IC_{50} values were calculated using nonlinear regression, with the proviso that in BRCA1 proficient cell lines (Control HeLa and MCF7) cytotoxicity did not approach 50% in some cases, thus impairing extrapolation. Clonogenic assay demonstrated that BRCA1 HeLa cells, are more sensitive to NU7441 compared to Control HeLa cells (mean IC_{50}= 0.6 ± 0.16 vs. IC_{50} above the maximum level tested). Similarly, increased sensitivity was also demonstrated in BRCA1 mutated MDA-MB-436 cells compared to control MCF7 cells (mean IC_{50}= 0.44 ± 0.12 vs. mean IC_{50}= 0.64 ± 0.19).

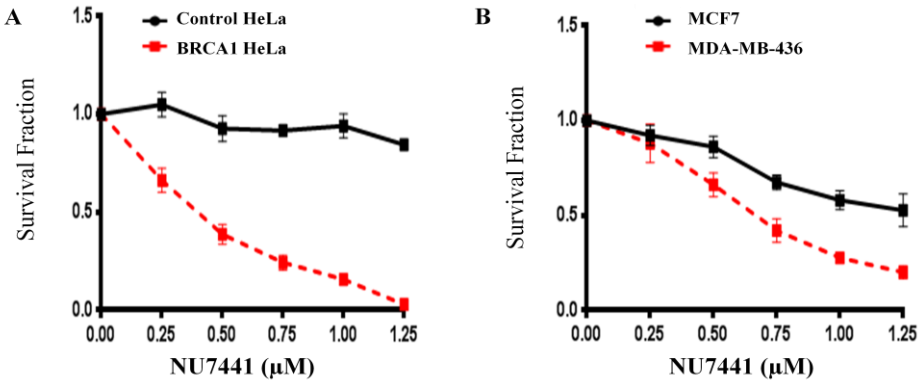

Figure 5.1. Clonogenic survival assay of DNA-PKcs inhibitor (NU7441).

Cell lines with reduced BRCA1 expression exhibited decreased colony forming ability after treatment with NU7441 inhibitor for 14 days, compared to BRCA1 proficient cell lines. (A) BRCA1 HeLa cells compared to Control HeLa cells. (B) MDA-MB-436 cells compared to MCF7 cells. Plating efficiencies of cell lines with standard error were as follows: (A) Control HeLa- 79.22% ± 1.79%; BRCA1 HeLa- 66.44% ± 5.22% (B) MCF7- 51.21% ± 3.82%; MDA-MB-436- 41.54% ± 4.33%. Clonogenic data are shown as the mean and SD values for each concentration from ≥ 2 independent experiments.

In general, increasing concentrations of NU7441 inhibitor reduced the colony forming ability in BRCA1 deficient cells compared to the BRCA1 proficient cells. To validate further, an alternative clonogenic assay protocol was performed, where cells were treated with DNA-PKcs inhibitor for 24 hours then culture media was replaced with fresh media and the remaining assay was conducted as described in 2.3.4.3. Results are illustrated in Figure 5.2.

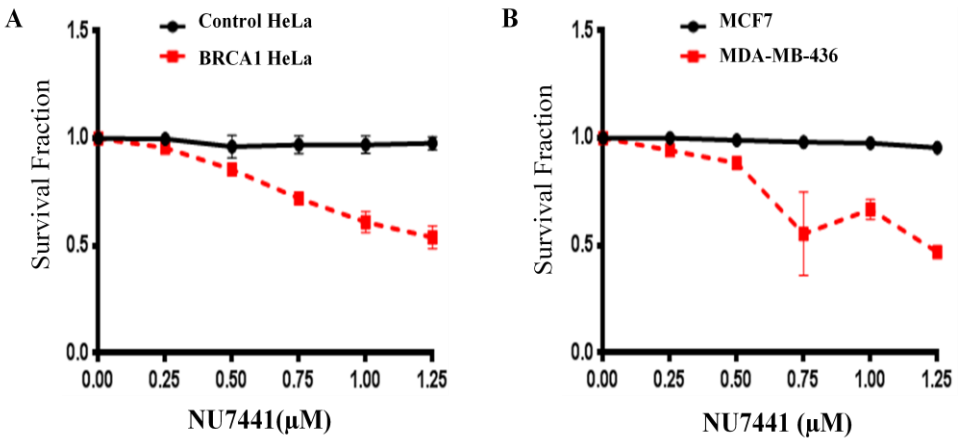

Figure 5.2. Clonogenic survival assay of inhibitor NU7441 (24 hour treatment protocol).

Cell lines with reduced BRCA1 expression exhibited decreased colony forming ability after treatment with NU7441 inhibitor for 24 hours. (A) BRCA1 HeLa cells compared to Control HeLa cells. (B) MDA-MB-436 cells compared to MCF7 cells. Plating efficiencies of cell lines with standard error were as follows: (A) Control HeLa- 90.30% ± 0.90%; BRCA1 HeLa- 83.60% ± 2.40% (B) MCF7- 55.58% ± 0.02%; MDA-MB-436- 54.28% ± 1.05%. Clonogenic data are shown as the mean and SD values for each concentration from 2 independent experiments.

The alternative clonogenic assay results demonstrated that BRCA1 HeLa cells are more sensitive to NU7441 than Control HeLa cells. Similarly, sensitivity was demonstrated in BRCA1 mutated MDA-MB-436 cells compared to control MCF7 cells. However, data did not approach 50%, thus impairing extrapolation of IC_{50} values. Though, both the 24 hour NU7441 treatment protocol and the 14 day treatment protocol, provide evidence that increasing concentration of NU7441 inhibitor reduces the colony forming ability of BRCA1 deficient cell lines compared to the BRCA1 proficient cell lines. The 14 day treatment protocol was used for all subsequent clonogenic assays described in the rest of the thesis.

For additional validation, the proliferation assay (MTS assay) was used to determine cell growth in response to NU7441. As shown in Figure 5.3, BRCA1 deficient HeLa cells were more sensitive to NU7441 than the Control HeLa cells. Similar sensitivity was demonstrated in BRCA1 mutated MDA-MB-436 cells compared to control MCF7 cells.

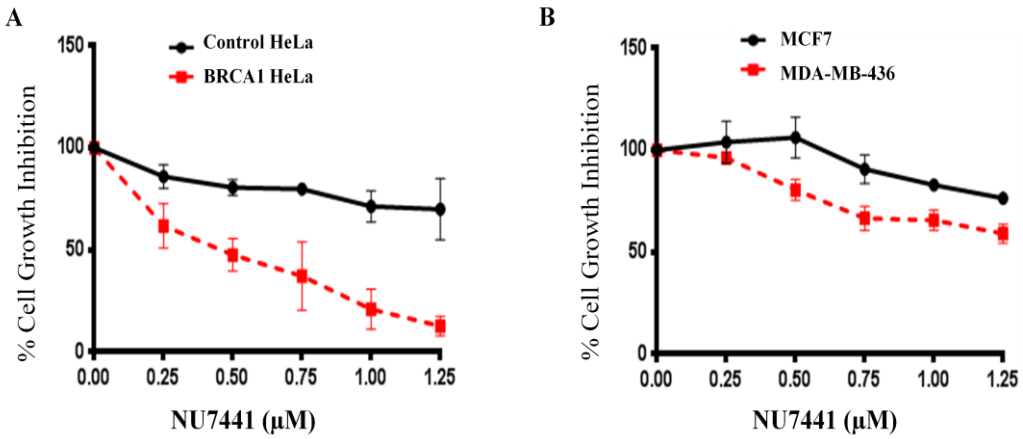

Figure 5.3. MTS cell growth inhibition assays of DNA-PKcs inhibitor (NU7441).

Cell lines with reduced BRCA1 expression exhibited decreased cell growth after treatment with NU7441 inhibitor for 6 days, compared to BRCA1 proficient cell lines. (A) BRCA1 HeLa cells compared to Control HeLa cells. (B) MDA-MB-436 cells compared to MCF7 cells. Data are shown as the mean and SD values for each concentration from ≥ 2 independent experiments.

For further validation NU7026 ($C_{17}H_{15}NO_3$), another potent kinase inhibitor of DNA-PKcs, was investigated (Hollick et al., 2003, Veuger et al., 2003, Amrein et al., 2007). As shown in Figure 5.4 clonogenic cell survival assays, BRCA1 HeLa cells are more sensitive to NU7026 than Control HeLa cells. Similar sensitivity was also demonstrated in BRCA1 mutated MDA-MB-436 cells compared to control MCF7 cells. Taken together, these data provide strong evidence that BRCA1 deficient cells are sensitive to DNA-PKcs inhibition.

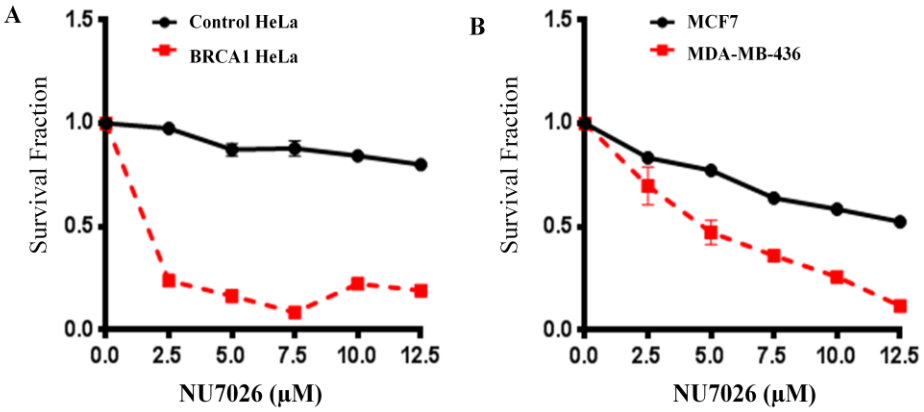

Figure 5.4. Clonogenic survival assay of DNA-PKcs inhibitor (NU7026).

Cell lines with reduced BRCA1 expression exhibited decreased colony forming ability after treatment with NU7026 inhibitor for 14 days, compared to BRCA1 proficient cell lines. (A) BRCA1 HeLa cells compared to Control HeLa cells. (B) MDA-MB-436 cells compared to MCF7 cells. Plating efficiencies of cell lines with standard error were as follows: (A) Control HeLa- 82.50% ± 0.50%; BRCA1 HeLa- 76.00% ± 6.50% (B) MCF7- 58.21% ± 2.21%; MDA-MB-436- 41.50% ± 2.25%. Clonogenic data are shown as the mean and SD values for each concentration from ≥ 2 independent experiments.

5.3.2. γH2AX focus immunofluorescence microscopy assay

To determine whether DSBs accumulate after treatment with NU7441, DSBs were measured using the γH2AX immunofluorescence microscopy assay. As described in Chapter 2 section 2.3.5, cells were treated with 1.5 μM of NU7441 for 24 hours and 48 hours. A significant increase in foci formation was observed in BRCA1 deficient cells after 48 hours treatment. Cells were then treated with 1 μM of NU7441 for 48 hours, but no significant accumulation of γH2AX foci in BRCA1 deficient cells was observed. The data support a dose response effect of DNA-PKcs inhibition in BRCA1 deficient cells.

5.3.2.1. γH2AX formation in response to DNA-PKcs inhibitors

BRCA1 proficient and BRCA1 deficient cell lines following treatment with 1.5 μM of NU7441 for 48 hours are shown in Figure 5.5. The data demonstrates a statistically significant increase in the accumulation of γH2AX foci in treated BRCA1 HeLa cells compared to untreated BRCA1 HeLa cells (mean 62.50% ± 7.50 vs. mean 17.50% ± 0.50; $p = 0.026$) and compared to corresponding treated Control HeLa cells (mean 8.00% ± 3.00; $p = 0.021$). Similar results were also observed in treated MDA-MB-436 cells in which accumulation of γH2AX foci were significantly higher compared to untreated MDA-MB-436 cells (mean 81.00% ± 9 vs. 7% ± 2; $p = 0.015$) and compared to corresponding treated MCF7 cells (mean 4.50% ± 1.50; $p = 0.013$).

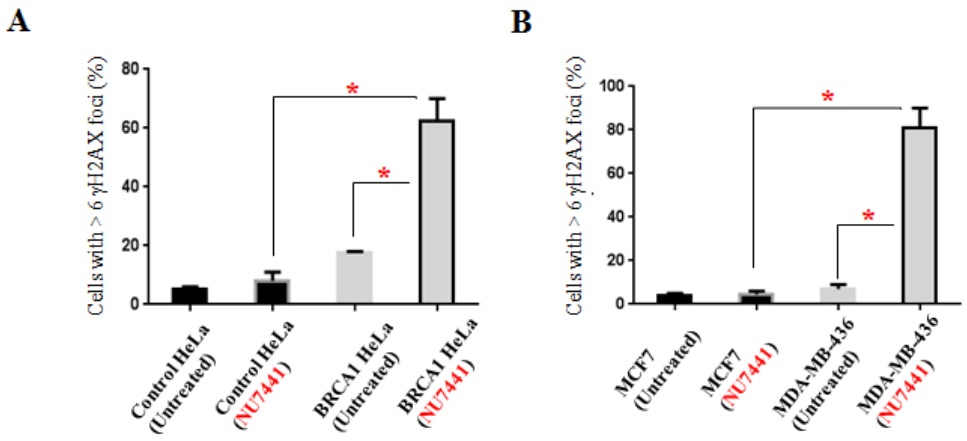

Figure 5.5. Immunofluorescence microscopy staining for γH2AX foci formation following NU7441 treatment for 48 hours.

(A) BRCA1 HeLa cells compared to Control HeLa cells. (B) MDA-MB-436 cells compared to MCF7 cells. Data are shown as the mean and SD values for each concentration from ≥ 2 independent experiments. * $p<0.05$, p value was assessed by a t-test comparing BRCA1 deficient cell lines to BRCA1 proficient cell lines. Graphs were produced and statistical analysis performed using GraphPad prism.

For further validation NU7026, another DNA-PKcs inhibitor, was investigated. Treatment with 1.5 µM of NU7026 produced similar results to NU7441. As shown in Figure 5.6, a statistically significant increase in the accumulation of γH2AX foci in treated BRCA1 HeLa cells compared to untreated BRCA1 HeLa cells (mean 46% ± 4 vs. 11% ± 1.0; $p = 0.013$), and compared to corresponding treated Control HeLa cells (mean 6.00% ± 2; $p = 0.012$) was observed. Similar results were also observed in treated MDA-MB-436 cells in which accumulation of γH2AX foci was significantly higher compared to untreated MDA-MB-436 cells (mean 80.50% ± 6.5 vs. 17.50% ± 1.5; $p = 0.011$), and compared to the corresponding treated MCF7 cells (mean 51% ± 1; $p = 0.046$). Even though MDA-MB-436 cells were more sensitive to NU7026 inhibitor, MCF7 cells showed similar changes (from 10% to 51%).

This result infers that NU7026 inhibitor maybe toxic to MCF7, especially as this increase was not seen with NU7441.

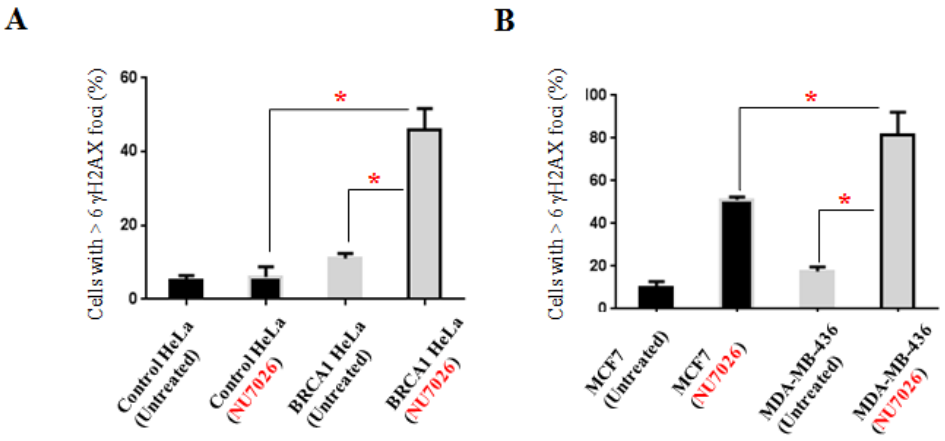

Figure 5.6. Immunofluorescence microscopy staining for γH2AX foci formation following NU7026 treatment for 48 hours.

(A) BRCA1 HeLa cells compared to Control HeLa cells. (B) MDA-MB-436 cells compared to MCF7 cells. Data are shown as the mean and SD values for each concentration from ≥ 2 independent experiments. * $p<0.05$, p value was assessed by a t-test comparing BRCA1 deficient cell lines to BRCA1 proficient cell lines. Graphs were produced and statistical analysis performed using GraphPad prism.

5.3.3. Cell cycle analysis by propidium iodide flow cytometry after treatment with DNA-PKcs inhibitors

Cells were treated as described in Chapter 2, section 2.3.6 for 24 hours and 48 hours with 1 µM or 1.5 µM of NU7441 (Figure 5.7). Although no significant difference was observed after 24 hours, at 48 hours in BRCA1 deficient cells treated with 1.5 µM NU7441 exhibited a significant increase in G1 phase arrest compared to control was observed.

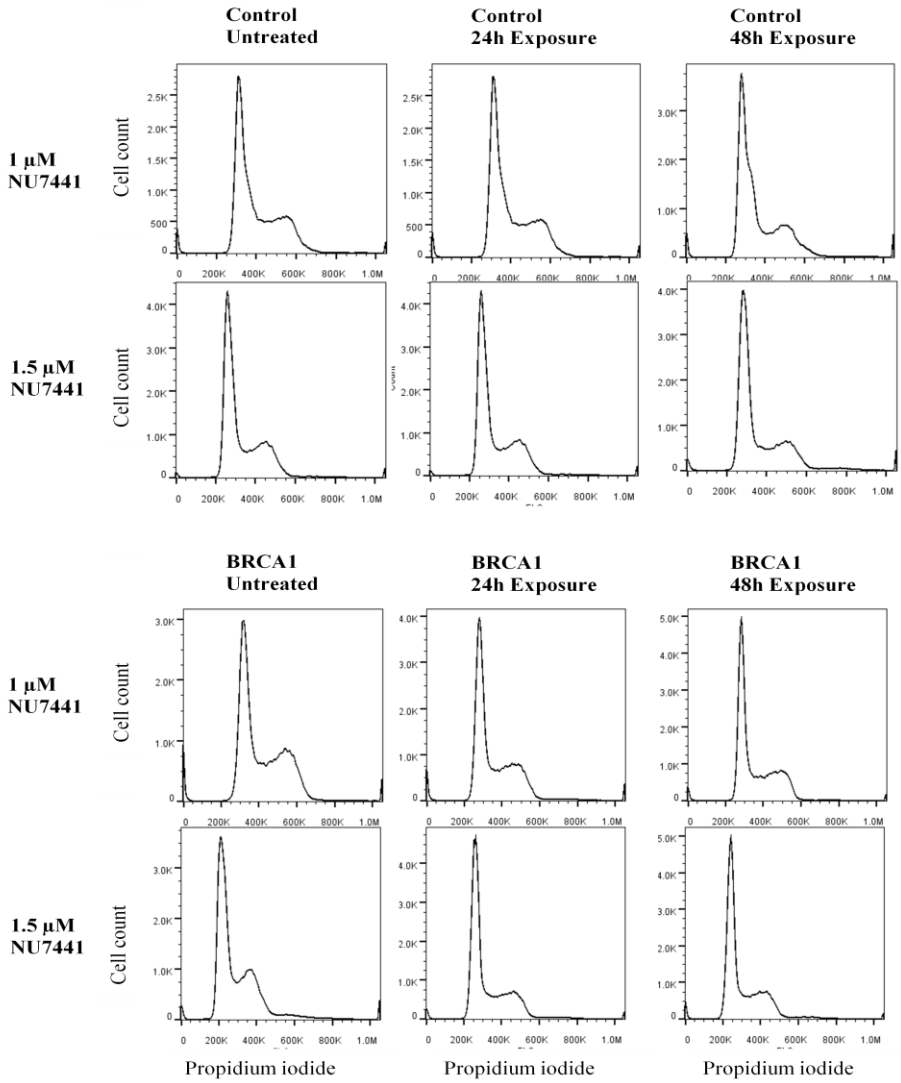

Figure 5.7. Representative graphs of flow cytometric cell cycle analysis following NU7441 treatment.

BRCA1 deficient HeLa cells and Control HeLa cells were treated with 1 µM or 1.5 µM for 24 hours or 48 hours. Y axis represents cell count and propidium iodides detected fluorescence is shown on the X axis.

Results for BRCA1 proficient and BRCA1 deficient cells following treatment with 1.5 µM (NU7441) for 48 hours are shown in Figure 5.8. The data demonstrate an increase in G1 arrest in treated BRCA1 HeLa cells compared with untreated BRCA1 HeLa cells (mean 60.6% ± 0.60 vs. 47.2% ± 3.80; though not significant $p = 0.07$), and compared to corresponding treated

Control HeLa cells (mean 32.4% ± 0.42; p = 0.0007). Results of treated MDA-MB-436 cells demonstrate an increase in G1 arrest compared to MDA-MB-436 untreated cells, though not significant (mean 49.4% ± 0.15 vs. mean 37.8% ± 3.6; p = 0.08). The observed G1 arrest was significantly higher in treated MDA-MB-436 cells compared to treated MCF7 cells (mean 30.4% ± 0.50; p < 0.0001). On the other hand, Control HeLa and MCF7 cells did not show the same rate of increase (i.e. ~12% increase like BRCA1 deficient cells) after treatment (Control HeLa and MCF7 cells, G1 arrest mean 41% to 32.4% and 25% to 30.4%, respectively).

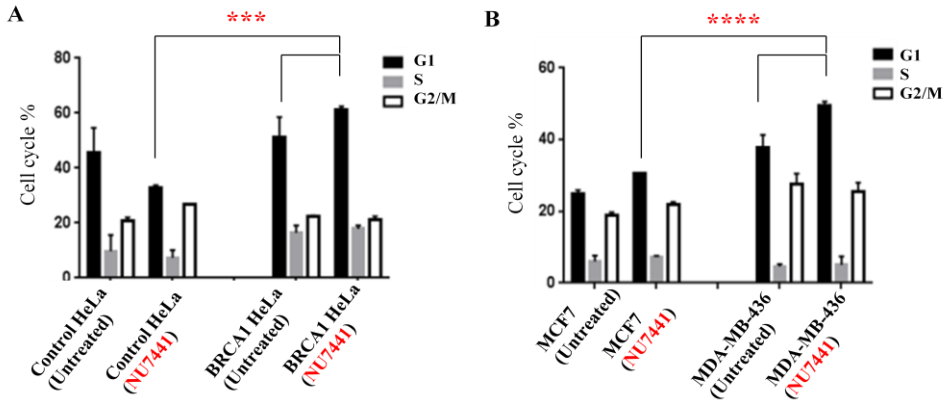

Figure 5.8. Flow cytometric cell cycle analysis following NU7441 treatment for 48 hours.

(A) BRCA1 HeLa cells compared to Control HeLa cells. (B) MDA-MB-436 cells compared to MCF7 cells. Data are shown as the mean and SD values for each concentration from ≥ 2 independent experiments. *** p<0.001 and **** p<0.0001, p value was assessed by a t-test comparing BRCA1 deficient cell lines to BRCA1 proficient cell lines. Graphs were produced and statistical analysis performed using GraphPad prism.

For further validation NU7026, another DNA-PKcs inhibitor, was investigated. Treatment with 10 µM of NU7026 produced similar results as with NU7441. As shown in Figure 5.9, increased G1 arrest in treated BRCA1 HeLa cells was demonstrated as compared to untreated BRCA1 HeLa cells (mean 61% ± 1 vs. 54.5% ± 0.5; p = 0.028). A modest, although not statistically significant, G1 arrest was also observed in treated MDA-MB-436 cells compared to untreated MDA-MB-436 cells (mean 40% ± 0.1 vs. 31.7% ± 3.8; p = 0.1). A statistically significant increase in G1 arrest was observed when treated MDA-MB-436 cells were compared to treated MCF7 cells (mean 27.25% ± 2.8; p = 0.04). In contrast, Control HeLa and MCF7 cells did not show the same increase.

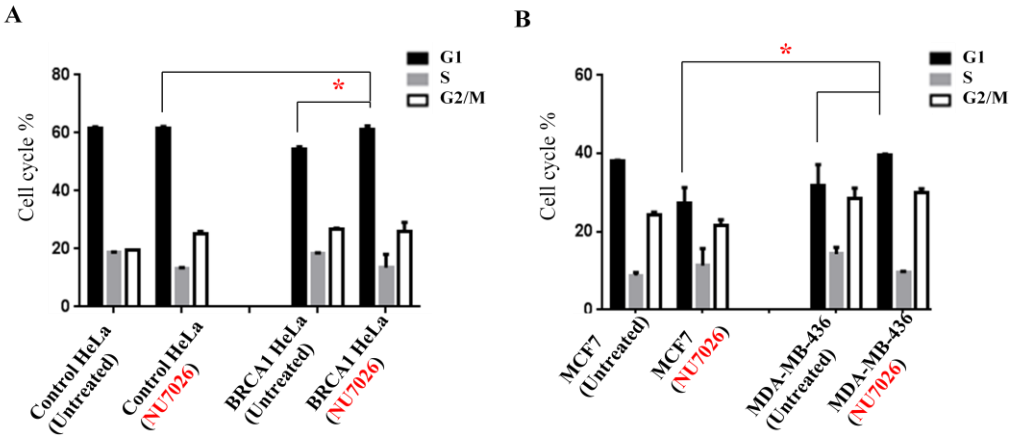

Figure 5.9. Flow cytometric cell cycle analysis following NU7026 treatment for 48 hours.

(A) BRCA1 HeLa cells compared to Control HeLa cells. (B) MDA-MB-436 cells compared to MCF7 cells. Data are shown as the mean and SD values for each concentration from ≥ 3 independent experiments. * $p<0.05$, p value was assessed by a t-test comparing BRCA1 deficient cell lines to BRCA1 proficient cell lines. Graphs were produced and statistical analysis performed using GraphPad prism.

5.3.4. Apoptosis detection by annexin V-FITC flow cytometry after treatment with DNA-PKcs inhibitors

Following evaluation of cell cycle arrest in BRCA1 deficient cells treated with DNA-PKcs inhibitors, Annexin V was used in conjunction with a propidium iodide (PI) for identification of early and late apoptotic cells as described in Chapter 2, section 2.3.7.

Arrest at the G1 phase of cell cycle may lead to apoptosis which could be the cause of the reduced survival observed in BRCA1 deficient cells in the clonogenic survival assay.

Cells were treated for 24 hours and 48 hours with 1.5 μM of NU7441. Although no significant increase in apoptosis was evident after 24 hours, at 48 hours in BRCA1 deficient cells treated with 1.5 μM of NU7441 significant increase in apoptosis compared to control cells was observed.

Results for BRCA1 proficient and BRCA1 deficient cells following treatment with 1.5 μM (NU7441) for 48 hours are shown in Figure 5.10, data were normalised against baseline apoptotic fraction (untreated cells) to determine the percentage increase in apoptosis. The data demonstrate a statistically significant increase in apoptosis with treated BRCA1 HeLa cells compared to untreated BRCA1 HeLa cells (mean 6.3% ± 0.36 vs. mean 3.6% ± 0.68; $p = 0.0057$). Similar results were also observed in treated MDA-MB-436 cells, in which a significant increase in apoptosis as compared to untreated MDA-MB-436 cells was observed (mean 13.5% ± 0.77 vs. 4.68% ± 0.07; $p < 0.0001$). On the other hand, Control HeLa and MCF7 cells did not show the same rate of increase (mean 2.44% to 3.25% and 4.06% to 4.76%, respectively).

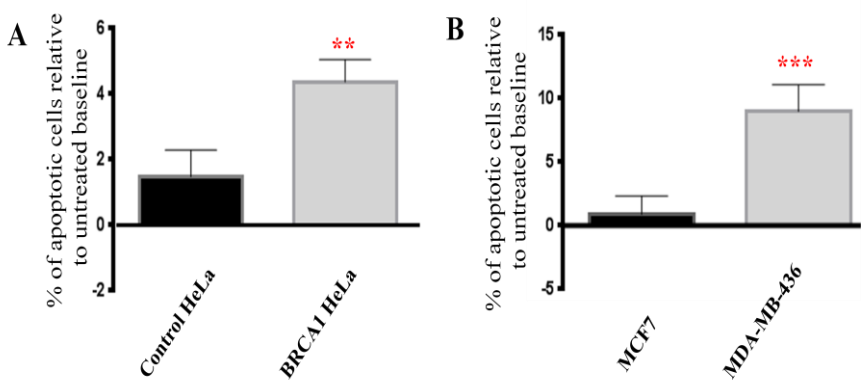

Figure 5.10. Apoptosis detection by annexin V-FITC flow cytometry in NU7441 treated cells.

Treatment with NU7441 inhibitor was associated with a significant increase in apoptotic cells. Data were normalised against baseline apoptotic fraction to determine the percentage increase in apoptosis. (A) BRCA1 HeLa cells compared to Control HeLa cells. (B) MDA-MB-436 cells compared to MCF7 cells. Data are shown as the mean and SD values for each concentration from ≥ 3 independent experiments. ** $p<0.01$ and *** $p<0.001$, p value was assessed by a t-test comparing BRCA1 deficient cell lines to BRCA1 proficient cell lines. Graphs were produced and statistical analysis performed using GraphPad prism.

For further validation NU7026, another DNA-PKcs inhibitor, was investigated. Treatment with 10 µM of NU7026 produced similar results as with NU7441. As shown in Figure 5.11, the data demonstrates a statistically significant increase in apoptosis in treated BRCA1 HeLa cells compared to the corresponding untreated BRCA1 HeLa cells (mean 8.71% ± 1.22 vs. mean 4.72% ± 0.34; $p = 0.034$). A similar increase was also observed in treated MDA-MB-436 cells as compared to untreated MDA-MB-436 cells (mean 9.13% vs. 4.67%; though was not significant $p=0.06$). On the other hand,

Control HeLa and MCF7 cells did not show the same rate of increase (mean 3.11% to 3.16% and 3.15% to 5.6%, respectively).

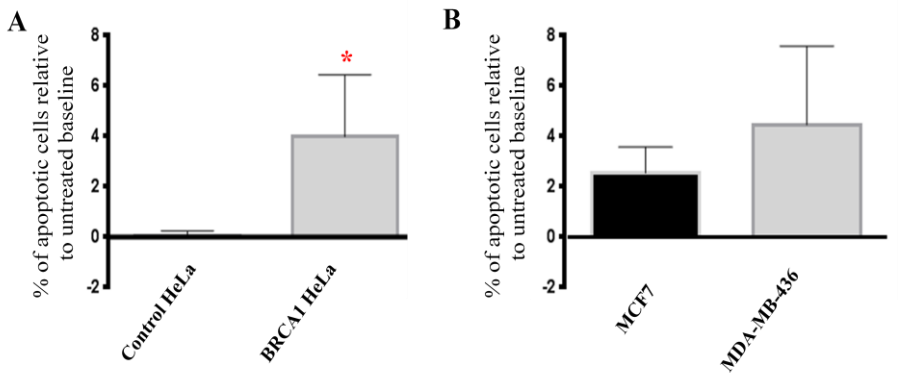

Figure 5.11. Apoptosis detection by annexin V-FITC flow cytometry in NU7026 treated cells.

Treatment with NU7026 inhibitor was associated with a significant increase in apoptotic cells. Data were normalised against baseline apoptotic fraction to determine the percentage increase in apoptosis. (A) BRCA1 HeLa cells compared to Control HeLa cells. (B) MDA-MB-436 cells compared to MCF7 cells. Data are shown as the mean and SD values for each concentration from ≥ 2 independent experiments. * $p<0.05$, p value was assessed by a t-test comparing BRCA1 deficient cell lines to BRCA1 proficient cell lines. Graphs were produced and statistical analysis performed using GraphPad prism.

5.4. Discussion and conclusions

The aim of this chapter was to investigate whether targeting BRCA1 deficiency by DNA-PKcs, a key player in NHEJ pathway, using NU7441 or NU7026 inhibitors, would be synthetically lethal.

The role of BRCA1 in regulating the NHEJ pathway has been investigated for a number of years. The data have been conflicting with a number of studies showing a major role of BRCA1 in NHEJ and maintenance of genomic integrity (Zhong et al., 2002, Bau et al., 2004), while others did not show a role of BRCA1 in NHEJ (Moynahan et al., 1999, Merel et al., 2002). The lack of consistency between these results may be partly explained by the use of different assays, which may measure different sub-pathways of NHEJ (Bau et al., 2006). Several studies have confirmed the interaction between BRCA1 and NHEJ factors. For example, one study showed that BRCA1 interacts with a subunit of the DNA-PK complex (KU80). Another study showed that BRCA1 is rapidly recruited to DSB and is dependent on its association with KU80 (Wei et al., 2008). A more recent study has found that DNA-PKcs interacts with BRCA1 in the absence of KU70 and KU80 (Davis et al., 2014b).

To test the importance of both BRCA1 and DNA-PKcs in the maintenance of cellular survival, clonogenic survival assays (inhibitor exposure for total assay period) were conducted to evaluate the cytotoxicity in BRCA1 knockdown HeLa cells and BRCA1 mutated MDA-MB-436 cells treated with DNA-PKcs inhibitors (NU7441 or NU7026), using Control HeLa and MCF7 cells as BRCA1 proficient controls, respectively. Then an alternative clonogenic assay protocol was performed (inhibitor exposure for 24 hours of assay period).

Results of both protocols showed high sensitivity in BRCA1 deficient cells compared to BRCA1 proficient cells. For additional validation, MTS assay was used to determine cell viability in response to DNA-PKcs inhibitor. Both NU7441 and NU7026 inhibitors induced significant cytotoxicity in BRCA1 deficient cells compared to BRCA1 proficient cells. Taken together, these data suggest that BRCA1 deficient cells are reliant on DNA-PKcs to maintain cellular survival. For mechanistic insights, several functional studies were conducted. BRCA1 deficient cell lines treated with DNA-PKcs inhibitors for 48 hours demonstrate a statistically significant increase in the accumulation of γH2AX foci compared to untreated BRCA1 cell lines. This finding supports previous publications showing accumulation of γH2AX foci with inhibition of DNA-PKcs (Shaheen et al., 2011, Sultana et al., 2013a). Interestingly MCF7 showed a slight increase after NU7026 inhibitor treatment but not with NU7441, this result infers that NU7026 may be toxic to MCF7 (Figure 5.6B); this could also be linked to the slight increase in apoptosis (Figure 5.11B). Results from Chapter 3 illustrate that ATM, ATR and DNA-PKcs are down regulated in BRCA1 deficient cells; these three enzymes are known to have a role in phosphorylation of H2AX (Podhorecka et al., 2010). Previously it had been shown that DSB deficient cells exhibited reduced phosphorylation of H2AX after ionizing radiation treatment, however they conclude that inhibitions of DNA-PKcs and ATM reduce, but do not eliminate, the accumulation of γH2AX foci (Paull et al., 2000). In the current study inhibition of DNA-PKcs or ATM in BRCA1 deficient cells have increased γH2AX foci formation around DSBs as compared to the untreated cells. The fact that γH2AX was still forming in my study can have two explanations. Firstly, with

a low expression of ATM and ATR, in the absence of DNA-PKcs, other enzymes (e.g. CHK2) may activate γH2AX, as has been shown in a previous study (Tu et al., 2013). Alternatively another signaling pathway may modulate γH2AX levels, for example DNA-PKcs has been suggested to phosphorylates H2AX directly and modulate γH2AX level indirectly through the Akt/GSK3ß signaling pathway (An et al., 2010). In the absence of DNA-PKcs it may be that the Akt/GSK3ß pathway can be activated by other factors. Secondly, the fact that ATM and ATR are down regulated in BRCA1 deficient cells does not mean it is completely silenced, and in the absence of DNA-PKcs low levels of ATM or ATR may be sufficient to phosphorylate H2AX. Taken together, these results support the hypothesis that DNA-PKcs inhibition in BRCA1-BER deficient cells causes DSB accumulation which cannot be repaired due to an actual defect in DSB pathway.

Monitoring cell cycle progression in BRCA1 deficient cell lines after treatment with DNA-PKcs inhibitors for 48 hours was associated with a modest increase arrest at the G1 phase compared to untreated BRCA1 deficient cell lines. However, this increase was not always significant and different time points should be tested in the future. These modest increases in G1 arrest support those previously published showing that G1 arrest increases after inhibition with DNA-PKcs (NU7441) inhibitor, in colon cancer (Zhao et al., 2006), prostate cancer (Shaheen et al., 2011, Yu et al., 2012) and breast cancer cell lines (Ciszewski et al., 2014). A more recent study showed that BRCA1 facilitates accurate repair during G1 phase through NHEJ (Jiang et al., 2013). To evaluate induction of apoptosis, a flow cytometry-based apoptosis detection assay was performed. Results demonstrated that BRCA1 deficient cell lines

treated with DNA-PKcs inhibitors for 48 hours exhibited increase in apoptosis rate compared to untreated BRCA1 deficient cell lines. These results support those previously published showing an increase in apoptosis after DNA-PKcs inhibition, in prostate cancer (Yu et al., 2012) and XRCC1 knockdown HeLa cell lines (Sultana et al., 2013a).

Taken together, the data presented here demonstrated that a potential synthetic lethality relationship which exists between BRCA1 deficiency and DNA-PKcs inhibition. Also the present study highlights the important role of DNA-PKcs in maintaining cellular survival in BRCA1 deficient cell. A model for synthetic lethality is shown in Figure 5.12. In brief, impaired expression of BER in BRCA1 deficient cell lines leads to accumulation of unrepaired SSBs followed by the formation of DSBs during DNA replication process. Therefore, it is suggested that cells are reliant on backup DSB pathway for cellular survival. Targeting the DSB pathway by DNA-PKcs inhibition would lead to the observed synthetic lethality. In contrast, in cells that are proficient in DSB repair the DSBs would be repaired and cells would survive.

It should be noted that these *in vitro* studies have limitations. Firstly, this investigation was restricted to two DNA-PKcs inhibitors. And a recent study has indicated that DNA-PKcs inhibitors currently available are limited by poor pharmacokinetics (Davidson et al., 2013). Secondly, cell cycle analysis showed modest G1 increase with DNA-PKcs treatment, this could be because samples were analysed after 24 and 48 hours. However, more time points should be tested in the future to monitor cells response after different treatments.

5.4.1. Conclusions

To conclude, this *in vitro* study has shown a potential synthetic lethality between BRCA1 deficiency and DNA-PKcs inhibition. Firstly, data have shown a selective toxicity in BRCA1 deficient cells to DNA-PKcs inhibitors (NU7441 or NU7026). Secondly, DNA DSB accumulation was observed after treatment with DNA-PKcs inhibitors in BRCA1 deficient cells compared to untreated cells. In addition modest increase in G1 phase arrest was detected, though this increase was not always significant and different time points should be tested in the future. Then again, DNA-PKcs inhibition was found to trigger apoptosis in BRCA1 deficient cells. Moreover, these findings present a potential new alternative synthetic lethality strategy in BRCA1 deficient cells. Finally, in agreement with previous studies this study shows the importance of DNA-PKcs in maintaining cellular survival.

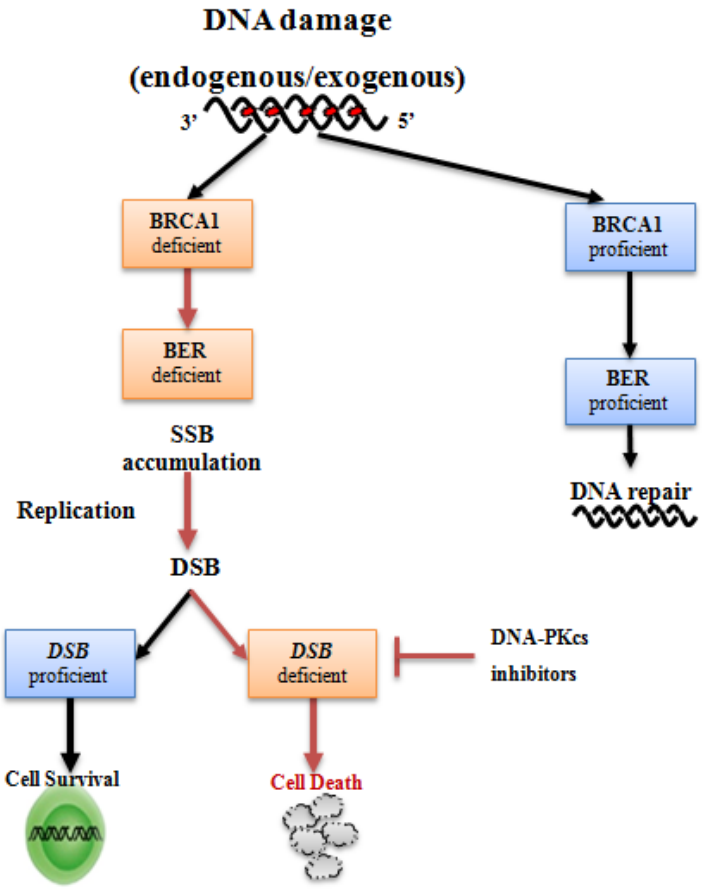

Figure 5.12. Proposed model of synthetic lethality between DNA-PKcs inhibitors and BRCA1-BER deficient system.

Chapter 6

Cisplatin in combination with Ataxia telangiectasia mutated (ATM) or DNA dependent protein kinase catalytic subunit (DNA-PKcs) inhibitor in BRCA1 deficient cells

6. Cisplatin in combination with Ataxia telangiectasia mutated (ATM) or DNA dependent protein kinase catalytic subunit (DNA-PKcs) inhibitor in BRCA1 deficient cells

6.1. Introduction

Cisplatin [cis-diamminedichloroplatinum(II)] is a platinating anticancer chemotherapeutic agent that acts by covalently binding to DNA and forming DNA damaging adducts. Cisplatin is effective in the treatment of many cancers including metastatic testicular cancers, bladder, cervical, ovarian, lung, head and neck cancers (Kelland, 2007, Ratanaphan, 2011).

Several preclinical studies have shown that BRCA1 deficient cell lines are hypersensitive to cisplatin treatment compared to their wild type matched controls (Bhattacharyya et al., 2000, Tassone et al., 2003, Tan et al., 2008). In addition, clinical studies have demonstrated similar hypersensitivity to cisplatin (Byrski et al., 2009, Taron et al., 2004, Quinn et al., 2007, Font et al., 2011, Silver et al., 2010).

In the previous chapters, a potential synthetic lethality was demonstrated between BRCA1 deficiency and ATM inhibition or DNA-PKcs inhibition in *in vitro* cell culture system. In light of these data, cisplatin was investigated in combination with ATM or DNA-PKcs inhibitor in BRCA1 proficient and BRCA1 deficient cells.

6.1.1. Rationale for study

The data presented in previous chapters suggested that BRCA1 deficiency is associated with low expression of BER. BRCA1-BER deficient cells are amenable to synthetic lethality targeting using ATM or DNA-PKcs inhibitors. As BRCA1 deficient cells are cisplatin sensitive, the potential of a combination strategy in BRCA1-BER proficient cells was investigated.

6.2. Aims

The aims of this study were as follows:

1. To investigate the effect of cisplatin in combination with ATM inhibitor (KU55933) or DNA-PKcs inhibitor (NU7441) in clonogenic cell survival assay.
2. To test the hypothesis that DNA double strand breaks accumulate in cells after treatment with cisplatin in combination with ATM inhibitor (KU55933) or DNA-PKcs inhibitor (NU7441) in BRCA1 deficient cells.
3. To determine the effect of cisplatin / ATM inhibitor (KU55933) or DNA-PKcs inhibitor (NU7441) combination on cell cycle progression in BRCA1 deficient cells.
4. To quantify apoptosis in BRCA1 deficient cells after treatment with cisplatin / ATM inhibitor (KU55933) or DNA-PKcs inhibitor (NU7441) combinations.

6.3. Results

6.3.1. Clonogenic cell survival assay in response to Cisplatin

BRCA1 mutated (MDA-MB-436) cells and knockdown (BRCA1 HeLa) cell lines along with control cells MCF7 and Control HeLa cell lines respectively, were treated with increasing concentrations of cisplatin ranging from (0.25 µM to 1.25 µM). Clonogenic survival assay results are shown in Figure 6.1. No colonies were obtained at any dose for BRCA1 HeLa and MDA-MB-436, showing high sensitivity in these cell lines and that the IC_{50} cannot be estimated from these data but must be below the minimum value tested. On the other hand, Control HeLa, mean IC_{50}= 0.25 µM ± 0.6 and MCF7, mean IC_{50}= 1.23 µM ± 0.9.

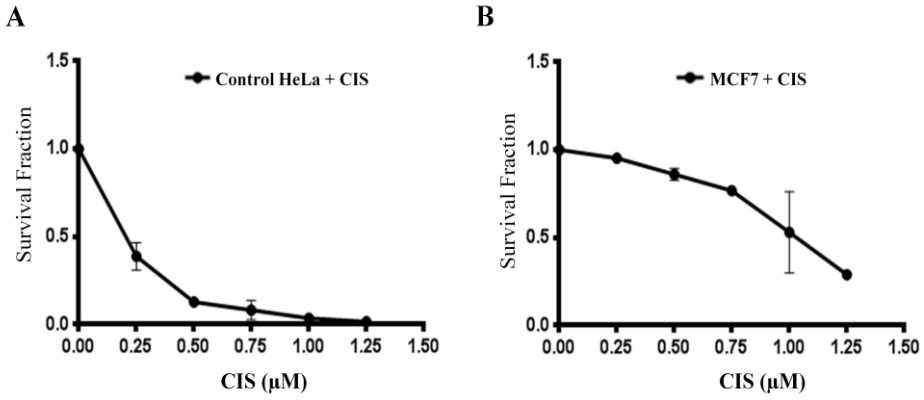

Figure 6.1. Clonogenic survival assay of cisplatin.

After exposure for 16 hours to cisplatin ranging from (0.25 µM to 1.25 µM), no colonies were obtained at any dose for BRCA1 HeLa and MDA-MB-436 showing high sensitivity in these lines compared to BRCA1 proficient cell lines. (A) BRCA1 HeLa cells compared to Control HeLa cells. (B) MDA-MB-436 cells compared to MCF7 cells. Plating efficiencies of cell lines were as follows: (A) Control HeLa- 75% ; BRCA1 HeLa- 75% (B) MCF7- 56.5% ; MDA-MB-436- 49.75%. Clonogenic data are shown as the mean and SD values for each concentration from 2 experiments.

6.3.2. Clonogenic cell survival assay in cells treated with KU55933 or NU7441 in combination with cisplatin

To evaluate the combination between cisplatin and ATM inhibitor (KU55933) or DNA-PKcs inhibitor (NU7441), cells were cultured with increasing concentrations of cisplatin. Cells were treated with increasing concentration of cisplatin ranging from (0.00001 µM to 0.1 µM) and KU55933 (5µM, HeLa cell lines and 7.5 µM, breast cancer cell lines) or NU7441 (0.5µM, HeLa cell lines and 0.75 µM, breast cancer cell lines). The concentration range for cisplatin in combination studies was lower as the cells were hypersensitive at higher concentrations and underwent profound cell death.

Clonogenic survival assays results for the combination of ATM inhibitor and cisplatin are shown in Figure 6.2. BRCA1 knockdown cells are more sensitive to combination treatment than cisplatin alone (mean IC_{50}= 0.00052 ± 0.00019 vs. IC_{50} above the maximum level tested), and compared to BRCA1 proficient Control HeLa cells. Similar sensitivity was also demonstrated in combination treated MDA-MB-436 cells compared to cisplatin alone (mean IC_{50}= 0.0003 ± 0.00013 vs. IC_{50}= 0.16 ± 0.026), and compared to control MCF7 cells.

Clonogenic survival assays results for the combination of DNA-PKcs inhibitor and cisplatin are shown in Figure 6.3. BRCA1 knockdown cells are more sensitive to combination treatment than cisplatin alone (mean IC_{50}= 0.09 ± 0.098 vs. IC_{50} above the maximum level tested), and comparing to BRCA1 proficient Control HeLa cells. Similar sensitivity was also demonstrated in

combination treated MDA-MB-436 cells compared to cisplatin alone (mean IC_{50}= 0.005 ± 0.0047 vs. IC_{50}= 0.16 ± 0.026), and compared to control MCF7 cells.

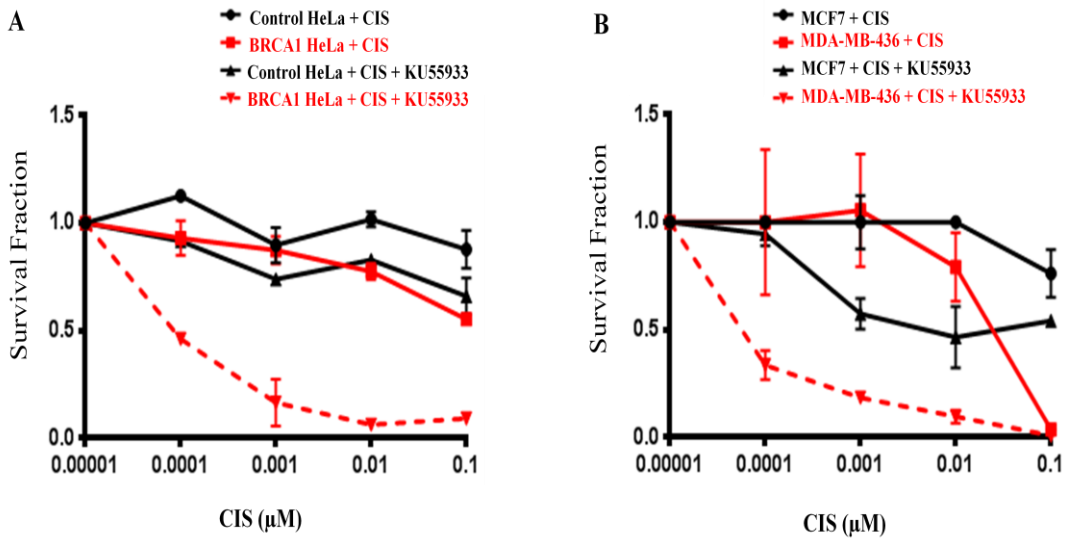

Figure 6.2. Clonogenic survival assay of ATM inhibitor (KU55933) in combination with cisplatin.

BRCA1 deficient cells show decreased colony forming ability after exposure for 16 hours to cisplatin ranging from (0.00001 µM to 0.1 µM) and then KU55933 (5 µM, HeLa cells lines and 7.5 µM, breast cancer cell lines), compared to BRCA1 proficient cell lines. (A) BRCA1 HeLa cells compared to Control HeLa cells. (B) MDA-MB-436 cells compared to MCF7 cells. Plating efficiencies of cell lines with standard error were as follows: (A) Control HeLa- 59.33% ± 1.69%; BRCA1 HeLa- 65.67% ± 0.60% (B) MCF7- 44.89% ± 0.72%; MDA-MB-436- 24.53% ± 2.76%. Clonogenic data are shown as the mean and SD values for each concentration from ≥ 2 independent experiments.

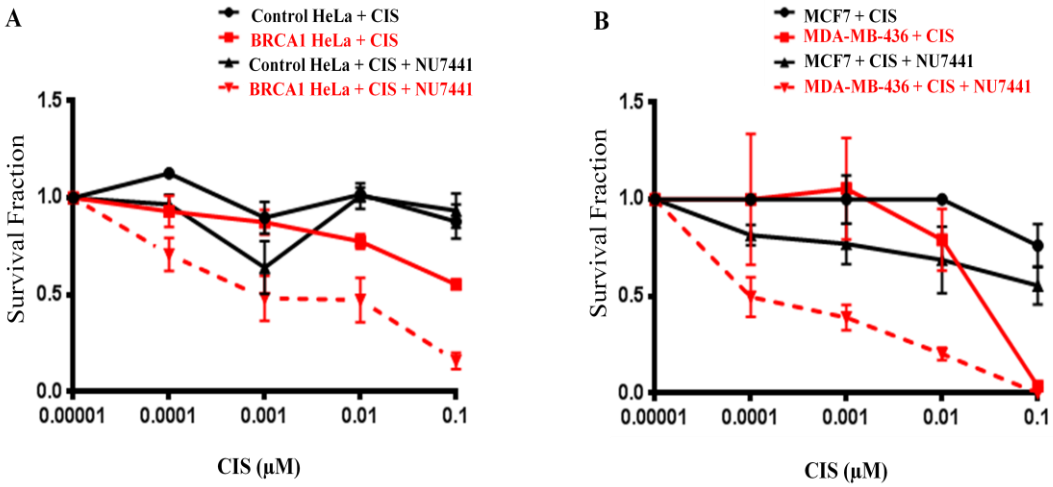

Figure 6.3. Clonogenic survival assay of DNA-PKcs inhibitor (NU7441) in combination with cisplatin.

BRCA1 deficient cells show decreased colony forming ability after exposure for 16 hours to cisplatin ranging from (0.00001 µM to 0.1 µM) and then NU7441 (0.5µM, HeLa cell lines and 0.75 µM, breast cancer cell lines), compared to BRCA1 proficient cell lines. (A) BRCA1 HeLa cells compared to Control HeLa cells. (B) MDA-MB-436 cells compared to MCF7 cells. Plating efficiencies of cell lines with standard error were as follows: (A) Control HeLa- 60% ± 1.36%; BRCA1 HeLa- 64.83% ± 1.55% (B) MCF7- 46.78% ± 2.61%; MDA-MB-436- 25.87% ± 2.36%. Clonogenic data are shown as the mean and SD values for each concentration from ≥ 2 independent experiments.

6.3.3. γH2AX immunofluorescence microscopy in response to KU55933 or NU7441 in combination with cisplatin

To determine whether DNA double strand breaks (DSBs) accumulate after treatment with KU55933 and cisplatin, DSBs were measured using the γH2AX immunofluorescence microscopy assay. As described in Chapter 2 section 2.3.5, cells were treated with cisplatin (0.1 μM) and KU55933 (for HeLa cell lines = 5 μM or breast cancer cell lines = 7.5 μM) for 24 hours and 48 hours. Although no significant changes were observed after 24 hours, at 48 hours a significant increase in foci formation was observed in BRCA1 deficient cells.

As shown in Figure 6.4, the data demonstrates a statistically significant increase in the accumulation of γH2AX foci in combination treated BRCA1 HeLa cells compared to corresponding cisplatin alone treated BRCA1 HeLa cells and untreated BRCA1 HeLa cells (76.50% vs. 18%; $p = 0.003$ and 76.50% vs. 11%; $p = 0.0017$, respectively) and compared to combination treated Control HeLa cells (15.00 %; $p = 0.0019$).

Similar results were also observed in combination treated MDA-MB-436 cells in which accumulation of γH2AX foci were higher compared to corresponding cisplatin alone treated MDA-MB-436 cells and untreated MDA-MB-436 cells (60.50% vs. 36%; $p = 0.06$ and 60.50% vs. 17.50%; $p = 0.012$, respectively) and compared to combination treated MCF7 cells (31 %; $p = 0.032$).

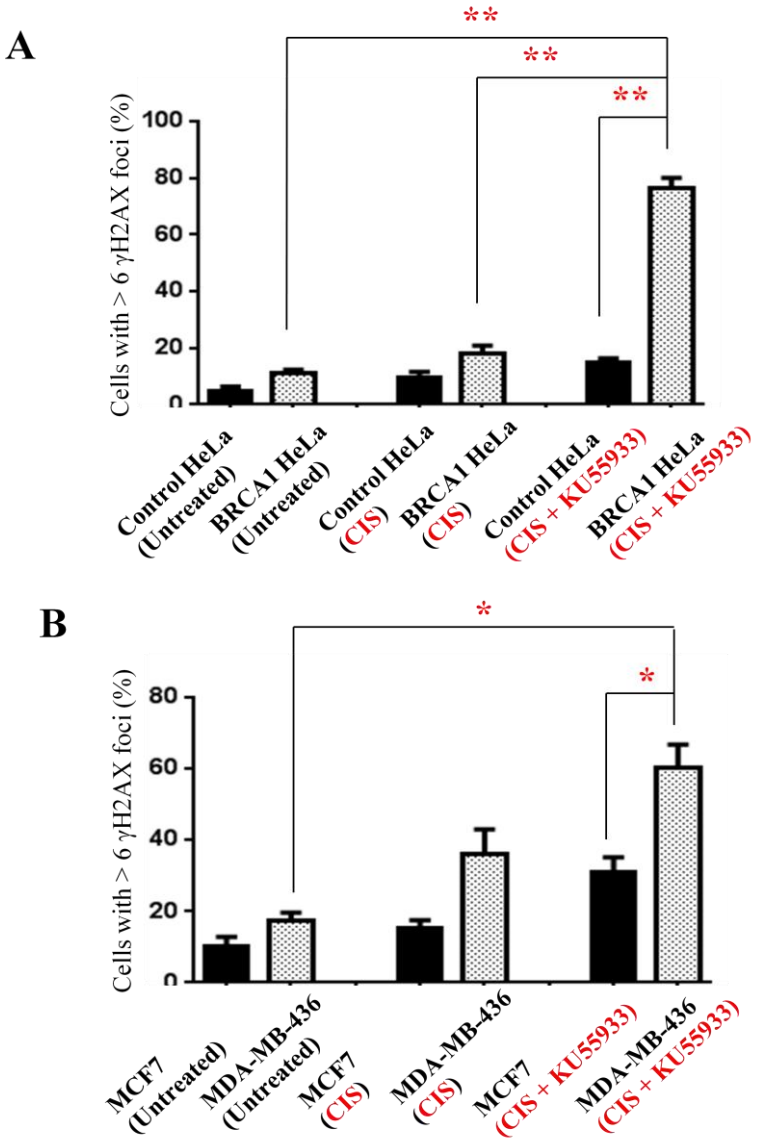

Figure 6.4. Immunofluorescence microscopy staining for γH2AX foci formation following ATM inhibitor (KU55933) in combination with cisplatin for 48 hours exposure.

(A) BRCA1 HeLa cells compared to Control HeLa cells. (B) MDA-MB-436 cells compared to MCF7 cells. Data are shown as the mean and SD values for each concentration from ≥ 2 independent experiments. * $p<0.05$ and ** $p<0.01$, p value was assessed by a t-test comparing BRCA1 deficient cell lines to BRCA1 proficient cell lines. Graphs were produced and statistical analysis performed using GraphPad prism.

Alternatively, cells were treated with cisplatin (0.1 μM) and NU7441 (for HeLa cell lines = 0.5 μM or breast cancer cell lines = 0.75 μM) for 24 hours and 48 hours. Although no significant changes were observed after 24 hours, at 48 hours in BRCA1 deficient cells a significant increase in foci formation was observed. As shown in Figure 6.5, the data demonstrates a statistically significant increase in the accumulation of γH2AX foci in combination treated BRCA1 HeLa cells compared to corresponding cisplatin alone treated BRCA1 HeLa cells and untreated BRCA1 HeLa cells (87% vs. 18%; $p = 0.0017$ and 87% vs. 11%; $p = 0.0009$, respectively) and compared to combination treated Control HeLa cells (16%; $p = 0.0026$).

Similar results were also observed in combination treated MDA-MB-436 cells in which accumulation of γH2AX foci were higher compared to corresponding cisplatin alone treated MDA-MB-436 cells and untreated MDA-MB-436 cells (81.5% vs. 36%; $p = 0.017$ and 81.5% vs. 17.50%; $p = 0.003$, respectively) and compared to combination treated MCF7 cells (38.5%; $p = 0.013$).

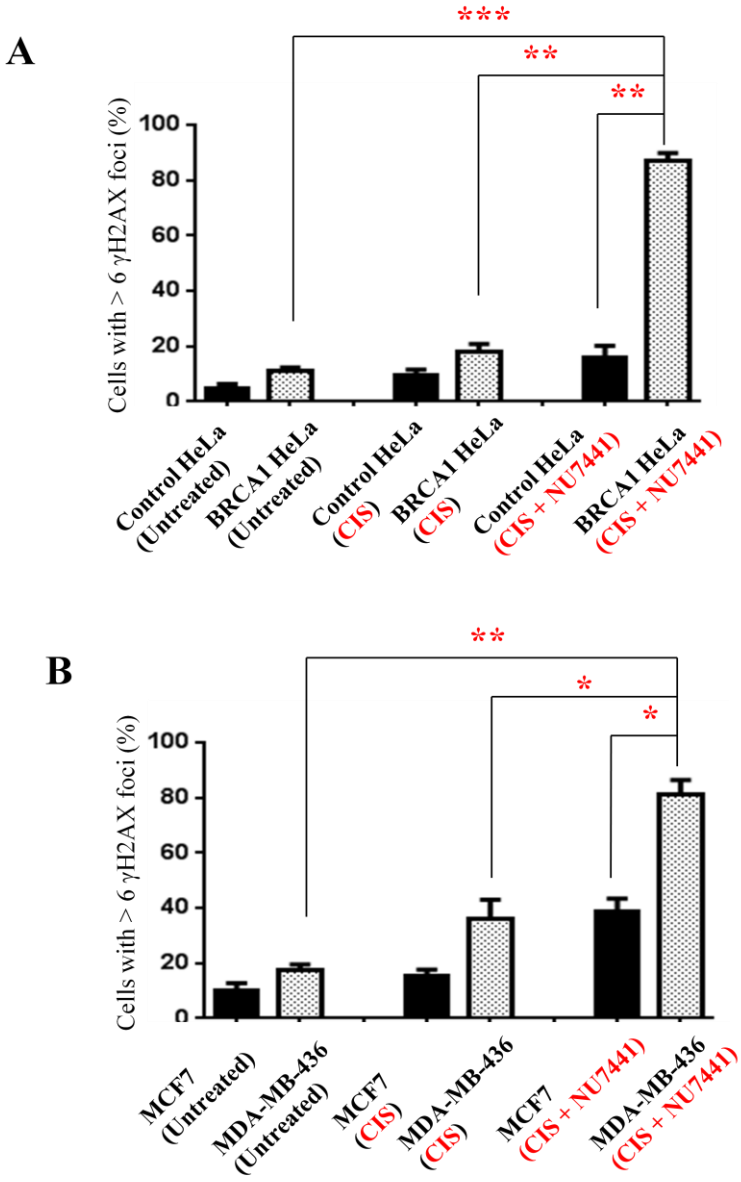

Figure 6.5. Immunofluorescence microscopy staining for γH2AX foci formation following DNA-PKcs inhibitor (NU7441) in combination with cisplatin for 48 hours exposure.

(A) BRCA1 HeLa cells compared to Control HeLa cells. (B) MDA-MB-436 cells compared to MCF7 cells. Data are shown as the mean and SD values for each concentration from ≥ 2 independent experiments. * $p<0.05$, ** $p<0.01$ and *** $p<0.001$, p value was assessed by a t-test comparing BRCA1 deficient cell lines to BRCA1 proficient cell lines. Graphs were produced and statistical analysis performed using GraphPad prism.

6.3.4. Flow cytometric cell cycle analysis in response to ATM inhibitor (KU55933) or DNA-PKcs inhibitor (NU7441) in combination with Cisplatin

For cell cycle analysis, cells were treated with cisplatin (0.1 µM) and KU55933 (for HeLa cell lines = 5 µM or breast cancer cell lines = 7.5 µM) for 48 hours. Results for BRCA1 proficient and BRCA1 deficient cells following combination treatment are shown in Figure 6.6. The data demonstrate an increase in G2/M arrest in combination treated BRCA1 HeLa cells compared to corresponding cisplatin alone treated BRCA1 HeLa cells and untreated BRCA1 HeLa cells (mean 37.6%, 29.5% and 25.8%; respectively). Similar results were also observed in combination treated MDA-MB-436 cells in which G2/M arrest were significantly higher compared to untreated MDA-MB-436 cells (mean 38% vs. 32.4%). On the other hand, cisplatin alone treated MDA-MB-436 cells showed mean of 41.4% G2/M arrest.

Conversely, cells were treated with cisplatin (0.1 µM) and NU7441 (for HeLa cell lines = 0.5 µM or breast cancer cell lines = 0.75 µM) for 48 hours. As shown in Figure 6.7, the data demonstrates an increase in G2/M arrest in combination treated BRCA1 HeLa cells compared with corresponding cisplatin alone treated BRCA1 HeLa cells and untreated BRCA1 HeLa cells (mean 34.2%, 29.5% and 25.8%; respectively). Similar results were also observed in combination treated MDA-MB-436 cells in which G2/M arrest was significantly higher compared to untreated MDA-MB-436 cells (mean 38.2% vs. 32.4%). On the other hand, cisplatin alone treated MDA-MB-436 cells showed a mean G2/M arrest of 41.4%. Control HeLa and MCF7 cells did not show the same increase as BRCA1 deficient cells with both combination treatments.

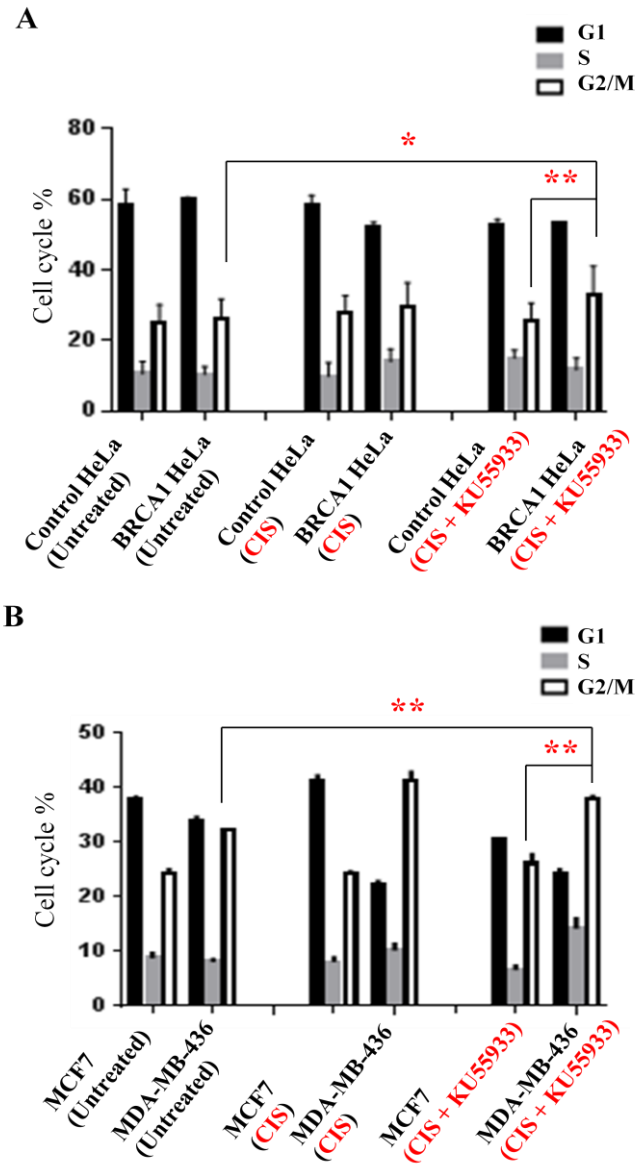

Figure 6.6. Flow cytometric cell cycle analysis following ATM inhibitor (KU55933) in combination with cisplatin

(A) BRCA1 HeLa cells compared to Control HeLa cells. (B) MDA-MB-436 cells compared to MCF7 cells. Data are shown as the mean and SD values for each concentration from ≥ 2 independent experiments. * $p<0.05$ and ** $p<0.01$, p value was assessed by a t-test comparing BRCA1 deficient cell lines to BRCA1 proficient cell lines. Graphs were produced and statistical analysis performed using GraphPad prism.

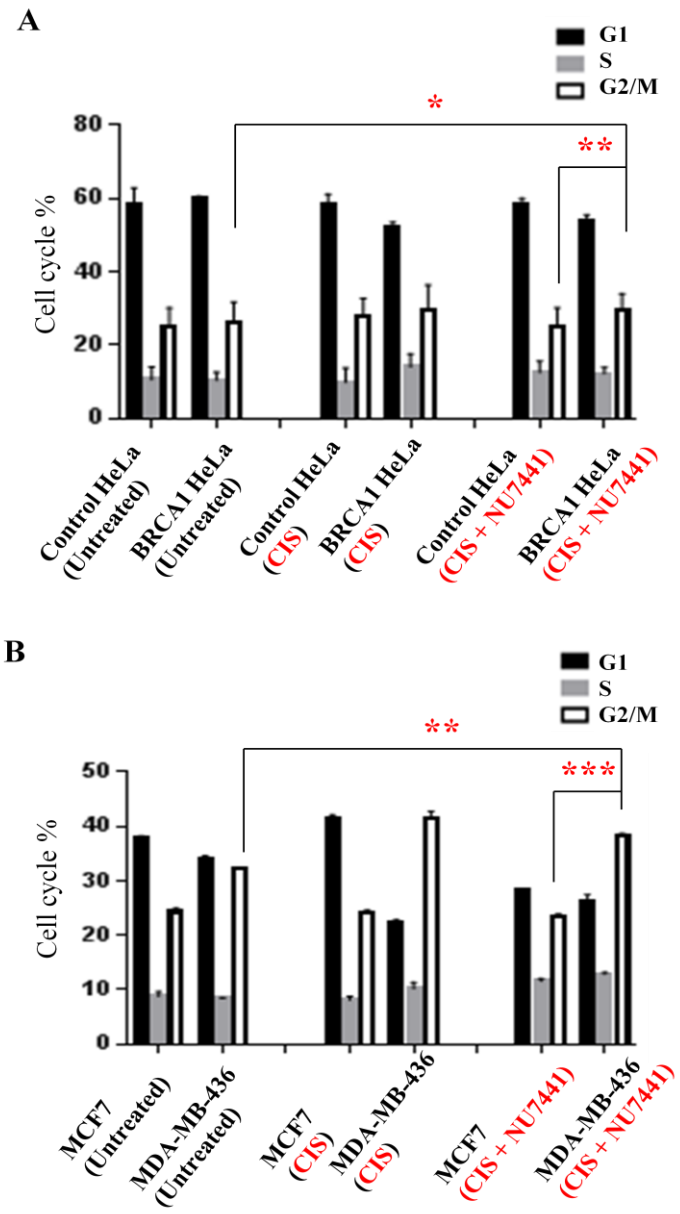

Figure 6.7. Flow cytometric cell cycle analysis following DNA-PKcs inhibitor (NU7441) in combination with cisplatin

(A) BRCA1 HeLa cells compared to Control HeLa cells. (B) MDA-MB-436 cells compared to MCF7 cells. Data are shown as the mean and SD values for each concentration from ≥ 2 independent experiments. * $p<0.05$ and ** $p<0.01$, *** $p<0.001$, p value was assessed by a t-test comparing BRCA1 deficient cell lines to BRCA1 proficient cell lines. Graphs were produced and statistical analysis performed using GraphPad prism.

6.3.5. Apoptosis detection by annexin V-FITC flow cytometry in response to KU55933 or NU7441 in combination with cisplatin

Cells were treated with cisplatin (0.1 µM) and KU55933 (for HeLa cell lines = 5 µM or breast cancer cell lines = 7.5 µM) for 48 hours. Results for BRCA1 proficient and BRCA1 deficient cells following combination treatment are shown in Figure 6.8, data were normalised against baseline apoptotic fraction (untreated cells) to determine the percentage increase in apoptosis. The data demonstrate a statistically significant increase in combination treated BRCA1 HeLa cells compared to corresponding cisplatin alone treated BRCA1 HeLa cells and untreated BRCA1 HeLa cells (mean 20.6%, 15.9% and 5.3%; respectively). Similar results were also observed in combination treated MDA-MB-436 cells in which the increase in apoptosis was significantly higher compared to cisplatin alone treated MDA-MB-436 and compared to untreated MDA-MB-436 cells (mean 17.6%, 7.4% and 4.9%; respectively). On the other hand, Control HeLa and MCF7 cells did not show the same high increase (i.e. around 14% increase with BRCA1 deficient cells) after cisplatin and KU55933 treatment (mean 4.35% to 7.49% and 3.17% to 9.25%, respectively).

Conversely, cells were treated with cisplatin (0.1 µM) and NU7441 (for HeLa cell lines = 0.5 µM or breast cancer cell lines = 0.75 µM) for 48 hours. As shown in Figure 6.9, the data demonstrates a statistically significant increase in combination treated BRCA1 HeLa cells compared to corresponding cisplatin alone treated BRCA1 HeLa cells and untreated BRCA1 HeLa cells (mean 25%, 15.9% and 5.3%; respectively). Similar results were also observed in combination treated MDA-MB-436 cells in which the increase in apoptosis was significantly higher compared to cisplatin alone treated MDA-MB-436

and compared to untreated MDA-MB-436 cells (mean 19.2%, 7.4% and 4.9%; respectively). On the other hand, Control HeLa and MCF7 cells did not show the same high increase (i.e. around 17% increase with BRCA1 deficient cells) after cisplatin and NU7441 treatment (mean 4.35% to 4.13% and 3.17% to 11%, respectively).

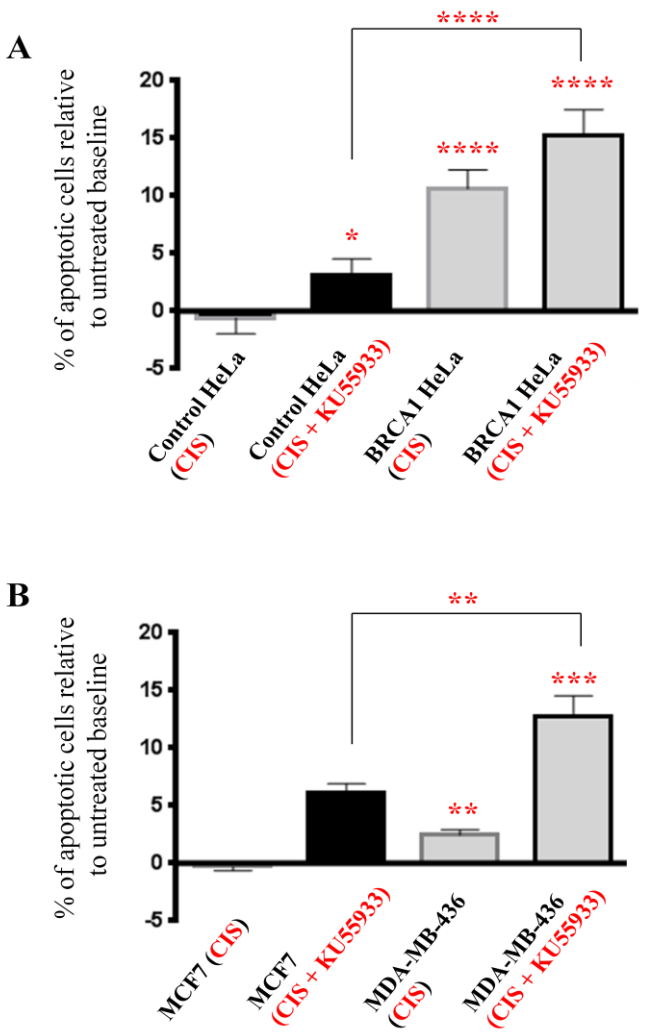

Figure 6.8. Apoptosis detection by annexin V-FITC flow cytometry in response to ATM inhibitor (KU55933) in combination with cisplatin

Treatment with combination KU55933 and cisplatin was associated with a significant increase in apoptotic. Data were normalised against baseline apoptotic fraction to determine the percentage increase in apoptosis. (A) BRCA1 HeLa cells compared to Control HeLa cells. (B) MDA-MB-436 cells compared to MCF7 cells. Data are shown as the mean and SD values for each concentration from 3 independent experiments. * $p<0.05$, ** $p<0.01$, *** $p<0.001$ and **** $p<0.0001$, p value was assessed by a t-test comparing BRCA1 deficient cell lines to BRCA1 proficient cell lines. Graphs were produced and statistical analysis performed using GraphPad prism.

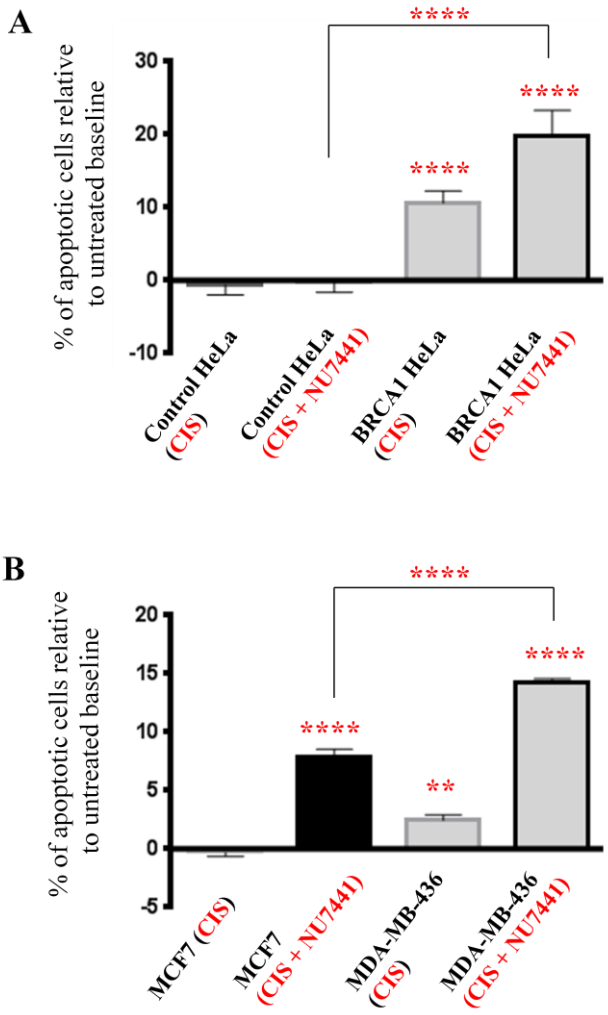

Figure 6.9. Apoptosis detection by annexin V-FITC flow cytometry in response to DNA-PKcs inhibitor (NU7441) in combination with cisplatin

Exposure to combination NU7441 and cisplatin was associated with a significant increase in apoptotic. Data were normalised against baseline apoptotic fraction to determine the percentage increase in apoptosis. (A) BRCA1 HeLa cell line compared to Control HeLa. (B) MDA-MB-436 compared to MCF7. Data are shown as the mean and SD values for each concentration from 3 independent experiments. ** $p<0.01$ and **** $p<0.0001$, p value was assessed by a t-test comparing BRCA1 deficient cell lines to BRCA1 proficient cell lines. Graphs were produced and statistical analysis performed using GraphPad prism.

6.4. Discussion and conclusions

In previous chapters (Chapter 4 and Chapter 5), it was suggested that there was a synthetic lethality relationship between BRCA1 deficiency and targeting DSB repair pathway by blockade of ATM or DNA-PKcs. ATM and DNA-PKcs modulation has been shown to enhance cisplatin cytotoxicity (Yoshida et al., 2008, Dejmek et al., 2009). Therefore, in this section of the study, the efficacy of combining cisplatin with ATM or DNA-PKcs inhibitor in BRCA1 proficient and BRCA1 deficient cells was investigated. To achieve this, clonogenic survival assay was conducted first to evaluate the cytotoxicity of cisplatin alone followed by combination studies using ATM (KU55933) or DNA-PKcs (NU7441) inhibitors. In agreement with previous studies, BRCA1 showed hypersensitivity to platinum therapy (Husain et al., 1998, Bhattacharyya et al., 2000, Tassone et al., 2003, Tan et al., 2008, Byrski et al., 2009, Taron et al., 2004, Quinn et al., 2007, Font et al., 2011, Silver et al., 2010). The dose of cisplatin used for the combination treatment in this study was $1/10^{th}$ the dose used in previous preclinical studies. The results of both combination treatments (cisplatin/ATM inhibitor and cisplatin/DNA-PKcs inhibitor) induced hypersensitivity in BRCA1 deficient cells compared to BRCA1 deficient cells treated with cisplatin alone. Formation of γH2AX foci in BRCA1 deficient cells following combination treatments increased compared to cisplatin alone and compared to either inhibitor alone. Whereas BRCA1 knockdown cells showed 76.5% increase in the accumulation of γH2AX foci following ATM inhibitor/cisplatin treatment (Figure 6.4A) and an 87% increase with DNA-PKcs inhibitor/cisplatin treatment (Figure 6.5A), ATM inhibitor alone showed 66.5% (Figure 4.9A) and DNA-PKcs inhibitor

alone showed 62.5% (Figure 5.5A). Interestingly, this increase in γH2AX foci formation was not seen following combination treatments in the BRCA1 mutated cells (Figure 6.4B and 6.5B) compared to each inhibitor alone (Figure 4.9B and 5.5B). This observation may be because MDA-MB-436 cells were found to be hypersensitive to the combination treatments and exhibited profound cell death. It should be noted that formation of γH2AX foci was analyzed after 48 hours with both single and combination treatments and to follow the damage after combination treatments different time points should be tested in the future.

The flow cytometry assay showed that BRCA1 deficient cells arrested significantly at G2/M phase after combination treatments compared to either inhibitor alone. Whereas BRCA1 deficient cell lines showed 37.6% and 38% increase in G2/M arrest following ATM inhibitor/cisplatin treatment (Figure 6.6), ATM inhibitor alone showed 26.6% and 32.45% (Figure 4.12), respectively. A similar increase was observed following DNA-PKcs inhibitor/cisplatin treatment with 34.25% and 38.25% (Figure 6.7), compared to 21.8% and 26.55% following DNA-PKcs inhibitor alone (Figure 5.8), respectively. In previous studies, G2/M arrest was demonstrated when combining KU55933 and NU7441 with Doxorubicin or Neocarzinostatin or Ionizing radiation (Zhao et al., 2006, Yu et al., 2012, Shaheen et al., 2011, Ciszewski et al., 2014). Cisplatin has been suggested to activate CHK1 and CHK2 which then leads to G2 arrest. Previous studies have also showed the selectivity of cisplatin in the killing of p53 defective tumor cells (Fan et al., 1995, Lee et al., 1999). Interestingly, targeting DNA-PKcs alone in BRCA1 deficient cells showed G1 arrest, whereas in the combination study G2/M

arrest was observed. This current study suggests that in combination treatments cisplatin activates G2/M arrest independent of DNA-PKcs inhibition. After G2/M arrest, BRCA1 deficient cells were unable to repair the DSBs and hence initiate apoptosis. A significant accumulation of apoptosis was observed in ATM inhibitor/cisplatin combination treatment, showing 20.6% and 17.6% (Figure 6.8) compared to 11.12% and 13.1% following ATM inhibitor alone (Figure 4.15) in BRCA1 HeLa and MDA-MB-436 cells, respectively. A similar increase in apoptosis was observed following DNA-PKcs inhibitor/cisplatin treatment with 25% and 19.2% (Figure 6.9) compared to 6.3% and 13.5% following DNA-PKcs inhibitor alone (Figure 5.10) in BRCA1 HeLa and MDA-MB-436 cells, respectively.

Taken together, several important observations have emerged from this chapter: firstly, the platinum anticancer drug cisplatin is selectively toxic to BRCA1 deficient cells. Cisplatin sensitivity in BRCA1 deficient cells observed here is consistent with previous publications. Secondly, inhibition of ATM or DNA-PKcs in combination with cisplatin enhances the cytotoxicity compared to either inhibitor alone. However, it should be noted that investigating drug combination interactions is an important area to study and it is one of the limitations in this chapter. For future studies in order to evaluate the interaction between ATM inhibitors and cisplatin or DNA-PKcs inhibitors and cisplatin, number of published methodologies can be used to evaluate the nature of drug-drug combination, e.g. isobologram, combination index, curve shift analysis (Evaluation of drug interaction methods are listed with more details in APPENDIX D). Thirdly, combination treatments increase DSB accumulation in BRCA1 deficient cells. Finally, combination treatments increase G2/M cell

cycle arrest, followed by an increase in apoptosis. A model for synthetic lethality is shown in Figure 6.10. In brief, impaired BER factors in BRCA1 deficient cell lines leads to accumulation of unrepaired SSBs followed by the formation of DSBs during DNA replication process. Therefore, it is suggested that cells are reliant on backup DSB pathways for cellular survival. Targeting DNA-PKcs or ATM along with cisplatin could induce extensive DSBs and over whelm BRCA1 deficient cells. This could lead to the observed synthetic lethality. In contrast, cells that are proficient in DSB repair (BRCA1-BER proficient), the DSBs would be repaired and cells would survive.

6.4.1. Conclusions

To conclude, this chapter of the study suggests that ATM and DNA-PKcs inhibition enhances cisplatin sensitivity in BRCA1 deficient cells. Firstly, data have shown that inhibition of ATM or DNA-PKcs in combination with cisplatin enhances the cytotoxicity compared to cisplatin alone. Secondly, combination treatments increase DSBs accumulation in BRCA1 deficient cells compared to cisplatin alone. In addition, combination treatments increase G2/M cell cycle arrest, followed by an increase in apoptosis. Finally, combination data were compared with corresponding cells treated with inhibitors alone (data presented in chapter 4 and chapter 5); the results generally suggested improved outcomes in combination treatments compared to each inhibitor alone. The data implies that the combination therapy could be an attractive strategy in BRCA1 cancer cells. However, advanced preclinical investigations with more cell lines and inhibitors are required.

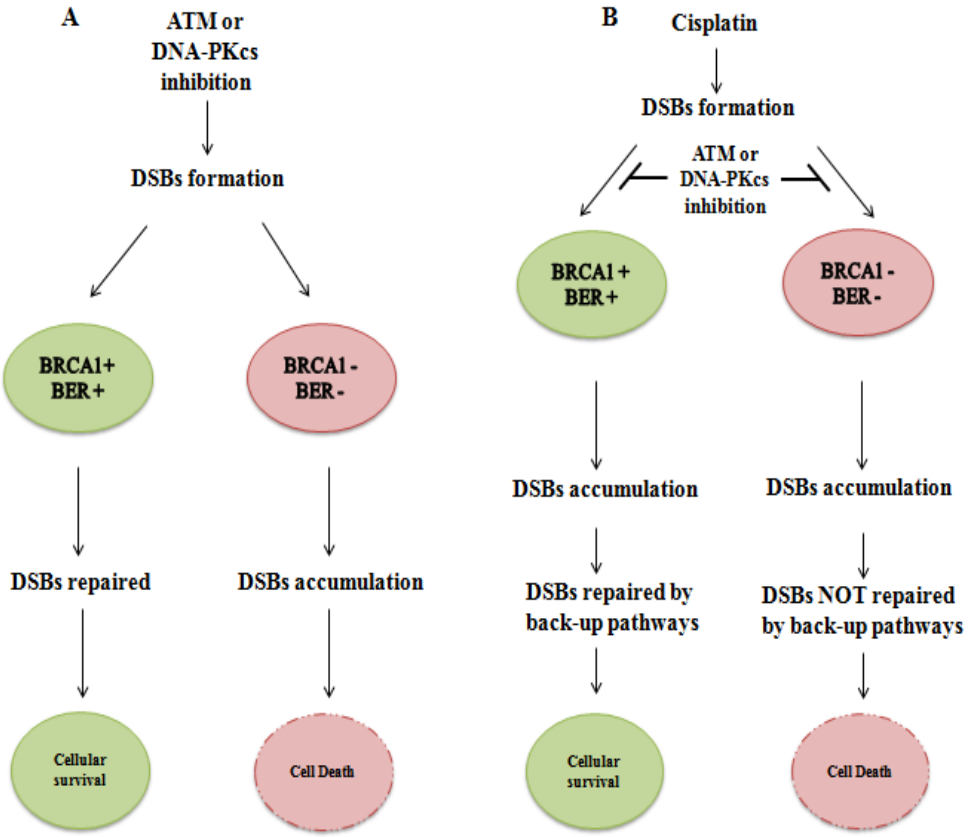

Figure 6.10. Working model for cisplatin and ATM or DNA-PKcs inhibitor as a synthetic lethality strategy in BRCA1-BER deficient cells.

(A) Inhibitors alone. (B) Cisplatin in combination with inhibitors. (BRCA1+/BER+) BRCA-BER proficient cells and (BRCA-/BER-) BRCA1-BER deficient cells.

Chapter 7

General discussion and suggestions for future studies

7. General Discussion and suggestions for future studies

Maintenance of genome stability is of primary importance for living organisms. However, DNA is under constant attack from numerous endogenous and exogenous DNA damaging agents. The accumulation of DNA damage can induce permanent changes that lead to carcinogenesis and could promote aggressive cancer biology. To counteract the deleterious effects of DNA damage, all organisms are equipped with DNA repair machinery to process DNA damage and maintain genomic integrity. Cancer cells on the other hand acquire defects in a certain DNA repair pathway and become dependent on a compensatory repair pathway in order to survive. More recently, inhibitions of the compensatory DNA repair (backup repair) pathway has emerged as a promising target for anticancer therapy. This strategy of selective killing of cancer cells is known as synthetic lethality (Abbotts et al., 2014b, Rassool and Tomkinson, 2010, Lord and Ashworth, 2008). Synthetic lethality is defined as a genetic combination of mutations in two or more genes/pathways that leads to cell death, whereas a mutation in only one of them does not. This represents a new approach of targeting DNA repair pathways with cancer therapies based on the genetic background of the tumour (Lord and Ashworth, 2008). The well known synthetic lethality relationship to date is targeting *BRCA* mutation with PARP inhibitors. BRCA/PARP synthetic lethality model proposes that targeting BRCA deficient tumours, which are HR deficient, with PARP inhibitor leads to the accumulation of SSBs. This is followed by the formation of DSBs during DNA replication, leading to cell death (Farmer et al., 2005, Bryant et al., 2005). On 23 October 2014, PARP

inhibitor (Olaparib, AstraZeneca©) has moved a step closer to being available for patients in the UK, after receiving a positive recommendation from the Committee for Medicinal products for Human Use (CHMP), which is part of the European Medicines Agency (EMA). The CHMP recommended that Olaparib (known as Lynparza™) be used as monotherapy for adult patients with relapsed, platinum sensitive epithelial ovarian, fallopian tube or primary peritoneal cancer with mutations in one of two genes *BRCA1* or *BRCA2*, and who have responded to platinum-based chemotherapy (EMA, 2014). This makes Lynparza™ the first in class drug depending on synthetic lethality strategy.

Clinical data provide compelling evidence that alterations in expression of DNA repair factors may have prognostic and predictive significance in patients. Germ-line mutations in *BRCA1* predispose to breast and ovarian cancer development. *BRCA1* mutation carriers have an 80% lifetime risk of developing breast cancer and 40-50% risk of developing ovarian cancer (Risch et al., 2001). In addition, *BRCA1* mutations has been found to increase the risk of pancreatic and prostate cancers (Thompson and Easton, 2002). A more recent study suggested that *BRCA1* mutation increases the risk of other types of cancer such as kidney, leukemia, lung, colorectal, myeloma, melanoma, stomach, thyroid and uterine cancers (Mersch et al., 2014). BRCA1 functions to maintain genomic stability through the assembly of multiple protein complexes involved in DNA repair pathways. BRCA deficiency on the other hand has been linked to genomic instability related to a defect in double strand break repair (Moynahan et al., 1999, Kass et al., 2013).

Alternative synthetic lethality target is an area of intense research. Our group has shown that targeting APE1, a central component of the BER pathway is synthetically lethal in HR deficient cells (Mohammed et al., 2011, Sultana et al., 2012). Similarly, targeting APE1 in PTEN deficient melanoma cell lines also shows synthetic lethality (Abbotts et al., 2014a). In addition, targeting XRCC1 deficient cell lines by ATM, DNA-PKcs or SSB repair inhibitor of ATR also induces synthetic lethality (Sultana et al., 2013a, Sultana et al., 2013b). Recently, BRCA1 has been suggested to be involved in the transcriptional regulation of three BER enzymes; OGG1, NTH1 and APE1 (Saha et al., 2010). A more recent study supports these observations and demonstrated down-regulation of APE1, NTH1, OGG1 and XRCC1 in *BRCA1* mutated and sporadic breast cancers (De Summa et al., 2014). Therefore impaired BER in BRCA1 deficient cell lines may be an opportunity for novel synthetic lethality strategy. The primary aim of the work described in this thesis was to investigate whether targeting BRCA1-BER deficient cells using ATM or DNA-PKcs inhibitors will be synthetically lethal. In order to achieve the aim, firstly DNA repair gene and protein expression in BRCA1 deficient and BRCA1 proficient cells were investigated (Chapter 3). Secondly, BRCA1 deficient cells were targeted by ATM inhibitors (KU55933 and KU60019) to investigate whether they would be synthetically lethal compared to BRCA1 proficient cells (Chapter 4). Then, BRCA1 deficient cells were targeted by DNA-PKcs inhibitors (NU7441 and NU7026) to investigate if they would also be synthetically lethal (Chapter 5). Finally, BRCA1 deficient cells were targeted by ATM or DNA-PKcs inhibitor in combination with cisplatin to

investigate whether it would enhance the observed synthetic lethality (Chapter 6).

Initially the RT² Profiler™ DNA Repair PCR Array was used to scan 84 DNA repair genes. Data demonstrated down-regulation of several DNA repair mRNAs in BRCA1 mutant/knockdown cell lines as compared to BRCA1 proficient cell lines. Low mRNA expression was demonstrated for *APE1*, *OGG1* and *NTHL1*, which is consistent with previous observations (Saha et al., 2010, De Summa et al., 2014). However RT² Profiler™ Array results did not always give statistical significance. Further assessments of the results were carried out using quantitative real time PCR (RT-qPCR) for a panel of selected DNA repair genes (*APE1*, *XRCC1*, *SMUG1*, *Pol ß*, *Lig3*, *ATM* and *DNA-PKcs*) which had previously be linked to BRCA1 (Abdel-Fatah et al., 2013, Masaoka et al., 2013, De Summa et al., 2014). RT-qPCR demonstrated statistically significant down-regulation of the selected genes. Protein expression was then analyzed for this selected group by western blot, which showed down-regulation consistent with the mRNAs expression. Taken together, these results suggest that BRCA1 deficiency may associate with a global defect in BER pathway. Interestingly, BRCA1 expression was also associated with a global reduction in HR (see section 3.4.2), NHEJ (see section 3.4.3), NER and MMR pathways (see section 3.4.4). However, further investigation is needed to measure the efficiency of these pathways.

As BRCA1 deficient cells were suggested to be BER deficient, cells may be amenable to synthetic lethality approach by targeting additional DSB repair targets. To examine this, clonogenic survival assays were conducted first to evaluate the cytotoxicity of ATM inhibitors (KU55933 and KU60019) against

BRCA1 knockdown HeLa cells and BRCA1 mutated MDA-MB-436 cells, using Control HeLa and MCF7 cells as BRCA1 proficient controls, respectively. Data demonstrated significant cytotoxicity in BRCA1 mutant/knockdown cell lines. For additional validation, the proliferation assay (MTS assay) was used to determine cell growth in response to ATM inhibitor, which showed consistent results with the clonogenic assay. Several functional studies were conducted to understand the mechanism behind this selective cytotoxicity. γH2AX immunofluorescence microscopy assay showed that BRCA1 deficient cell lines treated with ATM inhibitors (KU55933 or KU60019) for 48 hours were associated with statistically significant increase in the accumulation of DSBs (γH2AX foci) compared to untreated BRCA1 deficient cells. Cell cycle progression was arrested significantly at G2/M phase in treated BRCA1 HeLa cells compared to untreated BRCA1 HeLa cells. On the other hand, MDA-MB-436 cells showed a modest increase in G2/M arrest after 48 hours treatments which suggests a disturbance in cell cycle progression, though different time points should be tested in the future. Increases in G2/M arrest supports previously published data showing G2/M arrest after ATM inhibition (Sultana et al., 2013a, Lee et al., 2013, Nadkarni et al., 2012, Jazayeri et al., 2006). A flow cytometry-based apoptosis detection assay was performed after that and results demonstrated an increase in apoptosis rate in treated BRCA1 deficient cells compared to untreated BRCA1 deficient cells. These results support those previously published showing ATM inhibitor KU55933 treatment triggers apoptosis in different cancer cell lines (Sultana et al., 2013a, Li and Yang, 2010, Korwek et al., 2012) which again highlighted the importance of ATM in DNA repair and cell survival.

Altogether, these results support the hypothesis of BRCA1/ATM synthetic lethality and suggest that ATM plays a vital and irreplaceable role in genomic stability in BRCA1 deficient cells.

In light of the observed BRCA1/ATM synthetic lethality relationship, targeting BRCA1 deficiency by DNA-PKcs inhibitors (NU7441 and NU7026) was also carried out to investigate if there was a synthetically lethal relationship. Clonogenic survival assays results in Chapter 5 demonstrated that upon DNA-PKcs inhibition, BRCA1 mutant/knockdown cell lines showed increased cellular toxicity compared to BRCA1 proficient cell lines. For additional validation, MTS assay was used to determine cell viability in response to DNA-PKcs inhibitor. Both NU7441 and NU7026 inhibitors induced consistent results with the clonogenic assay. DSBs formation increased significantly after DNA-PKcs inhibition in BRCA1 mutant/knockdown cell lines. This finding supports previous publications showing accumulation of γH2AX foci with inhibition of DNA-PKcs (Shaheen et al., 2011, Sultana et al., 2013a). Monitoring cell cycle progression in BRCA1 deficient cell lines after treatment with DNA-PKcs inhibitors for 48 hours was associated with a modest arrest at G1 phase compared to untreated BRCA1 deficient cell lines. This suggests further investigation with different time points is required. The data demonstrate that a potential synthetic lethality relationship which exists between BRCA1 deficiency and DNA-PKcs inhibition, and highlights the role of DNA-PKcs in the maintenance of genomic stability of BRCA1 deficient cells.

Finally, combination strategy was investigated to demonstrate if targeting BRCA1 deficiency by ATM or DNA-PKcs inhibitor in combination with

cisplatin would enhance this synthetic lethality. Clonogenic combination results in Chapter 6 of both treatments (cisplatin/ATM inhibitor and cisplatin/DNA-PKcs inhibitor) induced hypersensitivity in BRCA1 deficient cells compared to BRCA1 deficient cells treated with cisplatin alone. Functional studies demonstrated that cisplatin enhanced cell death by increased accumulation of DSBs, G2/M cell cycle arrest and increased induction of apoptosis compared to either inhibitor alone. These data suggest that cisplatin can enhance the observed synthetic lethality effect.

Interestingly, it has always been assumed that cells lacking functional BRCA1 protein have impaired HR, and thus are suggested to depend on the more error-prone non-homologous end joining (NHEJ) pathway (Huen et al., 2010). In this thesis BRCA1 deficiency has been associated with a global impairment of expression of HR and NHEJ factors. Targeting NHEJ by DNA-PKcs inhibitors or HR by ATM inhibitors in BRCA1 deficient cells showed synthetic lethality. This observation supports that both DSB sub-pathways play an important role in maintaining chromosomal stability (Takata et al., 1998). Moreover, in BRCA1 proficient cells with functional BER, despite ATM or DNA-PKcs inhibition, DSBs may be rapidly repaired in backup DNA repair pathways and cells may continue to survive. The backup repair could operate through the complex overlap between HR, NHEJ and alternative non-homologous end joining (A-NHEJ) pathways (Schipler and Iliakis, 2013, Chapman et al., 2012). On the other hand, in BRCA1 deficient cells with low BER, ATM or DNA-PKcs inhibitors may lead to accumulation of DSBs which beyond a threshold, leading cells to cell cycle arrest and apoptosis. Recently our group has shown that ATM or DNA-PKcs inhibitors are synthetically lethal in XRCC1 deficient

cells (Sultana et al., 2013a). Given the potential role of XRCC1 in the A-NHEJ (Mladenov and Iliakis, 2011, Brandsma and Gent, 2012, Dueva and Iliakis, 2013), BRCA1 deficient cells with low XRCC1 may have impaired A-NHEJ in addition to BER resulting in an increased genomic instability and enhanced synthetic lethality when cisplatin was added in the current study. Moreover, ATM and DNA-PKcs modulation has been shown to enhance cisplatin cytotoxicity (Yoshida et al., 2008, Dejmek et al., 2009).

A limitation of my study is that this investigation was restricted to a few cell lines only. For future work, use of positive control drugs (e.g. several PARP inhibitors) in the functional studies will validate the results further. As with most research, the data presented here have thrown up as many questions as answers. Future *in vivo* studies are required to test these new findings and to evaluate the toxicity in normal tissue, which will validate the potential therapeutic benefit in clinical use. Another important area of investigation would be to evaluate potential biological mechanisms of resistance to ATM and DNA-PKcs inhibition. Moreover, the findings described here would also need further validation using pharmaceutical grade ATM and DNA-PKcs inhibitors that are currently under development. Also, to investigate if BRCA1 overexpression increases enzymatic activities related to DNA repair pathways (e.g. BER) a knock-in method using a BRCA1 expression plasmid created by cloning the BRCA1 cDNA into a vector could be used. In addition, ATM and DNA-PKcs knockdown cell lines can be targeted by BRCA1 small interfering (si) RNA to study the synthetic lethality relationship further.

This study suggests that BRCA1 deficiency may be associated with a global defect in DNA repair pathways, in particular base excision repair. The study

also provides proof that BRCA1 deficient cells could be targeted by inhibitors of the double strand break repair pathway, proposing that drug targets other than PARP can also be used for personalized cancer therapy.

7.1.Summary of key findings

- ✓ Loss of BRCA1 expression is associated with reduction in mRNA and protein expression of factors involved in Base excision repair.
- ✓ In cell lines, loss of BRCA1 expression is also associated with reduction in the expression of factors involved in Homologous recombination and Non-homologous end joining.
- ✓ BRCA1 mutated and knockdown cell lines are sensitive to ATM inhibitors (KU55933 & KU60019).
- ✓ ATM inhibitors treatment is associated with DNA double strand break accumulation and induction of apoptosis in BRCA1 deficient cells.
- ✓ BRCA1 mutated and knockdown cell lines are sensitive to DNA-PKcs inhibitors (NU7441 & NU7026).
- ✓ DNA-PKcs inhibitors treatment is associated with DNA double strand break accumulation and induction of apoptosis in BRCA1 deficient cells.
- ✓ Cisplatin in combination with ATM inhibitor (KU55933) or DNA-PKcs inhibitor (NU7441) enhances cytotoxicity in BRCA1 deficient cells.
- ✓ ATM inhibitor (KU55933) or DNA-PKcs inhibitor (NU7441) in combination with cisplatin treatment is associated with DNA double strand break accumulation, G2/M arrests and induction of apoptosis in BRCA1 deficient cells.

References

ABBOTTS, R., JEWELL, R., NSENGIMANA, J., MALONEY, D. J., SIMEONOV, A., SEEDHOUSE, C., ELLIOTT, F., LAYE, J., WALKER, C., JADHAV, A., GRABOWSKA, A., BALL, G., PATEL, P. M., NEWTON-BISHOP, J., WILSON, D. M., 3RD & MADHUSUDAN, S. 2014a. Targeting human apurinic/apyrimidinic endonuclease 1 (APE1) in phosphatase and tensin homolog (PTEN) deficient melanoma cells for personalized therapy. *Oncotarget,* 5**,** 3273-86.

ABBOTTS, R. & MADHUSUDAN, S. 2010. Human AP endonuclease 1 (APE1): from mechanistic insights to druggable target in cancer. *Cancer Treat Rev,* 36**,** 425-35.

ABBOTTS, R., THOMPSON, N. & MADHUSUDAN, S. 2014b. DNA repair in cancer: emerging targets for personalized therapy. *Cancer Manag Res,* 6**,** 77-92.

ABDEL-FATAH, T. M., ALBARAKATI, N., BOWELL, L., AGARWAL, D., MOSELEY, P., HAWKES, C., BALL, G., CHAN, S., ELLIS, I. O. & MADHUSUDAN, S. 2013. Single-strand selective monofunctional uracil-DNA glycosylase (SMUG1) deficiency is linked to aggressive breast cancer and predicts response to adjuvant therapy. *Breast Cancer Res Treat,* 142**,** 515-27.

ABDEL-FATAH, T. M., RUSSELL, R., AGARWAL, D., MOSELEY, P., ABAYOMI, M. A., PERRY, C., ALBARAKATI, N., BALL, G., CHAN, S., CALDAS, C., ELLIS, I. O. & MADHUSUDAN, S. 2014. DNA polymerase beta deficiency is linked to aggressive breast cancer: a comprehensive analysis of gene copy number, mRNA and protein expression in multiple cohorts. *Mol Oncol,* 8**,** 520-32.

ALLI, E., SHARMA, V. B., SUNDERESAKUMAR, P. & FORD, J. M. 2009. Defective repair of oxidative dna damage in triple-negative breast

cancer confers sensitivity to inhibition of poly(ADP-ribose) polymerase. *Cancer Res,* 69**,** 3589-96.

ALLINSON, S. L., DIANOVA, II & DIANOV, G. L. 2003. Poly(ADP-ribose) polymerase in base excision repair: always engaged, but not essential for DNA damage processing. *Acta Biochim Pol,* 50**,** 169-79.

AMREIN, L., LOIGNON, M., GOULET, A. C., DUNN, M., JEAN-CLAUDE, B., ALOYZ, R. & PANASCI, L. 2007. Chlorambucil cytotoxicity in malignant B lymphocytes is synergistically increased by 2-(morpholin-4-yl)-benzo[h]chomen-4-one (NU7026)-mediated inhibition of DNA double-strand break repair via inhibition of DNA-dependent protein kinase. *J Pharmacol Exp Ther,* 321**,** 848-55.

AN, J., HUANG, Y. C., XU, Q. Z., ZHOU, L. J., SHANG, Z. F., HUANG, B., WANG, Y., LIU, X. D., WU, D. C. & ZHOU, P. K. 2010. DNA-PKcs plays a dominant role in the regulation of H2AX phosphorylation in response to DNA damage and cell cycle progression. *BMC Mol Biol,* 11**,** 18.

ASHWORTH, A. 2008. A synthetic lethal therapeutic approach: poly(ADP) ribose polymerase inhibitors for the treatment of cancers deficient in DNA double-strand break repair. *J Clin Oncol,* 26**,** 3785-90.

AUDEH, M. W., CARMICHAEL, J., PENSON, R. T., FRIEDLANDER, M., POWELL, B., BELL-MCGUINN, K. M., SCOTT, C., WEITZEL, J. N., OAKNIN, A., LOMAN, N., LU, K., SCHMUTZLER, R. K., MATULONIS, U., WICKENS, M. & TUTT, A. 2010. Oral poly(ADP-ribose) polymerase inhibitor olaparib in patients with BRCA1 or BRCA2 mutations and recurrent ovarian cancer: a proof-of-concept trial. *Lancet,* 376**,** 245-51.

BAKKENIST, C. J. & KASTAN, M. B. 2003. DNA damage activates ATM through intermolecular autophosphorylation and dimer dissociation. *Nature,* 421**,** 499-506.

BAKKENIST, C. J. & KASTAN, M. B. 2004. Initiating cellular stress responses. *Cell,* 118**,** 9-17.

BALAKRISHNAN, L., BRANDT, P. D., LINDSEY-BOLTZ, L. A., SANCAR, A. & BAMBARA, R. A. 2009. Long patch base excision repair proceeds via coordinated stimulation of the multienzyme DNA repair complex. *J Biol Chem,* 284**,** 15158-72.

BALMANA, J., DIEZ, O., RUBIO, I. T. & CARDOSO, F. 2011. BRCA in breast cancer: ESMO Clinical Practice Guidelines. *Ann Oncol,* 22 Suppl 6**,** vi31-4.

BANIN, S., MOYAL, L., SHIEH, S., TAYA, Y., ANDERSON, C. W., CHESSA, L., SMORODINSKY, N. I., PRIVES, C., REISS, Y., SHILOH, Y. & ZIV, Y. 1998. Enhanced phosphorylation of p53 by ATM in response to DNA damage. *Science,* 281**,** 1674-7.

BAU, D. T., FU, Y. P., CHEN, S. T., CHENG, T. C., YU, J. C., WU, P. E. & SHEN, C. Y. 2004. Breast cancer risk and the DNA double-strand break end-joining capacity of nonhomologous end-joining genes are affected by BRCA1. *Cancer Res,* 64**,** 5013-9.

BAU, D. T., MAU, Y. C. & SHEN, C. Y. 2006. The role of BRCA1 in non-homologous end-joining. *Cancer Lett,* 240**,** 1-8.

BAYLIN, S. B. & JONES, P. A. 2011. A decade of exploring the cancer epigenome - biological and translational implications. *Nat Rev Cancer,* 11**,** 726-34.

BHATTACHARYYA, A., EAR, U. S., KOLLER, B. H., WEICHSELBAUM, R. R. & BISHOP, D. K. 2000. The breast cancer susceptibility gene BRCA1 is required for subnuclear assembly of Rad51 and survival following treatment with the DNA cross-linking agent cisplatin. *J Biol Chem,* 275**,** 23899-903.

BINDRA, R. S., SCHAFFER, P. J., MENG, A., WOO, J., MASEIDE, K., ROTH, M. E., LIZARDI, P., HEDLEY, D. W., BRISTOW, R. G. &

GLAZER, P. M. 2004. Down-regulation of Rad51 and decreased homologous recombination in hypoxic cancer cells. *Mol Cell Biol,* 24**,** 8504-18.

BOWMAN, K. J., WHITE, A., GOLDING, B. T., GRIFFIN, R. J. & CURTIN, N. J. 1998. Potentiation of anti-cancer agent cytotoxicity by the potent poly(ADP-ribose) polymerase inhibitors NU1025 and NU1064. *Br J Cancer,* 78**,** 1269-77.

BRADFORD, M. M. 1976. A rapid and sensitive method for the quantitation of microgram quantities of protein utilizing the principle of protein-dye binding. *Anal Biochem,* 72**,** 248-54.

BRANDSMA, I. & GENT, D. C. 2012. Pathway choice in DNA double strand break repair: observations of a balancing act. *Genome Integr,* 3**,** 9.

BRIDGE, W. L., VANDENBERG, C. J., FRANKLIN, R. J. & HIOM, K. 2005. The BRIP1 helicase functions independently of BRCA1 in the Fanconi anemia pathway for DNA crosslink repair. *Nat Genet,* 37**,** 953-7.

BRYANT, H. E., SCHULTZ, N., THOMAS, H. D., PARKER, K. M., FLOWER, D., LOPEZ, E., KYLE, S., MEUTH, M., CURTIN, N. J. & HELLEDAY, T. 2005. Specific killing of BRCA2-deficient tumours with inhibitors of poly(ADP-ribose) polymerase. *Nature,* 434**,** 913-7.

BUNTING, S. F., CALLEN, E., WONG, N., CHEN, H. T., POLATO, F., GUNN, A., BOTHMER, A., FELDHAHN, N., FERNANDEZ-CAPETILLO, O., CAO, L., XU, X., DENG, C. X., FINKEL, T., NUSSENZWEIG, M., STARK, J. M. & NUSSENZWEIG, A. 2010. 53BP1 inhibits homologous recombination in Brca1-deficient cells by blocking resection of DNA breaks. *Cell,* 141**,** 243-54.

BURMA, S., CHEN, B. P. & CHEN, D. J. 2006. Role of non-homologous end joining (NHEJ) in maintaining genomic integrity. *DNA Repair (Amst),* 5**,** 1042-8.

BURMA, S., CHEN, B. P., MURPHY, M., KURIMASA, A. & CHEN, D. J. 2001. ATM phosphorylates histone H2AX in response to DNA double-strand breaks. *J Biol Chem,* 276**,** 42462-7.

BURNETTE, W. N. 1981. "Western blotting": electrophoretic transfer of proteins from sodium dodecyl sulfate--polyacrylamide gels to unmodified nitrocellulose and radiographic detection with antibody and radioiodinated protein A. *Anal Biochem,* 112**,** 195-203.

BYRSKI, T., HUZARSKI, T., DENT, R., GRONWALD, J., ZUZIAK, D., CYBULSKI, C., KLADNY, J., GORSKI, B., LUBINSKI, J. & NAROD, S. A. 2009. Response to neoadjuvant therapy with cisplatin in BRCA1-positive breast cancer patients. *Breast Cancer Res Treat,* 115**,** 359-63.

CAESTECKER, K. W. & VAN DE WALLE, G. R. 2013. The role of BRCA1 in DNA double-strand repair: past and present. *Exp Cell Res,* 319**,** 575-87.

CALSOU, P., FRIT, P., HUMBERT, O., MULLER, C., CHEN, D. J. & SALLES, B. 1999. The DNA-dependent protein kinase catalytic activity regulates DNA end processing by means of Ku entry into DNA. *J Biol Chem,* 274**,** 7848-56.

CANMAN, C. E., LIM, D. S., CIMPRICH, K. A., TAYA, Y., TAMAI, K., SAKAGUCHI, K., APPELLA, E., KASTAN, M. B. & SILICIANO, J. D. 1998. Activation of the ATM kinase by ionizing radiation and phosphorylation of p53. *Science,* 281**,** 1677-9.

CHAI, Y. L., CUI, J., SHAO, N., SHYAM, E., REDDY, P. & RAO, V. N. 1999. The second BRCT domain of BRCA1 proteins interacts with p53 and stimulates transcription from the p21WAF1/CIP1 promoter. *Oncogene,* 18**,** 263-8.

CHAN, D. W., GATELY, D. P., URBAN, S., GALLOWAY, A. M., LEES-MILLER, S. P., YEN, T. & ALLALUNIS-TURNER, J. 1998. Lack of

correlation between ATM protein expression and tumour cell radiosensitivity. *Int J Radiat Biol,* 74**,** 217-24.

CHAN, D. W., YE, R., VEILLETTE, C. J. & LEES-MILLER, S. P. 1999. DNA-dependent protein kinase phosphorylation sites in Ku 70/80 heterodimer. *Biochemistry,* 38**,** 1819-28.

CHAN, S. L. & MOK, T. 2010. PARP inhibition in BRCA-mutated breast and ovarian cancers. *Lancet,* 376**,** 211-3.

CHAPMAN, J. R., TAYLOR, M. R. & BOULTON, S. J. 2012. Playing the end game: DNA double-strand break repair pathway choice. *Mol Cell,* 47**,** 497-510.

CHAUDHARY, M. W. & AL-BARADIE, R. S. 2014. Ataxia-telangiectasia: future prospects. *Appl Clin Genet,* 7**,** 159-67.

CHEN, B. P., CHAN, D. W., KOBAYASHI, J., BURMA, S., ASAITHAMBY, A., MOROTOMI-YANO, K., BOTVINICK, E., QIN, J. & CHEN, D. J. 2005. Cell cycle dependence of DNA-dependent protein kinase phosphorylation in response to DNA double strand breaks. *J Biol Chem,* 280**,** 14709-15.

CHEN, J., SILVER, D. P., WALPITA, D., CANTOR, S. B., GAZDAR, A. F., TOMLINSON, G., COUCH, F. J., WEBER, B. L., ASHLEY, T., LIVINGSTON, D. M. & SCULLY, R. 1998. Stable interaction between the products of the BRCA1 and BRCA2 tumor suppressor genes in mitotic and meiotic cells. *Mol Cell,* 2**,** 317-28.

CHEN, Y., GELFOND, J. A., MCMANUS, L. M. & SHIREMAN, P. K. 2009. Reproducibility of quantitative RT-PCR array in miRNA expression profiling and comparison with microarray analysis. *BMC Genomics,* 10**,** 407.

CHOU, T. C. & TALALAY, P. 1984. Quantitative analysis of dose-effect relationships: the combined effects of multiple drugs or enzyme inhibitors. *Adv Enzyme Regul,* 22**,** 27-55.

CHRISTMANN, M., TOMICIC, M. T., ROOS, W. P. & KAINA, B. 2003. Mechanisms of human DNA repair: an update. *Toxicology,* 193**,** 3-34.

CHUNG, D. C. & RUSTGI, A. K. 2003. The hereditary nonpolyposis colorectal cancer syndrome: genetics and clinical implications. *Ann Intern Med,* 138**,** 560-70.

CISZEWSKI, W. M., TAVECCHIO, M., DASTYCH, J. & CURTIN, N. J. 2014. DNA-PK inhibition by NU7441 sensitizes breast cancer cells to ionizing radiation and doxorubicin. *Breast Cancer Res Treat,* 143**,** 47-55.

CONNELLY, M. A., ZHANG, H., KIELECZAWA, J. & ANDERSON, C. W. 1998. The promoters for human DNA-PKcs (PRKDC) and MCM4: divergently transcribed genes located at chromosome 8 band q11. *Genomics,* 47**,** 71-83.

CORTEZ, D., WANG, Y., QIN, J. & ELLEDGE, S. J. 1999. Requirement of ATM-dependent phosphorylation of brca1 in the DNA damage response to double-strand breaks. *Science,* 286**,** 1162-6.

CORY, A. H., OWEN, T. C., BARLTROP, J. A. & CORY, J. G. 1991. Use of an aqueous soluble tetrazolium/formazan assay for cell growth assays in culture. *Cancer Commun,* 3**,** 207-12.

CRESCENZI, E., PALUMBO, G., DE BOER, J. & BRADY, H. J. 2008. Ataxia telangiectasia mutated and p21CIP1 modulate cell survival of drug-induced senescent tumor cells: implications for chemotherapy. *Clin Cancer Res,* 14**,** 1877-87.

DANTZER, F., DE LA RUBIA, G., MENISSIER-DE MURCIA, J., HOSTOMSKY, Z., DE MURCIA, G. & SCHREIBER, V. 2000. Base excision repair is impaired in mammalian cells lacking Poly(ADP-ribose) polymerase-1. *Biochemistry,* 39**,** 7559-69.

DAVIDSON, D., AMREIN, L., PANASCI, L. & ALOYZ, R. 2013. Small Molecules, Inhibitors of DNA-PK, Targeting DNA Repair, and Beyond. *Front Pharmacol,* 4**,** 5.

DAVIS, A. J., CHEN, B. P. & CHEN, D. J. 2014a. DNA-PK: a dynamic enzyme in a versatile DSB repair pathway. *DNA Repair (Amst),* 17**,** 21-9.

DAVIS, A. J. & CHEN, D. J. 2013. DNA double strand break repair via non-homologous end-joining. *Transl Cancer Res,* 2**,** 130-143.

DAVIS, A. J., CHI, L., SO, S., LEE, K. J., MORI, E., FATTAH, K., YANG, J. & CHEN, D. J. 2014b. BRCA1 modulates the autophosphorylation status of DNA-PKcs in S phase of the cell cycle. *Nucleic Acids Res*.

DE SUMMA, S., PINTO, R., PILATO, B., SAMBIASI, D., PORCELLI, L., GUIDA, G., MATTIOLI, E., PARADISO, A., MERLA, G., MICALE, L., DE NITTIS, P. & TOMMASI, S. 2014. Expression of base excision repair key factors and miR17 in familial and sporadic breast cancer. *Cell Death Dis,* 5**,** e1076.

DEJMEK, J., IGLEHART, J. D. & LAZARO, J. B. 2009. DNA-dependent protein kinase (DNA-PK)-dependent cisplatin-induced loss of nucleolar facilitator of chromatin transcription (FACT) and regulation of cisplatin sensitivity by DNA-PK and FACT. *Mol Cancer Res,* 7**,** 581-91.

DEVITA, V. T., JR. & CHU, E. 2008. A history of cancer chemotherapy. *Cancer Res,* 68**,** 8643-53.

DIANOV, G. L. & HUBSCHER, U. 2013. Mammalian base excision repair: the forgotten archangel. *Nucleic Acids Res,* 41**,** 3483-90.

DROST, R., BOUWMAN, P., ROTTENBERG, S., BOON, U., SCHUT, E., KLARENBEEK, S., KLIJN, C., VAN DER HEIJDEN, I., VAN DER GULDEN, H., WIENTJENS, E., PIETERSE, M., CATTEAU, A., GREEN, P., SOLOMON, E., MORRIS, J. R. & JONKERS, J. 2011.

BRCA1 RING function is essential for tumor suppression but dispensable for therapy resistance. *Cancer Cell,* 20**,** 797-809.

DUANGMANO, S., SAE-LIM, P., SUKSAMRARN, A., PATMASIRIWAT, P. & DOMANN, F. E. 2012. Cucurbitacin B Causes Increased Radiation Sensitivity of Human Breast Cancer Cells via G2/M Cell Cycle Arrest. *J Oncol,* 2012**,** 601682.

DUEVA, R. & ILIAKIS, G. 2013. Alternative pathways of non-homologous end joining (NHEJ) in genomic instability and cancer. *Translational Cancer Research,* 2**,** 163-177.

EDWARDS, S. L., BROUGH, R., LORD, C. J., NATRAJAN, R., VATCHEVA, R., LEVINE, D. A., BOYD, J., REIS-FILHO, J. S. & ASHWORTH, A. 2008. Resistance to therapy caused by intragenic deletion in BRCA2. *Nature,* 451**,** 1111-5.

ELLIS, I. O., GALEA, M., BROUGHTON, N., LOCKER, A., BLAMEY, R. W. & ELSTON, C. W. 1992. Pathological prognostic factors in breast cancer. II. Histological type. Relationship with survival in a large study with long-term follow-up. *Histopathology,* 20**,** 479-89.

ELSTRODT, F., HOLLESTELLE, A., NAGEL, J. H., GORIN, M., WASIELEWSKI, M., VAN DEN OUWELAND, A., MERAJVER, S. D., ETHIER, S. P. & SCHUTTE, M. 2006. BRCA1 mutation analysis of 41 human breast cancer cell lines reveals three new deleterious mutants. *Cancer Res,* 66**,** 41-5.

EMA. 2014. *Lynparza recommended for approval in ovarian cancer* [Online]. The European Medicines Agency. Available: www.ema.europa.eu [Accessed 8/11/ 2014].

ENGELBERGS, J., THOMALE, J. & RAJEWSKY, M. F. 2000. Role of DNA repair in carcinogen-induced ras mutation. *Mutat Res,* 450**,** 139-53.

EROLES, P., BOSCH, A., PEREZ-FIDALGO, J. A. & LLUCH, A. 2012. Molecular biology in breast cancer: intrinsic subtypes and signaling pathways. *Cancer Treat Rev,* 38**,** 698-707.

FAN, S., SMITH, M. L., RIVET, D. J., 2ND, DUBA, D., ZHAN, Q., KOHN, K. W., FORNACE, A. J., JR. & O'CONNOR, P. M. 1995. Disruption of p53 function sensitizes breast cancer MCF-7 cells to cisplatin and pentoxifylline. *Cancer Res,* 55**,** 1649-54.

FARMER, H., MCCABE, N., LORD, C. J., TUTT, A. N., JOHNSON, D. A., RICHARDSON, T. B., SANTAROSA, M., DILLON, K. J., HICKSON, I., KNIGHTS, C., MARTIN, N. M., JACKSON, S. P., SMITH, G. C. & ASHWORTH, A. 2005. Targeting the DNA repair defect in BRCA mutant cells as a therapeutic strategy. *Nature,* 434**,** 917-21.

FISHER, B., FISHER, E. R., REDMOND, C. & BROWN, A. 1986. Tumor nuclear grade, estrogen receptor, and progesterone receptor: their value alone or in combination as indicators of outcome following adjuvant therapy for breast cancer. *Breast Cancer Res Treat,* 7**,** 147-60.

FISHER, E. R., GREGORIO, R. M., FISHER, B., REDMOND, C., VELLIOS, F. & SOMMERS, S. C. 1975. The pathology of invasive breast cancer. A syllabus derived from findings of the National Surgical Adjuvant Breast Project (protocol no. 4). *Cancer,* 36**,** 1-85.

FLANAGAN, J. M., COCCIARDI, S., WADDELL, N., JOHNSTONE, C. N., MARSH, A., HENDERSON, S., SIMPSON, P., DA SILVA, L., KHANNA, K., LAKHANI, S., BOSHOFF, C. & CHENEVIX-TRENCH, G. 2010. DNA methylome of familial breast cancer identifies distinct profiles defined by mutation status. *Am J Hum Genet,* 86**,** 420-33.

FOJO, T. & BATES, S. 2013. Mechanisms of resistance to PARP inhibitors--three and counting. *Cancer Discov,* 3**,** 20-3.

FONG, P. C., YAP, T. A., BOSS, D. S., CARDEN, C. P., MERGUI-ROELVINK, M., GOURLEY, C., DE GREVE, J., LUBINSKI, J., SHANLEY, S., MESSIOU, C., A'HERN, R., TUTT, A., ASHWORTH, A., STONE, J., CARMICHAEL, J., SCHELLENS, J. H., DE BONO, J. S. & KAYE, S. B. 2010. Poly(ADP)-ribose polymerase inhibition: frequent durable responses in BRCA carrier ovarian cancer correlating with platinum-free interval. *J Clin Oncol,* 28**,** 2512-9.

FONT, A., TARON, M., GAGO, J. L., COSTA, C., SANCHEZ, J. J., CARRATO, C., MORA, M., CELIZ, P., PEREZ, L., RODRIGUEZ, D., GIMENEZ-CAPITAN, A., QUIROGA, V., BENLLOCH, S., IBARZ, L. & ROSELL, R. 2011. BRCA1 mRNA expression and outcome to neoadjuvant cisplatin-based chemotherapy in bladder cancer. *Ann Oncol,* 22**,** 139-44.

FORAY, N., MAROT, D., GABRIEL, A., RANDRIANARISON, V., CARR, A. M., PERRICAUDET, M., ASHWORTH, A. & JEGGO, P. 2003. A subset of ATM- and ATR-dependent phosphorylation events requires the BRCA1 protein. *EMBO J,* 22**,** 2860-71.

FORTINI, P. & DOGLIOTTI, E. 2007. Base damage and single-strand break repair: mechanisms and functional significance of short- and long-patch repair subpathways. *DNA Repair (Amst),* 6**,** 398-409.

FOULKES, W. D., GRAINGE, M. J., RAKHA, E. A., GREEN, A. R. & ELLIS, I. O. 2009. Tumor size is an unreliable predictor of prognosis in basal-like breast cancers and does not correlate closely with lymph node status. *Breast Cancer Res Treat,* 117**,** 199-204.

FU, D., CALVO, J. A. & SAMSON, L. D. 2012. Balancing repair and tolerance of DNA damage caused by alkylating agents. *Nat Rev Cancer,* 12**,** 104-20.

GARICOCHEA, B., MORELLE, A., ANDRIGHETTI, A. E., CANCELLA, A., BOS, A. & WERUTSKY, G. 2009. [Age as a prognostic factor in early breast cancer]. *Rev Saude Publica,* 43**,** 311-7.

GATES, K. S. 2009. An overview of chemical processes that damage cellular DNA: spontaneous hydrolysis, alkylation, and reactions with radicals. *Chem Res Toxicol,* 22**,** 1747-60.

GOLDING, S. E., ROSENBERG, E., VALERIE, N., HUSSAINI, I., FRIGERIO, M., COCKCROFT, X. F., CHONG, W. Y., HUMMERSONE, M., RIGOREAU, L., MENEAR, K. A., O'CONNOR, M. J., POVIRK, L. F., VAN METER, T. & VALERIE, K. 2009. Improved ATM kinase inhibitor KU-60019 radiosensitizes glioma cells, compromises insulin, AKT and ERK prosurvival signaling, and inhibits migration and invasion. *Mol Cancer Ther,* 8**,** 2894-902.

GORSKI, J. J., KENNEDY, R. D., HOSEY, A. M. & HARKIN, D. P. 2009. The complex relationship between BRCA1 and ERalpha in hereditary breast cancer. *Clin Cancer Res,* 15**,** 1514-8.

GOTTLICH, B., REICHENBERGER, S., FELDMANN, E. & PFEIFFER, P. 1998. Rejoining of DNA double-strand breaks in vitro by single-strand annealing. *Eur J Biochem,* 258**,** 387-95.

GRIFFIN, R. J., SRINIVASAN, S., BOWMAN, K., CALVERT, A. H., CURTIN, N. J., NEWELL, D. R., PEMBERTON, L. C. & GOLDING, B. T. 1998. Resistance-modifying agents. 5. Synthesis and biological properties of quinazolinone inhibitors of the DNA repair enzyme poly(ADP-ribose) polymerase (PARP). *J Med Chem,* 41**,** 5247-56.

GUNSOY, N. B., GARCIA-CLOSAS, M. & MOSS, S. M. 2014. Estimating breast cancer mortality reduction and overdiagnosis due to screening for different strategies in the United Kingdom. *Br J Cancer,* 110**,** 2412-2419.

HAINCE, J. F., KOZLOV, S., DAWSON, V. L., DAWSON, T. M., HENDZEL, M. J., LAVIN, M. F. & POIRIER, G. G. 2007. Ataxia telangiectasia mutated (ATM) signaling network is modulated by a

novel poly(ADP-ribose)-dependent pathway in the early response to DNA-damaging agents. *J Biol Chem,* 282**,** 16441-53.

HAINCE, J. F., MCDONALD, D., RODRIGUE, A., DERY, U., MASSON, J. Y., HENDZEL, M. J. & POIRIER, G. G. 2008. PARP1-dependent kinetics of recruitment of MRE11 and NBS1 proteins to multiple DNA damage sites. *J Biol Chem,* 283**,** 1197-208.

HALL, J. M., LEE, M. K., NEWMAN, B., MORROW, J. E., ANDERSON, L. A., HUEY, B. & KING, M. C. 1990. Linkage of early-onset familial breast cancer to chromosome 17q21. *Science,* 250**,** 1684-9.

HAMMARSTEN, O. & CHU, G. 1998. DNA-dependent protein kinase: DNA binding and activation in the absence of Ku. *Proc Natl Acad Sci U S A,* 95**,** 525-30.

HANAHAN, D. & WEINBERG, R. A. 2000. The hallmarks of cancer. *Cell,* 100**,** 57-70.

HANAHAN, D. & WEINBERG, R. A. 2011. Hallmarks of cancer: the next generation. *Cell,* 144**,** 646-74.

HARTLEY, K. O., GELL, D., SMITH, G. C., ZHANG, H., DIVECHA, N., CONNELLY, M. A., ADMON, A., LEES-MILLER, S. P., ANDERSON, C. W. & JACKSON, S. P. 1995. DNA-dependent protein kinase catalytic subunit: a relative of phosphatidylinositol 3-kinase and the ataxia telangiectasia gene product. *Cell,* 82**,** 849-56.

HARTMAN, A. R. & FORD, J. M. 2002. BRCA1 induces DNA damage recognition factors and enhances nucleotide excision repair. *Nat Genet,* 32**,** 180-4.

HEFTI, M. M., HU, R., KNOBLAUCH, N. W., COLLINS, L. C., HAIBE-KAINS, B., TAMIMI, R. M. & BECK, A. H. 2013. Estrogen receptor negative/progesterone receptor positive breast cancer is not a reproducible subtype. *Breast Cancer Res,* 15**,** R68.

HEGDE, M. L., HAZRA, T. K. & MITRA, S. 2008. Early steps in the DNA base excision/single-strand interruption repair pathway in mammalian cells. *Cell Res,* 18**,** 27-47.

HELLEDAY, T., LO, J., VAN GENT, D. C. & ENGELWARD, B. P. 2007. DNA double-strand break repair: from mechanistic understanding to cancer treatment. *DNA Repair (Amst),* 6**,** 923-35.

HICKSON, I., ZHAO, Y., RICHARDSON, C. J., GREEN, S. J., MARTIN, N. M., ORR, A. I., REAPER, P. M., JACKSON, S. P., CURTIN, N. J. & SMITH, G. C. 2004. Identification and characterization of a novel and specific inhibitor of the ataxia-telangiectasia mutated kinase ATM. *Cancer Res,* 64**,** 9152-9.

HOEIJMAKERS, J. H. 2001. Genome maintenance mechanisms for preventing cancer. *Nature,* 411**,** 366-74.

HOEIJMAKERS, J. H. 2009. DNA damage, aging, and cancer. *N Engl J Med,* 361**,** 1475-85.

HOLLICK, J. J., GOLDING, B. T., HARDCASTLE, I. R., MARTIN, N., RICHARDSON, C., RIGOREAU, L. J., SMITH, G. C. & GRIFFIN, R. J. 2003. 2,6-disubstituted pyran-4-one and thiopyran-4-one inhibitors of DNA-Dependent protein kinase (DNA-PK). *Bioorg Med Chem Lett,* 13**,** 3083-6.

HUEN, M. S., SY, S. M. & CHEN, J. 2010. BRCA1 and its toolbox for the maintenance of genome integrity. *Nat Rev Mol Cell Biol,* 11**,** 138-48.

HUSAIN, A., HE, G., VENKATRAMAN, E. S. & SPRIGGS, D. R. 1998. BRCA1 up-regulation is associated with repair-mediated resistance to cis-diamminedichloroplatinum(II). *Cancer Res,* 58**,** 1120-3.

IRMINGER-FINGER, I., SIEGEL, B. D. & LEUNG, W. C. 1999. The functions of breast cancer susceptibility gene 1 (BRCA1) product and its associated proteins. *Biol Chem,* 380**,** 117-28.

IVANOV, E. L., SUGAWARA, N., FISHMAN-LOBELL, J. & HABER, J. E. 1996. Genetic requirements for the single-strand annealing pathway of double-strand break repair in Saccharomyces cerevisiae. *Genetics,* 142**,** 693-704.

JAZAYERI, A., FALCK, J., LUKAS, C., BARTEK, J., SMITH, G. C., LUKAS, J. & JACKSON, S. P. 2006. ATM- and cell cycle-dependent regulation of ATR in response to DNA double-strand breaks. *Nat Cell Biol,* 8**,** 37-45.

JIANG, G., PLO, I., WANG, T., RAHMAN, M., CHO, J. H., YANG, E., LOPEZ, B. S. & XIA, F. 2013. BRCA1-Ku80 protein interaction enhances end-joining fidelity of chromosomal double-strand breaks in the G1 phase of the cell cycle. *J Biol Chem,* 288**,** 8966-76.

JIRICNY, J. 2006. The multifaceted mismatch-repair system. *Nat Rev Mol Cell Biol,* 7**,** 335-46.

KAELIN, W. G., JR. 2005. The concept of synthetic lethality in the context of anticancer therapy. *Nat Rev Cancer,* 5**,** 689-98.

KARASAWA, K., FUJITA, M., SHOJI, Y., HORIMOTO, Y., INOUE, T. & AL., E. 2014. Biological Effectiveness of Carbon-Ion Radiation on Various Human Breast Cancer Cell Lines. *J Cell Sci Ther,* 5:180.

KASHISHIAN, A., DOUANGPANYA, H., CLARK, D., SCHLACHTER, S. T., EARY, C. T., SCHIRO, J. G., HUANG, H., BURGESS, L. E., KESICKI, E. A. & HALBROOK, J. 2003. DNA-dependent protein kinase inhibitors as drug candidates for the treatment of cancer. *Mol Cancer Ther,* 2**,** 1257-64.

KASS, E. M., HELGADOTTIR, H. R., CHEN, C. C., BARBERA, M., WANG, R., WESTERMARK, U. K., LUDWIG, T., MOYNAHAN, M. E. & JASIN, M. 2013. Double-strand break repair by homologous recombination in primary mouse somatic cells requires BRCA1 but not the ATM kinase. *Proc Natl Acad Sci U S A,* 110**,** 5564-9.

KELLAND, L. 2007. The resurgence of platinum-based cancer chemotherapy. *Nat Rev Cancer,* 7**,** 573-84.

KHANNA, K. K. & JACKSON, S. P. 2001. DNA double-strand breaks: signaling, repair and the cancer connection. *Nat Genet,* 27**,** 247-54.

KHODYREVA, S. N., PRASAD, R., ILINA, E. S., SUKHANOVA, M. V., KUTUZOV, M. M., LIU, Y., HOU, E. W., WILSON, S. H. & LAVRIK, O. I. 2010. Apurinic/apyrimidinic (AP) site recognition by the 5'-dRP/AP lyase in poly(ADP-ribose) polymerase-1 (PARP-1). *Proc Natl Acad Sci U S A,* 107**,** 22090-5.

KNUDSON, A. G., JR. 1971. Mutation and cancer: statistical study of retinoblastoma. *Proc Natl Acad Sci U S A,* 68**,** 820-3.

KOOPMAN, G., REUTELINGSPERGER, C. P., KUIJTEN, G. A., KEEHNEN, R. M., PALS, S. T. & VAN OERS, M. H. 1994. Annexin V for flow cytometric detection of phosphatidylserine expression on B cells undergoing apoptosis. *Blood,* 84**,** 1415-20.

KORWEK, Z., SEWASTIANIK, T., BIELAK-ZMIJEWSKA, A., MOSIENIAK, G., ALSTER, O., MORENO-VILLANUEVA, M., BURKLE, A. & SIKORA, E. 2012. Inhibition of ATM blocks the etoposide-induced DNA damage response and apoptosis of resting human T cells. *DNA Repair (Amst),* 11**,** 864-73.

KOSCIELNY, S., ARRIAGADA, R., ADOLFSSON, J., FORNANDER, T. & BERGH, J. 2009. Impact of tumour size on axillary involvement and distant dissemination in breast cancer. *Br J Cancer,* 101**,** 902-7.

KRAEMER, K. H., PATRONAS, N. J., SCHIFFMANN, R., BROOKS, B. P., TAMURA, D. & DIGIOVANNA, J. J. 2007. Xeroderma pigmentosum, trichothiodystrophy and Cockayne syndrome: a complex genotype-phenotype relationship. *Neuroscience,* 145**,** 1388-96.

KROMAN, N., JENSEN, M. B., WOHLFAHRT, J., MOURIDSEN, H. T., ANDERSEN, P. K. & MELBYE, M. 2000. Factors influencing the

effect of age on prognosis in breast cancer: population based study. *BMJ,* 320**,** 474-8.

KURIMASA, A., KUMANO, S., BOUBNOV, N. V., STORY, M. D., TUNG, C. S., PETERSON, S. R. & CHEN, D. J. 1999. Requirement for the kinase activity of human DNA-dependent protein kinase catalytic subunit in DNA strand break rejoining. *Mol Cell Biol,* 19**,** 3877-84.

KURZ, E. U. & LEES-MILLER, S. P. 2004. DNA damage-induced activation of ATM and ATM-dependent signaling pathways. *DNA Repair (Amst),* 3**,** 889-900.

KUSUMOTO-MATSUO, R., GHOSH, D., KARMAKAR, P., MAY, A., RAMSDEN, D. & BOHR, V. A. 2014. Serines 440 and 467 in the Werner syndrome protein are phosphorylated by DNA-PK and affects its dynamics in response to DNA double strand breaks. *Aging (Albany NY),* 6**,** 70-81.

LANGELIER, M. F. & PASCAL, J. M. 2013. PARP-1 mechanism for coupling DNA damage detection to poly(ADP-ribose) synthesis. *Curr Opin Struct Biol,* 23**,** 134-43.

LE ROMANCER, M., COSULICH, S. C., JACKSON, S. P. & CLARKE, P. R. 1996. Cleavage and inactivation of DNA-dependent protein kinase catalytic subunit during apoptosis in Xenopus egg extracts. *J Cell Sci,* 109 (Pt 13)**,** 3121-7.

LEAHY, J. J., GOLDING, B. T., GRIFFIN, R. J., HARDCASTLE, I. R., RICHARDSON, C., RIGOREAU, L. & SMITH, G. C. 2004. Identification of a highly potent and selective DNA-dependent protein kinase (DNA-PK) inhibitor (NU7441) by screening of chromenone libraries. *Bioorg Med Chem Lett,* 14**,** 6083-7.

LEBER, R., WISE, T. W., MIZUTA, R. & MEEK, K. 1998. The XRCC4 gene product is a target for and interacts with the DNA-dependent protein kinase. *J Biol Chem,* 273**,** 1794-801.

LEE, J. G., KIM, J. H., AHN, J. H., LEE, K. T., BAEK, N. I. & CHOI, J. H. 2013. Jaceosidin, isolated from dietary mugwort (Artemisia princeps), induces G2/M cell cycle arrest by inactivating cdc25C-cdc2 via ATM-Chk1/2 activation. *Food Chem Toxicol,* 55**,** 214-21.

LEE, S. I., BROWN, M. K. & EASTMAN, A. 1999. Comparison of the efficacy of 7-hydroxystaurosporine (UCN-01) and other staurosporine analogs to abrogate cisplatin-induced cell cycle arrest in human breast cancer cell lines. *Biochem Pharmacol,* 58**,** 1713-21.

LI, G. M. 2008. Mechanisms and functions of DNA mismatch repair. *Cell Res,* 18**,** 85-98.

LI, X. & HEYER, W. D. 2008. Homologous recombination in DNA repair and DNA damage tolerance. *Cell Res,* 18**,** 99-113.

LI, Y. & YANG, D. Q. 2010. The ATM inhibitor KU-55933 suppresses cell proliferation and induces apoptosis by blocking Akt in cancer cells with overactivated Akt. *Mol Cancer Ther,* 9**,** 113-25.

LIFETECHNOLOGIES. 2012. *Basics of Real-Time PCR* [Online]. Available: http://find.lifetechnologies.com/qpcr/qpcrhandbook/email/qpcr-handbook-1467LW-3964VI.html [Accessed 10/7/2014].

LINDAHL, T. 1993. Instability and decay of the primary structure of DNA. *Nature,* 362**,** 709-15.

LINDAHL, T., SEDGWICK, B., SEKIGUCHI, M. & NAKABEPPU, Y. 1988. Regulation and expression of the adaptive response to alkylating agents. *Annu Rev Biochem,* 57**,** 133-57.

LIVAK, K. J. & SCHMITTGEN, T. D. 2001. Analysis of relative gene expression data using real-time quantitative PCR and the 2(-Delta Delta C(T)) Method. *Methods,* 25**,** 402-8.

LORD, C. J. & ASHWORTH, A. 2008. Targeted therapy for cancer using PARP inhibitors. *Curr Opin Pharmacol,* 8**,** 363-9.

LOSE, F., LOVELOCK, P., CHENEVIX-TRENCH, G., MANN, G. J., PUPO, G. M. & SPURDLE, A. B. 2006. Variation in the RAD51 gene and familial breast cancer. *Breast Cancer Res,* 8**,** R26.

LOVEDAY, C., TURNBULL, C., RAMSAY, E., HUGHES, D., RUARK, E., FRANKUM, J. R., BOWDEN, G., KALMYRZAEV, B., WARREN-PERRY, M., SNAPE, K., ADLARD, J. W., BARWELL, J., BERG, J., BRADY, A. F., BREWER, C., BRICE, G., CHAPMAN, C., COOK, J., DAVIDSON, R., DONALDSON, A., DOUGLAS, F., GREENHALGH, L., HENDERSON, A., IZATT, L., KUMAR, A., LALLOO, F., MIEDZYBRODZKA, Z., MORRISON, P. J., PATERSON, J., PORTEOUS, M., ROGERS, M. T., SHANLEY, S., WALKER, L., ECCLES, D., EVANS, D. G., RENWICK, A., SEAL, S., LORD, C. J., ASHWORTH, A., REIS-FILHO, J. S., ANTONIOU, A. C. & RAHMAN, N. 2011. Germline mutations in RAD51D confer susceptibility to ovarian cancer. *Nat Genet,* 43**,** 879-82.

LUO, M., HE, H., KELLEY, M. R. & GEORGIADIS, M. M. 2010. Redox regulation of DNA repair: implications for human health and cancer therapeutic development. *Antioxid Redox Signal,* 12**,** 1247-69.

MANGERICH, A. & BURKLE, A. 2011. How to kill tumor cells with inhibitors of poly(ADP-ribosyl)ation. *Int J Cancer,* 128**,** 251-65.

MARTINEZ, V. & AZZOPARDI, J. G. 1979. Invasive lobular carcinoma of the breast: incidence and variants. *Histopathology,* 3**,** 467-88.

MASAOKA, A., GASSMAN, N. R., HORTON, J. K., KEDAR, P. S., WITT, K. L., HOBBS, C. A., KISSLING, G. E., TANO, K., ASAGOSHI, K. & WILSON, S. H. 2013. Interaction between DNA Polymerase beta and BRCA1. *PLoS One,* 8**,** e66801.

MATROS, E., WANG, Z. C., LODEIRO, G., MIRON, A., IGLEHART, J. D. & RICHARDSON, A. L. 2005. BRCA1 promoter methylation in sporadic breast tumors: relationship to gene expression profiles. *Breast Cancer Res Treat,* 91**,** 179-86.

MCCORMACK, V. A. & BOFFETTA, P. 2011. Today's lifestyles, tomorrow's cancers: trends in lifestyle risk factors for cancer in low- and middle-income countries. *Ann Oncol,* 22**,** 2349-57.

MCVEY, M. & LEE, S. E. 2008. MMEJ repair of double-strand breaks (director's cut): deleted sequences and alternative endings. *Trends Genet,* 24**,** 529-38.

MEGNIN-CHANET, F., BOLLET, M. A. & HALL, J. 2010. Targeting poly(ADP-ribose) polymerase activity for cancer therapy. *Cell Mol Life Sci,* 67**,** 3649-62.

MERAJVER, S. D., FRANK, T. S., XU, J., PHAM, T. M., CALZONE, K. A., BENNETT-BAKER, P., CHAMBERLAIN, J., BOYD, J., GARBER, J. E., COLLINS, F. S. & ET AL. 1995. Germline BRCA1 mutations and loss of the wild-type allele in tumors from families with early onset breast and ovarian cancer. *Clin Cancer Res,* 1**,** 539-44.

MEREL, P., PRIEUR, A., PFEIFFER, P. & DELATTRE, O. 2002. Absence of major defects in non-homologous DNA end joining in human breast cancer cell lines. *Oncogene,* 21**,** 5654-9.

MERSCH, J., JACKSON, M. A., PARK, M., NEBGEN, D., PETERSON, S. K., SINGLETARY, C., ARUN, B. K. & LITTON, J. K. 2014. Cancers associated with BRCA1 and BRCA2 mutations other than breast and ovarian. *Cancer*.

MIKI, Y., SWENSEN, J., SHATTUCK-EIDENS, D., FUTREAL, P. A., HARSHMAN, K., TAVTIGIAN, S., LIU, Q., COCHRAN, C., BENNETT, L. M., DING, W. & ET AL. 1994. A strong candidate for the breast and ovarian cancer susceptibility gene BRCA1. *Science,* 266**,** 66-71.

MLADENOV, E. & ILIAKIS, G. 2011. Induction and repair of DNA double strand breaks: the increasing spectrum of non-homologous end joining pathways. *Mutat Res,* 711**,** 61-72.

MODRICH, P. & LAHUE, R. 1996. Mismatch repair in replication fidelity, genetic recombination, and cancer biology. *Annu Rev Biochem,* 65**,** 101-33.

MOHAMMED, M. Z., VYJAYANTI, V. N., LAUGHTON, C. A., DEKKER, L. V., FISCHER, P. M., WILSON, D. M., 3RD, ABBOTTS, R., SHAH, S., PATEL, P. M., HICKSON, I. D. & MADHUSUDAN, S. 2011. Development and evaluation of human AP endonuclease inhibitors in melanoma and glioma cell lines. *Br J Cancer,* 104**,** 653-63.

MONTONI, A., ROBU, M., POULIOT, E. & SHAH, G. M. 2013. Resistance to PARP-Inhibitors in Cancer Therapy. *Front Pharmacol,* 4**,** 18.

MOYNAHAN, M. E., CHIU, J. W., KOLLER, B. H. & JASIN, M. 1999. Brca1 controls homology-directed DNA repair. *Mol Cell,* 4**,** 511-8.

MUKHERJEE, A. & MARTIN, S. G. 2006. In vitro cytotoxicity of Phortress against colorectal cancer. *Int J Oncol,* 29**,** 1287-94.

MUKHERJEE, A., WESTWELL, A. D., BRADSHAW, T. D., STEVENS, M. F., CARMICHAEL, J. & MARTIN, S. G. 2005. Cytotoxic and antiangiogenic activity of AW464 (NSC 706704), a novel thioredoxin inhibitor: an in vitro study. *Br J Cancer,* 92**,** 350-8.

MULLAN, P. B., QUINN, J. E. & HARKIN, D. P. 2006. The role of BRCA1 in transcriptional regulation and cell cycle control. *Oncogene,* 25**,** 5854-63.

MUNSHI, A., HOBBS, M. & MEYN, R. E. 2005. Clonogenic cell survival assay. *Methods Mol Med,* 110**,** 21-8.

NADKARNI, A., SHRIVASTAV, M., MLADEK, A. C., SCHWINGLER, P. M., GROGAN, P. T., CHEN, J. & SARKARIA, J. N. 2012. ATM inhibitor KU-55933 increases the TMZ responsiveness of only inherently TMZ sensitive GBM cells. *J Neurooncol,* 110**,** 349-57.

NIJMAN, S. M. 2011. Synthetic lethality: general principles, utility and detection using genetic screens in human cells. *FEBS Lett,* 585**,** 1-6.

O'DRISCOLL, M. & JEGGO, P. A. 2006. The role of double-strand break repair - insights from human genetics. *Nat Rev Genet,* 7**,** 45-54.

ORMEROD, M. G. & KUBBIES, M. 1992. Cell cycle analysis of asynchronous cell populations by flow cytometry using bromodeoxyuridine label and Hoechst-propidium iodide stain. *Cytometry,* 13**,** 678-85.

PACHER, P. & SZABO, C. 2007. Role of poly(ADP-ribose) polymerase 1 (PARP-1) in cardiovascular diseases: the therapeutic potential of PARP inhibitors. *Cardiovasc Drug Rev,* 25**,** 235-60.

PAULL, T. T., ROGAKOU, E. P., YAMAZAKI, V., KIRCHGESSNER, C. U., GELLERT, M. & BONNER, W. M. 2000. A critical role for histone H2AX in recruitment of repair factors to nuclear foci after DNA damage. *Current Biology,* 10**,** 886-895.

PELTOMAKI, P. 2003. Role of DNA mismatch repair defects in the pathogenesis of human cancer. *J Clin Oncol,* 21**,** 1174-9.

PHAROAH, P. D., DAY, N. E., DUFFY, S., EASTON, D. F. & PONDER, B. A. 1997. Family history and the risk of breast cancer: a systematic review and meta-analysis. *Int J Cancer,* 71**,** 800-9.

PLUMMER, R., LORIGAN, P., EVANS, J., STEVEN, N., MIDDLETON, M., WILSON, R., SNOW, K., DEWJI, R. & CALVERT, H. Year. First and final report of a phase II study of the poly (ADP-ribose) polymerase (PARP) inhibitor, AG014699, in combination with temozolomide (TMZ) in patients with metastatic malignant melanoma (MM). *In:* ASCO Annual Meeting Proceedings, 2006. 8013.

PODHORECKA, M., SKLADANOWSKI, A. & BOZKO, P. 2010. H2AX Phosphorylation: Its Role in DNA Damage Response and Cancer Therapy. *J Nucleic Acids*, 2010.

POLTORATSKY, V. P., SHI, X., YORK, J. D., LIEBER, M. R. & CARTER, T. H. 1995. Human DNA-activated protein kinase (DNA-PK) is homologous to phosphatidylinositol kinases. *J Immunol,* 155**,** 4529-33.

POZAROWSKI, P. & DARZYNKIEWICZ, Z. 2004. Analysis of cell cycle by flow cytometry. *Methods Mol Biol,* 281**,** 301-11.

PUCK, T. T. & FISHER, H. W. 1956. Genetics of Somatic Mammalian Cells : I. Demonstration of the Existence of Mutants with Different Growth Requirements in a Human Cancer Cell Strain (Hela). *J Exp Med,* 104**,** 427-34.

PURNELL, M. R. & WHISH, W. J. 1980. Novel inhibitors of poly(ADP-ribose) synthetase. *Biochem J,* 185**,** 775-7.

QIAGEN. 2011. *RT2 Profiler PCR Arrays: Pathway Analysis* [Online]. Available: http://www.sabiosciences.com/pathwaymagazine/pcrhandbook-qiagen/pdfs/pcrarrayguide-qiagen.pdf [Accessed 11/7/2014].

QUINN, J. E., JAMES, C. R., STEWART, G. E., MULLIGAN, J. M., WHITE, P., CHANG, G. K., MULLAN, P. B., JOHNSTON, P. G., WILSON, R. H. & HARKIN, D. P. 2007. BRCA1 mRNA expression levels predict for overall survival in ovarian cancer after chemotherapy. *Clin Cancer Res,* 13**,** 7413-20.

RAFFERTY, K. A., JR. 1985. Growth potential of the cells of permanent lines (HeLa, BHK/21, NRK). *Virchows Arch B Cell Pathol Incl Mol Pathol,* 50**,** 167-80.

RAINEY, M. D., CHARLTON, M. E., STANTON, R. V. & KASTAN, M. B. 2008. Transient inhibition of ATM kinase is sufficient to enhance cellular sensitivity to ionizing radiation. *Cancer Res,* 68**,** 7466-74.

RAKHA, E. A., PATEL, A., POWE, D. G., BENHASOUNA, A., GREEN, A. R., LAMBROS, M. B., REIS-FILHO, J. S. & ELLIS, I. O. 2010.

Clinical and biological significance of E-cadherin protein expression in invasive lobular carcinoma of the breast. *Am J Surg Pathol,* 34**,** 1472-9.

RASSOOL, F. V. & TOMKINSON, A. E. 2010. Targeting abnormal DNA double strand break repair in cancer. *Cell Mol Life Sci,* 67**,** 3699-710.

RATANAPHAN, A. 2011. A DNA Repair Protein BRCA1 as a Potentially Molecular Target for the Anticancer Platinum Drug Cisplatin. *In:* KRUMAN, D. I. (ed.) *DNA Repair.*

REHMAN, F. L., LORD, C. J. & ASHWORTH, A. 2010. Synthetic lethal approaches to breast cancer therapy. *Nat Rev Clin Oncol,* 7**,** 718-24.

REINHARDT, H. C., ASLANIAN, A. S., LEES, J. A. & YAFFE, M. B. 2007. p53-deficient cells rely on ATM- and ATR-mediated checkpoint signaling through the p38MAPK/MK2 pathway for survival after DNA damage. *Cancer Cell,* 11**,** 175-89.

RIAZ, M., VAN JAARSVELD, M. T., HOLLESTELLE, A., PRAGER-VAN DER SMISSEN, W. J., HEINE, A. A., BOERSMA, A. W., LIU, J., HELMIJR, J., OZTURK, B., SMID, M., WIEMER, E. A., FOEKENS, J. A. & MARTENS, J. W. 2013. miRNA expression profiling of 51 human breast cancer cell lines reveals subtype and driver mutation-specific miRNAs. *Breast Cancer Res,* 15**,** R33.

RICCARDI, C. & NICOLETTI, I. 2006. Analysis of apoptosis by propidium iodide staining and flow cytometry. *Nat Protoc,* 1**,** 1458-61.

RISCH, H. A., MCLAUGHLIN, J. R., COLE, D. E., ROSEN, B., BRADLEY, L., KWAN, E., JACK, E., VESPRINI, D. J., KUPERSTEIN, G., ABRAHAMSON, J. L., FAN, I., WONG, B. & NAROD, S. A. 2001. Prevalence and penetrance of germline BRCA1 and BRCA2 mutations in a population series of 649 women with ovarian cancer. *Am J Hum Genet,* 68**,** 700-10.

RISS, T. L., MORAVEC, R. A. & NILES, A. L. 2011. Cytotoxicity testing: measuring viable cells, dead cells, and detecting mechanism of cell death. *Methods Mol Biol,* 740**,** 103-14.

ROBBINS, J. H., BRUMBACK, R. A., MENDIONES, M., BARRETT, S. F., CARL, J. R., CHO, S., DENCKLA, M. B., GANGES, M. B., GERBER, L. H., GUTHRIE, R. A. & ET AL. 1991. Neurological disease in xeroderma pigmentosum. Documentation of a late onset type of the juvenile onset form. *Brain,* 114 (Pt 3)**,** 1335-61.

ROGAKOU, E. P., BOON, C., REDON, C. & BONNER, W. M. 1999. Megabase chromatin domains involved in DNA double-strand breaks in vivo. *J Cell Biol,* 146**,** 905-16.

ROGAKOU, E. P., PILCH, D. R., ORR, A. H., IVANOVA, V. S. & BONNER, W. M. 1998. DNA double-stranded breaks induce histone H2AX phosphorylation on serine 139. *J Biol Chem,* 273**,** 5858-68.

ROSENZWEIG, K. E., YOUMELL, M. B., PALAYOOR, S. T. & PRICE, B. D. 1997. Radiosensitization of human tumor cells by the phosphatidylinositol3-kinase inhibitors wortmannin and LY294002 correlates with inhibition of DNA-dependent protein kinase and prolonged G2-M delay. *Clin Cancer Res,* 3**,** 1149-56.

ROSSO, S., GONDOS, A., ZANETTI, R., BRAY, F., ZAKELJ, M., ZAGAR, T., SMAILYTE, G., PONTI, A., BREWSTER, D. H., VOOGD, A. C., CROCETTI, E. & BRENNER, H. 2010. Up-to-date estimates of breast cancer survival for the years 2000-2004 in 11 European countries: the role of screening and a comparison with data from the United States. *Eur J Cancer,* 46**,** 3351-7.

ROTMAN, G. & SHILOH, Y. 1998. ATM: from gene to function. *Hum Mol Genet,* 7**,** 1555-63.

ROULEAU, M., PATEL, A., HENDZEL, M. J., KAUFMANN, S. H. & POIRIER, G. G. 2010. PARP inhibition: PARP1 and beyond. *Nat Rev Cancer,* 10**,** 293-301.

RUPNIK, A., GRENON, M. & LOWNDES, N. 2008. The MRN complex. *Curr Biol,* 18**,** R455-7.

SAHA, T., RIH, J. K. & ROSEN, E. M. 2009. BRCA1 down-regulates cellular levels of reactive oxygen species. *FEBS Lett,* 583**,** 1535-43.

SAHA, T., RIH, J. K., ROY, R., BALLAL, R. & ROSEN, E. M. 2010. Transcriptional regulation of the base excision repair pathway by BRCA1. *J Biol Chem,* 285**,** 19092-105.

SAMOL, J., RANSON, M., SCOTT, E., MACPHERSON, E., CARMICHAEL, J., THOMAS, A. & CASSIDY, J. 2012. Safety and tolerability of the poly(ADP-ribose) polymerase (PARP) inhibitor, olaparib (AZD2281) in combination with topotecan for the treatment of patients with advanced solid tumors: a phase I study. *Invest New Drugs,* 30**,** 1493-500.

SANCAR, A., LINDSEY-BOLTZ, L. A., UNSAL-KACMAZ, K. & LINN, S. 2004. Molecular mechanisms of mammalian DNA repair and the DNA damage checkpoints. *Annu Rev Biochem,* 73**,** 39-85.

SAVITSKY, K., BAR-SHIRA, A., GILAD, S., ROTMAN, G., ZIV, Y., VANAGAITE, L., TAGLE, D. A., SMITH, S., UZIEL, T., SFEZ, S., ASHKENAZI, M., PECKER, I., FRYDMAN, M., HARNIK, R., PATANJALI, S. R., SIMMONS, A., CLINES, G. A., SARTIEL, A., GATTI, R. A., CHESSA, L., SANAL, O., LAVIN, M. F., JASPERS, N. G., TAYLOR, A. M., ARLETT, C. F., MIKI, T., WEISSMAN, S. M., LOVETT, M., COLLINS, F. S. & SHILOH, Y. 1995. A single ataxia telangiectasia gene with a product similar to PI-3 kinase. *Science,* 268**,** 1749-53.

SCHIPLER, A. & ILIAKIS, G. 2013. DNA double-strand-break complexity levels and their possible contributions to the probability for error-prone processing and repair pathway choice. *Nucleic Acids Res,* 41**,** 7589-605.

SCHNITT, S. J. 2010. Classification and prognosis of invasive breast cancer: from morphology to molecular taxonomy. *Mod Pathol,* 23 Suppl 2**,** S60-4.

SCHREIBER, V., DANTZER, F., AME, J. C. & DE MURCIA, G. 2006. Poly(ADP-ribose): novel functions for an old molecule. *Nat Rev Mol Cell Biol,* 7**,** 517-28.

SCULLY, R., CHEN, J., PLUG, A., XIAO, Y., WEAVER, D., FEUNTEUN, J., ASHLEY, T. & LIVINGSTON, D. M. 1997. Association of BRCA1 with Rad51 in mitotic and meiotic cells. *Cell,* 88**,** 265-75.

SHAHEEN, F. S., ZNOJEK, P., FISHER, A., WEBSTER, M., PLUMMER, R., GAUGHAN, L., SMITH, G. C., LEUNG, H. Y., CURTIN, N. J. & ROBSON, C. N. 2011. Targeting the DNA double strand break repair machinery in prostate cancer. *PLoS One,* 6**,** e20311.

SHANG, Z., YU, L., LIN, Y. F., MATSUNAGA, S., SHEN, C. Y. & CHEN, B. P. 2014. DNA-PKcs activates the Chk2-Brca1 pathway during mitosis to ensure chromosomal stability. *Oncogenesis,* 3**,** e85.

SHIEH, S. Y., IKEDA, M., TAYA, Y. & PRIVES, C. 1997. DNA damage-induced phosphorylation of p53 alleviates inhibition by MDM2. *Cell,* 91**,** 325-34.

SILVER, D. P. & LIVINGSTON, D. M. 2012. Mechanisms of BRCA1 tumor suppression. *Cancer Discov,* 2**,** 679-84.

SILVER, D. P., RICHARDSON, A. L., EKLUND, A. C., WANG, Z. C., SZALLASI, Z., LI, Q., JUUL, N., LEONG, C. O., CALOGRIAS, D., BURAIMOH, A., FATIMA, A., GELMAN, R. S., RYAN, P. D., TUNG, N. M., DE NICOLO, A., GANESAN, S., MIRON, A., COLIN,

C., SGROI, D. C., ELLISEN, L. W., WINER, E. P. & GARBER, J. E. 2010. Efficacy of neoadjuvant Cisplatin in triple-negative breast cancer. *J Clin Oncol,* 28**,** 1145-53.

SMITH, J., THO, L. M., XU, N. & GILLESPIE, D. A. 2010. The ATM-Chk2 and ATR-Chk1 pathways in DNA damage signaling and cancer. *Adv Cancer Res,* 108**,** 73-112.

SOBOL, R. W., WATSON, D. E., NAKAMURA, J., YAKES, F. M., HOU, E., HORTON, J. K., LADAPO, J., VAN HOUTEN, B., SWENBERG, J. A., TINDALL, K. R., SAMSON, L. D. & WILSON, S. H. 2002. Mutations associated with base excision repair deficiency and methylation-induced genotoxic stress. *Proc Natl Acad Sci U S A,* 99**,** 6860-5.

SONG, H., CICEK, M. S., DICKS, E., HARRINGTON, P., RAMUS, S. J., CUNNINGHAM, J. M., FRIDLEY, B. L., TYRER, J. P., ALSOP, J., JIMENEZ-LINAN, M., GAYTHER, S. A., GOODE, E. L. & PHAROAH, P. D. 2014. The contribution of deleterious germline mutations in BRCA1, BRCA2 and the mismatch repair genes to ovarian cancer in the population. *Hum Mol Genet*.

STARCEVIC, D., DALAL, S. & SWEASY, J. B. 2004. Is there a link between DNA polymerase beta and cancer? *Cell Cycle,* 3**,** 998-1001.

STARK, J. M., PIERCE, A. J., OH, J., PASTINK, A. & JASIN, M. 2004. Genetic steps of mammalian homologous repair with distinct mutagenic consequences. *Mol Cell Biol,* 24**,** 9305-16.

STEVNSNER, T., MAY, A., PETERSEN, L. N., LARMINAT, F., PIRSEL, M. & BOHR, V. A. 1993. Repair of ribosomal RNA genes in hamster cells after UV irradiation, or treatment with cisplatin or alkylating agents. *Carcinogenesis,* 14**,** 1591-6.

STIFF, T., O'DRISCOLL, M., RIEF, N., IWABUCHI, K., LOBRICH, M. & JEGGO, P. A. 2004. ATM and DNA-PK function redundantly to

phosphorylate H2AX after exposure to ionizing radiation. *Cancer Res,* 64**,** 2390-6.

STROM, C. E., JOHANSSON, F., UHLEN, M., SZIGYARTO, C. A., ERIXON, K. & HELLEDAY, T. 2011. Poly (ADP-ribose) polymerase (PARP) is not involved in base excision repair but PARP inhibition traps a single-strand intermediate. *Nucleic Acids Res,* 39**,** 3166-75.

SUGASAWA, K. 2010. Regulation of damage recognition in mammalian global genomic nucleotide excision repair. *Mutat Res,* 685**,** 29-37.

SULTANA, R., ABDEL-FATAH, T., ABBOTTS, R., HAWKES, C., ALBARAKATI, N., SEEDHOUSE, C., BALL, G., CHAN, S., RAKHA, E. A., ELLIS, I. O. & MADHUSUDAN, S. 2013a. Targeting XRCC1 deficiency in breast cancer for personalized therapy. *Cancer Res,* 73**,** 1621-34.

SULTANA, R., ABDEL-FATAH, T., PERRY, C., MOSELEY, P., ALBARAKTI, N., MOHAN, V., SEEDHOUSE, C., CHAN, S. & MADHUSUDAN, S. 2013b. Ataxia telangiectasia mutated and Rad3 related (ATR) protein kinase inhibition is synthetically lethal in XRCC1 deficient ovarian cancer cells. *PLoS One,* 8**,** e57098.

SULTANA, R., MCNEILL, D. R., ABBOTTS, R., MOHAMMED, M. Z., ZDZIENICKA, M. Z., QUTOB, H., SEEDHOUSE, C., LAUGHTON, C. A., FISCHER, P. M., PATEL, P. M., WILSON, D. M., 3RD & MADHUSUDAN, S. 2012. Synthetic lethal targeting of DNA double-strand break repair deficient cells by human apurinic/apyrimidinic endonuclease inhibitors. *Int J Cancer,* 131**,** 2433-44.

TAKATA, M., SASAKI, M. S., SONODA, E., MORRISON, C., HASHIMOTO, M., UTSUMI, H., YAMAGUCHI-IWAI, Y., SHINOHARA, A. & TAKEDA, S. 1998. Homologous recombination and non-homologous end-joining pathways of DNA double-strand break repair have overlapping roles in the maintenance of chromosomal integrity in vertebrate cells. *EMBO J,* 17**,** 5497-508.

TAN, D. S., ROTHERMUNDT, C., THOMAS, K., BANCROFT, E., EELES, R., SHANLEY, S., ARDERN-JONES, A., NORMAN, A., KAYE, S. B. & GORE, M. E. 2008. "BRCAness" syndrome in ovarian cancer: a case-control study describing the clinical features and outcome of patients with epithelial ovarian cancer associated with BRCA1 and BRCA2 mutations. *J Clin Oncol,* 26**,** 5530-6.

TARON, M., ROSELL, R., FELIP, E., MENDEZ, P., SOUGLAKOS, J., RONCO, M. S., QUERALT, C., MAJO, J., SANCHEZ, J. M., SANCHEZ, J. J. & MAESTRE, J. 2004. BRCA1 mRNA expression levels as an indicator of chemoresistance in lung cancer. *Hum Mol Genet,* 13**,** 2443-9.

TASSONE, P., TAGLIAFERRI, P., PERRICELLI, A., BLOTTA, S., QUARESIMA, B., MARTELLI, M. L., GOEL, A., BARBIERI, V., COSTANZO, F., BOLAND, C. R. & VENUTA, S. 2003. BRCA1 expression modulates chemosensitivity of BRCA1-defective HCC1937 human breast cancer cells. *Br J Cancer,* 88**,** 1285-91.

TAVECCHIO, M., MUNCK, J. M., CANO, C., NEWELL, D. R. & CURTIN, N. J. 2012. Further characterisation of the cellular activity of the DNA-PK inhibitor, NU7441, reveals potential cross-talk with homologous recombination. *Cancer Chemother Pharmacol,* 69**,** 155-64.

THOMPSON, D. & EASTON, D. F. 2002. Cancer Incidence in BRCA1 mutation carriers. *J Natl Cancer Inst,* 94**,** 1358-65.

THOMS, K. M., KUSCHAL, C. & EMMERT, S. 2007. Lessons learned from DNA repair defective syndromes. *Exp Dermatol,* 16**,** 532-44.

TOMLINSON, G. E., CHEN, T. T., STASTNY, V. A., VIRMANI, A. K., SPILLMAN, M. A., TONK, V., BLUM, J. L., SCHNEIDER, N. R., WISTUBA, II, SHAY, J. W., MINNA, J. D. & GAZDAR, A. F. 1998. Characterization of a breast cancer cell line derived from a germ-line BRCA1 mutation carrier. *Cancer Res,* 58**,** 3237-42.

TU, W. Z., LI, B., HUANG, B., WANG, Y., LIU, X. D., GUAN, H., ZHANG, S. M., TANG, Y., RANG, W. Q. & ZHOU, P. K. 2013. gammaH2AX foci formation in the absence of DNA damage: mitotic H2AX phosphorylation is mediated by the DNA-PKcs/CHK2 pathway. *FEBS Lett,* 587**,** 3437-43.

TUDEK, B., CIESLA, Z., JANION, C., BOITEUX, S., BEBENEK, K., SHINAGAWA, H., BARTSCH, H., LAVAL, J., VAN ZEELAND, A. A., MULLENDERS, L. F., SZYFTER, K., COLLINS, A. & KRUSZEWSKI, M. 2003. 32nd annual meeting of European Environmental Mutagen Society. DNA damage and repair fundamental aspects and contribution to human disorders. *DNA Repair (Amst),* 2**,** 765-81.

TURNER, N., TUTT, A. & ASHWORTH, A. 2004. Hallmarks of 'BRCAness' in sporadic cancers. *Nat Rev Cancer,* 4**,** 814-9.

TUTT, A., ROBSON, M., GARBER, J. E., DOMCHEK, S. M., AUDEH, M. W., WEITZEL, J. N., FRIEDLANDER, M., ARUN, B., LOMAN, N., SCHMUTZLER, R. K., WARDLEY, A., MITCHELL, G., EARL, H., WICKENS, M. & CARMICHAEL, J. 2010. Oral poly(ADP-ribose) polymerase inhibitor olaparib in patients with BRCA1 or BRCA2 mutations and advanced breast cancer: a proof-of-concept trial. *Lancet,* 376**,** 235-44.

UNDERHILL, C., TOULMONDE, M. & BONNEFOI, H. 2011. A review of PARP inhibitors: from bench to bedside. *Ann Oncol,* 22**,** 268-79.

VAN DER SANGEN, M. J., VOOGD, A. C., VAN DE POLL-FRANSE, L. V. & TJAN-HEIJNEN, V. C. 2008. [Breast cancer in young women: epidemiology and treatment dilemmas]. *Ned Tijdschr Geneeskd,* 152**,** 2495-500.

VENKITARAMAN, A. R. 2002. Cancer susceptibility and the functions of BRCA1 and BRCA2. *Cell,* 108**,** 171-82.

VEUGER, S. J., CURTIN, N. J., RICHARDSON, C. J., SMITH, G. C. & DURKACZ, B. W. 2003. Radiosensitization and DNA repair inhibition by the combined use of novel inhibitors of DNA-dependent protein kinase and poly(ADP-ribose) polymerase-1. *Cancer Res,* 63**,** 6008-15.

VILAR, E., BARTNIK, C. M., STENZEL, S. L., RASKIN, L., AHN, J., MORENO, V., MUKHERJEE, B., INIESTA, M. D., MORGAN, M. A., RENNERT, G. & GRUBER, S. B. 2011. MRE11 deficiency increases sensitivity to poly(ADP-ribose) polymerase inhibition in microsatellite unstable colorectal cancers. *Cancer Res,* 71**,** 2632-42.

VLAHOS, C. J., MATTER, W. F., HUI, K. Y. & BROWN, R. F. 1994. A specific inhibitor of phosphatidylinositol 3-kinase, 2-(4-morpholinyl)-8-phenyl-4H-1-benzopyran-4-one (LY294002). *J Biol Chem,* 269**,** 5241-8.

VORGIAS, G., KOUKOURAS, D., PALEOGIANNI, V. & TZORACOELEFTHERAKIS, E. 2001. Prognostic significance of factors affecting disease free interval and overall survival for Stage II breast cancer in Greece. A multivariate cohort study. *Eur J Obstet Gynecol Reprod Biol,* 95**,** 100-4.

WAHLBERG, E., KARLBERG, T., KOUZNETSOVA, E., MARKOVA, N., MACCHIARULO, A., THORSELL, A. G., POL, E., FROSTELL, A., EKBLAD, T., ONCU, D., KULL, B., ROBERTSON, G. M., PELLICCIARI, R., SCHULER, H. & WEIGELT, J. 2012. Family-wide chemical profiling and structural analysis of PARP and tankyrase inhibitors. *Nat Biotechnol,* 30**,** 283-8.

WALLACE, S. S. 2014. Base excision repair: a critical player in many games. *DNA Repair (Amst),* 19**,** 14-26.

WANG, Y. G., NNAKWE, C., LANE, W. S., MODESTI, M. & FRANK, K. M. 2004. Phosphorylation and regulation of DNA ligase IV stability by DNA-dependent protein kinase. *J Biol Chem,* 279**,** 37282-90.

WARE, J. H., ZHOU, Z., GUAN, J., KENNEDY, A. R. & KOPELOVICH, L. 2007. Establishment of human cancer cell clones with different characteristics: a model for screening chemopreventive agents. *Anticancer Res,* 27**,** 1-16.

WEI, L., LAN, L., HONG, Z., YASUI, A., ISHIOKA, C. & CHIBA, N. 2008. Rapid recruitment of BRCA1 to DNA double-strand breaks is dependent on its association with Ku80. *Mol Cell Biol,* 28**,** 7380-93.

WEST, M., BLANCHETTE, C., DRESSMAN, H., HUANG, E., ISHIDA, S., SPANG, R., ZUZAN, H., OLSON, J. A., JR., MARKS, J. R. & NEVINS, J. R. 2001. Predicting the clinical status of human breast cancer by using gene expression profiles. *Proc Natl Acad Sci U S A,* 98**,** 11462-7.

WEST, R. B., YANEVA, M. & LIEBER, M. R. 1998. Productive and nonproductive complexes of Ku and DNA-dependent protein kinase at DNA termini. *Mol Cell Biol,* 18**,** 5908-20.

WETERINGS, E. & CHEN, D. J. 2008. The endless tale of non-homologous end-joining. *Cell Res,* 18**,** 114-24.

WILLIAMSON, C. T., KUBOTA, E., HAMILL, J. D., KLIMOWICZ, A., YE, R., MUZIK, H., DEAN, M., TU, L., GILLEY, D., MAGLIOCCO, A. M., MCKAY, B. C., BEBB, D. G. & LEES-MILLER, S. P. 2012. Enhanced cytotoxicity of PARP inhibition in mantle cell lymphoma harbouring mutations in both ATM and p53. *EMBO Mol Med,* 4**,** 515-27.

WILLMORE, E., DE CAUX, S., SUNTER, N. J., TILBY, M. J., JACKSON, G. H., AUSTIN, C. A. & DURKACZ, B. W. 2004. A novel DNA-dependent protein kinase inhibitor, NU7026, potentiates the cytotoxicity of topoisomerase II poisons used in the treatment of leukemia. *Blood,* 103**,** 4659-65.

WOOD, R. D. 1997. Nucleotide excision repair in mammalian cells. *J Biol Chem,* 272**,** 23465-8.

WU, J., LU, L. Y. & YU, X. 2010. The role of BRCA1 in DNA damage response. *Protein Cell,* 1**,** 117-23.

XU, B., KIM, S. & KASTAN, M. B. 2001. Involvement of Brca1 in S-phase and G(2)-phase checkpoints after ionizing irradiation. *Mol Cell Biol,* 21**,** 3445-50.

XU, B., O'DONNELL, A. H., KIM, S. T. & KASTAN, M. B. 2002. Phosphorylation of serine 1387 in Brca1 is specifically required for the Atm-mediated S-phase checkpoint after ionizing irradiation. *Cancer Res,* 62**,** 4588-91.

YAN, M., XU, H., WADDELL, N., SHIELD-ARTIN, K., HAVIV, I., MCKAY, M. J. & FOX, S. B. 2012. Enhanced RAD21 cohesin expression confers poor prognosis in BRCA2 and BRCAX, but not BRCA1 familial breast cancers. *Breast Cancer Res,* 14**,** R69.

YELAMOS, J., FARRES, J., LLACUNA, L., AMPURDANES, C. & MARTIN-CABALLERO, J. 2011. PARP-1 and PARP-2: New players in tumour development. *Am J Cancer Res,* 1**,** 328-346.

YOO, S. & DYNAN, W. S. 1999. Geometry of a complex formed by double strand break repair proteins at a single DNA end: recruitment of DNA-PKcs induces inward translocation of Ku protein. *Nucleic Acids Res,* 27**,** 4679-86.

YOSHIDA, K., OZAKI, T., FURUYA, K., NAKANISHI, M., KIKUCHI, H., YAMAMOTO, H., ONO, S., KODA, T., OMURA, K. & NAKAGAWARA, A. 2008. ATM-dependent nuclear accumulation of IKK-alpha plays an important role in the regulation of p73-mediated apoptosis in response to cisplatin. *Oncogene,* 27**,** 1183-8.

YOULDEN, D. R., CRAMB, S. M., DUNN, N. A., MULLER, J. M., PYKE, C. M. & BAADE, P. D. 2012. The descriptive epidemiology of female

breast cancer: an international comparison of screening, incidence, survival and mortality. *Cancer Epidemiol,* 36**,** 237-48.

YU, L., TUMATI, V., TSENG, S. F., HSU, F. M., KIM, D. N., HONG, D., HSIEH, J. T., JACOBS, C., KAPUR, P. & SAHA, D. 2012. DAB2IP regulates autophagy in prostate cancer in response to combined treatment of radiation and a DNA-PKcs inhibitor. *Neoplasia,* 14**,** 1203-12.

ZHANG, S., YAJIMA, H., HUYNH, H., ZHENG, J., CALLEN, E., CHEN, H. T., WONG, N., BUNTING, S., LIN, Y. F., LI, M., LEE, K. J., STORY, M., GAPUD, E., SLECKMAN, B. P., NUSSENZWEIG, A., ZHANG, C. C., CHEN, D. J. & CHEN, B. P. 2011. Congenital bone marrow failure in DNA-PKcs mutant mice associated with deficiencies in DNA repair. *J Cell Biol,* 193**,** 295-305.

ZHANG, Y., STORR, S. J., JOHNSON, K., GREEN, A. R., RAKHA, E. A., ELLIS, I. O., MORGAN, D. A. & MARTIN, S. G. 2014. Involvement of metformin and AMPK in the radioresponse and prognosis of luminal versus basal-like breast cancer treated with radiotherapy. *Oncotarget,* 5**,** 12936-49.

ZHAO, L., AU, J. L. & WIENTJES, M. G. 2010. Comparison of methods for evaluating drug-drug interaction. *Front Biosci (Elite Ed),* 2**,** 241-9.

ZHAO, Y., THOMAS, H. D., BATEY, M. A., COWELL, I. G., RICHARDSON, C. J., GRIFFIN, R. J., CALVERT, A. H., NEWELL, D. R., SMITH, G. C. & CURTIN, N. J. 2006. Preclinical evaluation of a potent novel DNA-dependent protein kinase inhibitor NU7441. *Cancer Res,* 66**,** 5354-62.

ZHONG, Q., BOYER, T. G., CHEN, P. L. & LEE, W. H. 2002. Deficient nonhomologous end-joining activity in cell-free extracts from Brca1-null fibroblasts. *Cancer Res,* 62**,** 3966-70.

Appendices

APPENDIX A. ΔΔCt Method

ΔΔCt method is a convenient way to analyze the relative changes in gene expression from real-time quantitative PCR experiments. This involves comparing the Ct values of the samples (BRCA1 deficient cells) of interest with a control (BRCA1 proficient cells). The Ct values of both the control and the samples of interest are normalized to a housekeeping gene (GAPDH). The ΔΔCt method is also known as the comparative Ct method and 2–[delta][delta]Ct method (Livak and Schmittgen, 2001), where

$$\Delta Ct1 = Ct(\text{target, control sample}) - Ct(\text{ref, control sample})$$

$$\Delta Ct2 = Ct(\text{target, deficient sample}) - Ct(\text{ref, deficient sample})$$

$$\Delta\Delta Ct = \Delta Ct1 - \Delta Ct2$$

Where
Ct (target, control sample) = Ct value of gene of interest in BRCA1 proficient sample
Ct (ref, control sample) = Ct value of housekeeping gene in BRCA1 proficient sample
Ct (target, deficient sample) = Ct value of gene of interest in BRCA1 deficient sample
Ct (ref, deficient sample) = Ct value of housekeeping gene in BRCA1 deficient sample

Then calculate the ratio of our target gene in our deficient sample relative to our control sample by taking $2^{\Delta\Delta CT}$.
Example:

	control sample	deficient sample
BRCA1	31.7	35.50
GAPDH	24.14	21.847

$$\Delta\Delta Ct = (31.7 - 24.14) - (35.50 - 21.847)$$

$$\Delta\Delta Ct = (7.56) - (13.653)$$

$$\Delta\Delta Ct = -6.093$$

$$2^{\Delta\Delta CT} = 2^{(0 - 6.093)} = 0.02 \text{ (Fold Change)}$$

So BRCA1 gene is decreased by 0.02 times in BRCA1 deficient sample versus BRCA1 proficient sample.

APPENDIX B. DNA repair genes assayed in Qiagen RT^2 Profiler DNA Repair

Symbol	*Description*
APE1	APEX nuclease (multifunctional DNA repair enzyme) 1
APE2	APEX nuclease (apurinic/apyrimidinic endonuclease) 2
ATM	Ataxia telangiectasia mutated
ATR	Ataxia telangiectasia and Rad3 related
ATXN3	Ataxin 3
BRCA1	Breast cancer 1, early onset
BRCA2	Breast cancer 2, early onset
BRIP1	BRCA1 interacting protein C-terminal helicase 1
CCNH	Cyclin H
CCNO	Cyclin O
CDK7	Cyclin-dependent kinase 7
DDB1	Damage-specific DNA binding protein 1, 127kDa
DDB2	Damage-specific DNA binding protein 2, 48kDa
DMC1	DMC1 dosage suppressor of mck1 homolog, meiosis-specific homologous recombination (yeast)
ERCC1	Excision repair cross-complementing rodent repair deficiency, complementation group 1
ERCC2	Excision repair cross-complementing rodent repair deficiency, complementation group 2
ERCC3	Excision repair cross-complementing rodent repair deficiency, complementation group 3
ERCC4	Excision repair cross-complementing rodent repair deficiency, complementation group 4
ERCC5	Excision repair cross-complementing rodent repair deficiency, complementation group 5
ERCC6	Excision repair cross-complementing rodent repair deficiency, complementation group 6
ERCC8	Excision repair cross-complementing rodent repair deficiency, complementation group 8
EXO1	Exonuclease 1
FEN1	Flap structure-specific endonuclease 1
LIG1	Ligase I, DNA, ATP-dependent
LIG3	Ligase III, DNA, ATP-dependent
LIG4	Ligase IV, DNA, ATP-dependent
MGMT	O-6-methylguanine-DNA methyltransferase
MLH1	MutL homolog 1, colon cancer, nonpolyposis type 2 (E. coli)
MLH3	MutL homolog 3 (E. coli)
MMS19	MMS19 nucleotide excision repair homolog (S. cerevisiae)
MPG	N-methylpurine-DNA glycosylase
MRE11A	MRE11 meiotic recombination 11 homolog A (S. cerevisiae)
MSH2	MutS homolog 2, colon cancer, nonpolyposis type 1 (E. coli)
MSH3	MutS homolog 3 (E. coli)
MSH4	MutS homolog 4 (E. coli)
MSH5	MutS homolog 5 (E. coli)
MSH6	MutS homolog 6 (E. coli)
MUTYH	MutY homolog (E. coli)
NEIL1	Nei endonuclease VIII-like 1 (E. coli)

NEIL2	Nei endonuclease VIII-like 2 (E. coli)
NEIL3	Nei endonuclease VIII-like 3 (E. coli)
NTHL1	Nth endonuclease III-like 1 (E. coli)
OGG1	8-oxoguanine DNA glycosylase
PARP1	Poly (ADP-ribose) polymerase 1
PARP2	Poly (ADP-ribose) polymerase 2
PARP3	Poly (ADP-ribose) polymerase family, member 3
PMS1	PMS1 postmeiotic segregation increased 1 (S. cerevisiae)
PMS2	PMS2 postmeiotic segregation increased 2 (S. cerevisiae)
PNKP	Polynucleotide kinase 3'-phosphatase
POLB	Polymerase (DNA directed), beta
POLD3	Polymerase (DNA-directed), delta 3, accessory subunit
POLL	Polymerase (DNA directed), lambda
DNA-PKcs	Protein kinase, DNA-activated, catalytic polypeptide
RAD18	RAD18 homolog (S. cerevisiae)
RAD21	RAD21 homolog (S. pombe)
RAD23A	RAD23 homolog A (S. cerevisiae)
RAD23B	RAD23 homolog B (S. cerevisiae)
RAD50	RAD50 homolog (S. cerevisiae)
RAD51	RAD51 homolog (S. cerevisiae)
RAD51B	RAD51 homolog B (S. cerevisiae)
RAD51C	RAD51 homolog C (S. cerevisiae)
RAD51D	RAD51 homolog D (S. cerevisiae)
RAD52	RAD52 homolog (S. cerevisiae)
RAD54L	RAD54-like (S. cerevisiae)
RFC1	Replication factor C (activator 1) 1, 145kDa
RPA1	Replication protein A1, 70kDa
RPA3	Replication protein A3, 14kDa
SLK	STE20-like kinase
SMUG1	Single-strand-selective monofunctional uracil-DNA glycosylase 1
TDG	Thymine-DNA glycosylase
TOP3A	Topoisomerase (DNA) III alpha
TOP3B	Topoisomerase (DNA) III beta
TREX1	Three prime repair exonuclease 1
UNG	Uracil-DNA glycosylase
XAB2	XPA binding protein 2
XPA	Xeroderma pigmentosum, complementation group A
XPC	Xeroderma pigmentosum, complementation group C
XRCC1	X-ray repair complementing defective repair in Chinese hamster cells 1
XRCC2	X-ray repair complementing defective repair in Chinese hamster cells 2
XRCC3	X-ray repair complementing defective repair in Chinese hamster cells 3
XRCC4	X-ray repair complementing defective repair in Chinese hamster cells 4
XRCC5	X-ray repair complementing defective repair in Chinese hamster cells 5 (double-strand-break rejoining)

XRCC6	X-ray repair complementing defective repair in Chinese hamster cells 6
XRCC6BP1	XRCC6 binding protein 1

APPENDIX C. Other related DNA repair genes under-expressed in BRCA1 deficient cell lines compared to BRCA1 proficient cell lines.

Statistical significance determined using the Bonferroni correction for multiple testing, with p values less than 0.05 (threshold $p < 0.000595 = 0.05/84$).

	Fold Change	***P Value***	***Fold Change***	***P Value***
Other related DNA repair genes				
	BRCA1 knockdown cell compared to Control cells		***MDA-MB-436 cells compared to MCF7 cells***	
ATR	**0.8129**	0.622017	**0.1521**	0.00402
EXO1	**0.7888**	0.572304	**0.143**	0.002984
MGMT	**0.3817**	0.022209	**0.2671**	0.043123
RAD18	**0.7589**	0.511457	**0.2366**	0.02729
RFC1	**0.7687**	0.531243	**0.4667**	0.242016
TOP3A	**0.7281**	0.450213	**0.2772**	0.049293
TOP3B	**0.6541**	0.312452	**0.3977**	0.1571
MRE11A	**0.7363**	0.466241	**0.1613**	0.005307
MMS19	**0.7137**	0.422161	**0.3424**	0.100227
TDG	**1.1639**	0.717939	**0.147**	0.003411

APPENDIX D. Evaluation of drug interaction

Isobologram, combination index and curve shift analysis are useful methods for analyzing drug-drug interaction, and provide complimentary information.

Isobologram analysis: The isobologram analysis provides a graphical presentation of the nature of interaction of two drugs (e.g. drug A and drug B). Firstly, in a two-coordinate plot with one coordinate representing concentration of drug A ($IC_{50(A)}$) and the other representing concentration of drug B ($IC_{50(B)}$), the concentrations of drugs A and B required to produce a defined effect x,

when used as single agents, are placed on the X and Y axes, respectively. The line of additivity is constructed by connecting these two points. Secondly, the concentrations of the two drugs used in combination to provide the same effect x, denoted by point ($C_{(A, X)}$, $C_{(B, X)}$), are placed in the same plot. Synergy, additivity, or antagonism is indicated when this point is located below, on, or above the line, respectively.

Combination index analysis: Combination index (CI) provides a quantitative measure of the extent of drug interaction at a given effect level. That is, the combination concentrations of first drug (A) and second drug (B) to produce an effect (D), combination drugs are normalized by their corresponding concentrations that produces the same effect as a single agent (Chou and Talalay, 1984). This is a useful method for analysing drug-drug interactions (Zhao et al., 2010). The effect of the combined treatment is analysed for the combination of drugs by applying the following CI equation: (Ac/Ae) + (Bc/Be) = D, where Ac and Bc correspond to the concentrations of drugs used in the combination treatment, and Ae and Be corresponds to the concentrations of drugs able to produce the same effect by themselves. CI is considered synergistic if D (combination index) is < 1, whereas considered additive if D = 1 or antagonistic if D is > 1.

Curve shift analysis: Curve shift analysis allows simultaneous presentation of the studied concentration-effect curves of single agent and combination treatments in a single plot. The effects of combination therapy can be analysed by applying the following equation:

$$Combination\ Therapy\ Effect = \frac{E_{\max}\left(\frac{C_{A,x}}{IC_{50,A}} + \frac{C_{B,x}}{IC_{50,B}}\right)^{n_{combo}}}{\left(\frac{C_{A,x}}{IC_{50,A}} + \frac{C_{B,x}}{IC_{50,B}}\right)^{n_{combo}} + (IC_{50,combo})^{n_{combo}}}$$

Where E_{max} is the full range of drug effect; $C_{A,x}$ or $C_{B,x}$ is the IC_{50}-equivalent concentration of drug A or B in combination; IC_{50} is the drug concentration producing the median effect of 50%; and n is the curve shape parameter describing the steepness of the concentration-effect relationship; $IC_{50, X}$ is the IC_{50} value of drug X; $IC_{50,combo}$ and n_{combo} are the values for the combination therapy.

Plotting the effects of both single agents and combinations against (IC_{50}-equivalent drug concentrations) enables the simultaneous presentation of these concentration effect curves in a single plot. Due to the normalization, the curves for the single agents will have an IC_{50} value of one, while synergistic combinations will have a lower IC_{50} value resulting in a leftward shift, and antagonistic combinations will show a rightward shift (Zhao et al., 2010).